Hurricane Resilient Wind Plant Concept Study Final Report

Besart Dibra, Zachary Finucane, Benjamin Foley and Rudy Hall
Keystone Engineering Inc.

Rick Damiani, Benjamin Maples, Zachary Parker, Amy Robertson, George Scott, Tyler Stehly, and Fabian Wendt
National Renewable Energy Laboratory

Mads Boel Overgaard Andersen and Kevin Standish
Siemens Wind Power A/S

Ken Lee, Amool Raina, and Kyle Wetzel
Wetzel Engineering Inc.

Walter Musial and Scott Schreck (Editors/Project Managers)
National Renewable Energy Laboratory

NREL is a national laboratory of the U.S. Department of Energy
Office of Energy Efficiency & Renewable Energy
Operated by the Alliance for Sustainable Energy, LLC

This report is available at no cost from the National Renewable Energy Laboratory (NREL) at www.nrel.gov/publications.

Technical Report
NREL/TP-5000-66869
October 2016

Contract No. DE-AC36-08GO28308

NREL
NATIONAL RENEWABLE ENERGY LABORATORY

Hurricane Resilient Wind Plant Concept Study Final Report

Besart Dibra, Zachary Finucane, Benjamin Foley and Rudy Hall
Keystone Engineering Inc.

Rick Damiani, Benjamin Maples, Zachary Parker, Amy Robertson, George Scott, Tyler Stehly, and Fabian Wendt
National Renewable Energy Laboratory

Mads Boel Overgaard Andersen and Kevin Standish
Siemens Wind Power A/S

Ken Lee, Amool Raina, and Kyle Wetzel
Wetzel Engineering Inc.

Walter Musial and Scott Schreck (Editors/Project Managers)
National Renewable Energy Laboratory

Prepared under Task No(s). WE11.5076 and LRDS3006

NREL is a national laboratory of the U.S. Department of Energy
Office of Energy Efficiency & Renewable Energy
Operated by the Alliance for Sustainable Energy, LLC

This report is available at no cost from the National Renewable Energy Laboratory (NREL) at www.nrel.gov/publications.

National Renewable Energy Laboratory
15013 Denver West Parkway
Golden, CO 80401
303-275-3000 • www.nrel.gov

Technical Report
NREL/TP-5000-66869
October 2016

Contract No. DE-AC36-08GO28308

NOTICE

This report is available at no cost from the National Renewable Energy Laboratory (NREL) at www.nrel.gov/publications.

Available electronically at SciTech Connect http:/www.osti.gov/scitech

Available for a processing fee to U.S. Department of Energy and its contractors, in paper, from:

U.S. Department of Energy
Office of Scientific and Technical Information
P.O. Box 62
Oak Ridge, TN 37831-0062
OSTI http://www.osti.gov
Phone: 865.576.8401
Fax: 865.576.5728
Email: reports@osti.gov

Available for sale to the public, in paper, from:

U.S. Department of Commerce
National Technical Information Service
5301 Shawnee Road
Alexandria, VA 22312
NTIS http://www.ntis.gov
Phone: 800.553.6847 or 703.605.6000
Fax: 703.605.6900
Email: orders@ntis.gov

Cover Photos by Dennis Schroeder: (left to right) NREL 26173, NREL 18302, NREL 19758, NREL 29642, NREL 19795.

NREL prints on paper that contains recycled content.

Nomenclature

ABS	American Bureau of Shipping
AC	alternating current
AEP	annual energy production
AEP_{net}	net annual energy production
AOE	annual operating expenses
API	American Petroleum Institute
BOM	bill of materials
BOS	balance of system
C_A	added mass coefficient
C_D	drag coefficient
CMS	conditional monitoring system
COE	cost of energy
CS	coordinate system
Demob	demobilization
DLC	design load case
DOE	U.S. Department of Energy
DR	discount rate
DTR	outside diamter (OD) to wall thickness ratio
ECN	Energy Research Center of the Netherlands
FE	finite element
FEA	finite-element analysis
FEED	front-end engineering design
FF	fiber failure
FOA	funding opportunity announcement
FTC	fault-type classification
GI	Germanischer Lloyd
HH	hub height
Hmax	maximum wave height
HorWindV	horizontal wind speed
HsSignificant	eave height
IBGS	inward battered guide structure
ICC	installed capital cost
IEC	International Electrotechnical Commission
IFF	interfiber failure
IntfFXss	interface reaction force in x-direction at the TP reference point
IntfFYss	interface reaction force in y-direction at the TP reference point
IntfFZs	interface reaction force in z-direction at the TP reference point
IntfMXss	interface reaction moment about the x-axis at the TP reference point

IntfMYss	interface reaction moment about the y-axis at the TP reference point
IntfMZss	interface reaction moment about the z-axis at the TP reference point
IntfRDXss	interface rotation at the TP reference point about the x-axis
IntfRDYss	interface rotation at the TP reference point about the y-axis
IntfRDZss	interface rotation at the TP reference point about the z-axis
IntfTDXss	interface displacement at the TP reference point along the x-axis
IntfTDYss	interface displacement at the TP reference point along the y-axis
IntfTDZss	interface displacement at the TP reference point along the z-axis
IPDefl1	in-plane blade tip deflection of blade 1
IWF	insurance, warranty, and other fees
kg	kilogram
km	kilometer
kN	kilonewton
kNm	kilonewton meter
kV	kilovolt
kW	kilowatt
kWh	kilowatt-hour
LCOE	levelized cost of energy
m	meter
min	minute(s)
m/s	meters per second
MC	maintenance category
Mob	mobilization
MSL	mean sea level
MW	megawatt
MWh	megawatt-hour
M_{XY}	maximum root bending moment
NCF	net capacity factor
NOAA	National Oceanic and Atmospheric Administration
NREL	National Renewable Energy Laboratory
O&M	operation and maintenance
OEM	original equipment manufacturer
OoP	defl1 out-of-plane blade tip deflection of blade 1
PMDD	permanent-magnet direct-drive
RDS-PP	reference designation system for power plant
ReactFXss	reaction force at the mudline along the x-axis
ReactFYss	reaction force at the mudline along the y-axis

ReactFZss	reaction force at the mudline along the z-axis
ReactMXss	reaction moment at the mudline about the x-axis
ReactMYss	reaction moment at the mudline about the y-axis
ReactMZss	reaction moment at the mudline about the z-axis
RNA	rotor nacelle assembly
RootF1	total blade 1 root shear force in the x/y-plane (FAST blade CS)
RootFxc1	blade 1 root force along the x-axis (FAST blade CS)
RootFyc1	blade 1 root force along the y-axis (FAST blade CS)
RootFzc1	blade 1 root force along the z-axis (FAST blade CS)
RootM1	total blade 1 root bending moment
RootMzc1	blade 1 root moment about the z-axis (FAST blade CS)
s	second(s)
SACS	finite-element analysis software package used by Keystone Engineering
SWT	Siemens Wind Turbine
t	ton(s)
T	metric ton (tonne)
TBC	torsion bend coupling
TCC	turbine capital costs
TI	turbulence intensity
Tmax	maximum wave period
TP	spectral peak period
TR	effective state and federal tax rate
TTDspFA	tower-top displacement in the fore-aft direction
TTDspSS	tower-top displacement in the side-to-side direction
TwrBsF	total tower base shear force
TwrBsFxt	tower base shear force along the x-axis
TwrBsFyt	tower base shear force along the y-axis
TwrBsFzt	tower base shear force along the z-axis
TwrBsM	total tower base bending moment
TwrBsMxt	tower base moment about the x-axis
TwrBsMyt	tower base moment about the y-axis
TwrBsMzt	tower base moment about the z-axis
ULS	ultimate-limit states
USACE	U.S. Army Corps of Engineers
Wave1Elev	wave elevation
WEI	Wetzel Engineering, Inc.
WindPACT	Wind Partnerships for Advanced Component Technology
WIS	wave information system
WS	wind speed
WT	wind turbine
WTG	wind turbine generator

YawBrFxp	yaw bearing force along the x-axis
YawBrFyp	yaw bearing force along the y-axis
YawBrFzp	yaw bearing force along the z-axis
YawBrMxp	yaw bearing moment about the x-axis
YawBrMyp	yaw bearing moment about the y-axis
YawBrMzp	yaw bearing moment about the z-axis
yr	year

Executive Summary

Hurricanes occur over much of the U.S. Atlantic and Gulf coasts, from Long Island to the U.S.-Mexico border, encompassing much of the nation's primary offshore wind resource. Category 5 hurricanes have made landfall as far north as North Carolina, with Category 3 hurricanes reaching New York with some frequency. Along the US West coast, typhoons strike with similar frequency and severity. At present, offshore wind turbine design practices do not fully consider the severe operating conditions imposed by hurricanes. Although universally applied to most turbine designs, International Electrotechnical Commission (IEC) standards do not sufficiently address the duration, directionality, magnitude, or character of hurricanes.

To assess advanced design features that could mitigate hurricane loading in various ways, this *Hurricane-Resilient Wind Plant Concept Study* considered a concept design study of a 500-megawatt (MW) wind power plant consisting of 10-MW wind turbines deployed in 25-meter (m) water depths in the Western Gulf of Mexico. This location was selected because hurricane frequency and severity provided a unique set of design challenges that would enable assessment of hurricane risk and projection of cost of energy (COE) changes, all in response to specific U.S. Department of Energy (DOE) objectives. Notably, the concept study pursued a holistic approach that incorporated multiple advanced system elements at the wind turbine and wind power plant levels to meet objectives for system performance and reduced COE. Principal turbine system elements included a 10-MW rotor with structurally efficient, low-solidity blades; a lightweight, permanent-magnet, direct-drive generator, and an innovative fixed substructure. At the wind power plant level, turbines were arrayed in a large-scale wind power plant in a manner aimed at balancing energy production against capital, installation, and operation and maintenance (O&M) costs to achieve significant overall reductions in COE (National Renewable Energy Laboratory (NREL) 2012).

The baseline turbine adopted for this effort was intended to be representative of the current state of the art for offshore wind turbine technology, and consisted of a utility-scale 5-MW turbine, also known as the NREL offshore 5-MW baseline wind turbine. This turbine has been used extensively worldwide as the basis for offshore wind turbine analyses (Jonkman 2009). Baseline turbine configuration consisted of a conventional three-bladed, upwind, variable-speed, variable blade-pitch-to-feather-controlled rotor designed against IEC Class 1A criteria. It employed a modular gear-driven system with full power conversion. Overall, the turbine was a hybrid concept based on published design documents from the REpower 5M turbine and the Wind Partnerships for Advanced Component (WindPACT), RECommendations for OFFshore wind turbines (RECOFF), and Dutch Offshore Wind Energy Converter projects. Baseline turbine rotor diameter was 126 m, mounted on a 90-m steel tubular tower, on a classic monopile substructure.

To successfully complete this challenging, multi-faceted concept design, partners were recruited from across the international wind energy research and development community to carry out various constituent component designs and studies. All of these designs and studies are documented in detail in this report.

Optimization of the hurricane-resilient blade and rotor for aerodynamic and structural performance**,** carried out by Wetzel Engineering, culminated in a downwind three-bladed rotor rated at 10 MW, having a swept diameter of 218 m, and hub height of 132 m. The optimization procedure produced a rotor with no precone and with the highest solidity geometry in the design space. The rotor operates at a maximum tip speed of 85 meters per second (m/s) and achieves a power coefficient of 0.47. The blade is constructed of glass fiber infused with epoxy resin, with the skin laminate utilizing quadraxial and triaxial glass fabric, and selectively reinforced with pultruded high-modulus glass fiber composites. The main spar cap and trailing edge spar cap are composed of fiber composites that are primarily unidirectional pultruded carbon fiber composites of tailored cross-sections and unidirectional glass fabric, respectively.

The basis for the Siemens Windpower hub, nacelle, and generator design for the hurricane-resilient wind turbine is the direct-drive Siemens 3.0 MW and 6.0 MW platforms, which achieve a straightforward turbine geometry. In this study, three 10-MW design concepts were created corresponding to three blade lengths, rated rotational speeds, and rated torques. Based on input parameters obtained from other turbine component designs in this study, the main parameters for hub, generator, and nacelle were found by extrapolating from the 3.0- and 6.0-MW baselines to 10 MW by applying simple physics-based scaling laws**.** The scaling relationship of the generator mass equation is based on the torque density of the Siemens SWT-6.0 MW turbine. The generator mass increases with higher-rated torques and lower-rated rotational speeds.

NREL designed a minimum mass tower to support the hurricane-resilient wind turbine, which achieved a first system eigenfrequency of approximately 0.163 hertz (Hz). This preliminary design was based solely on load-bearing strength and a soft-stiff frequency approach, considering both parked and operating states. A parametric study was conducted to show what mass penalty would need to be incurred if the geometric parameters were to change, or if a higher eigenfrequency were selected. Given the uncertainties in soil characteristics and design details, tower first natural frequency was not fine tuned, leaving this and other comparable design refinements to subsequent design stages in future studies.

Keystone Engineering's goal for the substructure and foundation design was to support the hurricane-resilient wind turbine system at a Western Gulf of Mexico site where it would encounter hurricane-loading conditions. A medium-consequence failure was adopted for the offshore wind turbine support structure, corresponding to an L-2 exposure category. Based on that, a coupled design and analysis for the substructure and foundation were completed for ultimate-limit states (ULS) and robustness conditions, for return periods of 50 years and 500 years, respectively. In addition, fabrication and installation cost comparisons were provided involving the Keystone inward battered guide structure (IBGS) design and a typical four-pile jacket to show reductions in capital cost that contribute to an overall decrease in cost of energy.

To obtain a realistic estimation of turbine system loads, NREL performed a fully coupled aero-hydro-elastic model of the integrated turbine system, which included the wind turbine, tower, and IBGS jacket substructure. Modeling was done to predict the maximum loads that the 10-MW hurricane-resilient turbine would encounter in a parked state during a hurricane event. Maximum structural load values were extracted from a series of nonoperating (parked) load cases modeled

for hurricane inflow conditions for 50-, 100-, and 500-year extreme events. It is important to note that, for integrated system modeling, only parked rotor conditions were considered. This was because the turbine would be shut down during hurricane conditions, and blade and rotor design optimization showed these produced higher loads than operating conditions.

For the NREL wind power plant layout analysis, a surrogate site was identified in the Gulf of Mexico, approximately 60 kilometers (km) southeast of Corpus Christi, Texas. The site and alternative wind power plant layouts were selected to typify general development scenarios for the hurricane-resilient technology. The AWS Truepower's windTrends database was used in connection with ancillary analyses to produce wind input files, and ocean bathymetry data were obtained from the National Oceanic and Atmospheric Administration (NOAA) Coastal Relief Model (CRM) database. Wake losses were calculated for each layout configuration using the deep array eddy viscosity wake model in AWS Truepower's Openwind Enterprise. All other loss assumptions were manually entered into Openwind and applied to the calculation of net energy production. Using these inputs, the Openwind model was applied to investigate four wind power plant layouts with key criteria being energy capture, ocean depth, and export cable length.

NREL's O&M analysis compared two 500 MW wind plant scenarios: 1) A baseline offshore wind power plant consisting of 100 baseline NREL offshore 5-MW wind turbines, each rated at 5 MW and, 2) A hurricane-resilient offshore wind power plant comprised of 50 hurricane resilient 10 MW turbines developed in the current study. Both the baseline and hurricane-resilient offshore wind power plant scenarios are located in the Western Gulf of Mexico, approximately 60 km southeast of Corpus Christi, Texas. This region of the United States is prone to hurricane activity that can limit access to a wind turbine for maintenance activities. The prevention of access to a turbine for repair not only increases the downtime of the turbine but ultimately increases the levelized cost of energy (LCOE). The O&M analysis for the baseline and hurricane resilient offshore wind power plants was intended to quantify the O&M cost, wind power plant availability, and energy production for a wind power plant located in the Gulf of Mexico.

The NREL LCOE analysis showed how hurricane-resilient technology innovations reduced the LCOE for the notional 500-MW offshore wind power plant adopted for this study relative to baseline LCOE assumptions for the same size plant. The analysis of both the baseline and proposed hurricane-resilient configurations were customized to projects located in the Gulf of Mexico. This analysis characterized impacts to LCOE in response to perturbations to annual energy capture, turbine capital cost, balance-of-station costs, annual operating expenses, and operational service life. Overall, the NREL LCOE analysis predicted a 21.5% reduction in LCOE for the proposed hurricane-resilient turbine and plant technology concept.

Overall, it should be noted that the current concept design study achieved robust performance levels for the hurricane resilient components, turbine, and wind plant, and that these performance levels supported significant LCOE reductions. Nonetheless, it should be emphasized that this study relied substantially on up-scaling current technologies rather than undertaking *de novo* engineering designs. In addition, while major components were optimized themselves, the current study did not carry out iterative system level optimization of the turbine or wind plant.

Extrapolating from these considerations, it is reasonable to surmise that clean-sheet engineering approaches and well integrated full system optimizations could deliver even better performance and culminate in greater LCOE reductions.

This conceptual study shows that challenges posed by hurricanes to wind turbine survivability, operability, and cost effectiveness in the U.S. offshore environment can be successfully addressed using innovative research and development strategies. Though hurricane occurrence is possible or probable throughout most U.S. coastal regions, this need not be an insurmountable barrier to cost-effective offshore wind energy deployment and operation in these regions. Finally, promising results achieved in the current study should be extended using more detailed analysis approaches, to arrive at optimized turbine and plant designs, and to refine projections of LCOE impacts.

Table of Contents

List of Figures

List of Tables

1 Introduction

Hurricanes occur over much of the U.S. Atlantic and Gulf coasts, from Long Island to the U.S.-Mexico border, encompassing much of the nation's primary offshore wind resource. Category 5 hurricanes have made landfall as far north as North Carolina, with Category 3 hurricanes reaching New York with some frequency. At present, offshore wind turbine designs generally do not consider the severe operating conditions imposed by hurricanes. Although universally applied to most turbine designs, International Electrotechnical Commission (IEC) standards do not sufficiently address the duration, directionality, magnitude, or character of hurricanes.

To help address these shortfalls, this report documents a concept design study of a 500-megawatt (MW) wind power plant consisting of 10-MW wind turbines deployed in 25-meter (m) water depths in the Western Gulf of Mexico. This location was selected because hurricane frequency and severity provided a unique set of design challenges that would enable assessment of hurricane risk and projection of cost of energy (COE) reductions in response to specific DOE objectives. Notably, the concept study pursued a holistic approach that incorporated multiple advanced system elements at the wind turbine and wind power plant levels to meet objectives for system performance and reduced COE. Principal turbine system elements included a 10-MW rotor with structurally efficient low-solidity blades, a lightweight permanent-magnet direct-drive generator, and an innovative fixed substructure. At the wind power plant level, turbines were arrayed in a large-scale wind power plant in a manner aimed at balancing energy production against capital, installation, and operation and maintenance (O&M) costs to achieve significant overall reductions in COE (National Renewable Energy Laboratory (NREL) 2012).

To establish a reference datum for LCOE analyses and related assessments, a well known and broadly used baseline turbine, for which configuration and operating data were freely available, was adopted for this effort. It was intended to be representative of current state of the art for offshore wind turbine technology, and consisted of a utility-scale 5-MW turbine known as the NREL offshore 5-MW wind turbine. This turbine has been used extensively worldwide as the basis for offshore wind turbine analyses (Jonkman 2009). Baseline turbine configuration consisted of a conventional, three-bladed, upwind, variable-speed, variable blade-pitch-to-feather-controlled rotor designed against IEC Class 1A criteria. It employed a modular gear-driven system with full power conversion. Overall, the turbine was a hybrid concept based on published design documents from the REpower 5M turbine, the Wind Partnerships for Advanced Component Technology (WindPACT), RECommendations for OFFshore wind turbines (RECOFF), and the Dutch Offshore Wind Energy Convertor (DOWEC) projects. Baseline turbine rotor diameter was 126 m that was mounted on top of a traditional 90-m steel tubular tower that interfaced with a classic monopile substructure.

To successfully complete this challenging, multi-faceted concept design, partners were recruited from across the international wind energy research and development community to carry out various constituent component designs and studies. These partners, their respective roles, and the chapter in which their work is documented are listed in Table 1-1. All of these designs and studies are documented in the current report with partner contributions and corresponding report sections organized in the manner summarized below.

Table 1-1. Summary of Concept Study Partners and Roles

Partner	Role	Chapter
Wetzel Engineering	Advanced Blade and Rotor Design	2
Siemens Windpower	Hub, Nacelle, and Generator Scaling	3
NREL's National Wind Technology Center	Tower Conceptual Design	4
Keystone Engineering	Substructure and Foundation Concept Design	5
NREL's National Wind Technology Center	Turbine System Maximum Loads Prediction	6
NREL's National Wind Technology Center	Wind Plant Layout Analysis	7
NREL's National Wind Technology Center	Operation and Maintenance (O&M) Analysis	8
NREL's National Wind Technology Center	LCOE Analysis and Projection	9

The blade and rotor conceptual design for the 10-MW wind turbine was carried out by Wetzel Engineering and involved various advanced design concepts. These included definition of hurricane inflow conditions and design constraints, coupled aerostructural performance and loads optimization, blade aerodynamic design data compilation and blade planform design, and preliminary blade structural design. Design of the hub, nacelle, and generator was completed by Siemens Windpower based on their 3.0-MW and 6.0-MW direct-drive platforms. From this baseline, three 10-MW design concepts were extrapolated, corresponding to three blade lengths, rated rotational speeds, and rated torques. A tower design concept was produced by NREL, which included creation of a FAST model to generate the complete mass matrix at the tower top and an optimization algorithm to minimize the tower mass given suitable design constraints.

Conceptual design of the substructure and foundation was completed by Keystone Engineering Inc., including relevant standards that governed the design. This design incorporated their inward battered guide structure (IBGS) and compared it with a conventional four-piled jacket. Maximum loads encountered by the integrated turbine system during a hurricane event were modeled by NREL using a fully coupled aero-hydro-elastic model of the wind turbine, tower, and jacket substructure. For integrated system modeling, only parked rotor conditions were considered because blade and rotor design optimization showed these produced higher loads than operating conditions and because it was assumed the turbine would be shut down during hurricane conditions.

For wind power plant level studies, a surrogate site was selected in the Southwest Gulf of Mexico, approximately 60 kilometers (km) southeast of Corpus Christi, Texas. This site was chosen for its advantageous combination of high wind speeds, water depths less than 25 m, and minimum export cable length. Using this surrogate site, NREL conducted a wind power plant

layout analysis with key model inputs, including wind resource and bathymetry data, and model outputs encompassing plant array wind speeds, wake losses, and energy production. For the same surrogate site, an NREL O&M analysis compared a baseline scenario of 100 5-MW turbines and a hurricane-resilient scenario of 50 10-MW turbines. This analysis quantified O&M costs, taking into account wind resource and weather, as well as wind power plant availability and energy production. Finally, NREL carried out a levelized cost of energy (LCOE) analysis for the same surrogate site that compared the proposed hurricane-resilient turbine design and wind power plant scenario against a baseline turbine and scenario. The LCOE analysis considered perturbations to annual energy capture, turbine capital cost, balance-of-station costs, annual operating expenses, and operational service life, and projected a 21.5% reduction in LCOE for the hurricane-resilient turbine and plant concept, relative to the reference baselines adopted for the current study.

The following sections demonstrate that this concept design study achieved robust performance levels for the hurricane resilient components, turbine, and wind plant, and that these performance levels supported significant LCOE reductions. Nonetheless, it should be emphasized that this study relied substantially on up-scaling current technologies rather than undertaking *de novo* engineering designs. In addition, while major components were optimized themselves, the current study did not carry out iterative system level optimization of the turbine or wind plant. Extrapolating from these considerations, it is reasonable to surmise that clean-sheet engineering approaches and well integrated full system optimizations could deliver even better performance and culminate in greater LCOE reductions.

2 Advanced Blade and Rotor Design

This section presents details of the rotor design for the *Hurricane-Resilient Wind Power Plant Concept Design Study*—advanced blade and rotor design project funded by the U.S. Department of Energy (DOE) through NREL.

2.1 Definition of Hurricane Inflow Conditions and Design Constraints

To perform the blade and rotor optimization analysis, it was necessary to define the design constraints for the aerostructural optimization analysis. As part of this task, all design constraints to be used for the optimization analysis were determined. These are summarized in Table 2-1.

Table 2-1. Summary of Blade and Rotor Design Space

Property	Value
Design wind class	Custom-defined
Turbulence intensity (TI)	14.6%
Blade spar cap/girder material	Carbon Spar Cap
Maximum tip speed	85 m/s[a], 95 m/s, and 105 m/s
Rated power	10 MW
Precone angle (equilibrium position)	0°, 4°
Blade air tip gap	23 m
Blade length	90 m, 95 m, 100 m, and 105 m
Shaft uptilt angle	4.5°
Root outer diameter	5.95 m
Overall system efficiency	90%
Cut-in and cut-out wind speed	3.5 m/s and 25 m/s

[a]meters per second

Given the unique nature of this project, apart from the design constraints provided in Table 2-1, four other design constraints were defined. These are:

- Definition of mean and extreme wind speeds
- Definition of blade air tip gap
- Safety factors for loads calculations
- Definition of TI.

The details of the methodology used for defining these parameters are provided below.

2.1.1 Definition of Mean and Extreme Wind Speeds

To determine the mean and extreme wind speeds, data, and methods from the American Bureau of Shipping (ABS) document and American Petroleum Institute (API) document were extracted and used (American Bureau of Shipping 2013, American Petroleum Institute 2010). The ABS document combines established ABS methods of engineering off-shore platforms with the IEC methods of loads analysis. Based on the data and methods provided in the ABS report, the following procedures were adopted:

- Fixed the mean and extreme wind speeds at a reference height above the water level for the purposes of analysis and allowed the mean and extreme wind speeds at hub height to vary as per a prescribed gradient model. It was understood that the hub-height wind speed would not necessarily be consistent with one of the IEC Standard Wind Classes.
    - The exponent is provided in the ABS document sections 3-2/9 as 0.14 for the Normal Wind Profile and for the Normal Turbulence Model. This is consistent with Germanischer Lloyd's (GL's) 2012 Guidelines (2010) for offshore wind turbines and the IEC 61400-3 (International Electrotechnical Commission 2009).
    - The exponent is provided in the ABS document sections 3-2/11 as 0.11 for Extreme Wind Model. This is consistent with GL's 2012 Guidelines for offshore wind turbines (2010) and the IEC 61400-3 (International Electrotechnical Commission 2009).
- For the extreme wind speeds at 10-m height, the data from the API guideline (Figure C.10 and Table C.22 in the API document) that is based on the 50-year -recurrence-period hurricane was used (American Petroleum Institute 2010).
- D. Elliot of NREL extracted 90 m annual wind resource data for the concept study wind plant, sited at 27.25° N X 97.12° W. Average annual wind speed was 8.71 m/s at 90 m and 8.16 m/s at 50 m, with shear exponent $\alpha = 0.11$. These data were extracted from a database produced by AWS Truepower using their MesoMap system and historical weather data. Extrapolating from these data to a hub height of 135 m, gave a mean wind speed of 9 m/s, using $\alpha = 0.11$ for shear. These values were used in final optimization.
- Average wind speed at 90-m height of 8.5 m/s, was extrapolated to hub height using a power law relationship with an exponent of 0.14. As a reference, this became 9.0 m/s average at 135-m hub height.
- Normal extreme winds per the 50-year recurrence API Western Gulf of Mexico model (American Petroleum Institute 2010) (Figure C.10 and Table C.22 in the API document), with 3-second (s) gust wind speed at 10 m height of 52.9 m/s and a 10-minute (min) mean of 40.6 m/s, were extrapolated to hub height using a power law with $\alpha = 0.11$. As a reference, this yielded 70 m/s, 3-s wind at 135-m height, and a 54 m/s 10-min mean. This was substantially higher than the IEC-prescribed 50-year extreme, which, for a 9-m/s mean hub height would translate into a 45-m/s, 10-min mean, 50-year recurrence and a 63 m/s, 3-s gust. These conditions were comparable with IEC Class I extreme conditions.

- Abnormal extreme winds per the 100-year recurrence API western Gulf model (American Petroleum Institute 2010) (Figure C.10 and Table C.22 in the API document), with 3-s gust wind speed at 10-m height of 60.2 m/s and a 10-min mean of 45.6 m/s, were extrapolated to hub height using a power law with an exponent of 0.11. As a reference, this became an 80 m/s, 3-s wind at 135-m height and a 60.6 m/s, 10-min mean. Again, these were much higher than the IEC Class I conditions, but with a lower safety factor.

2.1.2 Definition of Blade Tip Air Gap

Analysis performed by NREL resulted in a blade tip air gap dimension of 23.2 m as shown in Figure 2-1. At 6 o'clock, the tip of the blade is 23.2 m above the mean sea level (MSL). In the current optimization study, blade tip air gap was held constant at 23.2 m whereas rotor diameter and hub height were varied consistent with each other. For example, a 224-m diameter rotor would result in a hub height of 135 m. We used this setting for the optimization studies to determine power performance and energy capture assuming a power law relationship with an exponent of 0.14 measured from the MSL.

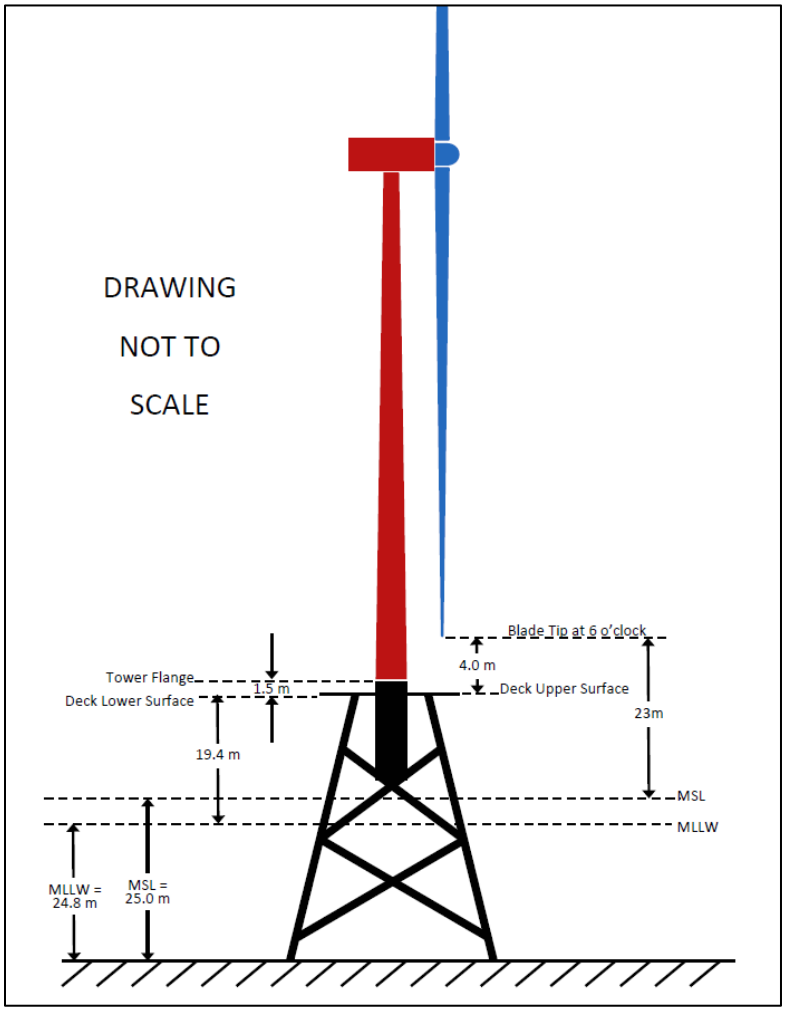

Figure 2-1. Blade tip air gap definition

2.1.3 Safety Factors

The safety factors are consistent with GL/IEC guidelines for wind turbine design and operation. A safety factor of 1.35 was used for normal extreme winds, and a safety factor of 1.10 was used for abnormal extreme winds.

Table 2-2 summarizes wind conditions for the rotor design, whereas Table 2-3 summarizes reduction factors for combining independent extremes into load cases for shallow water depth (American Petroleum Institute 2010).

Table 2-2. Extreme Operating Wind and Wave Conditions for Rotor Design

Parameter	Value
V_extreme at 10-m height (3-s gust, –50-year (yr) recurrence)	52.9 m/s
V_extreme at hub-height (3-s gust, 50-yr recurrence)	70 m/s
Safety factor for 50-yr recurrence	1.35
V_extreme at 10-m height (3-s gust, 100-yr recurrence)	60.2 m/s
V_extreme at hub-height (3-s gust, 100-yr recurrence)	80 m/s
Safety factor for 100-yr recurrence	1.1

Table 2-3. Factors for Combining Independent Extremes into Load Cases for Shallow Water Depth (American Petroleum Institute 2010, Table C.25)

Load case	Return period (years)						
	10	25	50	100	200	1,000	2,000
Wind dominant							
Wind speed	1.00	1.00	1.00	1.00	1.00	1.00	1.00
Wave height	1.00	0.95	0.95	0.95	0.95	0.95	0.95
Uniform current	0.80	0.80	0.80	0.80	0.80	0.80	0.80
Wind direction from wave (deg)	–15	–15	–15	–15	–15	–15	–15
Wave dominant							
Wind speed	1.00	0.95	0.95	0.95	0.95	0.95	0.95
Wave height	1.00	1.00	1.00	1.00	1.00	1.00	1.00
Uniform current	0.80	0.80	0.80	0.80	0.80	0.80	0.80
Wind direction from wave (deg)	–15	–15	–15	–15	–15	–15	–15
Current dominant							
Wind speed	0.80	0.75	0.75	0.75	0.75	0.75	0.75
Wave height	0.80	0.75	0.75	0.75	0.75	0.75	0.75
Uniform current	1.00	1.00	1.00	1.00	1.00	1.00	1.00
Wind direction from wave (deg)	0	0	0	0	0	0	0

2.1.4 Determination of TI

A study was carried out using NREL's TurbSim software (Jonkman 2009) to determine a correlation between the 3-s gust and 10-min average for 50- and 100-year extreme wind profiles as provided in API guidelines (American Petroleum Institute 2010). The adopted approach used the 10-min mean wind speed from API as an input reference wind speed in TurbSim. Different values for TI were used to determine the peak value for the wind velocity corresponding to the 3-s gust. Six seeds for wind speeds were used for the analysis. Two models were used (i.e., Normal Turbulence Model (NTM) and Extreme Turbulence Model (ETM)) to predict the TI required to match the 3-s gust from the API standard. Seventy-two cases were run with different TI values and 3-s and 1-min mean values were recorded and reported. For each of the 72 cases, six seeds were used. Results for the TI study are provided in Table 2-4 and Table 2-5.

Table 2-4. 3-s and 1-min Mean Calculation for TI = 14.6%, 50-Year Recurrence at 10-m Height

Seed Number	3-s Mean	1min Mean	API Predicted Value
1	51.04	43.32	52.9 m/s for 3-s gust 45.9 m/s for 1-min gust
2	53.60	44.03	
3	51.64	43.93	
4	52.30	43.68	
5	51.75	43.81	
6	52.15	43.75	

Table 2-5. 3-s and 1-min Mean Calculation for TI = 15%, 100-Year Recurrence at 10-m Height

Seed Number	3-s Mean	1-min Mean	API Predicted Value
1	57.61	48.61	60.2 m/s for 3-s gust 52.0 m/s for 1-min gust
2	60.34	49.40	
3	58.02	49.29	
4	58.98	49.03	
5	58.44	49.13	
6	58.79	49.08	

Based on these results and existing data being used by Wetzel Engineering Inc. (WEI) for other 10-MW blade designs, the recommended value of 14.6% TI was used for the 50-year recurrence period and 15% for the 100-year recurrence period. Note that the 1-min mean values did not match those predicted by API guidelines (American Petroleum Institute 2010).

2.1.5 Assumptions for Optimization Analysis

The effects of coning and prebend on the performance of different configurations for the 10-MW machine are considered. Two conditions were evaluated as part of this study—no precone and 4° precone.

The influence of tower wake noise was not considered as part of this optimization.

2.2 AeroStructural Optimization

Wetzel Engineering performed a design optimization analysis to determine the optimal blade configuration for the 10-MW rotor. The conceptual design optimization provided the results to understand the tradeoffs between different design parameters such as maximum blade root bending moment, blade mass, blade cost, annual energy production (AEP), and COE. These optimization analyses were based on the design requirements specified above.

2.2.1 Optimization Setup and Techniques

The following steps were performed as part of the optimization analysis:

- Final design requirements and the optimization parameter space were established based on the design requirements for operation of the 10-MW turbine.(Table 2-1)
- Table 2-1 summarizes inputs used for optimization analysis for the 10-MW rotor blade.
- The WEI flatback (WEI-FB), Delft University (DU), and NACA airfoil families were used for this optimization. Tables 2-6 and 2-7 show details of airfoil characteristics and geometric input variables for the optimization. WEI-FB airfoils were used at maximum chord station. For the outboard region of the blade, DU and NACA airfoils were used.

Table 2-6. Nominal Airfoil and Airfoil Designation

Airfoil Designation	Airfoil Thickness-to-Chord Ratio
WEI-FB-64	64.00%
WEI-FB-47	47.29%
DU-W-405LM	40.50%
DU99-350	35.09%
DU97-W-300LM	30.00%
DU91-W2-250LM	25.00%
NACA63621	21.00%

Table 2-7. Design Variables for 10-MW Rotor Blade Optimization Study

Design Variable	Choice of Selection	Comments
Airfoil family	WEI-FB, DU and NACA family	Airfoil family consisted of WEI-FB47, DU40, DU35, DU30, DU25, and NACA 63621 airfoils.
Thickness distributions	No. of thickness distributions = 6	6 distributions are defined to cover the entire design space, to yield both high aero performance and structurally efficiency. Extremely slender, high-aero efficiency blades are not considered because these blades result in unreasonable blade mass configurations which, in turn, do not yield an economical solution.
Chord distributions	Max chord variation: From 6.0 to 8.0 m	A spanwise distribution based on max chord variation was defined to obtain different blade planforms.
Materials	Carbon/carbon-glass hybrid	-

To study and evaluate various designs, it is essential to determine a design space that is based on constraints determined by WEI. These constraints are summarized in Table 2-1. To understand the contribution from several parameters defined in the design space, it is essential to develop and study the various trend lines obtained from different configurations. WEI-BladeOpt is used to generate and plot these trend lines or cloud plots. WEI-BladeOpt is a tool that allows a blade designer to select a design space as a preliminary estimate for the design of a wind turbine blade. The overall goal of the WEI-BladeOpt is to optimize the blade design taking into account the aerostructural properties and cost of the entire system. WEI-BladeOpt consists of the following modules that are used to define the optimal blade design (Figure 2-2):

- Aerodynamics module
- Structural module
- Loads module
- Cost module.

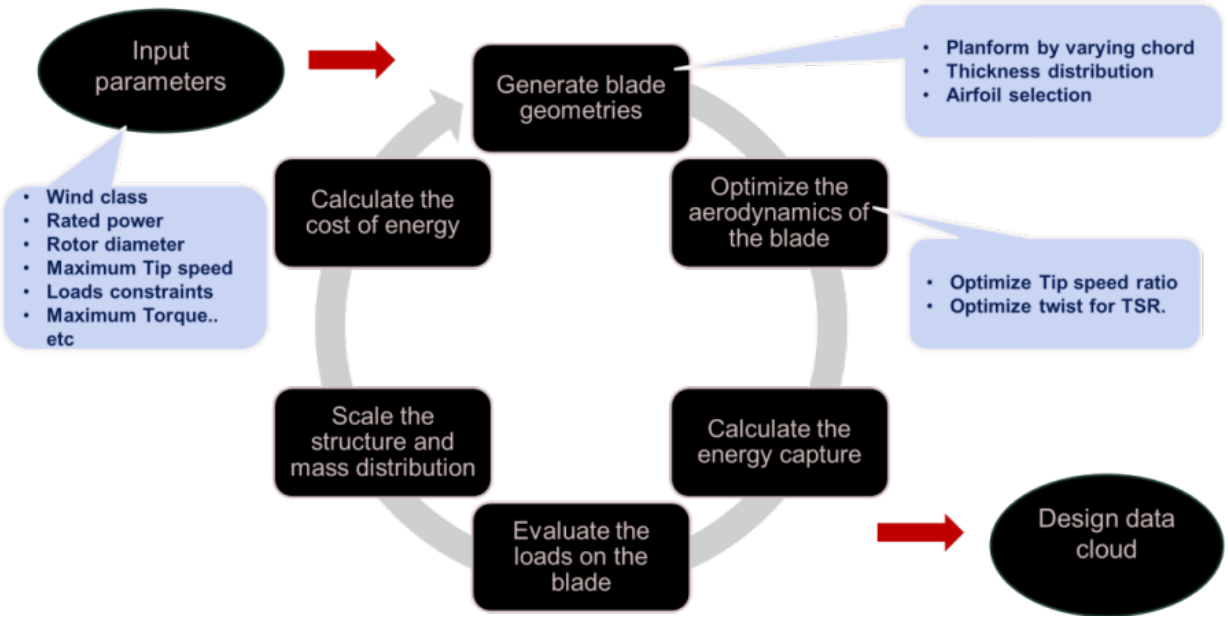

Figure 2-2. Schematic of WEI-BladeOpt

Once the cloud plots were generated, the chosen design space was evaluated based on four criteria:

- COE
- Maximum root bending moment loads
- AEP
- Aerodynamic coefficient of performance

Representative trend lines are shown in Figure 2-3. Based on these four criteria, a suitable blade design space was selected. Next, a refined stage of optimization was carried out for a restricted design space. Sample representative optimal planforms were then defined and the blade layout was initiated by fine-tuning the chosen optimal planforms in order to define a smooth profile for thickness and chord distributions. For advanced concepts such as torsion bend coupling (TBC), a structural optimization was undertaken, after the optimal planform had been defined, to determine the optimal internal structure for the blade.

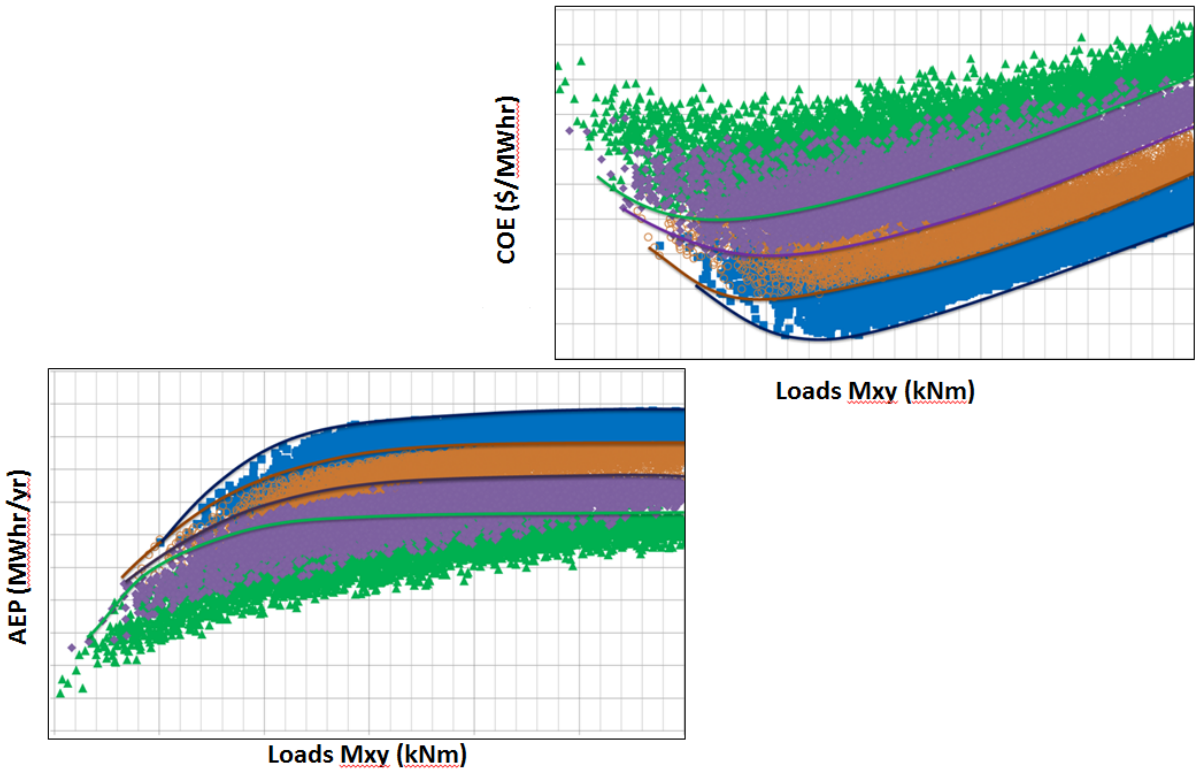

Figure 2-3. Representative cloud plots from WEI-BladeOpt

2.2.2 Aerodynamics Module

The aerodynamics module is based on the blade-element-momentum theory. However, to generate a cloud plot, several combinations of input parameters were defined. These input parameters include thickness, twist chord distributions, choice of airfoil families, blade length, and material definitions. Geometric parameters were defined at five radial stations that were interpolated to 27 nodes along the blade for aerodynamic performance and loads calculations.

2.2.3 Structural Module

Structures module defines the internal structure of the blade. The design philosophy is to use appropriate scaling laws to create a structural definition for each blade generated during the optimization process. Scaling laws are applied to a baseline blade. The choice of baseline blade is critical to the accuracy of the results. The scaling laws used for this model were developed from in-house expertise based on the structural design carried out for several blades. Some of the

design laws are listed in Table 2-8. At present, the final structure for a chosen optimal blade is not output as a part of the optimization routine. For example, for a given optimal blade that incorporates sweep or prebend, the amount of curvature required to achieve the loads constraint or to achieve the tower clearance constraint, respectively, is not explicitly defined as a part of the optimization routine. Once a particular planform is chosen, the internal structure will be optimized so the amount of curvature, material layout, laminate definitions, and similar quantities will be defined.

Table 2-8. Scaling Laws for the Structural Module

Parameter	Scaling Factor
Girder thickness	*f* (moment, blade thickness, blade length)
Girder width	*f* (baseline girder width)
Shell skin	*f* (moment, blade thickness, girder thickness)
Shell core	*f* (baseline shell core thickness)
Web skin	*f* (baseline web skin thickness)
Web height	*f* (baseline web height, blade thickness)
Web core	*f* (baseline web core thickness)
Root reinforcement thickness	*f* (baseline root reinforcement thickness, sectional arc length)

Despite not having accounted for the above-mentioned secondary details, the current approach provides a reasonable estimate for the optimal blade design that meets given design constraints.

2.2.4 Loads Module

The aerodynamic loads are calculated using BEM. The resultant moment is calculated as the vector sum of aerodynamic moments and inertial loads. The extreme loads are calculated based on several design load cases (DLCs). These DLCs include DLC 1.1 – NTM, DLC 1.3 – ECD, DLC 1.6 – EOG, DLC 1.7 – EWS, DLC 6.1 and 6.2 – EWM parked case. Example DLCs include ECD, EOG 1 year, EOG 50 years. Apart from the operating loads, the parked loads are calculated as well. The highest obtained loads are reported as the maximum loads for the particular blade design. Note that a safety factor, as described previously, is used during the loads calculation.

2.2.5 Cost Module

The cost module determines the COE based on the entire system cost. The cost of the system includes the blade, tower, and turbine costs. The blade cost is calculated based on the material and labor cost of a particular blade. A mass estimation tool is used to determine the mass of each component that then translates into the material cost and, hence, the total cost of the blade. The turbine cost is the sum of all component costs. The cost of each component is either fixed or

scales as a function of loads, power, or other turbine parameters. The cost module also accounts for the facilities costs and costs incurred toward blade tooling. Based on these costs, the COE is calculated. Inputs for the cost model are based on discussions in Raina (2013 and 2014).

2.2.6 Results of Optimization Analysis

Table 2-9 presents the results for the rotor optimization. The lowest cost of energy resulted from the configuration having a maximum tip speed of 85 m/s and a blade length of 105 m. The chosen configuration resulted from the highest solidity blade for the given rotor size. Increased tip speed led to more slender configurations that had, in turn, a lesser structural efficiency and increased COE compared to the chosen configuration. The impact of precone for loads alleviation leading to COE reduction was not prominent; a final configuration without pre-cone is recommended.

Table 2-9. Rotor Optimization Results (includes TBC corrections)

Precone 4 deg
V_tip 85 m/s

Blade Length in m		90	95	100	105
Mxy	[kNm]	56827	65667	74065	75452
AEP	[MWhr/yr]	43860	45461	47530	49185
COE (min)	[$/MWhr]	130.5	128.0	125.5	123.2

Precone 0 deg
V_tip 85 m/s

Blade Length in m		90	95	100	105
Mxy	[kNm]	59153	65722	75689	75244
AEP	[MWhr/yr]	44382	46268	48156	49480
COE (min)	[$/MWhr]	129.6	126.4	123.8	121.6

Precone 4 deg
V_tip 95 m/s

Blade Length in m		90	95	100	105
Mxy	[kNm]	57849	65965	74709	75577
AEP	[MWhr/yr]	43997	45762	47612	49113
COE (min)	[$/MWhr]	130.8	128.6	126.1	123.8

Precone 0 deg
V_tip 95 m/s

Blade Length in m		90	95	100	105
Mxy	[kNm]	59395	65794	75411	76433
AEP	[MWhr/yr]	44409	46355	48195	49682
COE (min)	[$/MWhr]	129.6	127.0	124.4	122.2

Precone 4 deg
V_tip 105 m/s

Blade Length in m		90	95	100	105
Mxy	[kNm]	58138	67980	75308	76251
AEP	[MWhr/yr]	43923	45792	47733	49166
COE (min)	[$/MWhr]	132.1	129.6	128.5	124.8

Precone 0 deg
V_tip 105 m/s

Blade Length in m		90	95	100	105
Mxy	[kNm]	59870	67605	76729	77427
AEP	[MWhr/yr]	44459	46346	48142	49634
COE (min)	[$/MWhr]	130.5	128.2	125.4	123.9

It should be noted that these results assume loads alleviation due to TBC, which is incorporated into the optimization analysis via loads alleviation scaling models developed by Wetzel Engineering based on field test data. Because there are no readily available dynamic simulation tools that can model a torsionally active structure, the use of TBC material in this blade design is no longer considered. However, finite-element analysis could be used to model the blade response resulting from TBC but, given the scope and budget for this project, it was decided not to carry out such detailed analysis at this time. This design change will impact the loads and, hence, the COE. The final COE will be provided in the cost of energy document (Raina 2014).The final configuration for aerodynamic design and layout resulted in a 105-m blade (i.e., 218-m rotor diameter). This blade has no precone and operates with a max tip speed of 85 m/s.

2.3 Blade Aerodynamic Design Summary and Planform Design

This task consists of the aerodynamic design of the 105-m blade. Based on recommendations

obtained from the aerostructural optimization analysis, a blade length of 105 m was chosen. This blade originally was designed to incorporate TBC, so as to obtain an additional 8%–10% reduction in operating blade loads. Because a TBC blade twists under load, the twist must be adjusted (induced twist) to ensure that, under load, the blade geometry returns to something close to the twist distribution for optimal aerodynamic performance. The effect on aerodynamic performance due to this induced twist correction, resulting from a TBC configuration, is negligible. However, available resources for loads calculation (i.e., the NREL FAST program) cannot capture the TBC effect accurately. Furthermore, the driving loads for this case came from DLC 6.2 Parked Loads Case, consistent with anticipated turbine state during hurricane conditions. The resulting reduction from TBC would be significant for the operating conditions, but a significant reduction would not be obtained in the parked case. Therefore, for this reason and in the interest of the project schedule, it was decided to develop a non-TBC blade design, which is presented in this section. The loads presented in Table 2-9 will increase by 8% – 10% for a non-TBC configuration. Table 2-10 summarizes the aerodynamic characteristics of the WEI105.0-10.0M-A 105-m blade, and blade geometry is documented in Figure 2-4.

Table 2-10. Summary of the Aerodynamic Design of the WEI105.0-10.0M-A 105.0-m Blade

Radial Station		Spanwise Station	Chord	Solidity	Original Optimized Twist (TBC effect not included)	Sectional thickness	Thickness-to-Chord Ratio	Airfoil
r	r/R	$s = r - r_{hub}$	c	σ	θ	t	t/c	**Used for Aerodynamic Modelling Purposes
(m)		(m)	(m)		(°)	(m)		
4.000	3.67%	0.000	5.950	0.710	0.00	5.950	100.00%	Cylinder
5.000	4.59%	1.000	5.950	0.568	0.00	5.950	100.00%	Cylinder
6.000	5.50%	2.000	5.950	0.473	0.00	5.950	100.00%	Cylinder
8.720	8.00%	4.720	5.950	0.326	0.00	5.950	100.00%	Cylinder
11.990	11.00%	7.990	6.050	0.241	0.00	5.717	94.50%	Cylinder
16.350	15.00%	12.350	6.380	0.186	10.00	5.008	78.50%	Cylinder-WEI-FB64
21.800	20.00%	17.800	6.900	0.151	9.75	4.139	59.99%	WEI-FB64-WEI-FB47
27.250	25.00%	23.250	7.000	0.123	9.05	3.297	47.10%	WEI-FB47
32.700	30.00%	28.700	6.213	0.091	6.94	2.609	42.00%	WEI-FB47-DU-W-405LM
38.150	35.00%	34.150	5.112	0.064	4.58	2.070	40.50%	DU-W-405LM
43.600	40.00%	39.600	4.356	0.048	3.08	1.668	38.30%	DU-W-405LM-DU99-350
49.050	45.00%	45.050	3.900	0.038	2.03	1.365	35.00%	DU99-350
54.500	50.00%	50.500	3.584	0.031	1.26	1.154	32.20%	DU99-350-DU97-W-300LM
59.950	55.00%	55.950	3.310	0.026	0.70	0.986	29.80%	DU97-W-300LM
65.400	60.00%	61.400	3.045	0.022	0.35	0.837	27.50%	DU97-W-300LM-DU91-W2-250LM
70.850	65.00%	66.850	2.788	0.019	0.18	0.711	25.50%	DU91-W2-250LM
76.300	70.00%	72.300	2.533	0.016	0.05	0.608	24.00%	DU91-W2-250LM-NACA63621
81.750	75.00%	77.750	2.270	0.013	-0.15	0.513	22.60%	DU91-W2-250LM-NACA63621
87.200	80.00%	83.200	2.020	0.011	-0.80	0.432	21.40%	NACA63621
92.650	85.00%	88.650	1.760	0.009	-1.86	0.370	21.00%	NACA63621
98.100	90.00%	94.100	1.507	0.007	-3.00	0.316	21.00%	NACA63621
100.280	92.00%	96.280	1.403	0.007	-3.30	0.295	21.00%	NACA63621
102.460	94.00%	98.460	1.294	0.006	-3.36	0.272	21.00%	NACA63621
104.640	96.00%	100.640	1.144	0.005	-3.20	0.240	21.00%	NACA63621
106.820	98.00%	102.820	0.844	0.004	-2.50	0.177	21.00%	NACA63621
108.150	99.22%	104.150	0.452	0.002	-1.00	0.095	21.00%	NACA63621
109.000	100.00%	105.000	0.100	0.000	0.50	0.021	21.00%	NACA63622

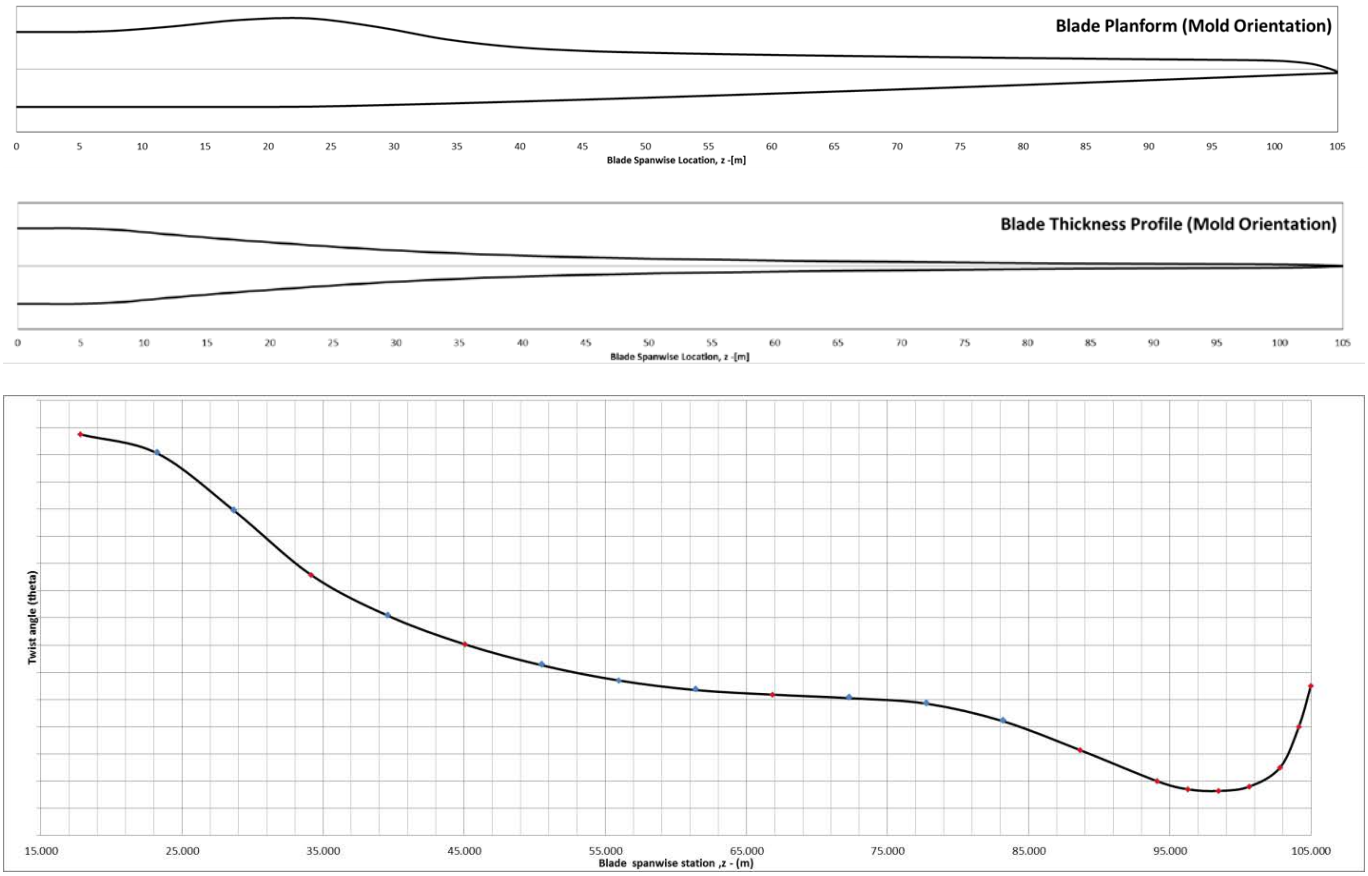

Figure 2-4. Planform definition for WEI105.0-10.0M-A blade

2.4 Rotor Performance Analysis Data Summary

The aerodynamic performance, based on steady inflow conditions, of the 105-m blade is provided in Table 2-11. Maximum aerodynamic power coefficient, C_{pmax} = 0.473, is achieved, whereas AEP based on IEC Class S Rayleigh distribution is AEP = 49,241 MWh.

Table 2-11. Performance for Prated = 10.0 MW (Assumes drivetrain efficiency of (peak 90%) and clean performance of airfoil sections and steady power)

ROTOR PERFORMANCE OUTPUT PARAMETERS								
Wind Speed	Shaft Speed	Tip Speed Ratio	Pitch Angle	Aero Power Coefficient	Aero Power	Electric Power	Aero Power	Electric Power
V (m/s)	Ω (rpm)	X (~)	β (°)	C_{paero} (~)	P_{aero} (kW)	P_{elec} (kW)	P_{aero} (MW)	P_{elec} (MW)
3.50	3.25	10.60	0.00	0.473	464	417	0.46	0.42
4.00	3.61	10.31	0.00	0.474	693	624	0.69	0.62
4.50	4.06	10.31	0.00	0.474	987	889	0.99	0.89
5.00	4.52	10.31	0.00	0.474	1354	1219	1.35	1.22
5.50	4.97	10.31	0.00	0.474	1803	1622	1.80	1.62
6.00	5.42	10.31	0.00	0.474	2340	2106	2.34	2.11
6.50	5.87	10.31	0.00	0.474	2975	2678	2.98	2.68
7.00	6.32	10.31	0.00	0.474	3716	3345	3.72	3.34
7.50	6.77	10.31	0.00	0.474	4571	4114	4.57	4.11
8.00	7.23	10.31	0.00	0.474	5547	4993	5.55	4.99
8.50	7.45	10.00	0.00	0.473	6635	5971	6.63	5.97
9.00	7.45	9.45	0.00	0.465	7746	6972	7.75	6.97
9.50	7.45	8.95	0.00	0.450	8826	7943	8.83	7.94
10.00	7.45	8.50	0.00	0.433	9908	8917	9.91	8.92
10.50	7.45	8.10	0.00	0.415	10981	9883	10.98	9.88
11.00	7.45	7.73	3.33	0.365	11109	9998	11.11	10.00
12.00	7.45	7.09	6.80	0.281	11111	10000	11.11	10.00
13.00	7.45	6.54	9.07	0.221	11111	10000	11.11	10.00
14.00	7.45	6.07	10.98	0.177	11111	10000	11.11	10.00
15.00	7.45	5.67	12.69	0.144	11111	10000	11.11	10.00
16.00	7.45	5.31	14.27	0.119	11111	10000	11.11	10.00
17.00	7.45	5.00	15.76	0.099	11111	10000	11.11	10.00
18.00	7.45	4.72	17.15	0.083	11111	10000	11.11	10.00
19.00	7.45	4.48	18.51	0.071	11111	10000	11.11	10.00
20.00	7.45	4.25	19.81	0.061	11111	10000	11.11	10.00
21.00	7.45	4.05	21.06	0.052	11111	10000	11.11	10.00
22.00	7.45	3.87	22.27	0.046	11111	10000	11.11	10.00
23.00	7.45	3.70	23.42	0.040	11111	10000	11.11	10.00
24.00	7.45	3.54	24.52	0.035	11111	10000	11.11	10.00
25.00	7.45	3.40	25.60	0.031	11111	10000	11.11	10.00

Figure 2-5 shows the tip-speed ratio and shaft-speed schedule for the WEI105.0-10.0M-A blade. Figure 2-6 shows the coefficient of performance distribution versus wind speed for this configuration.

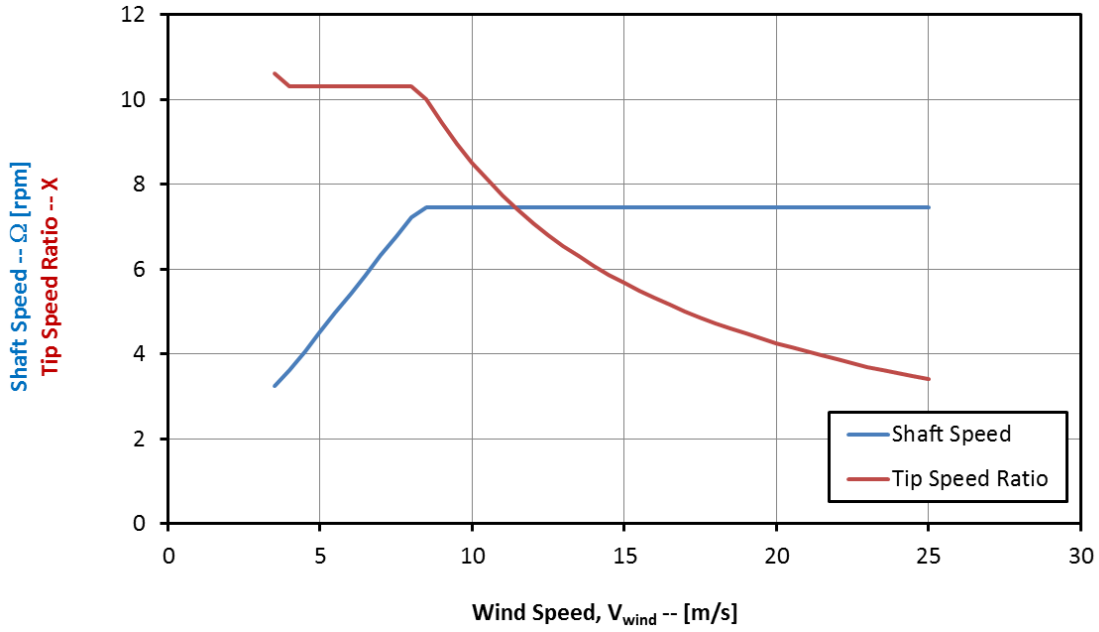

Figure 2-5. Shaft-speed schedule and tip-speed ratio for the WEI105.0-10.0M-A blade

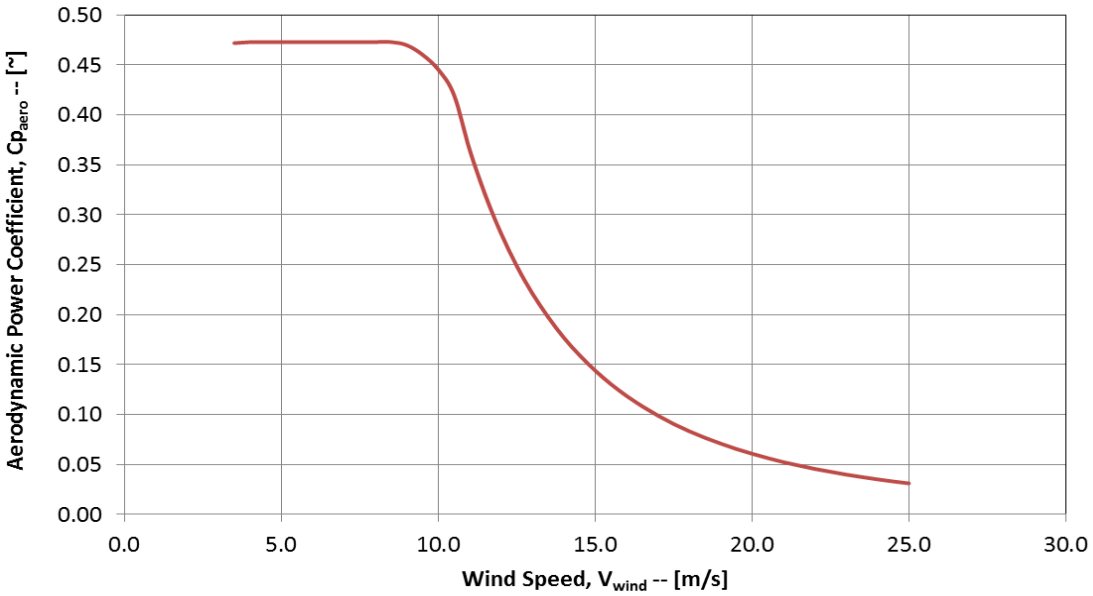

Figure 2-6. Aerodynamic power coefficient for WEI105.0-10.0M-A blade

Figure 2-7 and Figure 2-8 show the electric and aerodynamic power curves for the designed configurations.

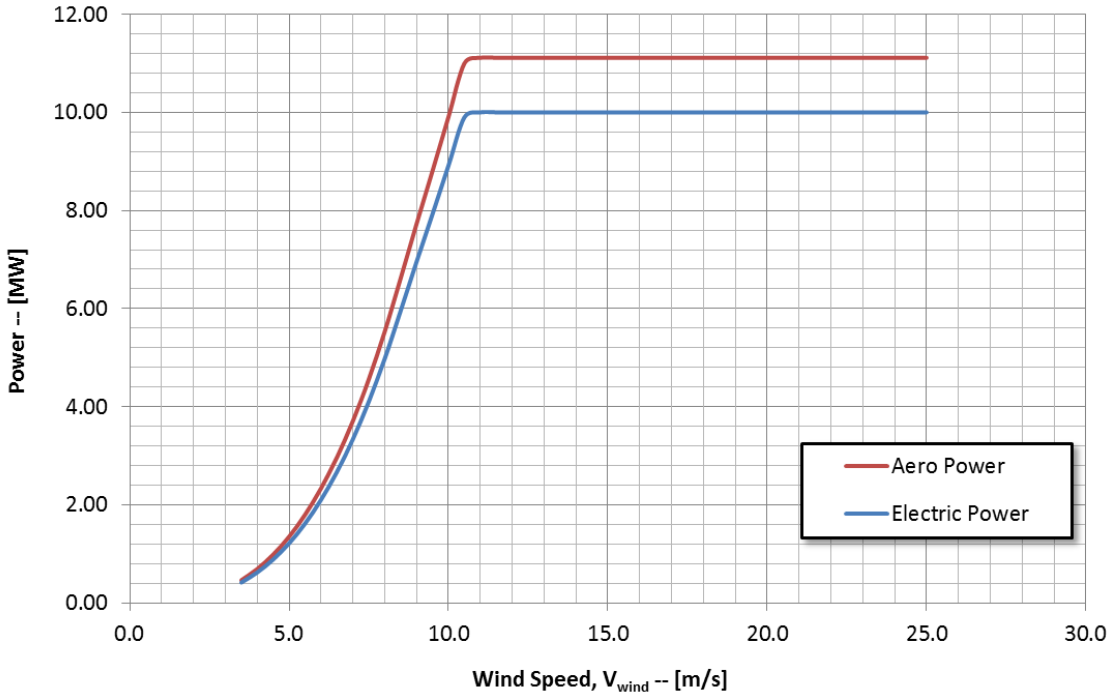

Figure 2-7. Power curves for the WEI105.0-10.0M-A blade

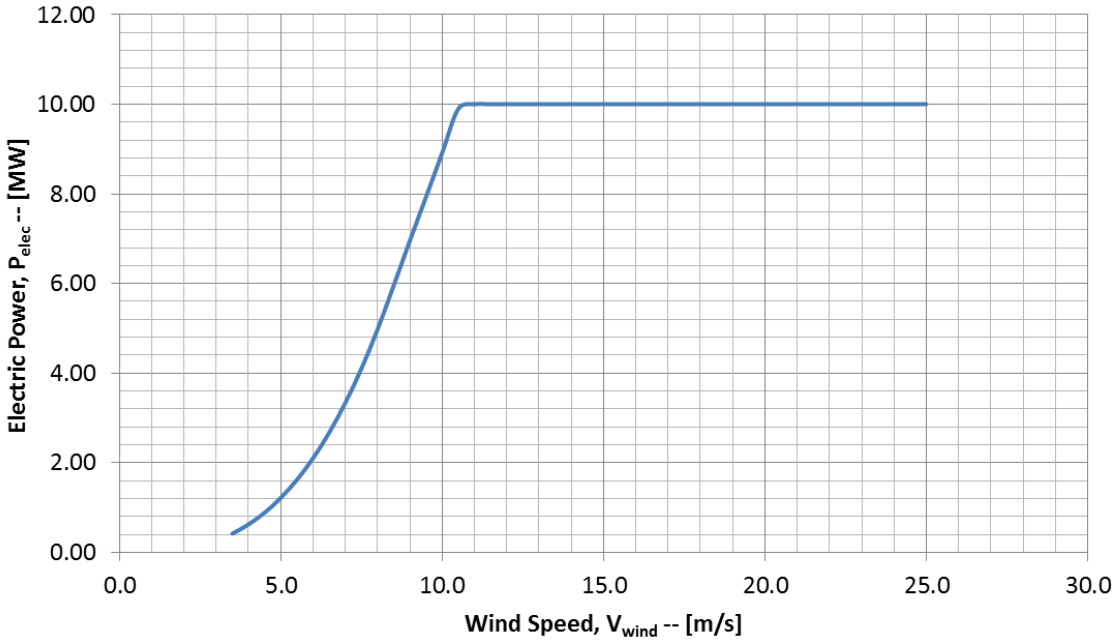

Figure 2-8. Electric power curve for the WEI105.0-10.0M-A blade

2.4.1 Airfoil Sections in Inboard Blade Region

For the inboard and transition region of the blade, custom airfoils developed by Wetzel Engineering were used. These airfoils were 64% and 47% thick flatback airfoil sections. Performance data for these airfoils is provided in a Wetzel Engineering report '98.01.03.002 Airfoil Data Generic Set' (Raina 2014). These airfoils have not been tested in a wind tunnel, and the performance characteristics of these airfoils were obtained from numerical simulations using computational fluid dynamics tools (ANSYS ICEM and FLUENT).

2.4.2 Airfoil Sections in Outboard Blade Region

The airfoil sections of the rotor blade were designed using commercially available airfoils with reliable aerodynamic lift and drag data. These airfoils are: DU-W-405LM, DU-99-350, DU97-W-300LM, DU91-W2-250LM, and NACA63621. These airfoils were tested in a wind tunnel and proved to deliver well-behaved aerodynamic characteristics for good overall rotor performance. An in-house aerodynamic-structural optimization code was used to determine a combination of chord lengths and selection of airfoil sections so as to optimize for maximum energy capture given the rotor design constraints. The aerodynamic lift and drag data for the airfoils used in the design of the blade (from the maximum chord location to the blade tip) are presented in Raina (2013).

2.4.3 Airfoil Data Interpolation

To define the airfoil data for loads-analysis input, we interpolated the airfoil data for the outboard sections using the pure airfoil sectional data. A simple weighted interpolation technique was used to perform this exercise, which simply calculates the performance of a given section based on interpolation of data from adjacent pure airfoil stations. For a section on the blade that contains a blend of two pure airfoils, we used a weighted average of the pure airfoil stations' properties to obtain those for the chosen section which lies in between the two pure airfoil stations. For example, 38.30% t/c airfoil consists of 66% of DU-W-405LM and 34% of DU99-350.

2.5 Preliminary Structural Design of the Advanced Rotor Concept

This section summarizes the analyses of the preliminary structural design of the WEI105.0-10M-A blade. The aerodynamic blade planform was designed by Wetzel Engineering and was the basis for preliminary structural design. This structural design, while performed with exceptional attention to detail and engineering judgment indicative of the standards of practice for the wind industry, is not representative of a certification-worthy blade. This report is intended to outline the general structural characteristics of the WEI105.0 m blade, including maximum blade deflection, first and second natural frequencies of vibration, and material exertion factors. Details of the blade internal structural layout can be found in Appendix A.

The aerodynamic and structural design of the blade is documented in Raina (2013) and in Lee (2014). An equivalent beam model consisting of finite-element models of multiple spanwise stations was built for this analysis. Wetzel Engineering used an in-house equivalent beam model tool during the preliminary design phase. The in-house blade sectional analysis tool was used to analyze the blade structure at multiple, distinct spanwise sections. Each section contour was

divided into regions (13 in the present study), and the laminate structure in each region was defined. The code meshed the cross-section of the laminated structure with nine-node, two-dimensional (2-D) elements. The output from the blade sectional model was 4-by-4 beam-equivalent stiffness and compliance matrices (including axial tension, edgewise bending, flapwise bending, and torsional degrees of freedom) and the 6-by-6 inertial matrix. These matrices can be used to construct an equivalent beam model of the blade suitable for dynamic simulations. If sectional loads are provided, the program will also calculate full strain fields on all elements and find the maximum strain values for all components for all materials. Wetzel Engineering found exceptional agreement between this model and the full finite-element analysis (FEA), generally within 1%–2% in strain estimation.

Material characteristics (Lee 2014) employed in the current analysis are summarized below. Lee tabulates the material models employed in the present analysis, including the unfactored stiffness and strength values used for analyses. The material models employed in the present analysis have reduced characteristic strengths for static strength analyses. These factors are given by $\gamma_{ma} = 2.205$ for R_{11} and $\gamma_{IFF} = 1.688$ for R_{12} and R_{22}. As per GL, the multi-axial fiber-reinforced materials are analyzed on a first-ply failure basis, ply by ply. As such, each ply is analyzed as an oriented unidirectional. The strength characteristics of the unidirectional glass were used for this analysis. However, we employed the LaRC03 criteria for analyzing the multi-axial materials. Davila and Camanho (2003) and Hermann (2011) provide details regarding LaRC03 criteria. It uses the fracture toughness of the composite to improve the failure prediction of the matrix-dominated failure modes.

The preliminary loads used for the design and analysis of the WEI105.0 m blade are established from WEI's internal software used for determining rotor blade steady aerodynamic performance and rigid aeroelastic loads under specific critical design load cases per the GL 2012 guidelines (2012). Additional design load cases to account for extreme wind conditions during a hurricane were also included in the analysis. These represent the predicted peak loads for the rigid planform during nominal operation as described below.

Based on nearly 20 years of wind turbine design, including loads analysis and blade design, Wetzel Engineering engineers have developed relationships between turbine design parameters and typical loads derived from critical design load cases that can be used to estimate ultimate design loads for new turbine designs at early stages of development.

Wetzel Engineering utilized an in-house rotor analysis code to study the rotor blade steady aerodynamic performance and rigid aeroelastic loads under critical design load cases as per the GL 2012 requirements (2012). A pre-defined set of DLCs were evaluated for the analyzed rotor blade to determine ultimate loads for preliminary structural design. The code can be customized and used to construct wind loading conditions outside of the definitions in the GL 2010 requirements (Germanischer Lloyd 2010), in this present case, for wind loading on the rotor blade under hurricane-like conditions.

Table 2-12 and Table 2-13 outline the loads used for structural analysis of the WEI105.0 m blade.

Table 2-12. Ultimate Loads

Station [m]	M_x [kNm] In-Plane	M_y [kNm] Out-of-Plane
0	33549.43	84748.14
1.5748	32641.09	81714.34
3.150	31732.76	78680.54
4.729	30856.94	76689.12
6.909	29884.24	74651.95
12.359	26861.78	68995.94
17.808	22764.16	61853.09
23.258	20071.82	54868.01
28.707	17715.43	48136.55
34.157	15501.04	41716.25
39.606	13406.28	35648.49
45.056	11425.65	29973.08
50.505	9565.20	24728.39
55.955	7818.85	19946.23
61.404	6196.37	15653.35
66.854	4720.33	11874.32
72.303	3417.19	8625.98
77.753	2318.05	5912.40
83.202	1445.83	3730.44
88.652	802.75	2076.05
94.101	299.83	754.86
96.281	160.67	390.06
98.461	85.63	198.72
100.640	36.36	79.34
102.820	7.68	15.22
103.910	1.47	2.55
105.000	0.15	0.26

Table 2-13. Maximum Flapwise Deflection Loads

Station [m]	M_x [kNm] In-Plane	M_y [kNm] Out-of-Plane
0	19390.69	62776.40
1.5748	18610.35	60934.07
3.150	17978.38	60139.47
4.729	16101.94	56228.23
6.909	14548.79	52935.00
12.359	12287.16	48099.46
17.808	9114.61	40786.68
23.258	6523.25	34119.17
28.707	4596.21	28325.22
34.157	3334.83	23353.76
39.606	2833.10	19070.35
45.056	2373.60	15369.73
50.505	1962.78	12181.37
55.955	1597.06	9454.35
61.404	1270.66	7148.38
66.854	979.96	5228.97
72.303	723.00	3664.54
77.753	500.58	2425.49
83.202	316.13	1482.45
88.652	173.81	804.24
94.101	60.63	287.30
96.281	30.03	148.07
98.461	14.64	75.91
100.640	5.50	30.72
102.820	0.96	6.06
103.910	0.08	0.66
105.000	0.01	0.11

The analysis and documentation within the scope of the preliminary design were conducted and are presented as per the GL 2010 requirements for the certification of wind turbines (2010). The blade was analyzed with respect to the following structural design considerations:

- Peak deflection constraints
- Modal analysis constraints
- Static strength analysis
- Ply-by-ply analysis of the fiber-reinforced structure using LaRC03 failure criteria (Davila and Camanho 2003, Hermann 2011) for fiber failure (FF) and interfiber failure (IFF).

2.5.1 Mass and Stiffness

The mass distribution of the blade was determined using the equivalent beam model as well as other internal tools used for modeling the preliminary structural design. These models assume a preliminary estimation of an assumed configuration for the root fastener concept, proprietary to WEI, and account for the mass of the root fasteners except for root studs. Figure 2-8 displays the mass distribution for the WEI105.0 m blade. The trend of the plot shows that most of the mass is concentrated between 30%–75% of the blade span. Mass is concentrated at the blade root because of the root ring, and the trend monotonically decreases as the plot approaches the maximum chord station. The plot also shows a general decreasing trend as it approaches the tip, whereby, overall mass of the blade decreases due to structural changes and termination points to various structural components of the blade such as the spar cap and shear webs. The total blade mass and breakdown can be found in Lee (2014).

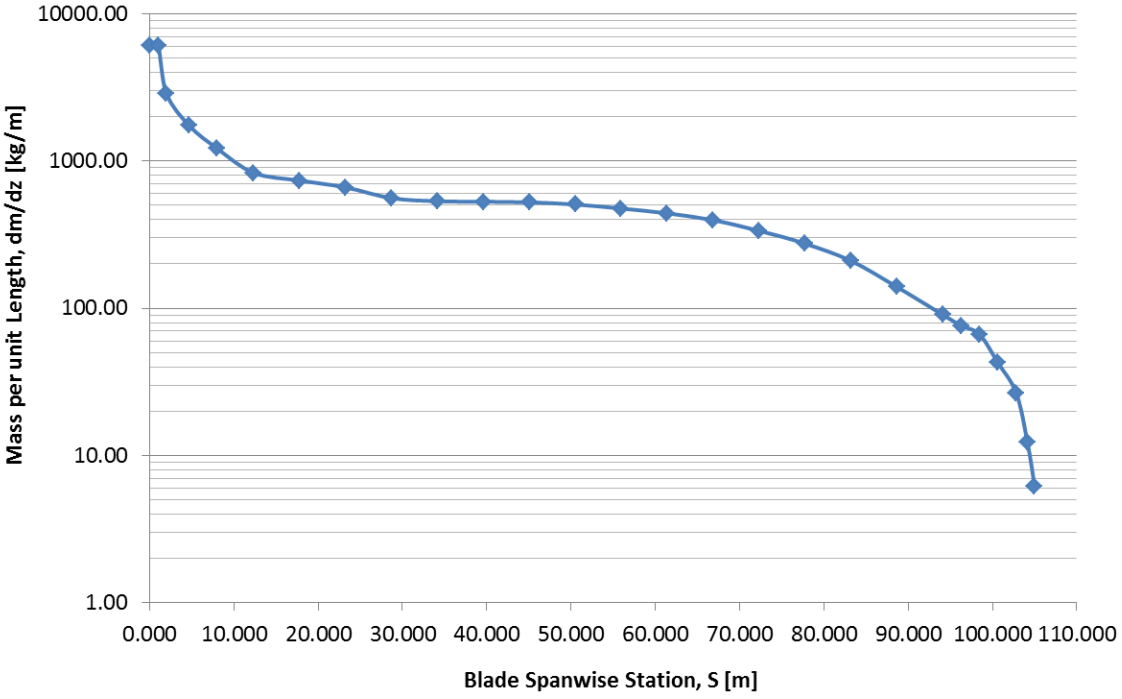

Figure 2-9. Mass distribution for the WEI105.0-m blade

2.5.2 Deformation

Because of the large amount of available clearance for this turbine configuration (downwind turbine), the blade tip deflection was constrained by Wetzel Engineering to be no more than 15% of the total blade length, $\Delta x = 15.75$ m. The present equivalent beam model predicts a maximum out-of-plane deflection of 11.44 m (10.9% of the total blade length) under extreme flapwise loading. The model results also predict an in-plane deflection of 1.05 m under the same loading conditions.

The benefit of the downwind configuration of the NREL 10-MW hurricane-resilient wind turbine is that it presents an opportunity to optimize the structural design of the 105-m blade with blade

deflection as a secondary design driver. This allows the design of the blade to be kept at a minimum weight to satisfy primary design drivers such as the strength of the spar cap, desired stiffness, and frequency characteristics of the blade. This also means direct material costs are kept as low as possible.

Figure 2-10 is a spanwise plot of the out-of-plane (or flapwise) deflection, and Figure 2-11 is a spanwise plot of the in-plane (or edgewise) deflection of the WEI105.0-m blade. Under the blade extreme flapwise loading, the resulting flapwise deflection of the 105.0-m blade of 11.44 m is about 10.9% of the total blade length. Results show out-of-plane blade deflection in the direction that is downwind of the tower, and in-plane blade deflection is in the direction toward the leading edge.

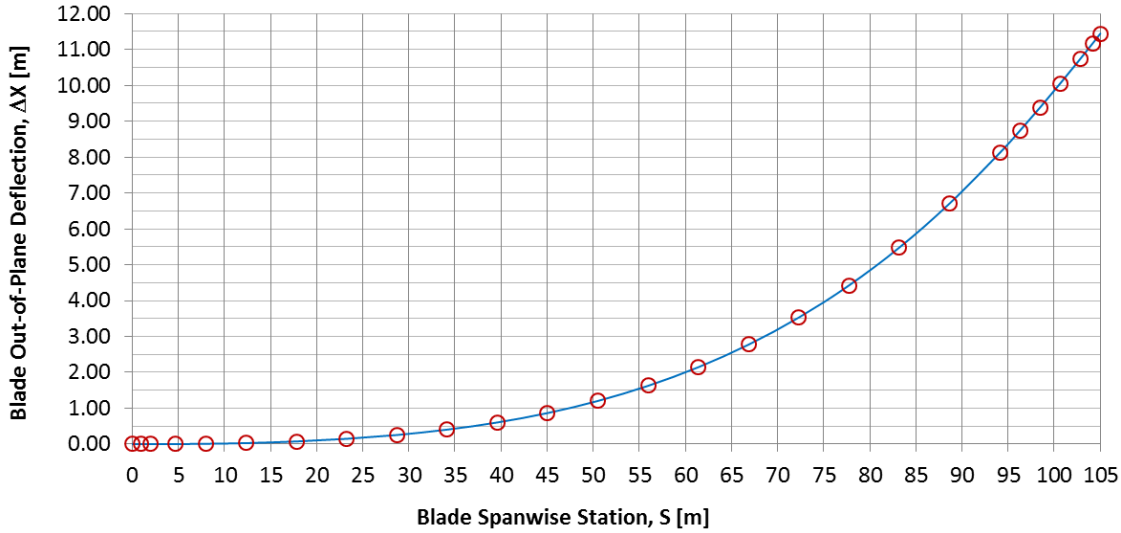

Figure 2-10. Out-of-plane deflection of the WEI105.0-m blade under maximum flapwise loading

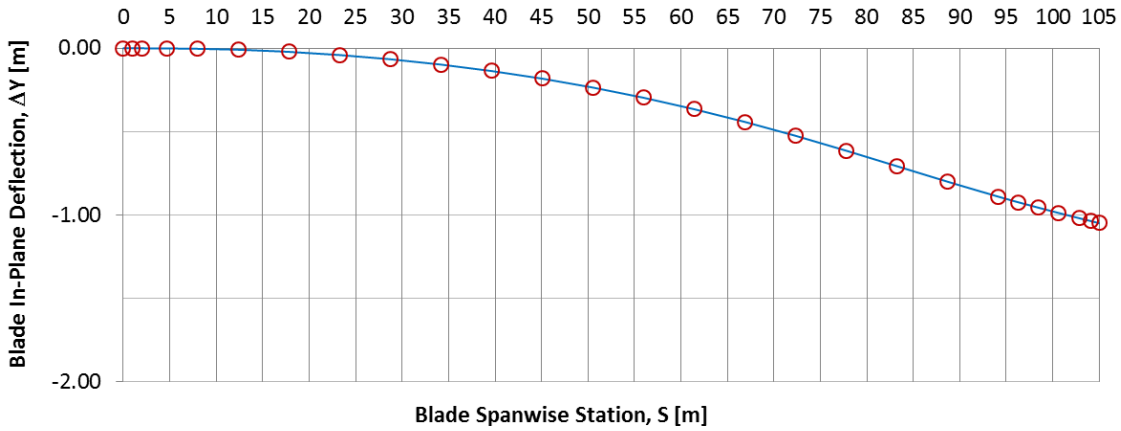

Figure 2-11. In-plane deflection of the WEI105.0-m blade under maximum edgewise loading

2.5.3 Modal Analysis

A modal analysis was conducted with inputs determined from WEI's internal sectional FEA tool using the NWTC Modes program that calculates uncoupled mode shapes from the beam equivalent model. Table 2-14 describes the frequency characteristics.

General blade design practice at Wetzel Engineering and throughout the industry is to design and optimize the blade structure so the target range for first flapwise frequency, f_1, is defined as 3P+10% < f_1 < 3P-10%. Additionally, the target range for first edgewise frequency, f_2, is defined as $f_2 > 1.35*f_1$ and 6P+5% < f_2 < 6P-5%.

This means the target range for first flapwise frequency shall be outside the range of three times the rotational frequency of one revolution of the rotor (1P). Similarly, the target range for first edgewise frequency shall be outside the range of six times the rotational frequency of one revolution of the rotor—and the first edgewise frequency is at least 35% higher than the first flapwise frequency to avoid resonance issues related to the first modes of flap and edge.

The WEI105.0-m blade has desirable frequency characteristics. Table 2-14 shows the isolated blade first flapwise frequency to be about five times per rotor revolution (5P) and the first edgewise frequency to be about 8P at rated shaft speed and cut-in shaft speed during normal operation. These isolated blade frequencies stay clear of any resonance with 3P and 6P. In addition, the first edgewise frequency is about 61% higher than the first flapwise frequency.

Table 2-14. Summary of the WEI105.0-m Blade Frequency Characteristics

Natural Frequencies - Mode Shape	Parked	Rotating			
		Minimum, Ω = 3.25rpm		Rated, Ω = 7.45 rpm	
1st Flapwise Mode	0.577 Hz	0.582 Hz	4.69 P	0.604 Hz	4.87 P
1st Edgewise Mode	0.964 Hz	0.966 Hz	7.78 P	0.976 Hz	7.86 P
2nd Flapwise Mode	1.550 Hz	1.556 Hz	12.53 P	1.583 Hz	12.75 P
2nd Edgewise Mode	3.457 Hz	3.459 Hz	27.86 P	3.469 Hz	27.94 P

2.5.4 Exertion Factors

Each component was analyzed for FF and IFF per the method described in Appendix E. The static exertion factors of the fiber-reinforced plastic components can be seen in Figure 2-12 through Figure 2-14. Note that discontinuities correlate with locations of ply drops in the laminate structure.

For the glass fiber-reinforced material, the strength was assessed on a ply-by-ply basis. Unidirectional glass material was analyzed for FF and IFF using the methods of Puck. The multi-axial glass fabrics were analyzed for FF and IFF using the LaRC03 criteria. A description of the theory and methods applied using LaRC03 in the FF and IFF evaluation of the WEI105.0-m blade can be found in Davila and Camanho (2003) and Hermann (2011).

Figure 2-10 through Figure 2-12 shows the general trend of the static exertion factors of FF and IFF of the composite laminates in the root ring, blade shell, spar cap, and shear webs, respectively. Static exertion factors greater than one indicate strain to failure at the ply level in the primary fiber direction (FF) and transverse fiber direction (IFF). All exertion factors presented in the figures below are less than 1.0.

The exertion factors in the spar cap of the WEI105.0-m blade is shown to be maximized and optimal under extreme blade loading. This indicates the blade spar cap was designed to the strength of the carbon materials in the spar cap while under consideration for maximum blade deflection constraints. The exertion factors in the blade shell and shear webs show sufficient margin in the design. The general trends of the plots below also show the overall buildup of laminate structure in various structural components of the WEI105.0-m blade from blade root to blade tip—with most of the structure concentrated toward 30%–75% of the blade span.

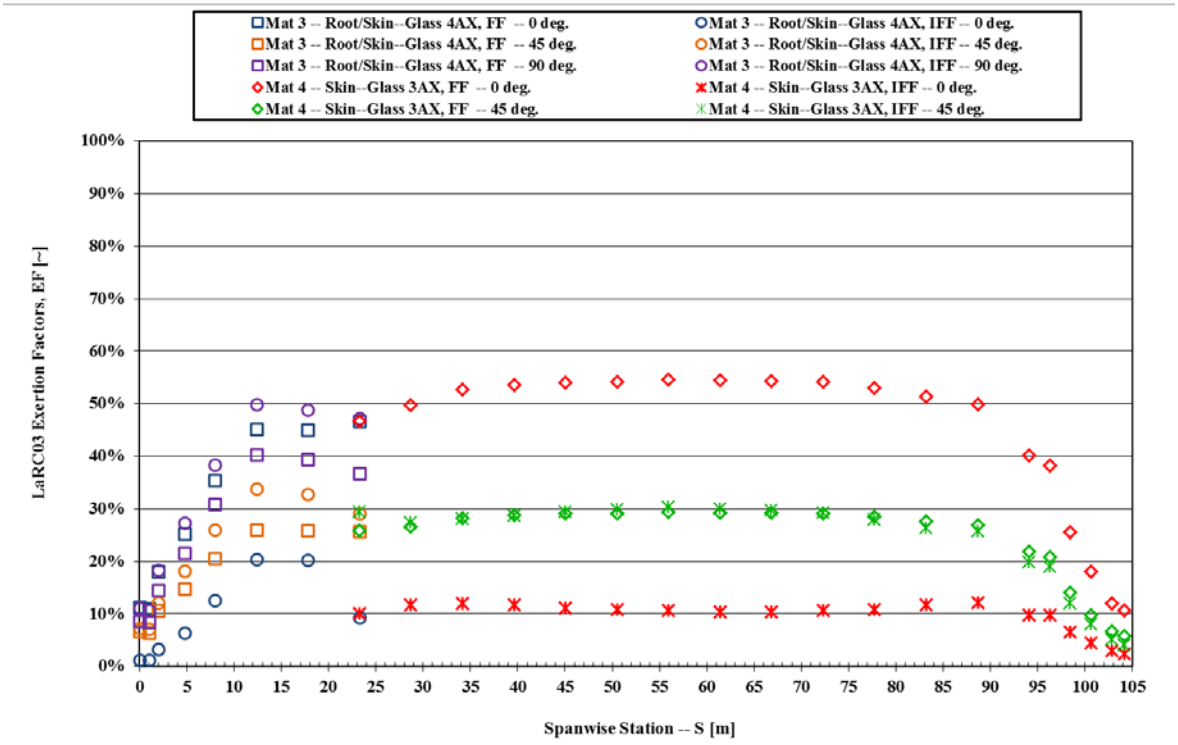

Figure 2-12. Sectional exertion factors for shell glass materials of the WEI105.0-m blade

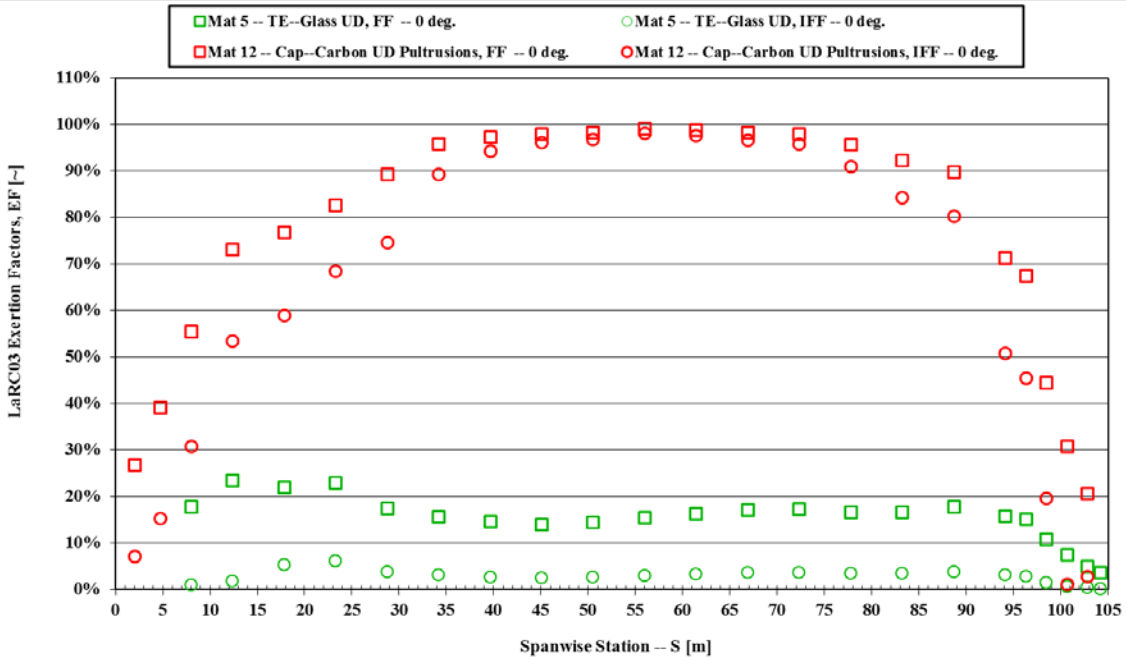

Figure 2-13. Sectional exertion factors for girder materials of the WEI105.0-m blade

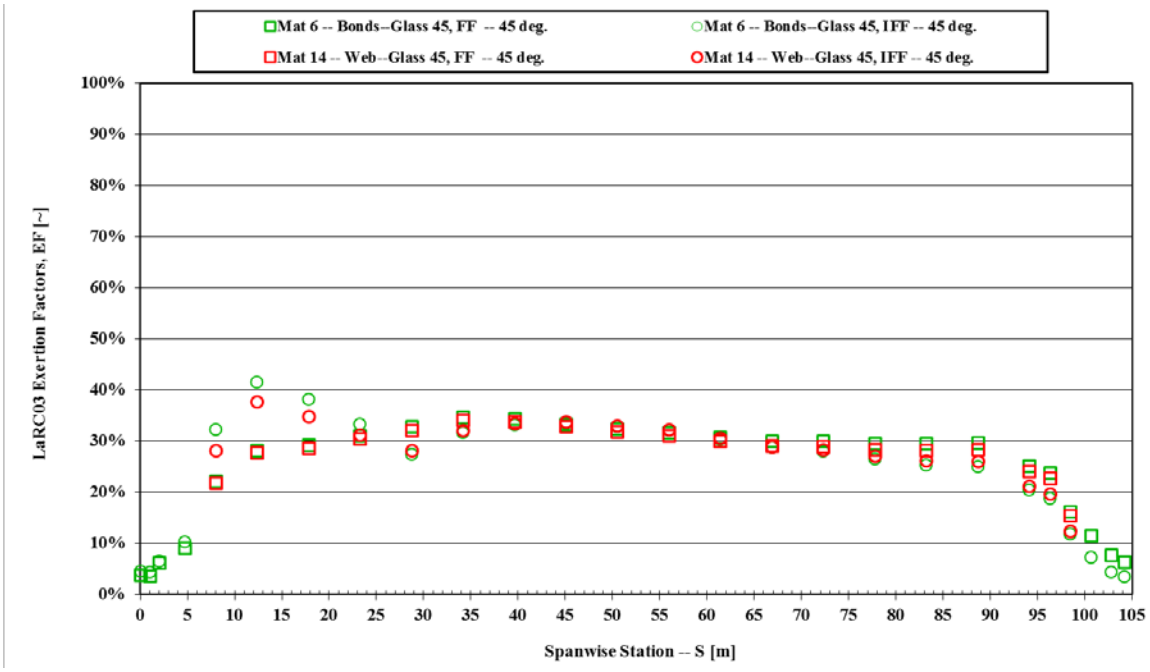

Figure 2-14. Sectional exertion factors for double-bias glass materials of the WEI105.0-m blade

The stiffness distributions for the blade were calculated using the equivalent beam model at each defined station. Figure 2-15 through Figure 2-17 displays the results of these calculations.

The distributed blade structural properties are reflected in the figures below, showing the flapwise, edgewise, and torsional section stiffness at each station, given about the principal structural axes of each cross section as oriented by the structural twist angle. The blade's sectional stiffness properties were used to determine the isolated blade modal frequencies and can be used as input for aeroelastic simulations of the 10-MW wind turbine in FAST or GH BLADED.

The in-plane (edgewise) stiffness at each cross section along the blade span is about 10 times larger than the out-of-plane (flapwise) stiffness at each station along the blade in magnitude. The overall trend in the blade stiffness shown in the following plots is smooth and monotonically decreasing from blade root to blade tip of the WEIU105.0-m blade. It can be observed from the figures below that the trend tapers off at the tip because of changes and termination points of some of the structural components within the blade structural layout.

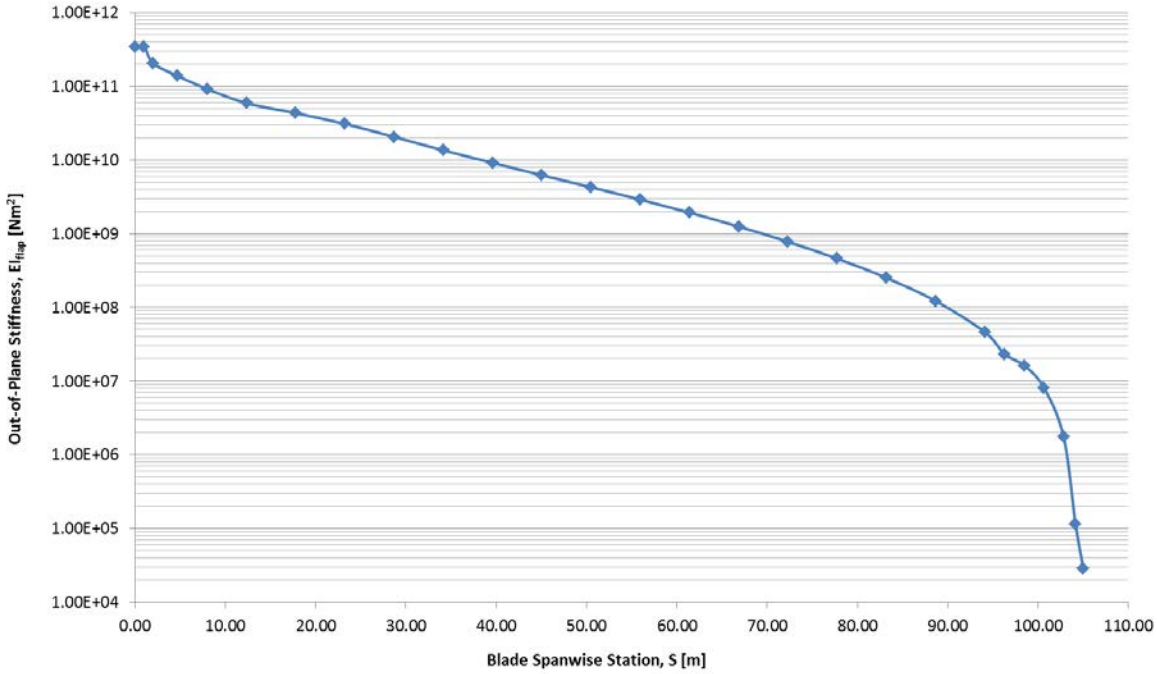

Figure 2-15. Out-of-plane stiffness distribution for the WEI105.0-m blade

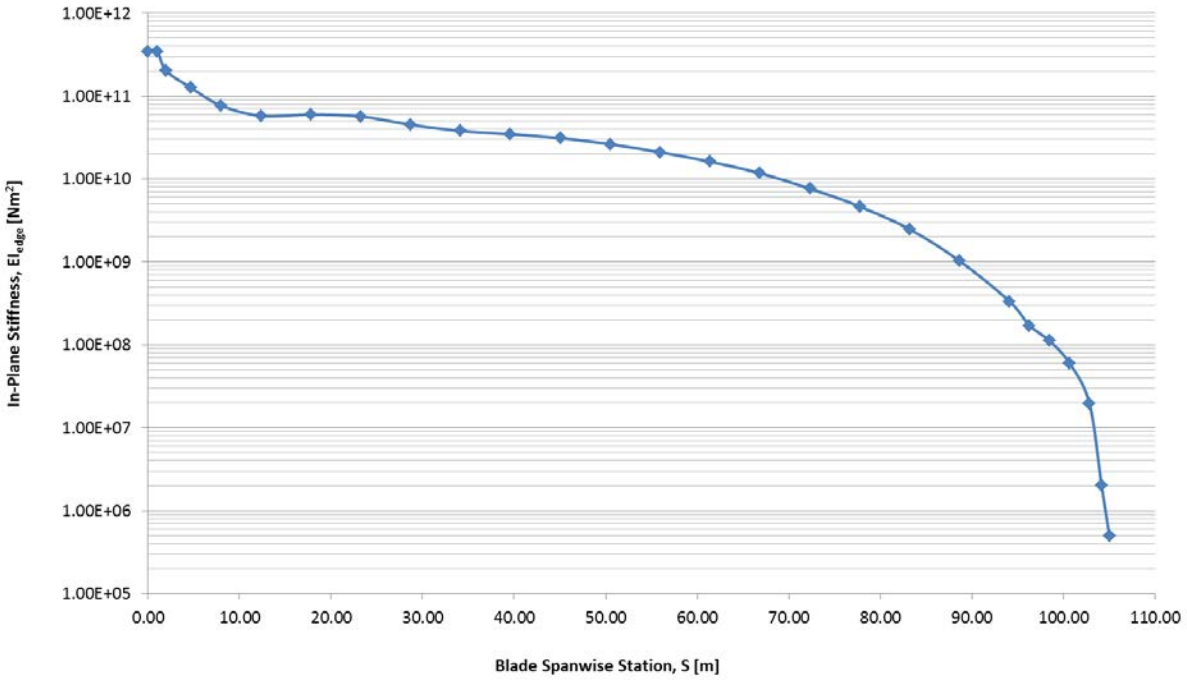

Figure 2-16. In-plane stiffness distribution for the WEI105.0-m blade

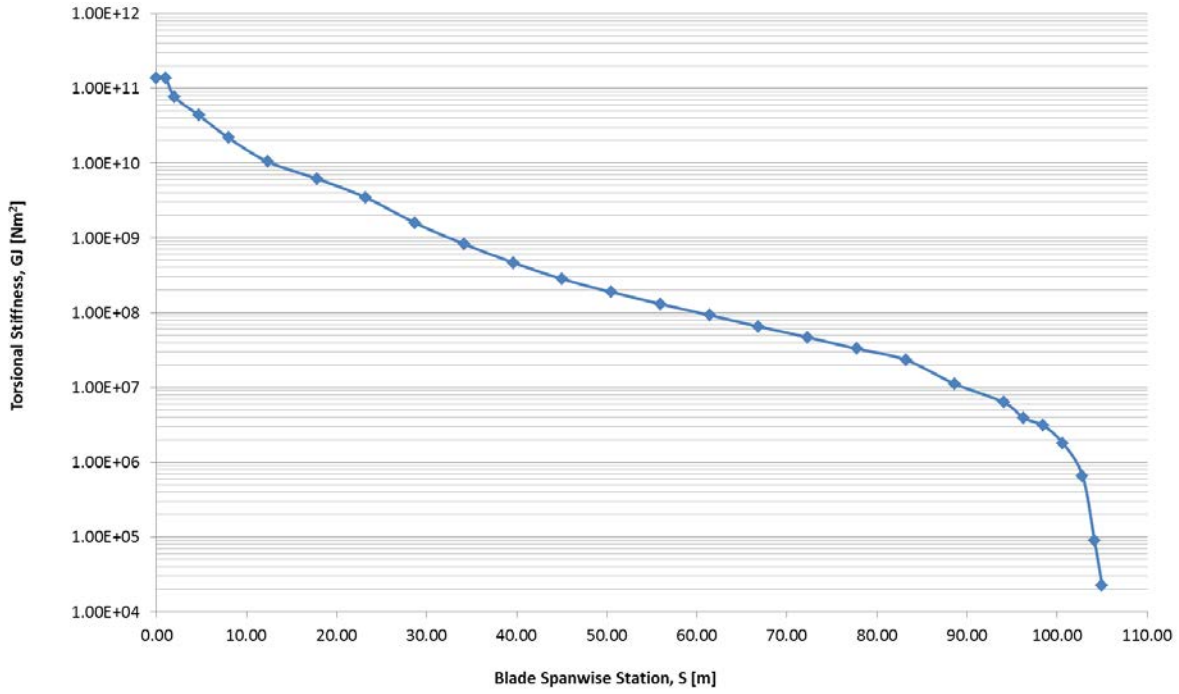

Figure 2-17. Torsional stiffness distribution for the WEI105.0-m blade

2.6 Summary of Blade Construction

Key geometry details of the blade are summarized in Table 2-13. Lee (2014) provides documentation of the laminate construction of the blade. The following is a summary of the key characteristics of the blade's construction:

- Constructed of glass fiber infused with epoxy resin and includes end-grain balsa as a core for sandwich constructions
- Skin laminate is constructed using quadraxial and triaxial glass fabric, and balsa core
- Lightweight sandwich core construction of the blade shell laminate is reinforced with pultruded high-modulus glass fiber composites with tailored cross-sections (proprietary to WEI) to achieve the required panel stiffness for buckling resistance
- Main spar cap and trailing-edge spar cap are composed of fiber composites that are primarily unidirectional pultruded carbon fiber composites of tailored cross-sections (proprietary to WEI) and unidirectional glass fabric, respectively. These were infused with the rest of the shell. The spar caps were sandwiched between the dry glass layers in the shell prior to the infusion of the shells with resin.
- Shear webs laminate is constructed using double-bias glass fabric and balsa core
- Structural components are fabricated using an open-molding method combined with a vacuum-assisted resin infusion molding process
- Root is fastened to the hub by passing external bolts through the root according to the requirements of the associated hardware. These bolts will have to be torqued to achieve the desired pretension.

Details of the material distribution and requirements are tabulated in Lee (2014).

Table 2-15. Key Geometry of the WEI105.0-m Blade

General Geometry		
	Blade Length	105.00m
	Length of Tip Chord	0.10m
	Position of Largest Chord	23.25m
	Length of Largest Chord	7.00m
Root Configuration		
	Root Outer Diameter	5.95m
	Root Inner Diameter	5.65m
	Root Bolt Circle Diameter	5.80m
	Bolt Count	WEI Proprietary
	Bolt Size	WEI Proprietary
*Preliminary Estimates		

3 Hub, Nacelle, and Generator Scaling

The basis for the NREL 10-MW aeroelastic hub, nacelle, and generator concept design is the direct-drive Siemens 3.0-MW and 6.0-MW platforms. Siemens' direct-drive technology provides a simple, straightforward wind turbine design. Replacing gearbox, coupling, and high-speed generator with a low-speed generator eliminates two-thirds of the conventional drivetrain configuration.

In this study, three 10-MW design concepts were created corresponding to three blade lengths, rated rotational speeds, and rated torques. Each of the three design concepts consisted of a hub, generator, and nacelle.

3.1 Model Assumptions and Constraints

Extrapolating to a 10-MW design based on current Siemens Wind Turbine (SWT) 3.0 MW and 6.0 MW components can only provide estimates because many factors will impact the key figures provided for this design concept. Extrapolation becomes especially difficult to forecast when dealing with large components for a high-level design.

This study assumes that parts can be produced without consideration for challenges related to component size. For example, challenges such as machining components at the 10-MW scale are assumed to be no different than those for the 3.0-MW and 6.0-MW baselines. Likewise, considerations about transportation and installation at 10 MW are assumed to be the same for the 6.0-MW components.

3.2 Scaling Methodology

The 10-MW turbine concept design was broken into modules that were created separately. Only a few key input and output parameters were passed between modules from which the individual module design was to originate. The rotor design was the important module interface for the hub, generator, and nacelle with the input for rated power, rated torque, and rated rotational speed.

Based on the input parameters from the 10-MW rotor concept design, main parameters for hub, generator, and nacelle were found by extrapolation from the 3.0 MW and 6.0 MW baselines by using simple, physics-based scaling laws. Hub, generator, and nacelle aeroelastic 10-MW concept designs were developed from the extrapolated main parameters and the corresponding 3.0-MW and 6.0-MW aeroelastic models. In the following paragraphs, we present details on the scaling methodology for each of the modules encompassed in this study.

A compromise between rotor module and hub, generator, and nacelle modules could be found by iterating on these input and output parameters between the modules.

Overall mass and volume figures were estimated from a combination of scaling by torque and rated power because, for simplified scaling of mass and volume, some components are governed by torque while others, primarily electrical components, are governed by rated power. Hence, the location of nacelle center of gravity is based on component mass scaling and the associated location in the nacelle. Mass scaling is split on the components included in Eq. 1, as follows:

$$\textbf{Total Mass} = \textbf{Hub} + \textbf{Generator} + \textbf{Main Electrical Components} + \textbf{Nacelle Misc.}$$

- Hub includes the casting as well as blade bearings, pitch system, and spinner
- Generator includes the main bearing, fixed shaft, stator, rotor, and cooling
- Main electrical components include the converter, transformer, and cabinets
- Nacelle misc. includes the bedframe and rear-end structure.

3.2.1 Hub

The hub assembled mass was scaled by the blade length. Other significant factors such as blade root diameter were not taken into account for this concept design because these factors were not considered in the module interfaces for this study. Hub mass was scaled according to square-cube law. At constant density, mass increases by the cube, and area increases by the square:

$$\textbf{Hub Mass} = \mathbf{C_3} \times \textbf{Blade Length}^3$$

Where the coefficient C_3 is $m_{Hub} \; / \; L_{Blade}^3$ for the SWT-6.0.

3.2.2 Generator

Generator mass was scaled based on torque:

$$\textbf{Generator Mass} = \mathbf{C_1} \times \textbf{Torque}$$

where the coefficient C_1 is based on data from Siemens' direct-drive turbines.

The scaling relationship of the generator mass equation was based on the torque density of the SWT-6.0 MW and is plotted in Figure 3-1 for the three concept designs. For reference, the torque mass relationship for the SWT-3.0 MW is also included in Figure 3-1.

The generator mass increases with higher-rated torques and lower-rated rotational speeds. For the three 10-MW designs, concept number 1 had the highest-rated torque and the lowest-rated rotational speed, whereas concept number 3 had the lowest-rated torque and highest-rated rotational speed.

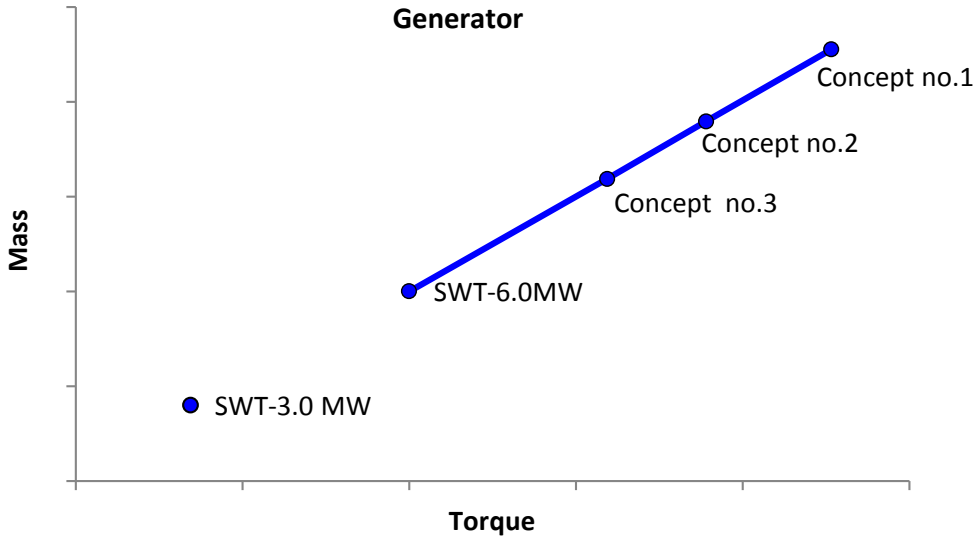

Figure 3-1. Generator mass as a function of torque

3.2.3 Primary Electrical Components

For the SWT-3.0 MW, the transformer and converter were placed in the tower; for the SWT-6.0 MW, these were placed in the nacelle. For the concept design, the transformer and converter were also considered to be in the nacelle and thus the SWT-6.0 MW platform was used as scaling basis. Primary electrical components were divided into the converter, transformer, and electrical cabinets. These were scaled according to estimates provided by Siemens' experts:

$$\textbf{Electrical Components Mass} = \mathbf{m}_{\textbf{converter}} + \mathbf{m}_{\textbf{transformer}} + \mathbf{m}_{\textbf{electrical cabinets}}$$

3.2.4 Nacelle Miscellaneous

The remainder of the nacelle mass was scaled based on rated power:

$$\textbf{Nacelle Mass} = \mathbf{C}_2 \times \textbf{Rated Power}$$

where the coefficient C_2 was based on data from Siemens' direct-drive turbines.

3.2.5 Volume and Overall Dimensions

Siemens' direct-drive turbines have a cylindrical-shaped nacelle and generator. Generator volume is scaled directly with mass and governed by length and diameter, which, for this concept design, were estimated by Siemens' experts. Nacelle diameter is equal to generator diameter, whereas nacelle length is kept the same as the SWT-6.0 MW.

3.3 Electrical System Efficiency

Electrical system efficiency was estimated by taking into account losses from the generator, main bearing, converter, transformer, auxiliary, and cables. This means that efficiency describes the conversion from mechanical-to-electrical power at the grid. The system efficiency was estimated by Siemens' experts.

3.4 Model Topology

The hub, nacelle, and generator model topology is according to the beam element topology of Siemens' direct-drive turbines. The nacelle was connected to the tower at the top tower flange in node nTi. The nacelle bedframe was modeled between nTi and nN2. An element placed downwind of the top tower flange represented the nacelle aft end (not shown in Figure 3-2). The fixed shaft was tilted 6.0 degrees and placed between node nN2 and nN5; it was connected to the bedframe at node nN2 and to the main bearing at node nN5. The nacelle and hub interface is in node nN6.

Overall, nacelle and hub masses were controlled by assigning mass per length for element beams and adding individual masses at selected nodes to represent the turbine physical components.

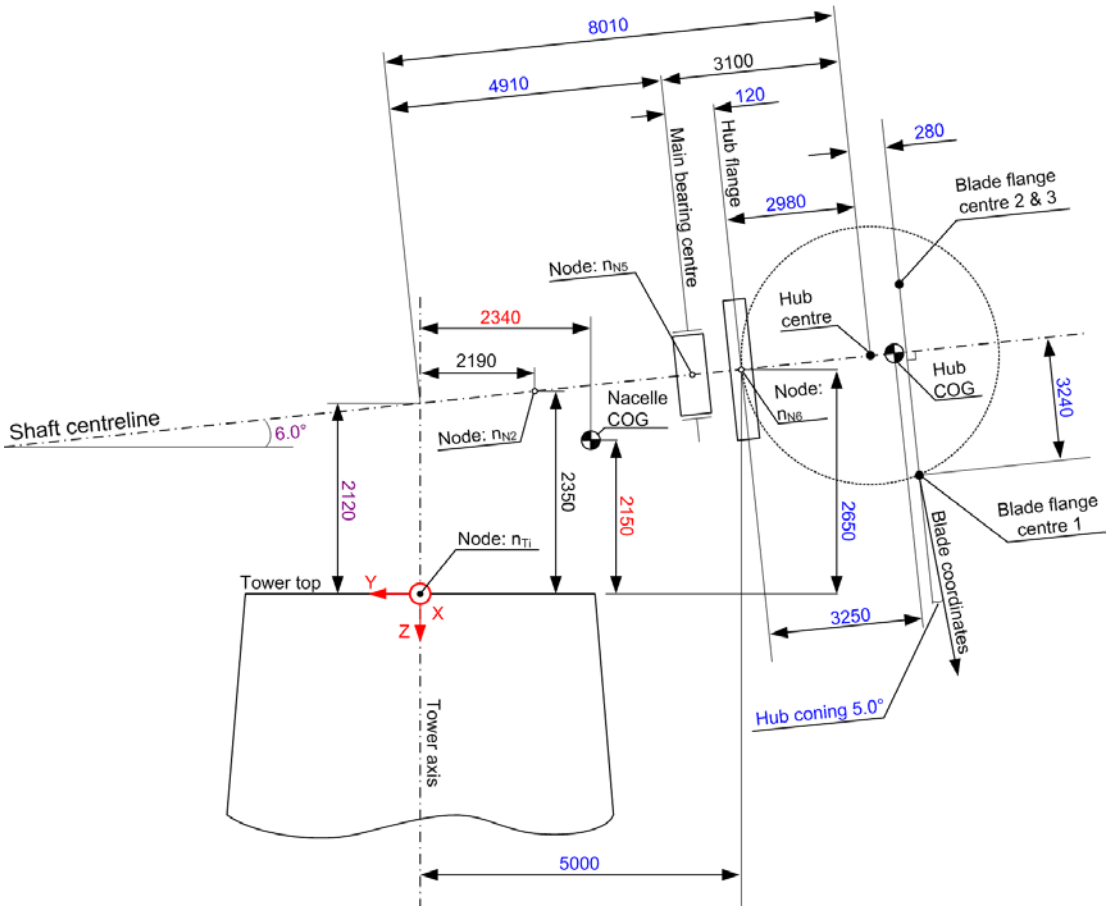

Figure 3-2. Concept design number 1 nacelle and hub geometry

3.5 Cost Estimate

Cost projections were generated based on the 3.0-MW and 6.0-MW baselines and are approximations. Many factors impact final cost, including the individual detailed component designs, manufacturing possibilities, and quantity produced. Furthermore, cost estimates do not cover transportation and installation.

4 Tower Conceptual Design

The team was tasked to create a design for a hurricane resilient offshore wind turbine system to be deployable in the Gulf of Mexico region. The turbine rotor was optimized by WEI; the nacelle components, including the permanent-magnet generator, were sized by Siemens; and the substructure information was provided by Keystone Engineering. Based on geometric and load data produced by these partners, NREL generated a preliminary design of the tower. This included the creation of a FAST model to generate the complete mass matrix at the tower top as well as an optimization algorithm to minimize the tower mass given a few design constraints.

A minimum mass tower design was achieved that would place the first system eigenfrequency at approximately 0.163 Hz (see below). A parametric study was conducted to show what mass penalty would need to be incurred if the geometric parameters were to change or if a higher eigenfrequency was selected.

This preliminary design was solely based on load-bearing strength and a soft-stiff frequency approach. Future efforts will need to focus on iterating the solution based on revised substructure parameters and on fatigue design. It was noted that the downwind configuration (forcing the rotor nacelle assembly (RNA) center of mass downwind of the tower centerline) causes the tower mass to increase by some 100 tonnes or 16%.

4.1 Introduction

The project team produced a complete design of a wind turbine system to be deployable in the Gulf of Mexico region. The turbine and its support structure would be subjected to hurricane loading conditions. The design accounted for ULS conditions that would be encountered during a 100-year, return-period event. This report discusses the tower preliminary structural design. The tubular tower was made of standard ASTM A992 steel with up to three tubular segments. The base was fastened to a transition piece at the top of an IBGS substructure. Hub-height was fixed at 135 m, and the tower-base flange level was chosen at 20.7 m MSL. Wetzel Engineering provided basic properties of the blades whereas nacelle and hub inertial and geometric properties were either calculated or derived from Siemens' report on the generator design. A FAST model was produced that helped with the determination of the tower-top overall inertial properties. An optimization algorithm was utilized to arrive at a tower of minimum mass that would pass GL (2005) and Eurocode (2007) checks for global and local (shell) buckling strength while simultaneously achieving a desired natural frequency range.

It was demonstrated that the tower mass can be reduced if a higher first natural frequency is accepted, which would require the controller to incorporate frequency-hopping features to avoid 3P-forcing frequencies. If the substructure is designed with greater stiffness, it is possible to produce a lighter tower and still meet the design criteria, but the full system optimization (Damiani and Song 2013) was outside the scope of this study.

In Section 4.2, details are provided of the design parameter bounds, main assumptions, and criteria to be met. Section 4.3 discusses the main algorithm to arrive at the optimum design. The achieved geometry is provided in Section 4.4. Section 4.5 offers a sensitivity analysis to the

results and obtained design parameters. Conclusions and a summary of main observations are presented in Section 6.

4.2 Specifications and Design Criteria

Generally speaking, there are three criteria that drive the design of a turbine tower. The first one is tied to the geometric parameters. The tower must allow for the hub to be located at the prescribed height above MSL to guarantee the expected rotor performance and loading levels. And, one must guarantee the fabricability of the structure and the viability of interfacing with both the nacelle and the substructure. Geometry parameters and constraints are shown in Table 4-1. Note that the hub-height was provided by WEI whereas the interface level was chosen based on wave-crest clearance criteria dictated by the American Wind Energy Association (AWEA) (2012) and GL (2005). The RNA inertial properties were derived after a preliminary FAST model was created and a linearization performed that helped obtain the mass matrix at the tower top. The tower base and top outer diameters and diameter-to-thickness ratios were selected based on best practice and to guarantee ease of manufacturing. The tower-top outer diameter was limited to 4.5 meters, which is on the upper limit of manufacturability for yaw bearings. Furthermore, due to the high maximum wind speeds expected in hurricane-prone areas, it is imperative to minimize tower drag and therefore limit the support structure windage area. The tower material was the common ASTM A992 steel but with an artificially increased (by 12%) density to account for secondary steel, cables, and coatings.

The second design criterion ensures the structural strength of the tower. Because of the reduced scope of this study, and because its focus was on hurricane resiliency, the tower was primarily designed against ULS cases and no fatigue treatment was conducted. Two main loading situations were considered: 1) An operational case with maximum rotor thrust (typical of an IEC 61400-3, 1.6 case (IEC 2005)); and 2) A parked case with maximum wind speed (typical of an IEC DLC 6.1/6.2 case). The values of the prescribed rotor loads were supplied by Wetzel engineering and are shown in Table 4-2. Additionally, a tower drag coefficient of 0.7 was selected based on the expected Reynolds numbers. The coordinate system assumed in the tables has the x-axis aligned with the wind (thrust direction), z-axis vertically upward, and y-axis following the right-hand rule.

The third criterion aims at reducing the possibility for harmful resonance. The main forcing derives from the rotor dynamics, primarily associated with the rotor and blade passing frequencies (i.e.,1P and 3P; rotor RPM range provided by WEI). Additionally, it is customary to avoid the wave-forcing frequency spectrum, which features high-energy content below 0.2 Hz. Table 4-3 presents the main frequency response parameters used for this study. Note that the substructure equivalent-stiffness characteristics were provided by Keystone Engineering based on their best estimate at this initial stage of the design. Keystone Engineering further recommended a target first natural frequency of 0.14 Hz. While this frequency is outside the rotor forcing frequency band, it falls in the wave spectrum high-energy content band. This fact is further discussed in Section 4.4.

Normally, the tower and substructure would be designed through an iterative process, where loads at the tower base are passed from the turbine-loads analysis to the substructure designer

who, in return, would update the substructure geometry and provide new stiffness to the turbine and tower designer for a new iteration. A better approach, which allows for direct optimization of the entire support structural mass, consists of a simultaneous sizing of tower and substructure (Damiani and Song 2013) and of associated coupled loads analyses with aero-hydro-servo-elastic tools such as FAST-8 with Subdyn and Hydrodyn (Damiani et al. 2014). In this research, we did not have enough resources and budget to perform more detailed analyses and design iterations; therefore, the design is left at the preliminary stage, but it is considered to be an accurate representation of the general geometry and structural properties of the final tower design.

Table 4-1. Geometry Parameters for Tower Design

Parameter	Value	Units
Deck height/flange level	20.7	m
Hub Height	135	m
Tower length (hub height-tower2hub-deck height)	111.2	m
RNA CMzOFF (center of mass z offset from tower-top flange)	2.61E+00	m
RNA CMxOFF (center of mass x offset from tower centerline, positive = downwind)	5.87E+00	m
RNA mass	8.646E+05	kilogram (kg)
RNA_Ixx	342033606	$kg*m^2$
RNA_Iyy	215922606	$kg*m^2$
RNA_Izz	213483330	$kg*m^2$
RNA_Ixy	0.664878088	$kg*m^2$
RNA_Izx	669586684.7	$kg*m^2$
RNA_Iyz	8.351770841	$kg*m^2$
Tower Db (base OD) max	8	m
Tower Dt (top OD) min	3	m
Tower Dt max	4.5	m
Tower DTR (OD-to-wall thickness) max	200	-
Tower DTR (OD-to-wall thickness) min	120	-
Number of unsupported segments	3 (~30 m unsupported length)	-
Steel density	8792	kg/m^3

Table 4-2. Loading Parameters for Tower Design (Rotor load values provided by WEI)

Maximum Thrust—Operational DLC		
Parameter	**Value**	**Units**
Maximum rotor thrust	1.903E+06	N
Yaw bearing Mxx @max thrust	1.300E+07	Nm
Yaw bearing Myy @max thrust	1.660E+06	Nm
HH (hub-height) wind speed @max thrust	33.0	m/s
Wind shear exponent @max thrust	0.14	-
Maximum Parked Yaw-Bearing Shear Force—Parked DLC		
Parameter	**Value**	**Units**
Maximum shear force at yaw bearing (aligned with wind)	4.300E+05	N
Yaw bearing Mxx @max thrust	1.130E+07	Nm
Yaw bearing Myy @max thrust	3.250E+05	Nm
Design wind speed for driving parked case	70.0	m/s
Wind shear exponent for driving parked case	0.11	-
Tower 2-D drag coefficient	0.7 (both cases)	-

Table 4-3. Resonance Avoidance Parameters for Tower Design (Stiffness and target natural frequency supplied by Keystone Engineering)

Parameter	Value	Units
Min RPM	3.25 (1P/3P=0.054/0.1625Hz)	RPM
Max RPM	7.45(1P/3P=0.124/0.3725Hz)	RPM
Substructure equivalent Lateral spring constant	5.80E+04	kilonewton (kN)/m
Substructure equivalent Rotational spring constant	4.40E+07	kilonewton meter (kNm)/rad
Substructure equivalent Axial spring constant	6.46E+06	kN/m
Target 1st natural frequency	0.14 (soft-stiff approach)	Hz

4.3 Design Optimization Algorithm

The algorithm used to optimize the design was based on a constrained optimization by linear approximation. The function to minimize is the overall structural mass. The constraints are as follows:

- First natural frequency within a prescribed range of the target frequency
- ULS utilization (global buckling and strength) (Germanischer Lloyd 2005) and shell buckling (Eurocode 2007) less than unity

- Uniform cross-section segment length less than or equal to one-quarter of total tower length
- Tower-base outer diameter bounds: 5m < D_b <8m
- Tower-top outer diameter bounds: 3m < D_t < 4.5m
- Diameter-to-thickness ratio bounds: 120 < DTR < 200
- Basic IEC PSFs (partial safety factors) are considered (1.35 for aerodynamic loads and 1.1 for gravity loads) whereas other safety factors are per GL (2005).

The algorithm made use of a finite-element-analysis tool (FEA) largely based on Frame3DD (http://frame3dd.sourceforge.net/), and of an analytical treatment of the loading distribution and geometry build-up. The FEA provided the eigenvalue analysis whereas the main utilization calculations were performed analytically by the program. Verification of results was achieved through an ANSYS model and excellent agreement was observed.

The method was implemented as a Python program (sizing tool) capable of sizing towers, monopiles and tower-jacket assemblies (Damiani and Song 2013).

4.4 Results and Final Geometry

The tower-sizing tool was exercised in optimization mode to reach a design that would meet the prescribed criteria, including a target natural frequency of 0.14 Hz. This frequency is outside the main forcing bands (1P and 3P) of the rotor forcing dynamics (soft-stiff approach) but falls within the high-energy content band of the wave spectrum and may give rise to harmful resonance (this should be checked against local meteorological ocean (metocean) conditions and with a more detailed study). Nevertheless, based on Keystone Engineering recommendations, it was decided to attempt to generate a tower design that would lead to that eigenfrequency for the support structure.

It was quickly observed that the parked case was considerably less exerting for the tower, and designs optimized for that DLC were not going to satisfy the operational DLC strength requirement (Figure 4-1). Furthermore, a design fully satisfying the operational DLC and the eigenfrequency criteria could not be found under the adopted design assumptions. The loads were elevated enough that in order to obtain a sufficient cross-sectional bending modulus, the outer diameter had to be above 6 m. This yielded high stiffness and, therefore, natural frequencies could be rather high unless a reduced wall thickness was chosen.

Worth noting is the RNA center of mass was displaced downwind of the tower centerline by almost 6 m; therefore, the RNA weight contributes to the deflection and bending moment values for the tower. While a more in-depth study is outside the scope of this project, it has to be recognized that this downwind configuration adds some 100 tonnes to the tower mass with respect to an upwind configuration. Future studies will be needed to account for second-order effects such as the P-Δ effect associated with the additional moment created by the increased displacement of the mass at tower-top.

Figure 4-2 shows the ULS utilization for a tower optimized to have its first eigenfrequency in the 0.14 Hz ±10% range. As can be seen, the tower fails the global buckling and strength checks.

And, the obtained eigenfrequency was 0.157 Hz—greater than 0.154 Hz (=1.1*0.14 Hz), which was chosen as the acceptable eigenfrequency upper limit. There might be other designs, based on different geometric-optimization parameters and assumptions, that could achieve the desired characteristics, but this is outside the scope of this research.

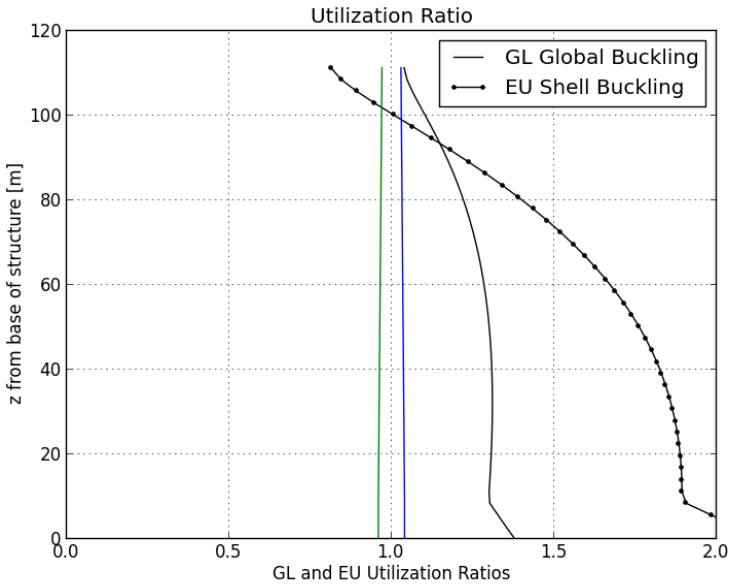

Figure 4-1. Utilization ratios per GL (2005) and Eurocode (2007), for the operational DLC, for the configuration that was optimized under the parked DLC (first eigenfrequency at 0.14 Hz)

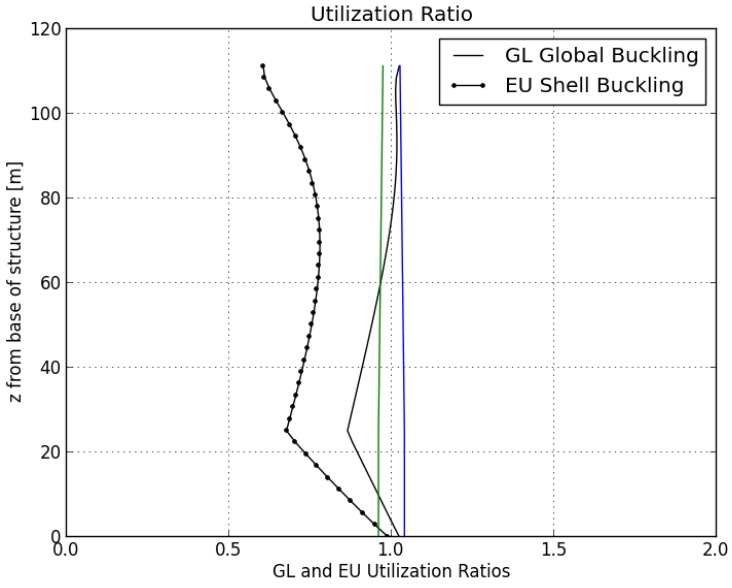

Figure 4-2. Utilization ratio for a configuration seeking a first natural frequency of 0.14 ± 10% Hz (first eigenfrequency at 0.157 Hz)

By allowing for an acceptable eigenfrequency range of 0.14 Hz ± 15%, the optimizer returned a design that met all of the design criteria and featured a tower mass that is about 10% lighter than the above configuration. Details of the geometry and tower base resulting loads are provided in Table 4-4.

Table 4-4. Optimized Tower Design with a Target System First Natural Frequency of 0.14 Hz ± 15% as well as Tower Base Loads for Parked and Operational DLCs

Parameter	Value	Units
Db	6.845	m
Dt	4.5	m
DTR	157	-
Constant cross-section tower segment length	10	m
Tower mass	659	tonnes
Expected system 1st natural frequency	0.161	Hz
Tower base shear force (ULS, unfactored)	2,571 (parked)/2,354 (operational)	kN
Tower base bending moment (ULS, unfactored)	165,744 (parked)/ 283,478 (operational)	kNm
Tower base vertical load (tower+RNA weight, unfactored)	14,945	kN
Max tower-top displacement (unfactored)	2.37	m

Given the observed trend of mass versus eigenfrequency, a parametric study was conducted to highlight the actual effects of the optimization parameters and to explore the solution space. The main optimization variables were varied in a multidimensional sweep: mass, eigenfrequencies, and utilization values were computed for each realization of the new configurations. Some 2,350 configurations were processed. In Figure 4-3, the obtained tower mass is plotted against tower DTR and first eigenfrequency; colors represent maximum utilization ratios per Germanischer Lloyd (2005). A similar plot was produced in which the number of configurations was limited to those featuring maximum ULS utilizations below unity (Figure 4-4). That figure also shows what mass change would result if utilization was relaxed to 1.01 (1% reduction in safety margin).

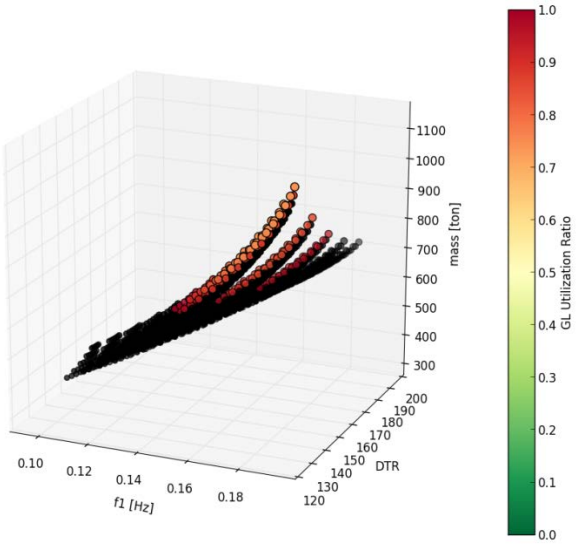

Figure 4-3. Parametric plot of utilization ratio per GL (2005) versus first eigenfrequency and DTR. Utilization values above unity are shown in black.

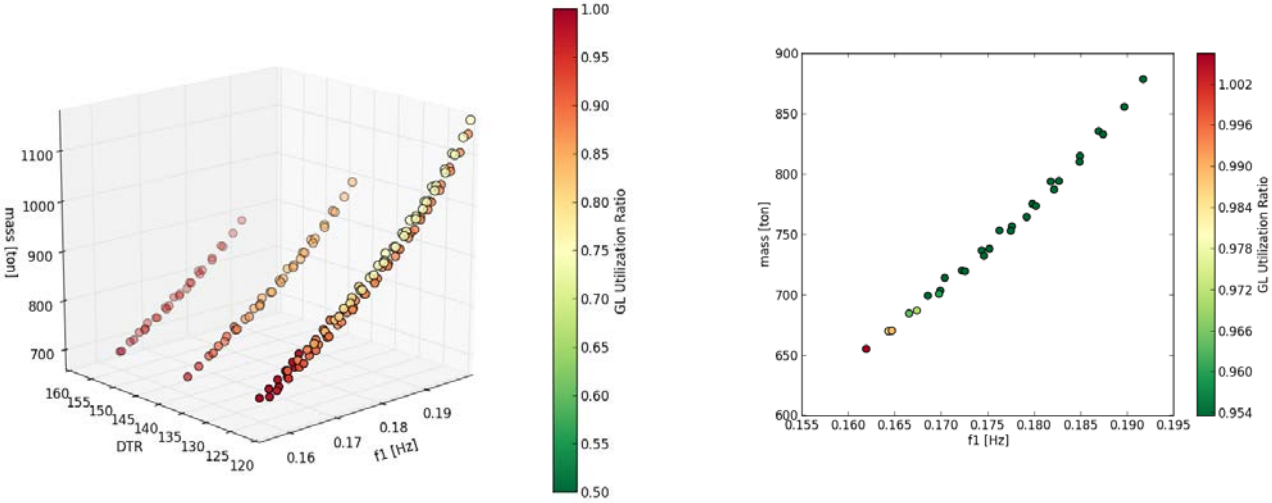

Figure 4-4. as in Figure 4-3, for configurations with utilization values < 1.0 (left) and < 1.01 (right)

These graphs show that for a given DTR, tower mass increases with the desired natural frequency as expected. Yet, it is possible to vary the DTR to achieve a minimum in mass for any given frequency. Note also that reducing wall thickness beyond DTR ~160 does not produce acceptable utilizations in most cases. The plots also show that the minimum achievable system frequency with acceptable maximum utilization is above 0.16 Hz, thus 0.14 Hz cannot be achieved with the current material, soil, and substructure characteristics.

Given these results, it was decided to allow for the first natural frequency to be above 0.16 Hz, and the obtained optimal configuration is provided in Table 4-5. A plot of the calculated utilization is shown in Figure 4-5. An ANSYS model was created to verify results. The

calculated maximum deflection, stresses, and eigenfrequencies (Figure 4-6) were in excellent agreement with the model employed with relative errors less than 5%.

Table 4-5. Optimized Tower Design with a Target System First Natural Frequency of 0.16 Hz as well as Tower Base Loads for Parked and Operational DLCs

Parameter	Value	Units
Db	6.96	m
Dt	4.5	m
DTR	163.5	-
Constant cross-section tower segment length	13.35	m
Tower mass	656	tonnes
Expected system first natural frequency	0.163	Hz
Tower base shear force (ULS, unfactored)	2,606 (parked)/2,361 (operational)	kN
Tower base bending moment (ULS, unfactored)	166,598 (parked)/ 283,660 (operational)	kNm
Tower base vertical load (tower+RNA weight, unfactored)	14,918	kN
Max tower-top displacement (unfactored)	2.30	m

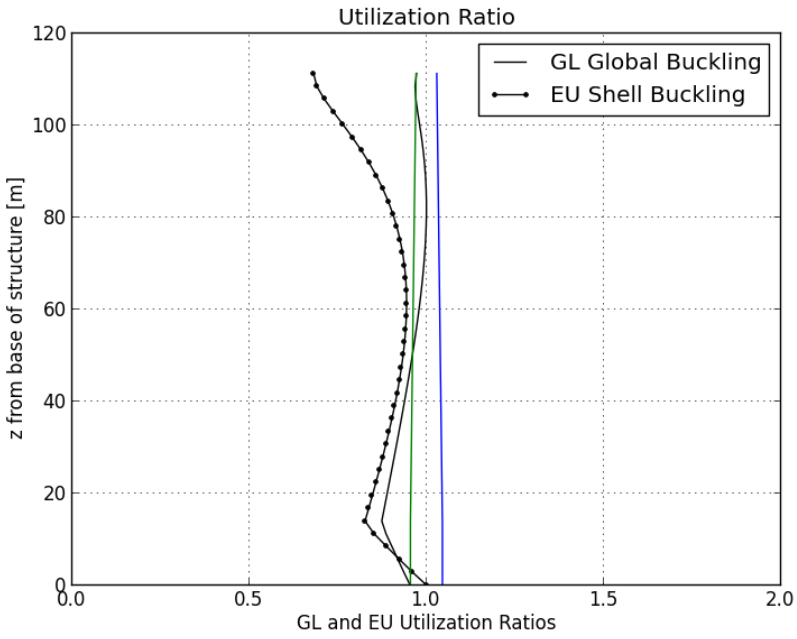

Figure 4-5. Utilization for the configuration depicted in Table 4-5

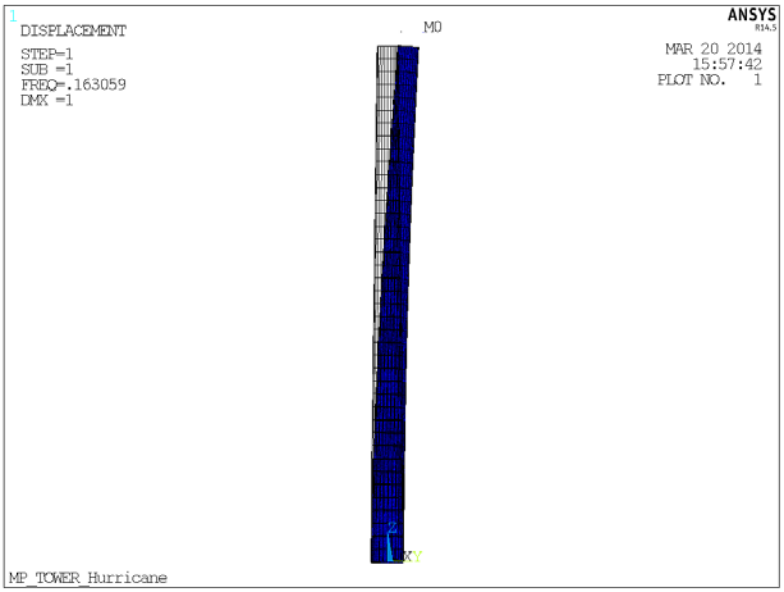

Figure 4-6. First mode shape calculated by ANSYS for tower configuration in Table 4-5 Sensitivity Analysis and Alternative Designs

The achieved system frequency of 0.163 Hz is extremely close to the lower bound of the 3P range (Table 4-3); therefore, it might create harmful resonance during start-up phases. It may be more prudent to establish a frequency-hopping strategy in the controller for a frequency in the middle of the 3P range—something closer to 0.18 Hz. This would need to be evaluated with respect to the control system capabilities in detailed design.

Figure 4-7 through Figure 4-10 show contours of tower mass, utilization, and first natural frequency as a function of tower base outer diameter and DTR for a given tower-top outer diameter and for a given length of the segment at constant cross-section. The plots confirm that for acceptable utilization values eigenfrequencies must be above 0.16 Hz. Furthermore, it can be seen that the original configuration of Figure 4-2 can be approximately located in Figure 4-8 in a region of utilization values above unity. From the same Figure 4-8, one could attempt to reach an acceptable design by further reducing DTR and increasing the tower base outer diameter at the cost of a large increase in mass. However, Figure 4-9 and Figure 4-10 show that a reduced mass configuration can be achieved by pushing the tower-top diameter to its upper limit of 4.5 m and fine-tuning the constant cross-section segment length. The configuration depicted in Table 4-4 can be approximately located in Figure 4-10.

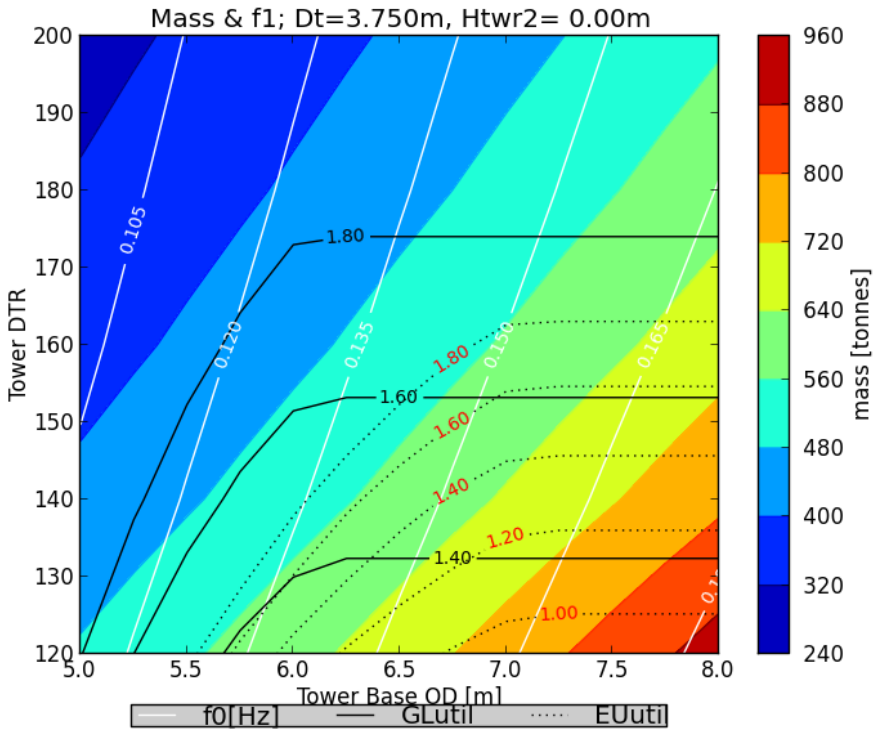

Figure 4-7. Parametric plot showing tower mass in filled contours, first eigenfrequency, utilization ratios contours per GL and Eurocode, as a function of tower base diameter and DTR for a given tower-top outer diameter and constant cross-section segment length shown at the top

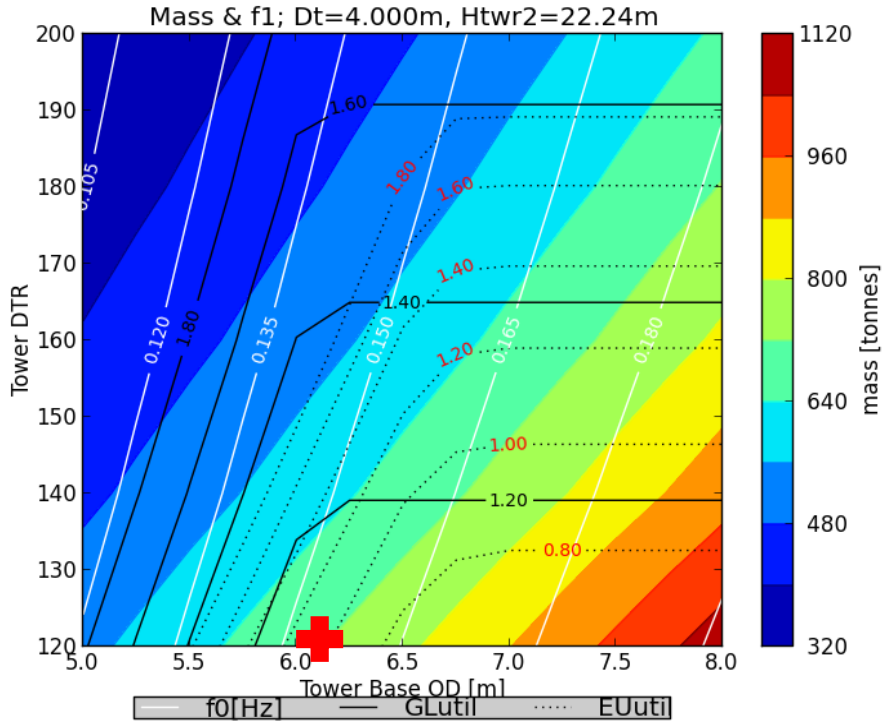

Figure 4-8. As in Figure 4-7, for a longer segment at constant cross-section. The cross loosely represents the configuration of Figure 4-2.

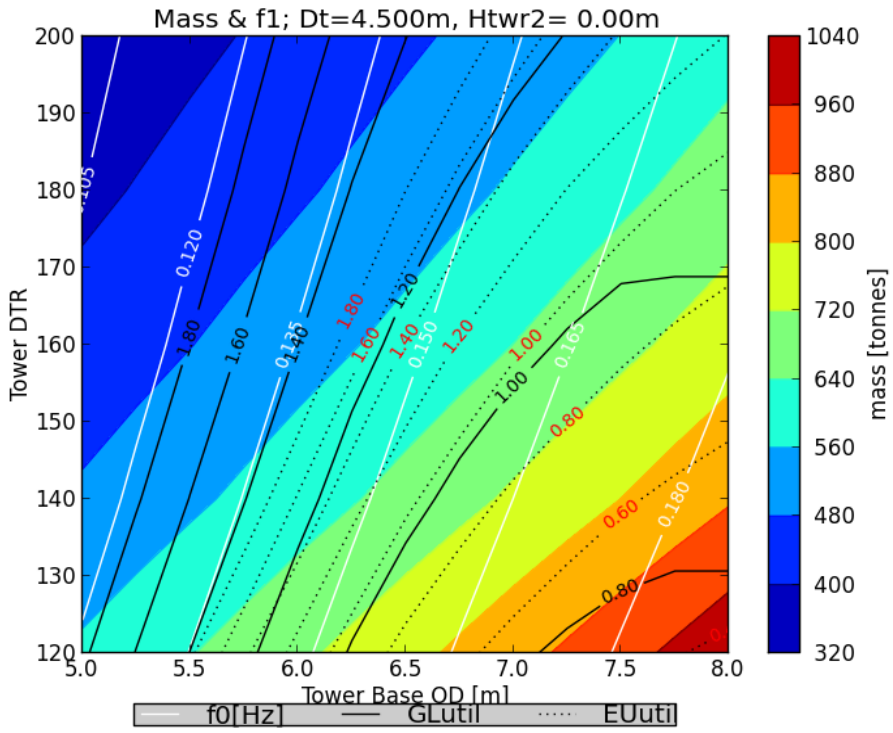

Figure 4-9. As in Figure 4-7, for a new value of the tower-top diameter and a fully tapered tower

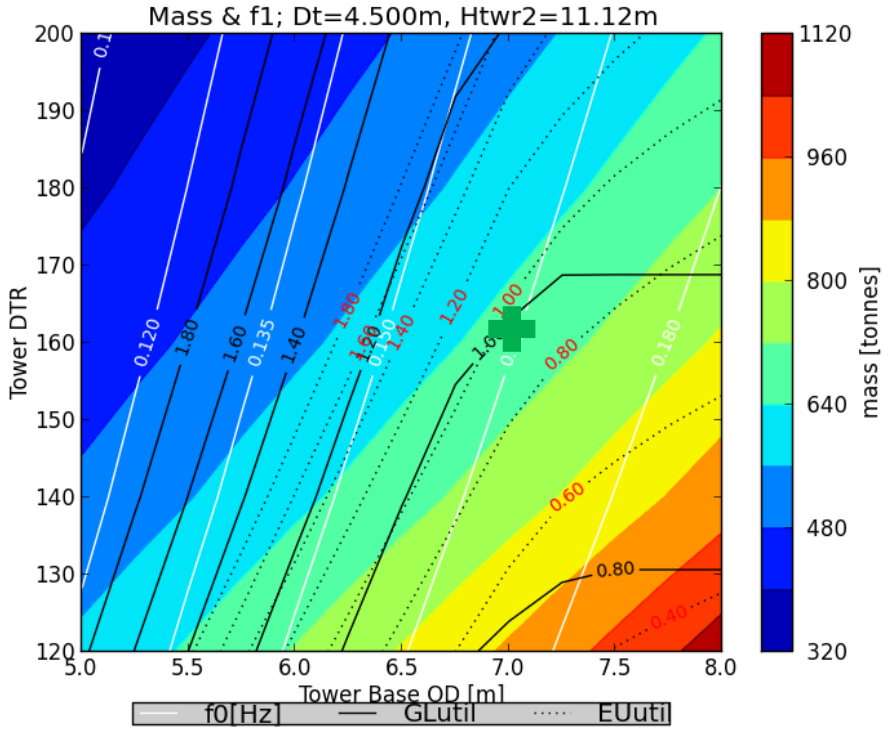

Figure 4-10. As in Figure 4-9, for a tower with an 11.12-m-long constant cross-section segment. The green cross denotes the approximate location of the optimized configuration depicted in Table 4-5 (that configuration has a slightly different length for the tower base segment).

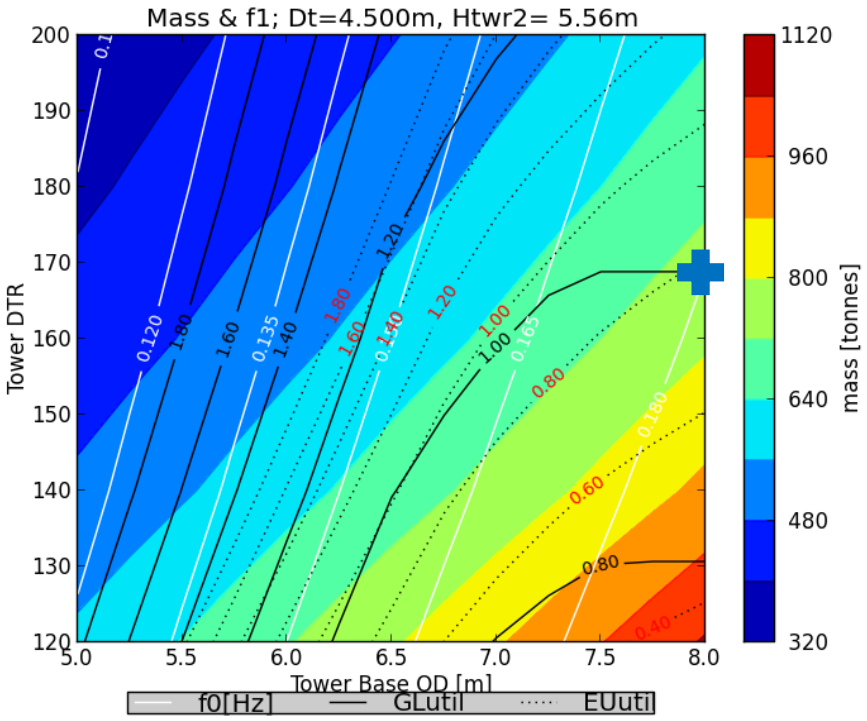

Figure 4-11. As in Figure 4-10, for different length of the constant cross-section segment. The blue cross denotes the approximate location on the graph of the configuration depicted in Table 4-7.

The plots could be used further to evaluate the mass penalty incurred when departing from the minimum mass solution. For example, by allowing for the eigenfrequency to reach 0.17 Hz (0.18 Hz), the mass would increase by some 3% (13%), to yield the configuration in Table 4-6 (Table 4-7).

From these results, and carefully analyzing Figure 4-4, we can observe that the overall minimum in tower mass is reached for a frequency of 0.163 Hz to yield the configuration in Table 4-5. For frequencies below 0.163 Hz, the mass would increase and the utilization ratio may also exceed unity. For eigenfrequencies above 0.163 Hz, whereas utilizations are acceptable, the mass would rapidly increase.

Table 4-6. Optimized Tower Design with a System First Natural Frequency of 0.17 Hz as well as Tower Base Loads

Parameter	Value	Units
Db	7.634	m
Dt	4.5	m
DTR	169	-
Constant cross-section tower segment length	0	m
Tower mass	680.1	tonnes
Expected system first natural frequency	0.17	Hz
Tower base shear force (ULS, unfactored)	2,667 (parked)/2,374 (operational)	Nm
Tower base bending moment (ULS, unfactored)	167,955 (parked)/283,946 (operational)	kNm
Tower base vertical load (tower+RNA weight, unfactored)	15,156	kN
Max tower-top displacement (unfactored)	2.13	m

Table 4-7. Optimized Tower Design with a System First Natural Frequency of 0.18 Hz as well as Tower Base Loads

Parameter	Value	Units
Db	8	m
Dt	4.5	m
DTR	169	-
Constant cross-section tower segment length	5.7	m
Tower mass	747	tonnes
Expected system first natural frequency	0.18	Hz
Tower base shear force (ULS, unfactored)	2,761 (parked)/2,393 (operational)	Nm
Tower base bending moment (ULS, unfactored)	170,145 (parked)/284,410 (operational)	kNm
Tower base vertical load (tower+RNA weight, unfactored)	15,811	kN
Max tower-top displacement (unfactored)	1.88	m

4.5 Conclusions

This study focused on an optimized design for the hurricane-resilient turbine project.

Blade aerodynamic, mass, and stiffness properties were provided by WEI. Details on the nacelle inertial parameters and main geometric parameters were provided by Siemens. An initial FAST model was developed to extract tower-top inertial characteristics. The derived tower-top mass matrix was combined with ultimate rotor loads and further design constraints on the tower geometry to arrive at a design that would demonstrate enough load-bearing capacity and the desired stiffness characteristics. The substructure and soil equivalent stiffness was provided by Keystone Engineering whereas other design constraints based on utilization and manufacturability were set up by NREL based on Germanischer Lloyd (2005) and Eurocode (2007). Keystone Engineering recommended a target system natural frequency of 0.14 Hz, which would place the support structure in the soft-stiff frequency band (between the 1P and 3P rotor forcing bands). This frequency, however, falls within close proximity of the typical wave spectrum energy mode (Figure 4-12). An optimization algorithm was devised that allowed us to achieve a minimum mass configuration while meeting the design constraints and a target first natural frequency.

The findings in this study indicate that a 0.14-Hz system first eigenfrequency cannot be easily achieved given the employed design, geometric, and substructure stiffness assumptions. A minimum mass tower configuration was found with an OWT frequency of approximately 0.163 Hz. However, this value is very close to the cut-in value of the blade passing frequency (0.163 Hz). Tower base loads associated with the parked and operational DLCs were also provided so the substructure can be appropriately sized.

It is recommended that structural resonance be avoided in detailed design by: 1) verifying that the wave-forcing spectrum is characterized by low-energy content at the system's lowest (2 or 3) eigenfrequencies, and 2) designing a control system capable of frequency hopping in case the system's first eigenfrequency falls within the 3P range.

We provided additional design configurations that featured a first natural frequency some 5%–10% higher (0.17–0.18 Hz) than the cut-in 3P frequency. Whereas those solutions likely avoid the start-up phase dynamics and reduce the risk of resonance under wave dynamics (forcing energy peaks at approximately 0.15 Hz), they do require a dedicated controller to minimize the possibility of resonance in the turbine power-curve region two and are associated with a 3%–13% mass penalty.

Given the uncertainties in soil characteristics and in the details of the final design, fine-tuning the first natural frequency may not provide additional value to this research; a more in-depth study should be performed at a later stage in the detail design phase.

Finally, it is worth underlining the fact that the downwind placement of the RNA center of mass adds some 100 tonnes (>15%) to the design when compared to an upwind configuration. Additionally, fatigue loads should be calculated and the integrity of the structure verified. If the

substructure stiffness changes, new iterations should be carried out to ensure the system response is still as desired and avoids resonance.

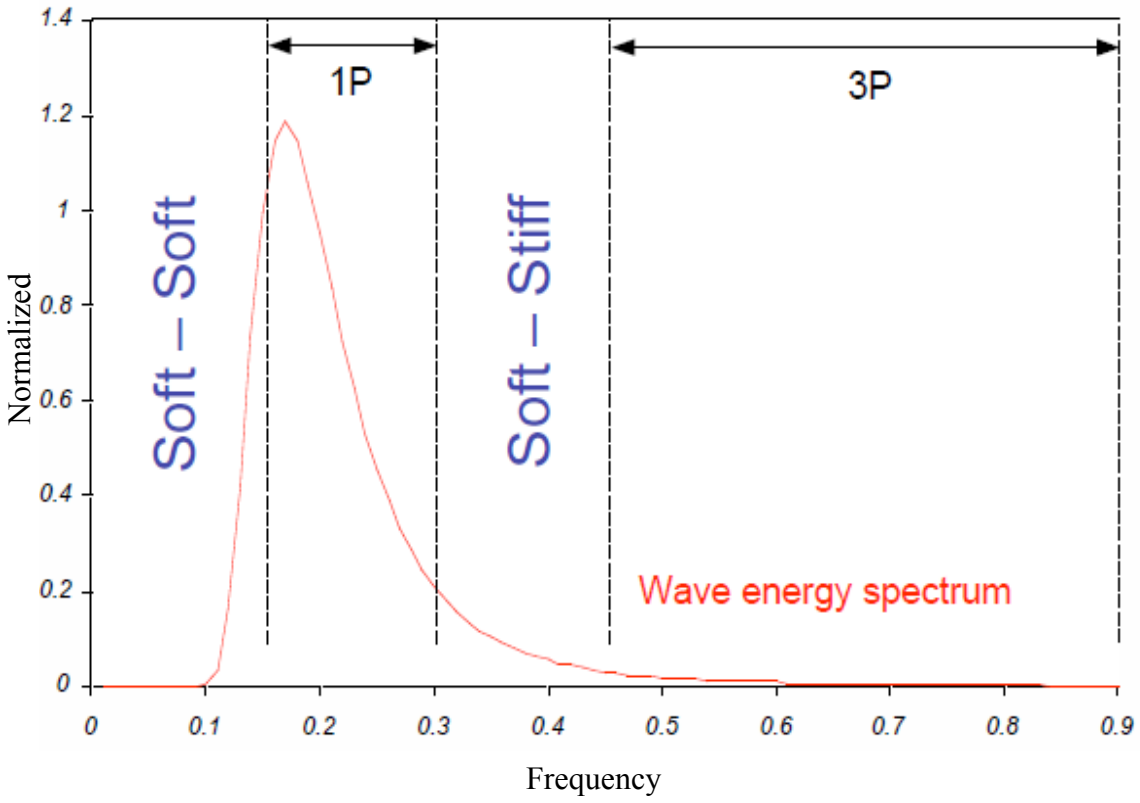

Figure 4-12. Typical arrangement for offshore wind support structures. For the OWT in this study, the 1P and 3P ranges are between [0.054; 0.124] and [0.163; 0.373] Hz, respectively

5 Substructure and Foundation Concept Design

This section was prepared by Keystone Engineering Inc. for NREL to assist in the design of an offshore wind turbine system to be deployable in the Western Gulf of Mexico region. This section contains specific information about the design methodology and results of the conceptual design of the substructure and foundation. A fabrication and installation cost comparison between the final IBGS design and a typical four-piled jacket is also presented. This document includes the relevant standards according to which the design was carried out.

5.1 Background and Objective

The goal of this work was to design the substructure and foundation for an offshore wind turbine system to be deployable in the Western Gulf of Mexico region. As such, the wind turbine system would be subjected to hurricane loading conditions. Per AWEA (2012), a medium-consequence failure was considered for an offshore wind turbine support structure, which corresponds to L-2 exposure category as specified in API RP 2A (American Petroleum Institute 2014). Based on that, the structure would be designed for ULS and robustness conditions for return periods of 50 years and 500 years, respectively. This design work ties in with the remainder of the offshore wind system design developed by the team. The turbine rotor was optimized by WEI; the nacelle components, including the permanent-magnet generator, were sized by Siemens; and the preliminary substructure information was provided by Keystone Engineering. Based on geometric and load data produced by these partners, NREL generated a preliminary design tower with associated load parameters. Afterward, Keystone Engineering developed a final design of the substructure, which is summarized in this section.

The objective of this section is to describe the procedures and basic parameters used to perform a preliminary design of the substructure and foundation. It also provides a summary of analyses results as well as the verification parameters for a coupled analysis of the complete system. The second objective is to perform a fabrication and installation cost comparison between the IBGS and a typical jacket to show a reduction in capital that contributes to an overall reduction in the COE.

Primary steel design conforms to guidelines as outlined in IEC 61400-3 (International Electrotechnical Commission 2009), ISO 19902 (ISO 2007), API RP2A (American Petroleum Institute 2014), and API RP2 MET (American Petroleum Institute 2010) wherever applicable. Primary steel is designed in accordance with IEC 61400-3 (International Electrotechnical Commission 2009). IEC 61400-3 provides load factors for ultimate loads and refers to ISO 19902 for resistance factors. API provides guidance for performing robustness checks in hurricane regions.

5.2 Design Premise

The purpose of the analyses described below is to demonstrate that, based on estimated tower loadings provided by NREL, the substructure and foundation meet the criteria defined in this report as well as have the required strength to resist ULS hurricane loadings. The structural natural frequency will be checked to comply for operating turbine limits.

Three analyses are included in this stage of design:

- Natural Frequency Analysis—To demonstrate that the natural frequency of the support structure is within the allowable range as specified in the *Tower Conceptual Design Report* (Chapter 4). The minimum allowable frequency considered for this preliminary design is provided in Section 4.5.
- ULS—To demonstrate that the substructure and foundation are designed to resist extreme loading without overstressing any primary steel member or foundation failure.
- Robustness Limit State—To confirm that the substructure and foundation have adequate strength to withstand the extreme storm loads and tolerate damage without failure or collapse as recommended by API RP2A 22nd edition (American Petroleum Institute 2014).

The design of the heavy wall sleeve sections, reinforced by the grouted pile or caisson, is largely driven by fatigue or necessitated by the interconnecting brace thickness. Fatigue analysis was not within the scope of this study, but the joints were conservatively sized according to experience-based estimates.

5.3 Design Basis

This section describes the criteria and methodology used to perform the primary design of the substructure and foundation. It also states the relevant standards according to which the design was carried out. Section 4.4 describes the design procedure.

5.3.1 Reference Datum

The Bentley Systems SACS V8i, 5.6 offshore FEA structural analysis package was used to develop a space frame model that represents the mass and stiffness of the primary steel members of the support structure.

All elevations shall be relative to mean lower low water. In the SACS global coordinate system, X is “true west,” Y is “true south,” and Z is positive up (Figure 5-1). The SACS local coordinate system is such that the positive X direction is along the member length. The positive member end force directions can be seen in Figure 5-2.

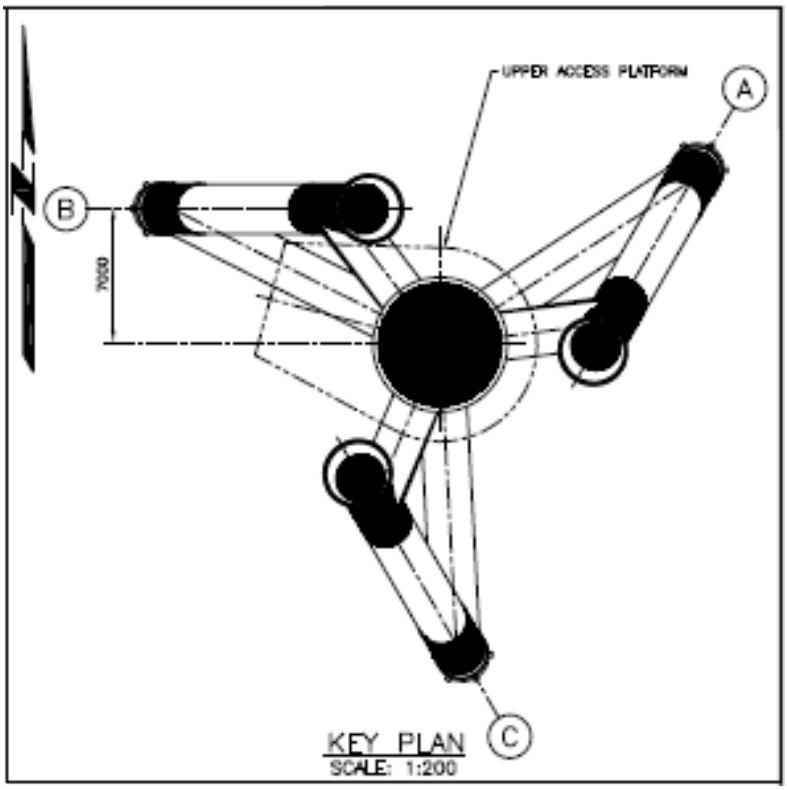

Figure 5-1. Platform orientation

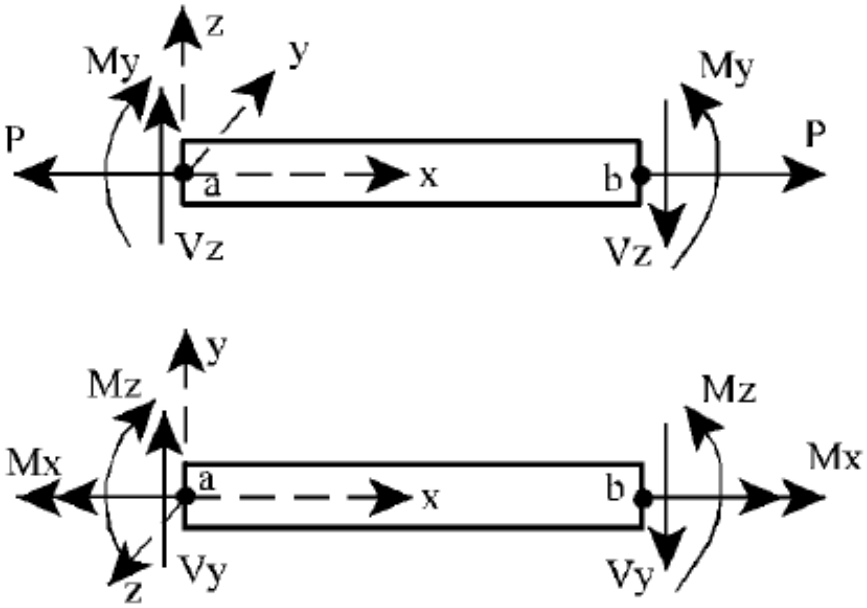

Figure 5-2. SACS positive member end force directions

5.3.2 Wind Turbine

The wind turbine rotor was optimized by Wetzel Engineering and the nacelle components, including the permanent-magnet generator, were sized by Siemens. The tower was designed by NREL and is documented in Section 4 herein. Data in Table 5-1, Table 5-2, and Table 5-3, were extracted from Section 4), presents the main parameters utilized to model the wind turbine in SACS and to perform the analyses.

Table 5-1. Main Geometry Parameters Utilized To Generate the Tower SACS Model

Parameter	Value	Units
Deck elevation	20.7	m
Interface elevation	20.9	m
Hub elevation	135	m
Tower outside diameter at interface elevation	6.96	m
Tower outside diameter at tower-top flange elevation	4.5	m
Maximum outside diameter to thickness along the tower length	163.5	-
RNA center of mass offset from the tower-top flange, in Z direction	2.61	m
RNA center of mass offset downwind along the RNA axis	6	m
Steel density	8,792	kgm^3
Mass of tower	656	tonnes
Mass of RNA	8.646 E+05	kg

Two main loading conditions were considered for the ULS —operational condition and parked condition (Table 5-2). The operational condition represents the maximum rotor thrust; the parked condition represents the situation with the maximum wind speed.

Table 5-2. Turbine-Generated Loads

Turbine Load Condition	Load Description	Value
Extreme loads ULS at interface elevation (parked condition)	Tower base shear force	Fxy = 2,606 kN
	Tower base bending moment	Mxy = 166,598 kN-m
	Tower base vertical load (Tower + RNA)	Fz = 14,918 kN
Extreme loads ULS at interface elevation (operational condition)	Tower base shear force	Fxy = 2,361 kN
	Tower base bending moment	Mxy = 283,660 kN-m
	Tower Base vertical Load (Tower + RNA)	Fz = 14,918 kN

The additional tower parameters used to perform the frequency analysis are provided in Table 5-3. RNA characteristics are applied to the SACS model to capture the mode shape of the integrated system compromised of the tower, substructure, and foundation. The frequency analysis is described in Section 4.5.

Table 5-3. RNA Parameters Used to Perform the Frequency Analysis

Parameter	Value	Units
RNA_ Ixx	342,033,606	kgm^2
RNA_Iyy	215,922,606	kgm^2
RNA_Izz	213,483,330	kgm^2
Expected system first natural frequency	0.16	Hz

5.3.3 Metocean Wave and Wind Criteria

The metocean criteria and environmental data were selected based on a 25-m water depth in the Western Gulf of Mexico as specified by NREL. The critical environmental parameters associated with a 25-m water depth were determined per the Western Gulf of Mexico region addressed in API RP 2MET (American Petroleum Institute 2010) and are listed below:

- Design environmental parameters (50-year return period)
  - H_{max} = 15.0 m
  - T_{Hmax} = 13.0 s
  - Surge/Tide = 1.7 m
  - Current = 2.1 m/s (constant profile)
  - Wind = 39.5 m/s 1-hour mean wind speed at10-m elevation
- Design environmental parameters (10-year return period)
  - H_{max} = 10.1 m
  - T_{Hmax} = 11.3 s
  - Surge/Tide = 1.1 m
  - Current = 1.52 m/s (constant profile)
  - Wind = 30.7 m/s 1-hour mean wind speed at 10-m elevation
- Design environmental parameters (500-year return period)
  - H_{max} = 21.0 m
  - T_{Hmax} = 14.8 s
  - Surge/Tide =2.45 m
  - Current = 2.44 m/s (constant profile)
  - Wind = 52.1 m/s 1-hour mean wind speed at 10-m elevation.

The above values are the extreme environmental loads provided by API RP 2MET (American Petroleum Institute 2010). Combining these extreme values to generate the sea state representing

the simultaneous occurrence of wave, wind, current, and surge loads, at the same return period, is very conservative. To more accurately combine statistically independent extreme environmental loads, load factors per Table C.25 of API RP 2MET were applied accordingly.

For load cases corresponding to a 50-year return period and 500-year return period, the following load conditions were considered:

- For wave-dominant load cases, the wind speed was reduced by a factor of 0.95, whereas the wave height was reduced by a factor of 0.95 for wind-dominant load cases.
- For the environmental cases using metocean criteria of each return period, the current was reduced by a factor of 0.8.
- To consider the directional offset of wind-heading from wave-heading, and current-heading from wave-heading, a (-)15-degree offset was applied to the ULS and robustness analyses load combinations for both wind- and wave-dominant load cases.

5.3.4 Marine Growth

The marine growth profile was selected as specified in Table C.21 of API RP 2MET (American Petroleum Institute 2010). Thirty-eight mm of marine growth thickness was considered for the design from 0 m to (-)10 m. Marine growth thickness was then linearly interpolated between 38 mm to 10 mm from (-)10 m to (-)50 m. The specific gravity of the marine growth was assumed to be 1.2.

5.3.5 Soil Properties

The soil profile was based on a geotechnical report generated in 2006 for a previous project in the vicinity of South Padre Island, Texas. The report included p-y data, pile bearing capacity, and skin friction factors used to simulate the pile soil interaction in SACS. The generalized soil stratigraphy describing soil properties for this location is shown in Table 5-4.

Table 5-4. General Soil Stratigraphy

Stratum	Depth (m)	Description
I	0–25	Very soft to very stiff clay
II	25–35	Medium-dense to dense-fine sand
III	35–50	Very stiff clay
IV	50–60	Medium-dense to dense-silty fine sand
V	60–75	Very stiff to hard clay

5.4 Design Procedure

5.4.1 Model

SACS is used to develop a space frame model that represents the mass and stiffness of the primary steel members of the support structure. The foundation (i.e., piles) is represented by

nonlinear pile-soil interactions along the length of the piles. For preliminary analyses, secondary steel is modeled as point masses at the center of gravity of each particular item (e.g., boat landing, access and egress system, j-tubes, and platforms.). To account for the loads generated by the environmental loading on the nonmodeled secondary steel, a representative area is also included that allows the nonmodeled secondary steel to attract wave loading, current loading, and wind loading. SACS is used to generate the loads associated with the waves by discretely stepping the wave through the structure. The static equivalent of the aerodynamic wind turbine generator (WTG) loads are added at the interface flange, the interface between the connection flange of the turbine and the connection flange of the substructure. The analyses consider the integrated system, comprised of the RNA and the support structure, including the tower, substructure, and the foundation.

5.4.2 Natural Frequency Analysis

To determine the eigenfrequencies of the support structure, it is necessary to linearize the soil curves. To predict the minimum stiffness at which the turbine would still be operating, the maximum operational turbine load is applied coincidentally with the metocean loading associated with a 10-year return period storm. Based on the pile deflections calculated under this loading, a pile super element is calculated that represents linear mudline stiffness. The frequency calculations are then performed in SACS.

5.4.3 ULS Analysis

Preliminary ULS analysis is performed by applying the wind turbine loadings (weight, shear, and overturning moment) on the interface flange, along with the metocean loadings (wave, wind, and current) corresponding to a 50-year return period and the gravity loading. The WTG and the metocean loads were combined per IEC 61400-3 (International Electrotechnical Commission 2009) and applied omni-directionally in 30-degree increments for each load case (Table 5-5). A load factor of 1.35 is included for the environmental and turbine loads per IEC 61400-3 (International Electrotechnical Commission 2009).

For the operational design load cases (DLC 1.6), the 10-year extreme hurricane environmental loading characteristics were used as an estimate of the metocean conditions associated with a severe sea state per section 6.1.4.3 of IEC 61400-3 (International Electrotechnical Commission 2009). For the extreme design load case (DLC 6.1), the 50-Year extreme hurricane environmental loading characteristics were used as an estimate of the metocean conditions associated with an extreme sea state per section 6.1.4.5 of IEC 61400-3 (International Electrotechnical Commission 2009). The primary structural members, the pile capacities, and the soil capacity safety factors were code checked per ISO 19902 (ISO 2007).

Table 5-5. ULS Load Case Description

SACS Load Case	IEC Load Case	Turbine Loads	Wave Loads	Environmental Load Factor	Gravity Load Factor
A000 – A330	1.6	Operating case	10-year maximum wave	1.35	1.1
B000 – B330	1.6	Operating case	10-year maximum wave	1.35	0.9
C000 – C330	6.1	Parked case	50-year wave dominant	1.35	1.1
D000 – D330	6.1	Parked case	50-year wave dominant	1.35	0.9
E000 – E330	6.1	Parked case	50-year wind dominant	1.35	1.1
F000 – F330	6.1	Parked case	50-year wind dominant	1.35	0.9

5.4.4 Robustness Analysis

A preliminary robustness analysis was performed for unfactored metocean loads associated with a 500-year return period combined with WTG loads and gravity. The metocean and WTG loads were applied omni-directionally in 30-degree increments for each load case. The metocean loads and WTG loads are combined per IEC 61400-3 (International Electrotechnical Commission 2009) (Table 5-6). The WTG loads were obtained by factoring the WTG loads associated with a 50-year return period with the WTG in a parked condition. The factors were obtained by squaring the ratio of 500-year wind speed to the 50-year wind speed. Code checking of members is performed according to ISO 19902 (ISO 2007).

Table 5-6. Robustness Load Case Description

SACS Load Case	Turbine Loads	Wave Loads	Environmental Load Factor	Gravity Load Factor
H000 – H330	Parked case	500-year wave dominant	1.0	1.0
Y000 – Y330	Parked case	500-year wind dominant	1.0	1.0

All of the partial safety factors and material resistance factors were set to 1.0 per API (American Petroleum Institute 2014).

5.5 Frequency Analysis Results

The eigenfrequencies of the complete structural system, including the foundation, tower, and turbine, are tuned to avoid the operating 1P and 3P frequency ranges of the turbine. The sleeve spacing, batter (rake) angle, work point elevations, pile OD, pile wall thickness, caisson OD, caisson thickness, brace sizes, sleeve thicknesses, and elevation of braces can all be adjusted to tune the structural system frequency. Table 5-7 presents the conceptual design's first natural frequency. Natural frequencies are within the acceptable range discussed in Tower Conceptual Design (Section 4 herein).

Table 5-7. Natural Frequencies

Site	Allowed Frequency Range (Hz)	SACS Computed Frequency (Hz)
25-m water depth	0.16 – 0.19	0.174

This preliminary analysis only considers the checking of the first natural frequency because it contains the most energy. However, in the detail design, the possible resonances with the higher frequencies would be investigated.

5.6 ULS Analysis Results

5.6.1 Method of Analysis

SACS is used to develop a space frame dynamic analysis model that represents the mass and stiffness of primary and secondary structural steel members. The model includes the heavy wall joint cans and the major appurtenances. Typical analysis practices and the analysis results for the conceptual design are reviewed below.

Concentric grouted tubular members were used to represent the composite properties of IBGS piles and pile sleeves, and caisson and caisson sleeve, members. The mass of the grout in the annular space was accounted for by SACS (grout option).

Flooded members were identified in the model, and the entrapped water mass was included for all flooded members. The entrained (added water) mass factor was assumed to be 1.0 perpendicular to submerged members and zero in line with the member.

5.6.2 Member and Connection Utilization Ratio (Unity Check)

For the ULS analysis, the wind turbine loads (weight, shear, and overturning moment) corresponding to a parked and operational load condition on the IBGS foundation, along with the metocean loads (wind, wave, and current) corresponding to a 50-year and 10-year return period, were analyzed omni-directionally. All members and connections were designed per ISO 19902 (ISO 2007). The maximum member utilization ratio is 0.94 and occurs in the conical transition piece. The maximum joint utilization ratio is 0.83 and occurs in the upper pile sleeve can. The summary of the ULS steel utilization ratios for the guide structure members (transition, sleeves, and braces) and connections can be found in Appendix A.

5.6.3 Foundation Analysis Results

The pile utilization ratio is determined by the capacity of the pile caused by the combined effects of the axial and lateral loads transferred by the jacket. The maximum utilization ratio of the pile is 0.66 and the maximum utilization ratio of the caisson is 0.39.

The minimum safety factor against failure of the soil is 1.52. A summary of the pile utilization ratios and soil capacities can be found in Appendix B.

5.7 Robustness Analysis Results

5.7.1 Member and Connection Utilization Ratio (Unity Check)

For the robustness analysis, wind turbine and sea state loads corresponding to a 500-year return period were applied to the IBGS foundation omni-directionally. All members and connections were designed per ISO 19902 (ISO 2007). The maximum member utilization in the jacket structure is 0.96 and occurs in the lower diagonal brace. The maximum joint utilization is 0.80 and occurs in the upper pile sleeve can. A summary of the results from the robustness analysis can be found in Appendix C.

5.7.2 Foundation Analysis Results

The pile utilization ratio is determined by the capacity of the pile due to the combined effects of the axial and lateral loads transferred by the jacket. The maximum utilization ratio of the pile is 0.99 and the maximum utilization ratio of the caisson is 0.49. The minimum safety factor against failure of the soil is 1.03. A summary of the pile utilization ratios and soil capacities can be found in Appendix D.

5.8 Substructure Cost Comparison

The following cost comparisons reveal the associated savings realized when utilizing the patented Keystone Engineering IBGS. A comparison of the weight of primary steel, the weight of secondary steel, the piling weight, the fabrication cost, and the installation cost between the IBGS and a typical four-piled jacket substructure was performed. The traditional four-piled jacket was modeled using SACS and analyzed for the same tower load and metocean criteria as the IBGS. Frequency, ULS, and robustness analyses were performed. Both designs were optimized to reduce material weight yet still be able to sustain hurricane loads and to satisfy the frequency requirement. A comparison of the SACS models can be seen in Figure 5-3. Table 5-8 compares the ULS maximum utilization ratios and first eigenfrequency for the two jackets.

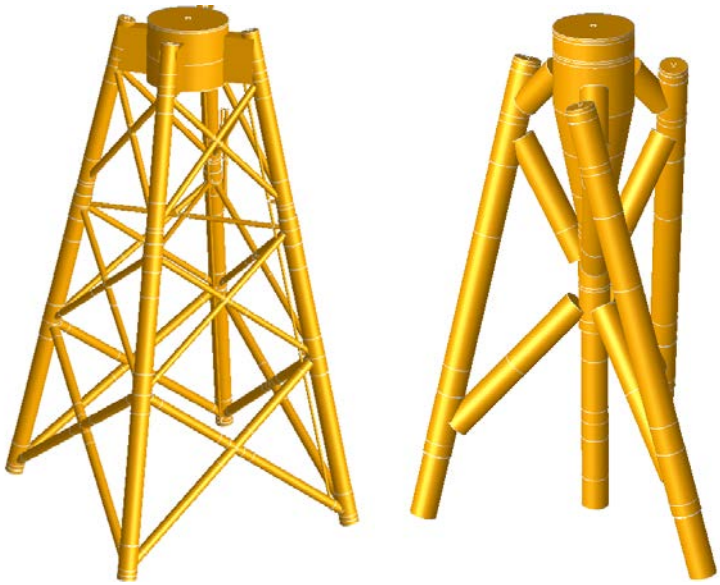

Figure 5-3. SACS models of the traditional jacket (left) and the IBGS (right)

Table 5-8. Comparison of IBGS and Traditional Jacket Analysis Results

ULS Analysis	IBGS	Traditional Jacket
Member UC	0.96	0.94
Joint UC	0.83	0.85
Pile UC	0.99	0.99
Frequency	0.174	0.160

A summary of the bill of materials, fabrication cost, and installation cost for the IBGS and the traditional jacket can be found in Table 5-9. A detailed bill of materials and cost breakdown can be found in Appendices E and F, respectively. As can be seen, the primary steel weights are similar between the IBGS and traditional jacket; however, after accounting for the increases in secondary steel and piling, the IBGS results in a substructure with a reduced total weight, fabrication cost, and installation cost. The increase in secondary steel for the traditional jacket is a result of increased anode weight caused by a higher number of members and the need for mud mats. Total jacket weight includes the weight of additional reinforcement for the transition piece.

Table 5-9. Weight and Cost Comparison of the IBGS and Traditional Jacket

	IBGS	Traditional Jacket	Savings (%)
Primary steel (tonne)	602	605	0
Secondary steel (tonne)	83	103	24
Total jacket weight (tonne)	745	767	3
Total pile weight (tonne)	604	734	17
Fabrication cost	$5,595,881	$ 6,116,435	9
Installation cost	$755,566	$ 1,011,595	25

Note that the fabrication cost savings is higher than the savings in jacket weight. This increase in the fabrication cost savings to 9% can be realized when implementing the IBGS because of the lower fabrication cost of the primary steel for the IBGS foundation. A large portion of the fabrication cost is due to welding of the steel members. The IBGS uses fewer members and, subsequently, less joint cans than the traditional jacket that results in a lower unit cost of steel. The IBGS is also well suited for a mass manufacturing assembly line approach.

A cost savings can also be realized when considering the installations of the different substructures. Because the height and footprint of the IBGS are less than the traditional jacket, more IBGS foundations can be transported on existing multipurpose transportation and installation vessels. The IBGS installation uses proven pre-piling (caisson installation similar to monopiles), above-water leveling, (guide structure installation similar to monopile transition), and post-piling (battered pile installation similar to jackets) procedures. Also, no diver or remotely operated vehicle intervention is required, thus providing advantages over traditional jacket pre- or post-piling installation scenarios. Welding of pile sections in the field during installation or to the jacket structure is also not required when using the IBGS foundation.

Decommissioning costs are not expected to be significant for the IBGS foundation since access to cut the piles is not limited. After salvaging the steel from the IBGS, decommissioning of the foundation can result in a positive net cost.

5.9 NREL SubDyn Model Validation

The following results may be used to validate the SubDyn model produced by NREL for the hurricane-resilient turbine. All results were generated from the SACS space frame models of the jacket structure without modeling the turbine.

5.9.1 IBGS Eigenfrequencies

The first 10 eigenfrequencies for the IBGS jacket are presented in Table 5-10. Two support conditions were investigated, including clamped pile heads and nonlinear pile-soil interaction. The frequencies were calculated assuming that all of the members were nonflooded, marine growth was not present, and added masses were neglected. To accurately model the pile soil interaction, the soil profile was linearized after applying ULS loads to the structure. The ULS loads include metocean criteria consistent with a 10-year return period, tower loads during the parked condition, and the self-weight of the structure. Environmental and tower loads were applied in both the platform zero and 90-degree directions to generate the pile head stiffness in two directions.

Table 5-10. IBGS Eigenfrequencies for Clamped and Nonlinear Soil Interaction Support Conditions

Mode	Clamped Pile Head Frequency (Hz)	Pile-Soil Interaction Frequency (Hz)
1	3.907080	2.361693
2	3.907459	2.365342
3	4.071976	3.712149
4	6.451437	6.407723
5	6.451947	6.412541
6	7.222403	7.626446
7	7.222419	7.627876
8	7.831278	8.482193
9	9.759542	12.283156
10	14.348294	14.101282

5.9.2 IBGS Mass and Stiffness Matrices

The global mass and stiffness matrices are presented in Table 5-11 and Table 5-12, respectively. The global matrices produced by SACS have been reduced so that only the degrees of freedom with respect to the transition piece work point have been retained. SACS reduces the global stiffness matrix by traditional matrix analysis methods and reduces the mass matrix by the Guyan method. Pile head or clamped supports were not modeled when determining the global matrices.

Table 5-11. Global IBGS Mass Matrix with Respect to the Transition Piece Work Point WP1A (0.0, 0.0, 20.9)[m]

Global Mass Matrix with Respect to WP1A (0.0, 0.0, 20.9)[m]							
(KG,M)							
JOINT		WP1A	WP1A	WP1A	WP1A	WP1A	WP1A
	DOF	DX	DY	DZ	RX	RY	RZ
WP1A	DX	5.565E+05	-1.906E+03	-6.142E+02	-8.181E+05	-5.845E+06	-3.654E+03
WP1A	DY	-1.906E+03	5.562E+05	-6.957E+01	5.854E+06	-7.503E+05	3.391E+02
WP1A	DZ	-6.142E+02	-6.957E+01	5.178E+05	3.244E+01	1.088E+04	9.530E+05
WP1A	RX	-8.181E+05	5.854E+06	3.244E+01	8.128E+07	5.715E+05	1.591E+04
WP1A	RY	-5.845E+06	-7.503E+05	1.088E+04	5.715E+05	8.089E+07	6.750E+04
WP1A	RZ	-3.654E+03	3.391E+02	9.530E+05	1.591E+04	6.750E+04	1.163E+07

Table 5-12. Global IBGS Stiffness Matrix with Respect to the Transition Piece Work Point WP1A (0.0, 0.0, 20.9)[m]

Global Stiffness Matrix with Respect to WP1A (0.0, 0.0, 20.9)[m]							
(N,M)							
JOINT		WP1A	WP1A	WP1A	WP1A	WP1A	WP1A
	DOF	DX	DY	DZ	RX	RY	RZ
WP1A	DX	1.826E+08	6.896E+05	5.523E+05	1.466E+09	-1.774E+09	2.331E+06
WP1A	DY	6.896E+05	1.828E+08	1.020E+05	1.773E+09	1.437E+09	-3.421E+05
WP1A	DZ	5.523E+05	1.020E+05	3.449E+09	8.222E+04	-1.121E+07	-3.786E+09
WP1A	RX	1.466E+09	1.773E+09	8.222E+04	9.633E+10	-2.706E+08	-1.109E+07
WP1A	RY	-1.774E+09	1.437E+09	-1.121E+07	-2.706E+08	9.647E+10	-4.255E+07
WP1A	RZ	2.331E+06	-3.421E+05	-3.786E+09	-1.109E+07	-4.255E+07	1.519E+10

5.9.3 IBGS Mass and Buoyancy

The total mass and buoyancy of the IBGS, as modeled in SACS, is presented in Table 5-13 and Table 5-14. The mass and buoyancy are reported while considering and neglecting marine growth per section 5.3.4

Table 5-13. Mass and Buoyancy of IBGS Neglecting Marine Growth

Mass (kg)		Buoyancy (kN)
948,929		3,007.5
Center of Mass (m)		
x	y	z
0	0	0.651
Center of Buoyancy (m)		
x	y	z
0	0	-10.264

Table 5-14. Mass and Buoyancy of IBGS Accounting for Marine Growth

Mass (kg)		Buoyancy (kN)
1,000,591		3,442.5
Center of Mass (m)		
x	**y**	**z**
0	0	0.035
Center of Buoyancy (m)		
x	**y**	**z**
0	0	-10.392

5.9.4 Pile-Soil Stiffness Matrices

To model the inherent flexibility of the pile foundations, the jacket supports were modeled in SACS with use of the pile-soil-interaction module. This module develops super elements to model the foundations based on user-generated soil "p-y" curves. The stiffness matrices for the pile and caisson super elements are presented in Table 5-15 through Table 5-18. The matrices were developed assuming all members were nonflooded, added masses were neglected, and no marine growth was present. ULS loads were applied to the structure, including metocean criteria representative of a 10-year return period and tower loads in the parked condition before extracting the pile head stiffness.

Table 5-15. Pile Head Stiffness (kN/m) for Joint WP1J (-13.116, -8.723, -25.0)[m]

	RX	RY	RZ	DX	DY	DZ
RX	1.1005E+09	1.8931E+05	7.6516E+09	-1.0224E+03	7.7627E+05	-1.9191E+05
RY	1.8931E+09	3.2905E+09	1.3265E+10	-7.7299E+05	8.7390E+02	1.1010E+05
RZ	7.6516E+09	1.3265E+10	5.3626E+10	1.9139E+05	-1.1100E+05	1.4846E+02
DX	-1.0223E+03	-7.7299E+05	1.9139E+05	1.8712E+05	1.2282E+05	4.9741E+05
DY	7.7627E+05	8.7390E+02	-1.1100E+05	1.2282E+05	3.3019E+05	8.6210E+05
DZ	-1.9191E+05	1.1010E+05	1.4846E+02	4.9741E+05	8.6210E+05	3.6013E+06

Table 5-16. Pile Head Stiffness (kN/m) for Joint WP1K (0.995, 15.723, -25.0)[m]

	RX	RY	RZ	DX	DY	DZ
RX	1.1020E+09	-1.8936E+09	7.6566E+09	-1.5683E+03	7.7569E+05	1.9206E+05
RY	-1.8936E+09	3.2881E+09	-1.3261E+10	-7.7359E+05	1.5781E+03	1.1086E+05
RZ	7.6566E+09	-1.3261E+10	5.3627E+10	-1.9109E+05	-1.1038E+05	-9.7819E+00
DX	-1.5683E+03	-7.7359E+05	-1.9109E+05	1.8732E+05	-1.2343E+05	4.9758E+05
DY	7.7569E+05	1.5781E+03	-1.1038E+05	-1.2343E+05	3.2989E+05	-8.6175E+05
DZ	1.9206E+05	1.1086E+05	-9.7819E+00	4.9758E+05	-8.6175E+05	3.6014E+06

Table 5-17. Pile Head Stiffness (kN/m) for Joint WP1L (14.115, -7.0, -25.0)[m]

	RX	RY	RZ	DX	DY	DZ
RX	4.3852E+09	1.8441E+04	-1.5318E+10	-1.8196E+03	7.7464E+05	-5.1988E+02
RY	1.8441E+04	8.5819E+06	5.2689E+03	-7.7459E+05	1.9681E+03	-2.2131E+05
RZ	-1.5318E+10	5.2689E+03	5.3623E+10	-5.1988E+02	2.2132E+05	-1.4853E+02
DX	-1.8196E+03	-7.7459E+05	-5.1988E+02	4.0096E+05	-4.2682E+02	-9.9559E+05
DY	7.7464E+05	1.9681E+03	2.2132E+05	-4.2682E+02	1.1652E+05	-1.2195E+02
DZ	-5.1988E+02	-2.2131E+05	-1.4853E+02	-9.9559E+05	-1.2195E+02	3.6011E+06

Table 5-18. Caisson Head Stiffness (kN/m) for Joint WP1P (0.0, 0.0, -25.0)[m]

	RX	RY	RZ	DX	DY	DZ
RX	7.3994E+06	5.1214E+02	0.0000E+00	-8.6488E+01	7.6575E+05	0.0000E+00
RY	5.1214E+02	7.4037E+06	0.0000E+00	-7.6647E+05	8.6488E+01	0.0000E+00
RZ	0.0000E+00	0.0000E+00	5.8000E+10	0.0000E+00	0.0000E+00	0.0000E+00
DX	-8.6488E+01	-7.6647E+05	0.0000E+00	1.2345E+05	-1.8526E+01	0.0000E+00
DY	7.6575E+05	8.6488E+01	0.0000E+00	-1.8526E+01	1.2329E+05	0.0000E+00
DZ	0.0000E+00	0.0000E+00	0.0000E+00	0.0000E+00	0.0000E+00	4.2867E+06

5.9.5 Static Load Results Summary

The following results are caused by a single static force and moment applied to the transition piece work point (SACS joint WP1A) of the jacket structure. For the purposes of this analysis, all environmental loads and the self-weight of the structure were neglected. One-thousand kN of shear were applied in the positive x-direction, and 100,000 kNm were applied about the y-axis in the positive direction. A summary of the member end forces is presented in Appendix G. Overall reactions and displacements of the transition piece work point can be found in Table 5-19 and Table 5-20.

Table 5-19. Global Reaction Relative to the Mudline

F_x (kN)	F_y (kN)	F_z (kN)	M_x (kNm)	M_y (kNm)	M_z (kNm)
1,000.0	0.0	0.0	0.0	145,900.2	0.0

Table 5-20. Displacements and Rotations of Joint WP1A (0.0, 0.0, 20.9)[m]

δ_x (cm)	δ_y (cm)	δ_z (cm)	θ_x (rad)	θ_y (rad)	θ_z (rad)
2.104	-1.104	-0.003	-1.068E-03	1.570E-03	1.780E-05

6 Turbine System Maximum Loads Prediction

This report section summarizes the work performed by NREL to estimate the maximum loads that the 10-MW hurricane-resilient WTG would encounter during a hurricane event. To obtain a realistic estimation of the loads, a fully coupled aero-hydro-elastic model of the system was built, including the wind turbine, tower, and Keystone Engineering jacket substructure. A series of simulations was run that encompasses possible nonoperating conditions that the turbine may encounter during a hurricane event. The maximum loads on the structure were taken from these results. Operational simulations were not performed because no turbine controller was developed and because it was found during the turbine optimization that the nonoperating condition was more likely to result in the largest loads.

In Section 6.3, the report summarizes the approach that was taken to develop the model of the system and the set of simulations run. Section 6.4 summarizes the results from these simulations in terms of the maximum loads on the system.

6.1 Modeling Approach

The following sections provide an overview of the wind system model and the process used to verify the model. Figure 6-1 illustrates the general coordinate system used within this project (shown schematically in relation to the analyzed downwind turbine).

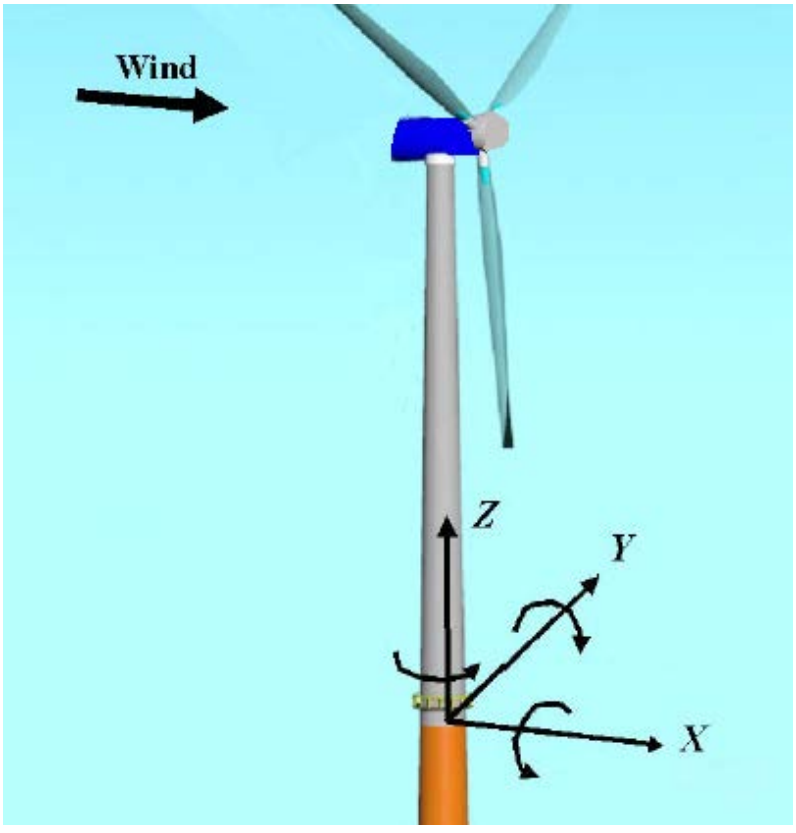

Figure 6-1. General coordinate system used within this project

6.2 Wind System Model

The wind system model was created in FASTv8 (v8.09.00a-bjj) (NREL 2014), NREL's publicly available aero-hydro-servo-elastic wind turbine simulation software. The major subcomponents and their FASTv8 implementation are presented in the following sections.

6.2.1 Blades

The rotor blades were designed by WEI. All simulations conducted within the scope of this project used the FAST blade input file provided by WEI. The mass of a single blade is 61548.047 kg. The blade length (root to tip) is 105 m. The blade was optimized for a rated power of 10 MW and maximum tip speed of 85 m/s (Section 2.2.6 herein).

6.3 Rotor Nacelle Assembly

The RNA model for FASTv8 was created by NREL. The structural properties required for the RNA definition were calculated from the information provided by Siemens (generator and hub) and Wetzel Engineering (rotor).

6.3.1 Tower

The tower was designed by NREL (Section 4). The tower height is 131.9 m (above MSL) and the total tower mass is 654970.375 kg. The tower starts at 20.9 m above MSL. Aerodynamic tower drag is considered in all simulations and a drag coefficient of $C_D = 0.7$ was applied to each segment of the tower. Nacelle drag is not considered within this model. The tower mode shapes, which are used to represent the flexibility of the tower in FAST, were recomputed in BModes (NREL 2014) after the substructure model was completed to consider the influence of the substructure stiffness on the dynamic response of the tower. The stiffness and mass matrices that were used to incorporate the influence of the substructure into the tower mode shape computation are shown in Table 6-1. These matrices were generated by SubDyn (NREL 2014), the substructure dynamics module within FAST (Table 6-1 and Table 6-2).

Table 6-1. Substructure Mass Matrix at TP Reference Point Used for Tower Mode Shape Computation (as reported by SubDyn) [kg, kg-m, kg-m^2]

	X	Y	Z	XX	YY	ZZ
X	4.50E+05	1.24E+00	3.73E+01	-3.98E+05	-2.57E+06	-6.84E+01
Y	1.24E+00	4.50E+05	-2.52E+01	2.57E+06	-3.98E+05	-1.95E+01
Z	3.73E+01	-2.52E+01	5.75E+05	-4.65E+02	-1.37E+02	1.05E+06
XX	-3.98E+05	2.57E+06	-4.65E+02	2.29E+07	1.07E+03	2.41E+02
YY	-2.57E+06	-3.98E+05	-1.37E+02	1.07E+03	2.29E+07	1.46E+03
ZZ	-6.84E+01	-1.95E+01	1.05E+06	2.41E+02	1.46E+03	1.02E+07

Table 6-2. Substructure Stiffness Matrix at TP Reference Point Used for Tower Mode Shape Computation (as reported by SubDyn) [N/m, N/rad, N-m/m, N-m/rad]

	X	Y	Z	XX	YY	ZZ
X	3.80E+08	-2.18E+04	-9.46E+04	1.05E+09	-4.15E+09	2.73E+05
Y	-1.85E+04	3.80E+08	-8.20E+02	4.15E+09	1.05E+09	-2.02E+05
Z	-9.39E+04	-2.95E+04	4.70E+09	8.83E+04	1.17E+06	-3.48E+09
XX	1.05E+09	4.15E+09	2.67E+05	1.23E+11	-8.83E+05	-1.85E+05
YY	-4.15E+09	1.05E+09	9.39E+05	-8.75E+05	1.23E+11	-2.42E+06
ZZ	2.19E+05	-1.46E+04	-3.48E+09	7.66E+05	-2.89E+06	1.78E+10

The first tower-bending frequency reported by BModes is 0.175 Hz, which agrees with what was computed by Keystone Engineering with their SACS model (0.174 Hz).

6.3.2 Substructure

The twisted jacket substructure for the 10-MW hurricane-resilient wind turbine system was designed by Keystone Engineering. The SubDyn model for the FASTv8 simulations was based on the information provided by Keystone Engineering. SubDyn is a finite-element (FE)-based code for the simulation of flexible offshore and land-based support structures that was developed by NREL (2014). SubDyn is distributed together with FASTv8. SubDyn v1.01.01a-rrd was used in this project. Because SubDyn only allows tubular substructure members and is not able to model double-walled tubes, grouting, and member offsets, a few modifications had to be introduced to the initial modeling data provided by Keystone Engineering. Also, the current version of SubDyn is not capable of considering any soil interaction effects. Due to this limitation of SubDyn, the substructure is assumed to be rigidly fixed at its four intersection points with the mudline.

For all double-walled tubes, tubes with grouting, and noncircular substructure members, an equivalent tubular member was introduced. This equivalent member has the same axial and bending stiffness and mass as the original member specified by Keystone Engineering. For double-walled circular tubes with grouting, the outer diameter of the equivalent member is kept constant and the wall thickness, density, and Young's modulus are varied to match the target properties of the original member defined by Keystone Engineering. This problem was solved numerically with a Python script.

The initial Keystone FE model of the substructure was created in SACS. SACS allows for the specification of offsets to avoid any unrealistic overlap between members. SubDyn has plans to model this overlap accurately but that capability has not yet been implemented. To address the overlaps, offset members were introduced to the SubDyn model (Figure 6-2 and Figure 6-3).

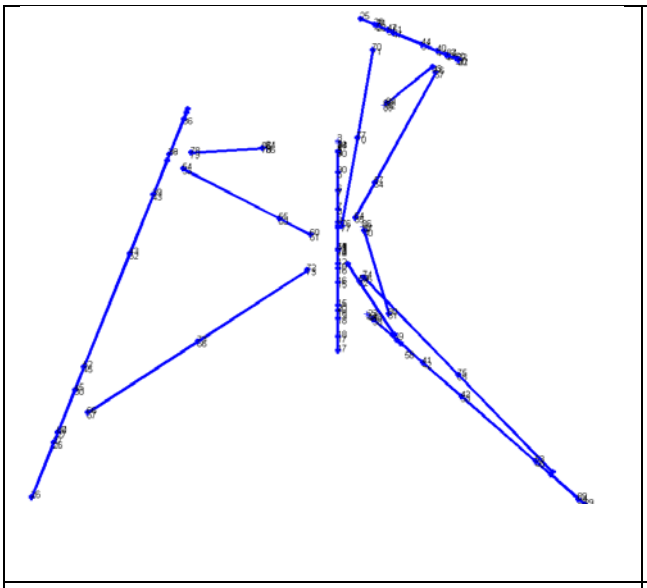

Figure 6-2. SACS substructure model with offsets

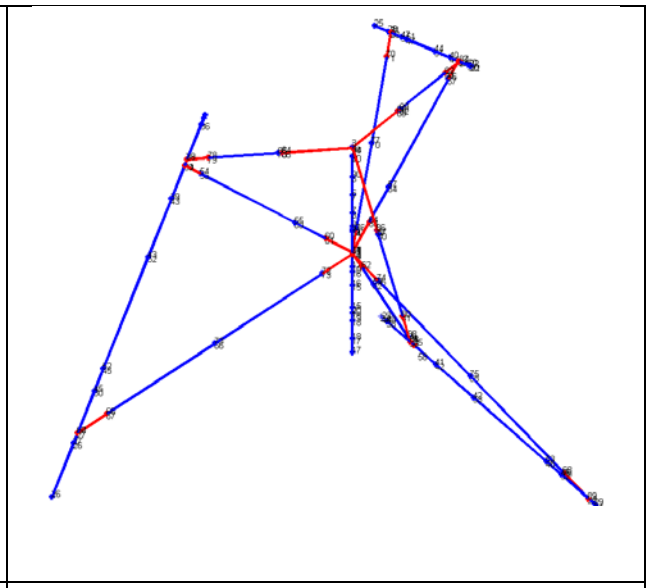

Figure 6-3. SubDyn substructure model with offset members (shown in red)

These offset members have standard steel moduli (Young's modulus: 2E11 N/m^2, shear modulus: 7.86E11 N/m^2), a cross-section diameter of 3.38 m (average of all substructure members), and a wall thickness of 6.04E-02 m (average of all substructure members). The density of the offset members is set to half the value of the average member density: 3.73E3 kg/m^3. Using these offset member properties yields a relatively good match between SACS and SubDyn for the overall substructure mass and the substructure eigenfrequencies.

Marine growth and hydrodynamic coefficients were specified in SubDyn as provided by Keystone Engineering. Marine growth of 38 mm is considered between 0 m and -10 m MSL; between -10 m and -50 m MSL, marine growth is interpolated between 38 mm and 10 mm. A drag coefficient of $C_D = 1.05$ and an added mass coefficient of $C_A = 1.2$ are used for all submerged members. These coefficients were provided by Keystone Engineering and are based on the recommendations in the API standard.

HydroDyn's ballasting feature was used to model the water mass in the flooded substructure members. HydroDyn is a FASTv8 module that computes hydrodynamic loads on fixed and floating substructures; it was developed by NREL and is distributed together with FASTv8. HydroDyn v2.02.00a-adp was used in this project. A Morison-based approach was selected to model the hydrodynamic loads on the substructure. The utilized hydrodynamic coefficients have already been specified in the preceding paragraph and the substructure geometry matches with the SubDyn model. Detailed information about the substructure design is provided in Dibra (2014).

6.4 Model Verification

To understand whether the FASTv8 model that was built was accurate and consistent with other models used in this project, verification of the model was performed. Because the rotor blade input files were provided directly by WEI, and the tower was an in-house NREL design, the main subcomponent that needed to be verified was the SubDyn substructure model.

6.4.1 Mass

The overall substructure mass reported by Keystone Engineering is 948,929 kg. This number reflects the dry substructure (no ballasting) without marine growth. The equivalent mass reported by SubDyn is 1,055,250 kg, which means the SubDyn model is 11.204% heavier than the SACS model. This is caused by the introduction of offset members in the SubDyn model. By further reducing the offset member mass density, this difference could have been easily reduced, but a reduction of the offset member mass density introduced larger differences between SACS and SubDyn in the substructure eigenfrequencies. Due to the nature of this fixed-bottom structure, we decided it was more important to match the eigenfrequencies than to match the mass. An overall mass difference of approximately 10% was considered acceptable for this project.

6.4.2 Eigenfrequencies

The eigenfrequencies of the dry, clamped substructure in air (without the turbine mounted on top of it) compare as shown in Table 6-3.

Table 6-3. Comparison of Eigenfrequencies Between SubDyn and SACS

SubDyn (from SD.SUM file)	SACS	Delta (%)
3.95E+00	3.907080	1.202944398
3.95E+00	3.907459	1.1990145
4.66E+00	4.071976	14.56059662
7.89E+00	6.451437	22.2225374
7.89E+00	6.451947	22.2245006
9.14E+00	7.222403	26.53530965
9.14E+00	7.222419	26.54942894
1.09E+01	7.831278	38.79216138
1.12E+01	9.759543	14.89779798
1.42E+01	14.438294	-1.959331206

The first two eigenfrequencies are the first fore-and-aft and side-to-side bending modes that are controlled by the mass and stiffness of the main legs and their distance from the neutral axis of the substructure. The higher eigenfrequencies contain components of torsional and axial motion. These torsional and axial components are strongly influenced by the properties of the substructure joints. Because the joints were modeled with different approaches in SACS and SubDyn, we expect larger differences between SACS and SubDyn for higher eigenfrequencies.

6.4.3 Marine Growth Mass

The marine growth mass was reported as 51,662 kg by Keystone Engineering. The marine growth mass reported by HydroDyn is 51,113.74 kg (1.06% difference between the HydroDyn and the Keystone Engineering marine growth mass).

6.4.4 Substructure Buoyancy

The substructure buoyancy without marine growth is reported as 3,007.5 kN by Keystone Engineering. The buoyancy of the substructure reported by HydroDyn is 3,079.31 kN (2.33% difference between the Keystone Engineering and the SubDyn buoyancy). These buoyancy values consider the displaced fluid by the submerged substructure as well as the weight force of the fluid in the flooded substructure members.

6.4.5 Static Load Deflection

A relatively simple static load case without gravity acceleration was used to verify the global stiffness properties of the substructure. A 1,000 kN force in the x-direction and a 100,000 kNm moment about the y-axis are applied to the transition piece or interface. In FASTv8, this is accomplished through a constant wind speed of 33 m/s (locked rotor, blades pitched to 0 deg, tower length adjusted to 120 m, no gravity acceleration). This approach leads to the following interface forces in FAST:

Table 6-4. Absolute Magnitude of FAST Interface Forces

IntfFXss [N]	IntfFYss [N]	IntfFZss [N]	IntfMXss [Nm]	IntfMYss [Nm]	IntfMZss [Nm]
9.98E+05	2.85E+02	1.69E+03	4.63E+06	9.88E+07	5.49E+03

As shown in Table 6-4, the interface force in x-direction and the moment about the y-axis are very close to what is used in SACS. However, due to the nature of the load case implementation in FAST, we can see nonzero values for all the other interface load components (which is different from the load case implementation in SACS). The corresponding mudline reaction forces predicted by FAST and SACS are compared in Table 6-5.

Table 6-5. Absolute Magnitude of Mudline Reaction Forces from FAST and SACS

	ReactFXss [N]	ReactFYss [N]	ReactFZss [N]	ReactMXss [Nm]	ReactMYss [Nm]	ReactMZss [Nm]
FAST	9.98E+05	3.00E+02	1.43E+03	4.62E+06	1.45E+08	7.85E+03
SACS	1E6	0	0	0	1.46E+08	0
Delta (%)	0.18	-	-	-	0.89	-

Excellent agreement was observed between FAST and SACS for the primary mudline reaction loads (ReactFXss and ReactMYss in Table 6-5), but larger differences between SACS and FAST were observed for the interface displacements. The primary (displacements IntfTDXss and IntfRDYss in Table 6-6) agree relatively well between FAST and SACS (considering the different load application approaches and the different implementations of member offsets).The secondary displacements are shown in grey (Table 6-6) because they are probably caused by the additional load components that are present in FAST but not in SACS (Table 6-4).

Table 6-6. Interface Displacements

	IntfTDXss [m]	IntfTDYss [m]	IntfTDZss [m]	IntfRDXss [rad]	IntfRDYss [rad]	IntfRDZss [rad]
FAST	0.01861	-0.00433	0.00000	0.00002	0.00147	0.00000
SACS	0.02104	-0.01104	-0.00003	1.07E-03	1.57E-03	1.78E-05
Delta (%)	11.55	60.75	99.47	97.66	6.49	98.22

6.5 Load Cases

To estimate the extreme loads that occur during a hurricane event, three load case scenarios were investigated. The choice of load cases was based on the work performed by both Keystone Engineering and Wetzel Engineering to understand the design drivers for the jacket substructure and turbine, respectively. Wetzel Engineering focused on a 50-year and a 100-year extreme event (Raina 2013) whereas Keystone Engineering examined a 50-year and a 500-year event (Dibra 2014). NREL ran all three of these conditions, which are summarized below.

For each event, a series of simulations was performed. Each 1-hr simulation was run with six different seeds. Three yaw positions were considered (352, 0, and 8 degrees) and four wave angles (0, 30, 60, and 90 degrees). The wind direction cannot be varied easily within FAST and was therefore not considered. It was assumed that wind turbines would be shut down during hurricane conditions, so operational conditions were not simulated. In total, 72 simulations were run for each of the three extreme events. To limit the number of simulations needed, knock down factors for combining independent extremes as defined in API RP2 MET (American Petroleum Institute, 2010) were not considered.

6.5.1 50-Year Extreme Event

The 50-year extreme load case is based on DLC 6.1 as described by the International Electrotechnical Commission (2008), which is an extreme wind and wave event during parked or idling conditions. The safety factor for this load case is 1.35. Wind conditions for this load case were based on the values set by Wetzel Engineering in its turbine design study. The maximum 3-second gust wind speed was considered to be the driving aerodynamic load event for the characterization of the maximum extreme loads and NREL, therefore, developed a turbulent wind file (using TurbSim) that matched Wetzel Engineering's prescribed turbulence intensity and maximum 3-second gust. The resulting wind file had a slightly different mean wind speed than that used by Wetzel Engineering and Keystone Engineering in their analyses.

Simulated sea state conditions were based on Keystone Engineering's prescribed maximum wave height (Hmax) and maximum period (Tmax) values for the same load case. FAST defines the wave condition using a Joint North Sea Wave Project spectrum with a prescribed significant wave height (Hs) rather than maximum wave height. Hs was set by scaling Hmax by a factor of 1.86 as defined within the API standard. An additional factor of 1.09 was applied to account for the 1 hour simulation time (American Bureau of Shipping, 2013). Hs was then scaled further to account for directional wave spreading by multiplying by a factor of 0.88 (American Petroleum Institute 2010). A gamma of 2.25 was chosen for the spectrum, as recommended for hurricane conditions in (American Petroleum Institute 2010).

Table 6-7. 50-Year Extreme Load Case Parameters

Safety Factor	1.35
WS @ HH (m/s)	49.28
3-sec gust (m/s)	70
Shear exponent	0.11
Turbulence intensity	14.60%
Hmax (m)	15
Hs (m)	8.79
Hs*0.88 (m)	7.74
Tmax (s)	13
Tide level above MSL (m)	1.7
Current (m/s)	2.1
Sim. length (s)	3600
Seeds (wind and waves)	6
Yaw error (deg)	352,0,8
Wave angles (deg)	0, 30, 60, 90
Total number of simulations	72

6.5.2 100-Year Extreme Event

For the 100-year extreme event (see Table 6-8), the load factor is reduced from 1.35 to 1.1. The wind and wave conditions are set using the same process as the 50-year event. The wind conditions were developed with the goal of achieving a maximum 3-second gust of 80 m/s.

Table 6-8. 100-Year Extreme Load Case Parameters

Safety Factor	1.1
WS @ HH (m/s)	55.78
3-sec gust (m/s)	80
Shear exponent	0.11
Turbulence intensity	15%
Hmax (m)	17.2
Hs (m)	10.08
HS*0.88 (m)	8.87
Tmax (s)	13.7
Tide level above MSL (m)	2.3
Current (m/s)	2.1
Sim. length (s)	3600
Seeds (wind and waves)	6
Yaw error (deg)	352,0,8
Wave angles (deg)	0, 30, 60, 90
Total number of simulations	72

6.5.3 500-Year Extreme Event

The 500-year extreme event (see Table 6-9) is considered a robustness check; therefore, the safety factor for this case was set at 1.0. Wetzel Engineering did not run this wind condition, so both the wind and wave conditions were based on those defined by Keystone Engineering. Keystone only prescribed a mean wind speed at 10-m height. Again, the focus was on the three-second gust so this mean speed was scaled to achieve the equivalent three-second gust value. First, the average wind speed at 10-m height was scaled to HH using a power-law extrapolation with a 0.11 exponent (mean wind speed at HH = 69.37 m/s). This value was then multiplied by a factor of 1.43 to obtain the maximum three-second gust. The 1.43 factor was found by comparing the average wind speed and maximum gusts from the 50-year and 100-year cases. A TurbSim file was then generated that matched the three-second gust criterion, which required a slightly altered wind speed at HH of 69.52 m/s.

Table 6-9. 500-Year Extreme Load Case Parameters

Safety Factor	1
WS @ HH [m/s]	69.52
3-sec gust [m/s]	99.01
Shear exponent	11%
Turbulence intensity	15%
Hmax [m]	21.00
Hs [m]	12.31
HS*0.88 [m]	10.83
Tmax [s]	14.8
Tide level above MSL [m]	2.45
Current [m/s]	2.44
Sim. length [s]	3600
Seeds (wind and waves)	6
Yaw error [deg]	352,0,8
Wave angles [deg]	0, 30, 60, 90
Total number of simulations	72

6.6 Loads Analysis

The results of the fully coupled loads analysis are presented and discussed in the following sections. The focus of this study was on extreme loads, which is why all simulation results are presented through extreme load event tables (generated through NREL's MExtremes post-processor (v.1.00.00h-gjh)). All conducted simulations have a total length of 4,600 s whereas the first 1,000 s were disregarded in order to remove any initial transients from the simulation results. The rotor blades are pitched to feather and the rotor is allowed to idle (no brake applied).

The extreme axial stress level of a few selected members was investigated as part of this study. The locations of the selected members are shown in Figure 6-4.

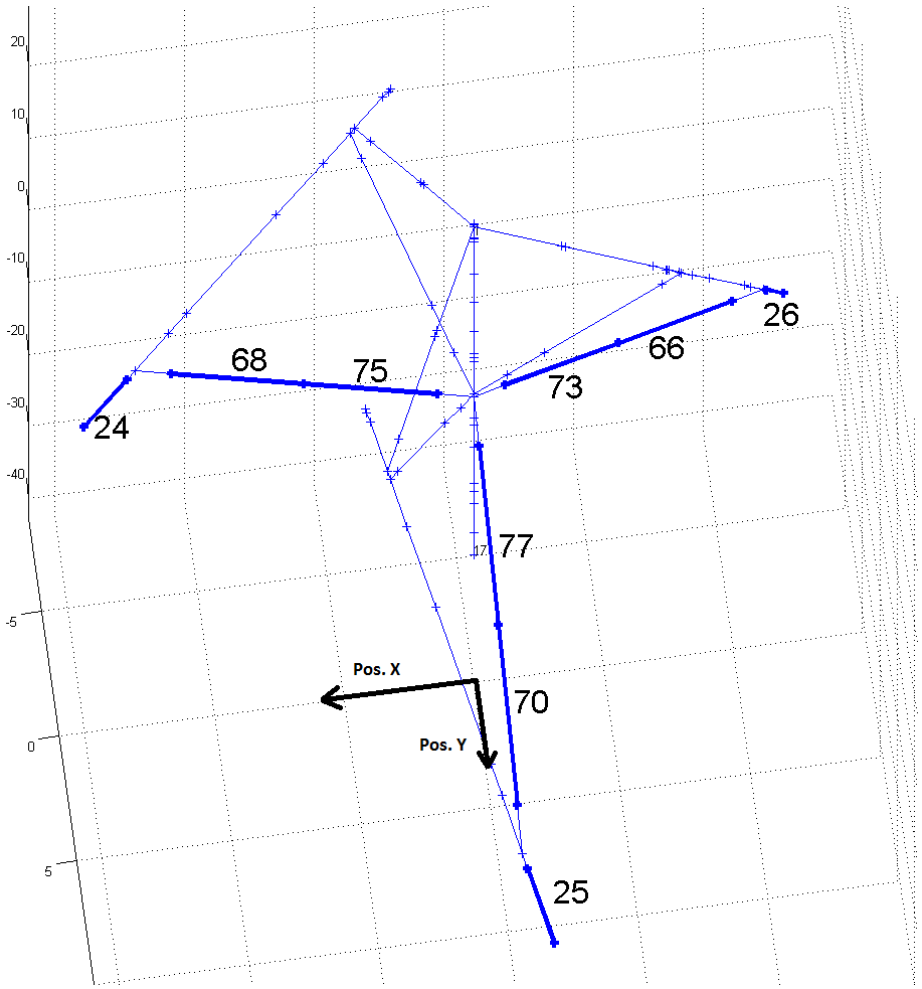

Figure 6-4. Illustration of members considered for axial stress-level evaluation

These members were identified as the most critical for parked extreme load cases by Keystone Engineering (SACS unity check values greater than 0.8).

The load analysis approaches implemented in FASTv8 and SACS are entirely different. While FASTv8 uses a time-domain-based approach, SACS uses a frequency-domain approach to predict system loads and responses. The load analysis in SACS is decoupled and based on superposition of different extreme load components (e.g., aerodynamic and hydrodynamic loads). FASTv8 uses a fully coupled approach that considers the actual turbine condition and motion and its interaction with environmental loads. Because of of FAST's time-domain analysis approach, a relatively large amount of simulated time is needed to statistically cover all relevant combinations of environmental load conditions, turbine conditions, and motions.

6.7 50-Year Extreme Event

To assess the 50-year extreme event loads, the 72 load cases in Table 6-10 were simulated.

Table 6-10. 50-Year Extreme Load Case Simulation Matrix

Load Case #	Wind Seed	Yaw Error	Wave Angle	WaveSeed1	WaveSeed2
1	1	-8	0	307452	3330741
2	1	-8	30	307452	3330741
3	1	-8	60	307452	3330741
4	1	-8	90	307452	3330741
5	1	0	0	307452	3330741
6	1	0	30	307452	3330741
7	1	0	60	307452	3330741
8	1	0	90	307452	3330741
9	1	8	0	307452	3330741
10	1	8	30	307452	3330741
11	1	8	60	307452	3330741
12	1	8	90	307452	3330741
13	2	-8	0	764372	138856
14	2	-8	30	764372	138856
15	2	-8	60	764372	138856
16	2	-8	90	764372	138856
17	2	0	0	764372	138856
18	2	0	30	764372	138856
19	2	0	60	764372	138856
20	2	0	90	764372	138856
21	2	8	0	764372	138856
22	2	8	30	764372	138856
23	2	8	60	764372	138856
24	2	8	90	764372	138856
25	3	-8	0	188856	744372
26	3	-8	30	188856	744372
27	3	-8	60	188856	744372
28	3	-8	90	188856	744372
29	3	0	0	188856	744372
30	3	0	30	188856	744372
31	3	0	60	188856	744372
32	3	0	90	188856	744372
33	3	8	0	188856	744372
34	3	8	30	188856	744372

35	3	8	60	188856	744372
36	3	8	90	188856	744372
37	4	-8	0	199956	700072
38	4	-8	30	199956	700072
39	4	-8	60	199956	700072
40	4	-8	90	199956	700072
41	4	0	0	199956	700072
42	4	0	30	199956	700072
43	4	0	60	199956	700072
44	4	0	90	199956	700072
45	4	8	0	199956	700072
46	4	8	30	199956	700072
47	4	8	60	199956	700072
48	4	8	90	199956	700072
49	5	-8	0	163756	766972
50	5	-8	30	163756	766972
51	5	-8	60	163756	766972
52	5	-8	90	163756	766972
53	5	0	0	163756	766972
54	5	0	30	163756	766972
55	5	0	60	163756	766972
56	5	0	90	163756	766972
57	5	8	0	163756	766972
58	5	8	30	163756	766972
59	5	8	60	163756	766972
60	5	8	90	163756	766972
61	6	-8	0	156789	765000
62	6	-8	30	156789	765000
63	6	-8	60	156789	765000
64	6	-8	90	156789	765000
65	6	0	0	156789	765000
66	6	0	30	156789	765000
67	6	0	60	156789	765000
68	6	0	90	156789	765000
69	6	8	0	156789	765000
70	6	8	30	156789	765000
71	6	8	60	156789	765000
72	6	8	90	156789	765000

6.7.1 Maximum Loads

Selected overall maximum and minimum loads from the 50-year extreme load case simulations are shown in Appendix F (Table F-1 through Table F-9). The "File Name" column indicates the load case.

Table 6-11 compares the mudline reaction forces with the values reported by Keystone Engineering (Dibra 2014). A safety factor of 1.35 has been applied to all loads for the 50-year case, except for ReactFZss, which includes a safety factor of 1.1 because this force component is primarily gravity controlled. Keystone Engineering applied a safety factor of 1.1 to all gravity loads presented in Dibra (Dibra 2014, p. 24). The mudline reaction force in the x-direction (ReactFXss) is significantly lower than the value estimated by Keystone Engineering. Comparing the tower-base x-direction force (TwrBsFxt), as shown in the first two rows of Table F-6, with the corresponding ReactFXss (Table F-7) values shows that the mudline reaction force in the x-direction is dominated by the hydrodynamic loads acting on the substructure. FASTv8 does not presently consider wave-stretching above the mean free surface; this is the reason for the underestimation by FAST.

The significantly larger mudline moment about the x-axis in FAST (ReactMXss) is related to larger aerodynamic loads in the y-direction as compared to Keystone Engineering (and also evident in the larger ReactFYss for FASTv8 in Table 6-11). The major part of these aerodynamic loads in the y-direction is generated by the rotor. This is clearly evident when applying the appropriate safety factor of 1.35 to the maximum yaw bearing loads reported in Table F-5, which yields a maximum 50-year yaw bearing load in the y-direction (YawBrFyp) of 2,114.37 kN. This number is very close to what is reported as ReactFYss in Table 6-11. Keystone Engineering only applies unidirectional wind and examines different possible wind angles. Therefore, the maximum aerodynamic load on the turbine in the y-direction occurs for case C090, which has a wind direction of 75 degrees. In the FAST simulations, wind is only prescribed at 0 degrees, but uses a complex flow field with components in all three directions. Thus, the y-component forces are not directly comparable between the two approaches.

Table 6-11 also shows that FASTv8 predicts a larger moment about the z-axis. The larger value in FASTv8 is because Keystone Engineering did not consider any moments about the z-axis that are induced by aerodynamic turbine loads. The underprediction of the mudline reaction moment about the y-axis (ReactMYss) is also related to the fact that the FAST solution does not consider any wave-stretching effects.

Table 6-11. Comparison of 50-Year Extreme Mudline Reaction Loads Between Keystone and FASTv8 (absolute values)

	Keystone Engineering (load case C000)	FASTv8 (overall extremes)
ReactFXss (kN)	15,992.17	12,285.00
ReactFYss (kN)	726.31	2,331.70
ReactFZss (kN)	25,430.85	26,313.00
ReactMXss (kNm)	83,127.50	339,240.00
ReactMYss (kNm)	611,385.30	563,040.00
ReactMZss (kNm)	1,308.20	24,795.00

Comparing Table F-2 and Table F-3 shows that the in-plane blade tip deflection is significantly higher than the out-of-plane deflection. This is caused by the blades being pitched to feather. For the present blade pitch orientation, in-plane blade deflection corresponds to the flap-wise direction. This is also visible in the blade root loads (Table F-4).

Table 6-12. Comparison of Maximum 50-Year Extreme Yaw Bearing Loads

	FASTv8, Flexible, LC25	**FASTv8, Rigid, LC25**	**WEI Rotor Loads**
YawBrFxp (N)	1.595E+006	4.436E+05	4.300E+05

Wetzel Engineering provided to NREL the aerodynamic rotor loads for the parked 50-year case, which were considered for the tower design process. Additional tower drag loads were added, and the corresponding tower base loads were supplied to Keystone Engineering for the substructure design process. A comparison of the initial rotor loads at the yaw bearing supplied by Wetzel Engineering and the final rotor loads generated by FASTv8 for the fully coupled 50-year analysis is shown in Table 6-12. LC25 has been simulated with two different model configurations in FASTv8. One configuration features a fully flexible model (as used in the 50-year, 100-year, and 500-year loads analysis). The other model configuration has a rigid tower to allow comparison to WEI's values and to show the impact of inertia loads from the tower motion on the yaw bearing loads. The yaw bearing load in the x-direction compares very well between the rigid FASTv8 model and the value provided by WEI. Adding a flexible tower, and therefore inertia loads from the tower motion, significantly increases the yaw bearing load in the x-direction. This effect can only be captured by a fully coupled loads analysis and was not considered in the tower and substructure design process, which emphasizes the importance of a fully coupled loads analysis.

6.7.2 Maximum Axial Stress in Critical Member

The following member shown in Table 6-13 has been identified as critical (SACS unity check larger than 0.8) for the parked 50-year extreme load case C000. As shown in Table 6-13, FASTv8 significantly overpredicts the extreme axial stress. This is probably caused by the larger aerodynamic turbine loads (especially considering the larger ReactMXss and ReactMZss shown in Table 6-11).

Table 6-13. Comparison of Axial Stress Levels for Critical Member

	Keystone Engineering (load case C000, 1.35 safety factor applied)	FASTv8 (overall extremes, 1.35 safety factor applied)
AxialStress68 (N/mm^2)	-45.19	-62.90298

6.8 500-Year Extreme Event

The load case matrix used for the 50-year extreme load case was also used for the 500-year extreme load case (Table 6-10).

6.8.1 Maximum Loads

Selected overall maximum and minimum loads from the 500-year extreme load case simulations are shown in the Appendix F (Table F-18 through Table F-25). The "File Name" column indicates the load case.

A comparison of the 500-year extreme mudline reaction loads between FASTv8 and SACS/Keystone is shown in Table 6-14. As previously discussed for the 50-year extreme load case,an underprediction by FASTv8 is evident in the mudline reaction force in the x-direction (ReactFXss) and the mudline reaction moment about the y-axis (ReactMYss). This underprediction is related to the fact that the current version of FASTv8 does not consider any wave-stretching effects, which have a significant impact on the extreme loads for fixed-bottom substructures in severe sea states. Because Keystone Engineering did not consider any aerodynamic turbine loads about the z-axis, we do see an over prediction of the mudline reaction moment about the z-axis (ReactMZss) by FASTv8. The significantly larger mudline moment about the x-axis in FASTv8 (ReactMXss) is related to larger aerodynamic loads on the turbine in the y-direction (also evident in the larger ReactFYss for FASTv8 in Table 6-14). This effect can be further related to the yaw bearing shear force in the y-direction as previously discussed for the 50-year load case in Section 6.5.1.

Table 6-14. Comparison of 500-Year Extreme Mudline Reaction Loads Between Keystone Engineering and FASTv8 (absolute values)

	Keystone Engineering (load case H000)	FASTv8 (overall extremes)
ReactFXss (kN)	22,400.93	15,212.72
ReactFYss (kN)	865.67	3,519.98
ReactFZss (kN)	23,611.51	25,665.31
ReactMXss (kNm)	102,886.80	487,896.92
ReactMYss (kNm)	928,446.70	795,285.95
ReactMZss (kNm)	1,790.00	37,663.35

6.8.2 Maximum Axial Stress Levels in Critical Substructure Members

Looking at the axial stresses of the critical members identified by Keystone Engineering (SACS unity check larger than 0.8), we see a similar trend as previously discussed for the 50-year load case in Section 6.5.1. The stresses in member 68 and 75 are slightly higher in FASTv8 whereas the axial stress in member 24 is predicted slightly lower by FASTv8 (Table 6-15).

Table 6-15. Comparison of Axial Stress Levels for Critical Members

	Keystone Engineering (load case H000)	FASTv8 (overall extremes)
AxialStress24 (N/mm^2)	-142.99	-132.21
AxialStress68 (N/mm^2)	-62.28	-71.64
AxialStress75 (N/mm^2)	-63.78	-71.11

6.9 Load Case Comparison

The following sections compare loads and member stresses predicted by FASTv8 for the 50-year, 100-year and 500-year extreme load cases. All loads and member stresses shown in this section include the appropriate load factors.

6.9.1 Maximum Loads

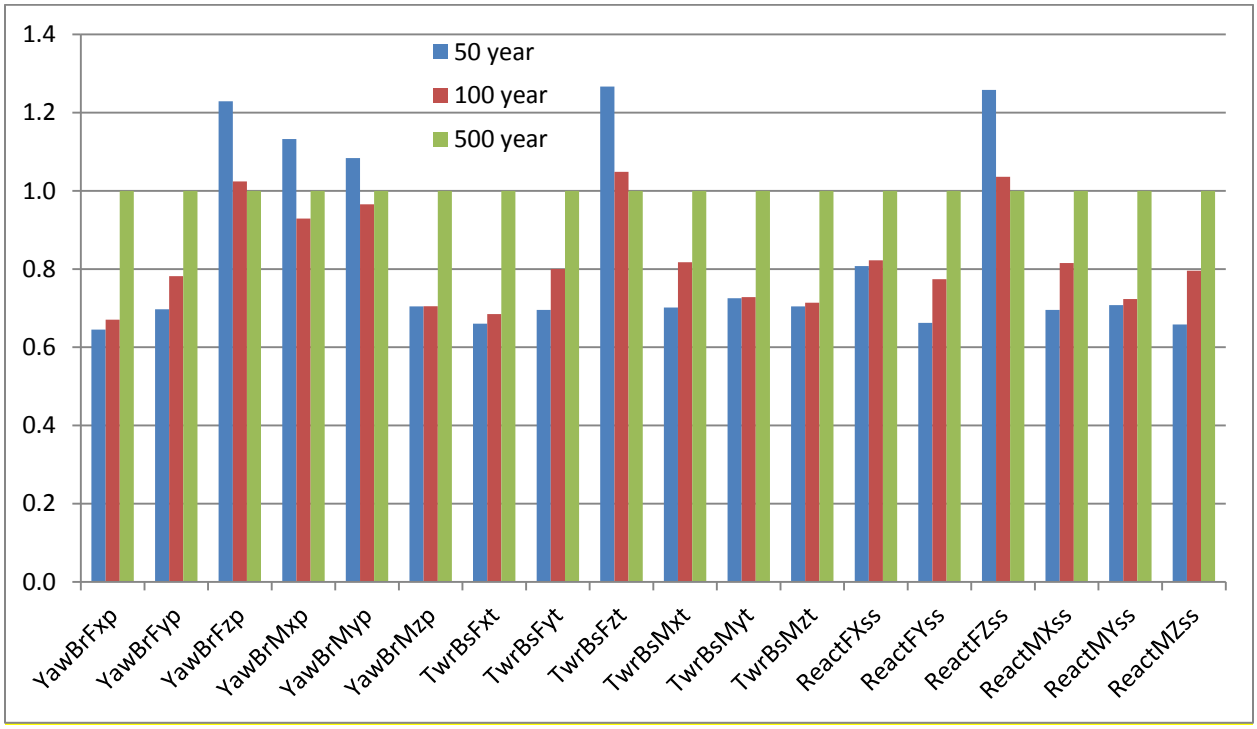

Figure 6-5. Comparison of extreme loads

A comparison between extreme loads for different reoccurrence periods is shown in Figure 6-5. In addition to load components that are controlled by gravity effects (YawBrFzp, YawBrMxp, YawBrMyp, TwrBsFzt, and ReactFZss), this comparison shows a similar trend for all investigated load components. The 50-year and 100-year loads are fairly close whereas the 500-year load case produces significantly higher loads. The average increase in extreme loads when moving from a 50-year to a 100-year reoccurrence period is 4.51%. When moving from a 100-year to a 500-year reoccurrence period, the extreme loads increase by 18.63% on average. These relative load increases were computed without considering the gravity-dominated load channels. The gravity-controlled load components primarily reflect the different load factors (1.35 for 50 years, 1.1 for 100 years, and 1.0 for 500 years) because the nonfactorized gravity loads are not significantly affected by changes in the considered recurrence period.

6.9.2 Maximum Axial Stress Levels in Critical Substructure Members

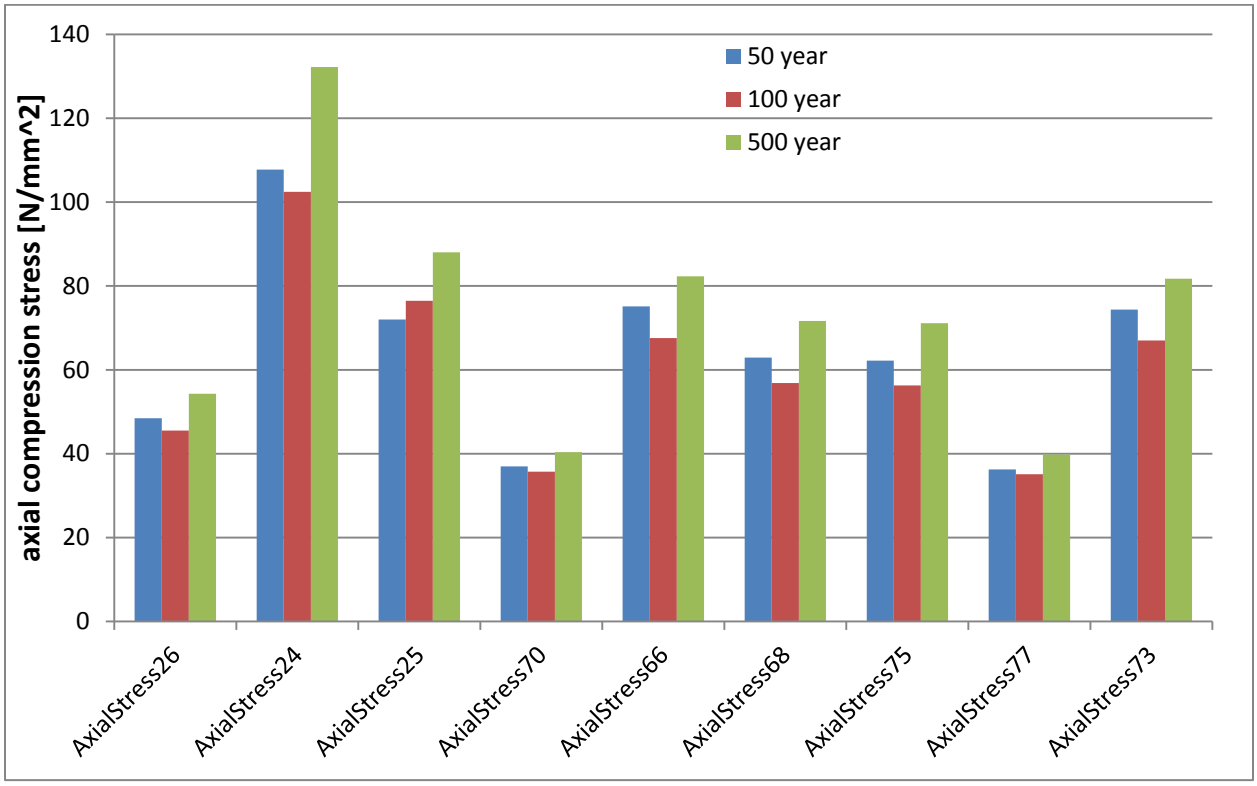

Figure 6-6. Comparison of axial member stresses (compression)

The axial member stresses for different recurrence periods are shown in Figure 6-6. The considered members were identified as critical by Keystone Engineering (SACS combined unity check larger than 0.8). Keystone Engineering considered incoming wind directions ranging from 0-360 degrees. Because the NREL analysis only considered a 0-deg wind direction, some of these members show relatively low stress levels. Keystone Engineering identified members 24, 68, and 75 as critical for the 500-year case with 15-deg wind direction; member 68 was also identified as critical for the corresponding 50-year case. For these members, the 50-year case appears to be producing slightly higher axial compression stresses in FAST than the 100-year case. The 500-year case produces higher stress levels for all members—especially member 24. The location of these members is illustrated in Figure 6-4.

6.10 Conclusions

To assess the extreme loads from a hurricane on a 10-MW fixed-bottom offshore wind turbine, a fully coupled model of the wind turbine system was created in FASTv8. The twisted jacket substructure (designed by Keystone Engineering) was modeled in SubDyn, an FE module for FASTv8 developed by NREL. The SubDyn model was verified against Keystone Engineering's SACS model through comparison of mass, buoyancy, and stiffness properties.

Hurricane extreme conditions were defined for 50-year, 100-year, and 500-year reoccurrence periods. The definition of these load conditions was based on what was originally specified by Keystone Engineering for the substructure design (50-year and 500-year reoccurrence periods) and Wetzel Engineering for the rotor blade design (50-year and 100-year reoccurrence periods).

A set of fully coupled FASTv8 time-domain simulations was conducted for each reoccurrence period (50 years, 100 years, and 500 years). Yaw errors of +/- 8 degrees, as well as wave angles of 0 degrees, 30 degrees, 60 degrees, and 90 degrees were considered. Six different wave and wind seeds were simulated for each combination of wave angles and yaw errors. This resulted in 72 simulations for each recurrence period.

The 50-year and 500-year substructure extreme loads were compared against what was predicted by Keystone Engineering. The mudline reaction force in the x-direction was found to be underpredicted by FASTv8. This is related to the fact that the present version of FASTv8 does not consider any wave-stretching effects. Wave-stretching has a significant impact on the extreme loads for fixed-bottom substructures in severe sea states. The mudline reaction moment around the z-axis and the y-direction force were higher in FASTv8 for a 0-degree wind direction because Keystone Engineering did not consider any off-axis aerodynamic loading.

The 50-year yaw bearing shear force in the x-direction that was used by Wetzel Engineering during its rotor blade design was smaller than the corresponding load component of the fully coupled FASTv8 loads analysis. This was found to be related to tower motion and, therefore, inertia loads could not be considered by WEI, because blade and rotor optimization necessarily preceded the fully coupled loads analysis. For later and more detailed design stages, this underlines the importance of a fully coupled loads analysis within an iterative turbine design methodology, in order to achieve most accurate load estimations.

Finally, the hurricane extreme loads for the 50-year, 100-year, and 500-year reoccurrence periods were compared. The extreme loads were found to increase by an average of 4.51% between a 50-year and 100-year reoccurrence period. An average increase of 18.63% in extreme loads was found between a 100-year and 500-year reoccurrence period. Aerodynamic loads were found to be more sensitive to changes in the considered reoccurrence period than the hydrodynamic extreme loads.

7 Wind Plant Layout Analysis

7.1 Site Selection Area

A site selection area was identified approximately 60 km to the southeast of Corpus Christi, Texas. The site was selected such that candidate layouts would represent a general development scenario for the given technology. The site selection sought the most appropriate combination of high wind speeds, depths less than 25 m, and minimum export cable length. Key required inputs were wind resource and bathymetry data. The site selection area is shown in Figure 7-1.

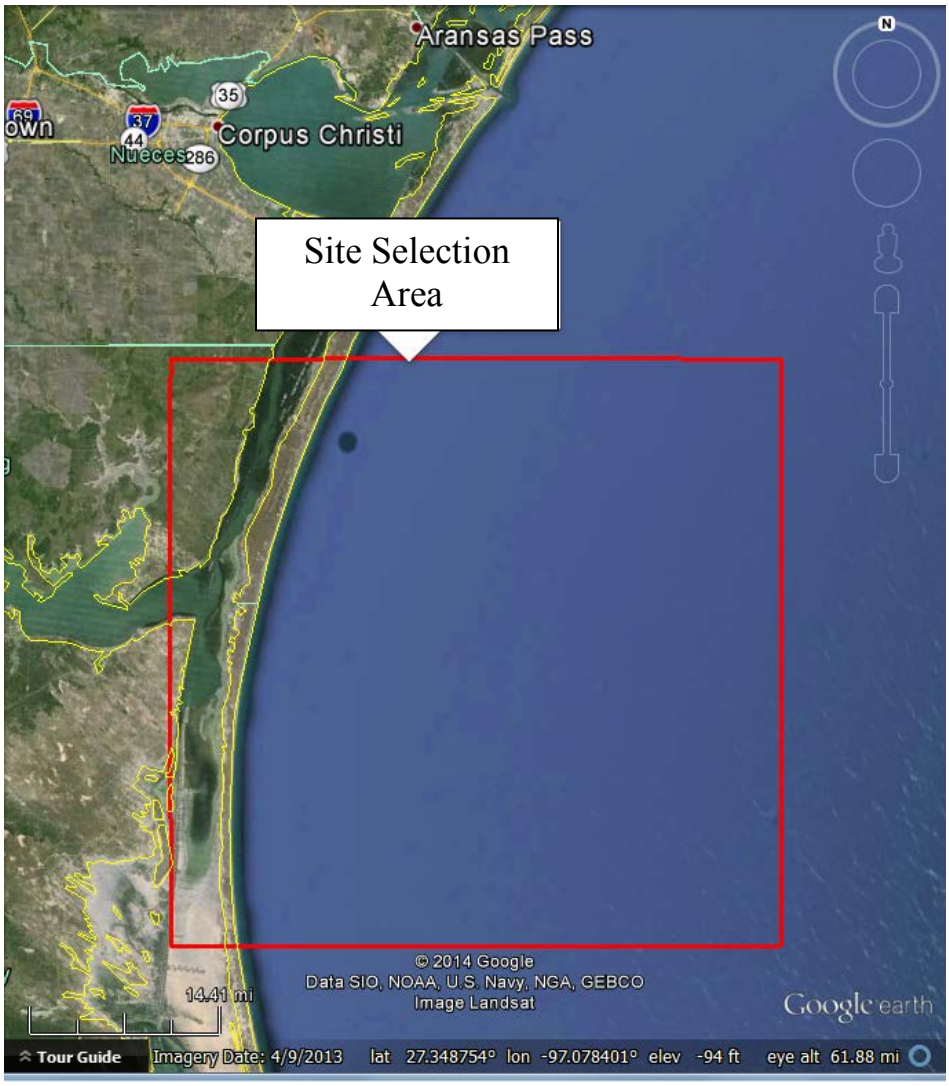

Figure 7-1. Site selection area Southeast of Corpus Christi, Texas

7.2 Wind Resource Data

The wind resource data used for the layout design was a high-resolution, long-term record obtained from AWS Truepower.

The mesoscale model, Mesoscale Atmospheric Simulations System, was used to simulate the atmosphere with a coarse horizontal grid spacing of 20 km over the United States and immediately offshore. The Mesoscale Atmospheric Simulations System is a numerical weather model that has been developed over the past 20 years by MESO, Inc., in partnership with AWS Truepower. The mesoscale simulations were processed to produce a long-term time series of weather information called windTrends. The windTrends dataset is available from 1997 to the present and contains hourly approximations of several meteorological fields, including wind speed and direction. This data set was used to produce an annual average wind speed map at a resolution of 20,000 m (20 km) and a set of statistical files containing information about the wind resource. This information was then used by NREL researchers, along with higher-resolution capacity factor data, to create and extrapolate a wind resource grid file at 200 m horizontal resolution. NREL researchers input these wind resource grid files into the Openwind model where the wind speed gradients and directional distributions were determined.

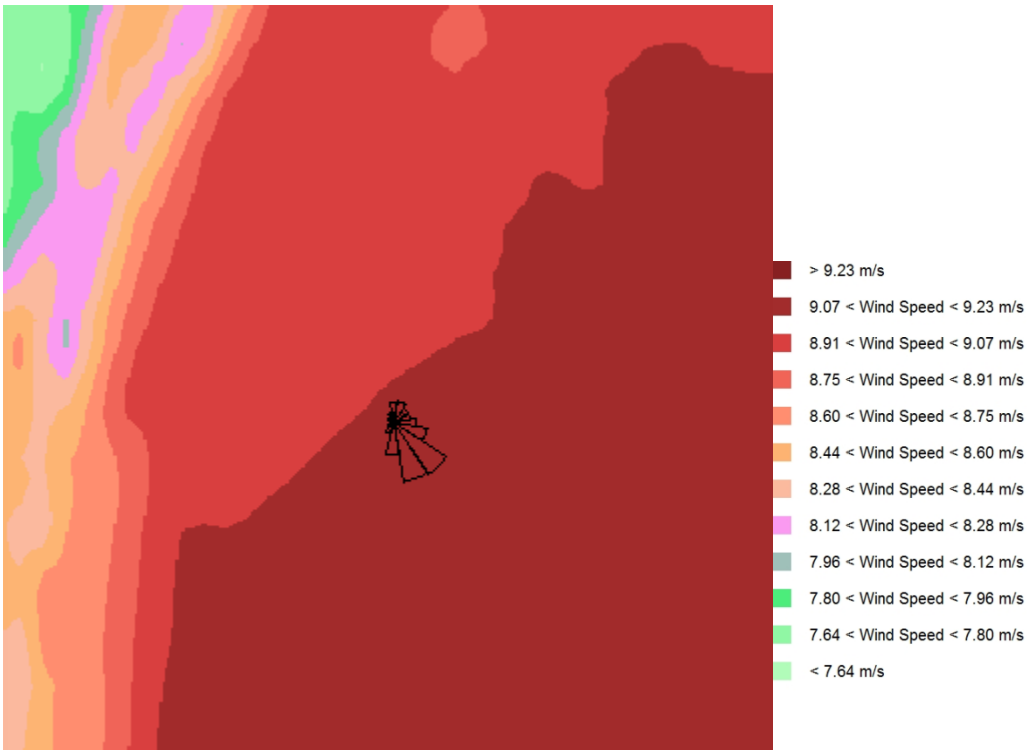

Figure 7-2. Annual average wind speed in the site selection area

As shown in Figure 7-2, average annual wind speeds range from 7.64 m/s to 9.23 m/s with wind speeds exceeding 9 m/s in much of the area. The winds are predominantly from the southeast as shown by the wind rose near the center of Figure 7-2.

7.3 Bathymetry Data

NOAA's Coastal Relief Model (CRM) is a nationally comprehensive dataset available at relatively high spatial resolution (3 arc-seconds) for the coastal waters of the contiguous United States and Hawaii. NOAA has integrated data from the U.S. National Ocean Service Hydrographic Database, the U.S. Geological Survey (USGS), the Monterey Bay Aquarium Research Institute, the U.S. Army Corps of Engineers, the International Bathymetric Chart of the Caribbean Sea and the Gulf of Mexico, and various academic institutions. The data are freely available to the public, allowing NREL to distribute the data used in our analysis to our partners and stakeholders. The data are downloadable from NOAA's National Geophysical Data Center (http://www.ngdc.noaa.gov/mgg/coastal/crm.html), which provides scientific stewardship for sea floor and lakebed geophysical data, including bathymetry (NOAA 2013). These bathymetry data for the site selection area are shown contour plotted in Figure 7-3.

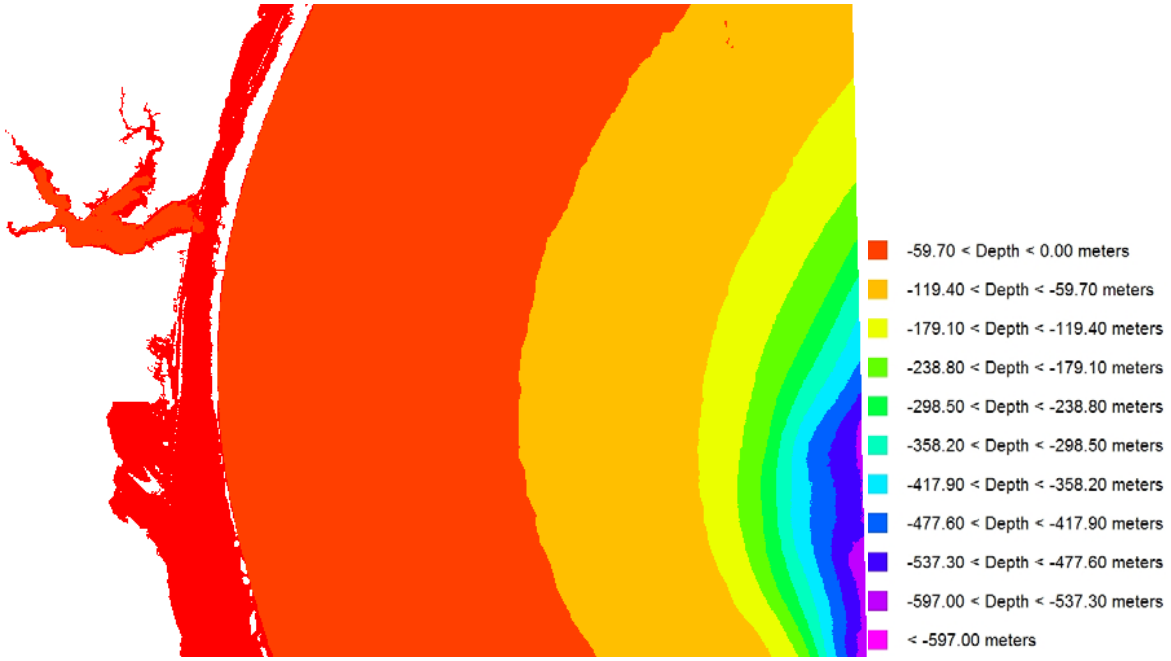

Figure 7-3. Bathymetry map showing ocean depth in and around the site selection area

7.4 Siting and Layout Design

The selected site and layout designs are shown in Figure 7-4 through Figure 7-7. The turbines are arranged in arrays with 8D-by-12D spacing at an orientation angle of 155 degrees from North. Each array is configured to optimize a different development parameter. Layout A is configured in a block to minimize depth and distance from shore. Layout B is configured in a north-south line to minimize depth and distance from shore while reducing wake losses. Layout C is configured in an east-west line to maximize wind speed. Layout D is configured in a 155-degree line to minimize wake losses.

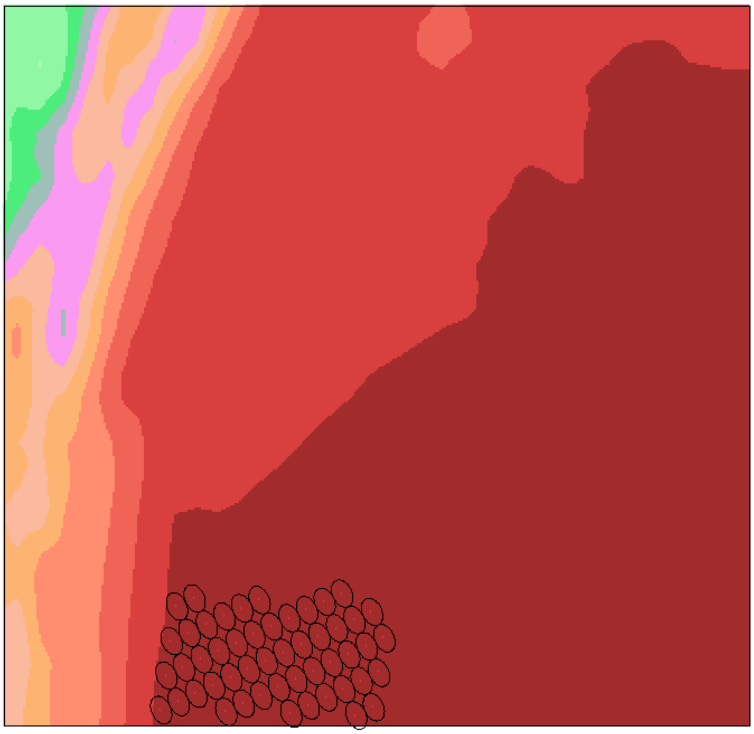

Figure 7-4. Layout A, block 500-MW layout in site selection area

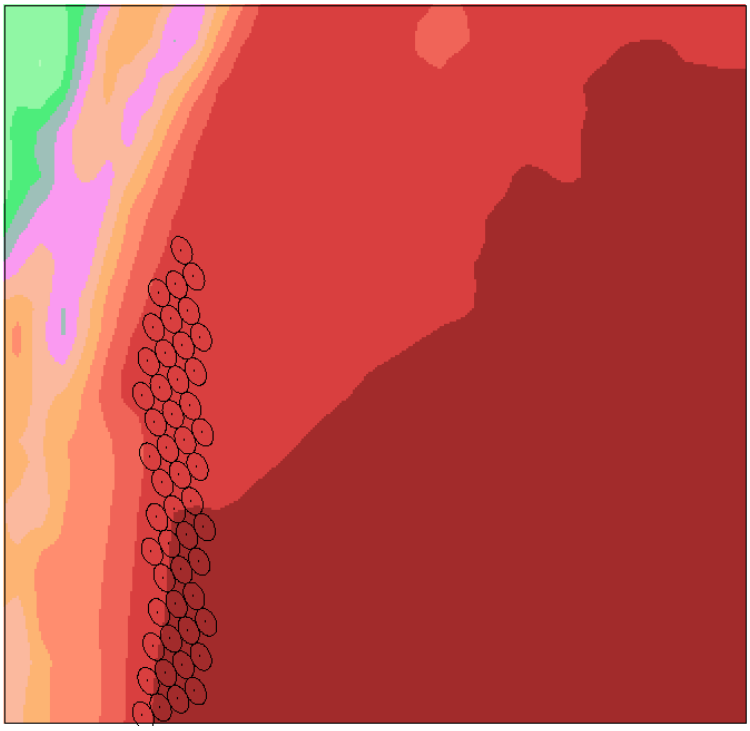

Figure 7-5. Layout B, north-south 500-MW layout in site selection area

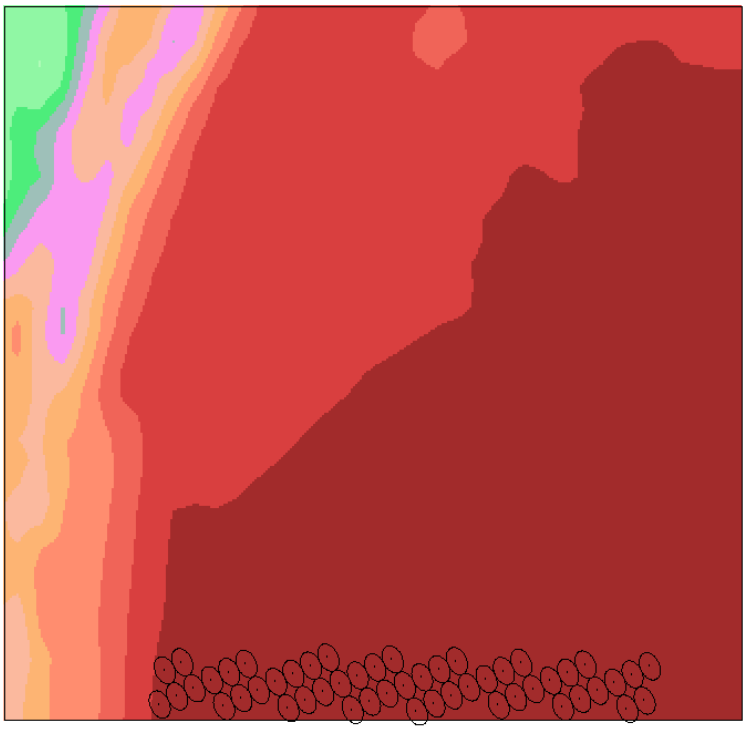

Figure 7-6. Layout C, east-west 500-MW layout in site selection area

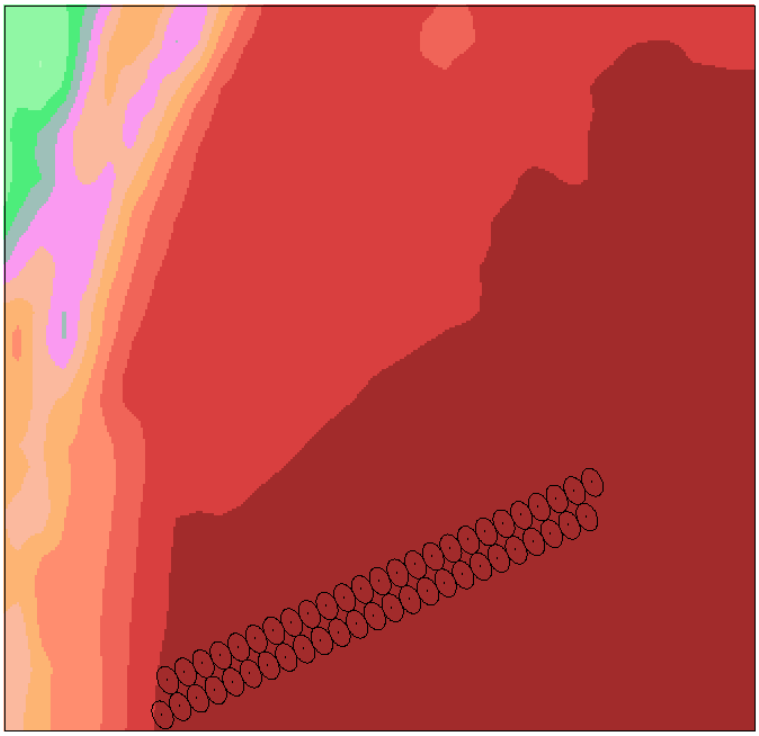

Figure 7-7. Layout D, 155-degree 500-MW layout in site selection area

Modeled wind speed, loss assumptions, and energy production are shown in Table 7-1. Wake losses are calculated for each layout configuration using the deep array eddy viscosity wake model in Openwind Enterprise. All other loss assumptions were manually entered into Openwind and applied to the calculation of net energy production. High-resolution lightning flash rate maps from NASA's Global Hydrology and Climate Center indicate that this area experiences an annual lightning flash rate between 4 and 10, shown in Figure 7-8. A corresponding loss of 0.9% has been assumed because of lightning. NASA MERRA data shows temperatures in the site selection area ranging from 18°C–30°C so temperature shutdown and icing losses are assumed to be zero (http://disc.sci.gsfc.nasa.gov/mdisc/).

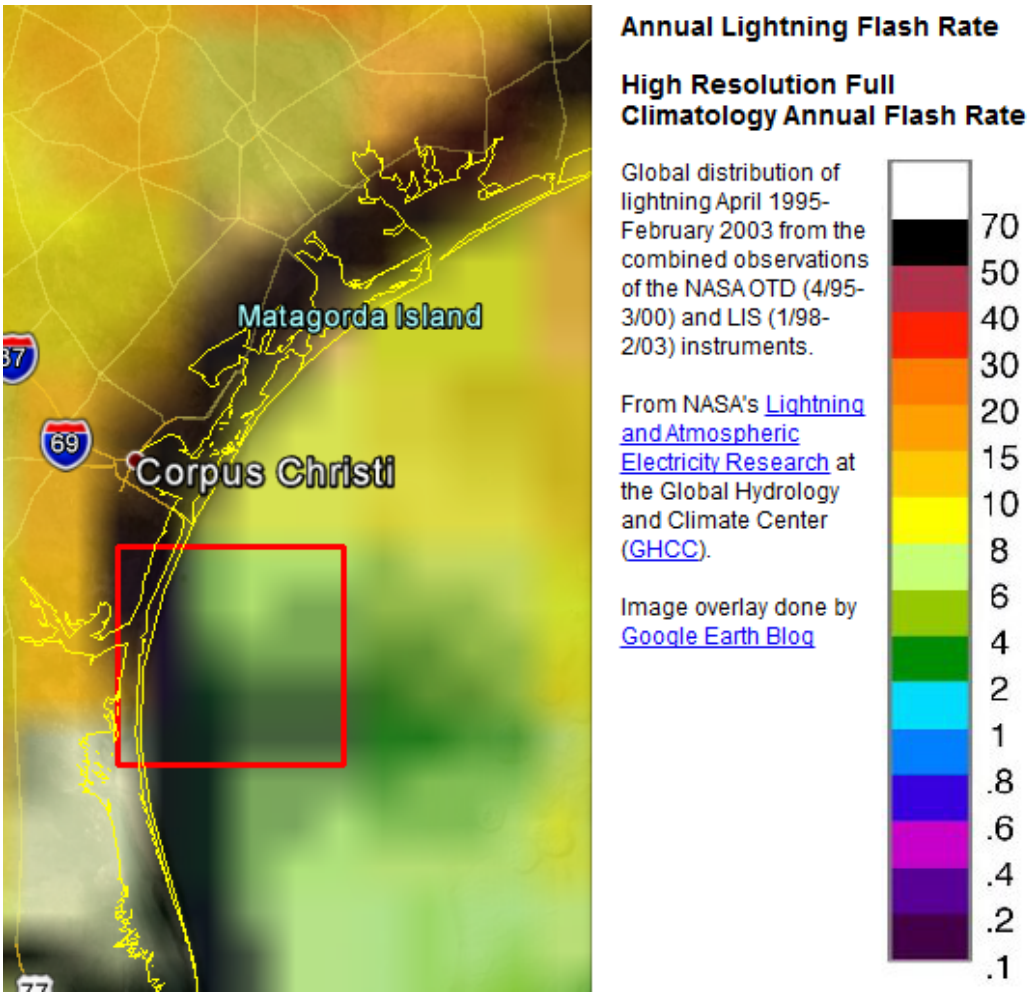

Figure 7-8. Annual lightning flash rate (http://thunder.nsstc.nasa.gov/)

Table 7-1. Wind Speed, Loss, Energy Production and Average Depth for Hurricane Layout Designs

Hurricane Layout Analysis	Layout A	Layout B	Layout C	Layout D
Capacity (MW)	500	500	500	500
Mean annual wind speed (m/s)	9.17	9.05	9.18	9.16
Gross energy production (GWh)	2426.3	2396.7	2430.4	2424.938
Gross capacity factor	**55.36%**	**54.68%**	**55.45%**	**55.33%**
Wake loss	3.05%	2.65%	2.06%	1.82%
Availability loss	4.00%	4.00%	4.00%	4.00%
High wind hysteresis	0.70%	0.70%	0.70%	0.70%
Lightning loss	0.90%	0.90%	0.90%	0.90%
Total electrical loss	2.00%	2.00%	2.00%	2.00%
Total losses	10.24%	9.87%	9.33%	9.10%
Net capacity factor	**49.68%**	**49.28%**	**50.28%**	**50.29%**
Net energy production (GWh)	2177.5	2160.1	2203.7	2204.1
Average depth (m)	28.06	20.43	38.56	34.82

The highest net energy production and lowest wake loss is associated with Layout D; Layout B is in the shallowest waters.

8 Operation and Maintenance (O&M) Analysis

This section is part of the *Hurricane-Resilient Wind Power Plant Concept Study* in response to Topic Area 2 of the U.S. Department of Energy Funding Opportunity DE-FOA-0000415, U.S. Offshore Wind: Technology Development. The goal of this section is to provide an analysis to better understand the impact on O&M for an offshore wind plant sited in a hurricane region.

The analysis assesses two O&M scenarios: 1) a baseline offshore wind power plant scenario consisting of 100 turbines, each rated at 5 MW, and 2) a hurricane-resilient offshore wind power plant scenario comprised of 50 turbines, each rated at 10 MW. Both the baseline and hurricane-resilient offshore wind power plant scenarios are located in the Western Gulf of Mexico, approximately 60 km southeast of Corpus Christi, Texas. This region of the United States is prone to hurricane activity that can limit access to a wind turbine for maintenance activities. The prevention of access to a turbine for repair not only increases the downtime of the turbine, but ultimately increases the LCOE. This O&M analysis for the baseline and hurricane-resilient offshore wind power plants is intended to quantify the O&M cost, wind power plant availability, and energy production for a wind power plant located in the Gulf of Mexico.

8.1 Description of the O&M Analysis Scenarios

8.1.1 Baseline Scenario

The baseline wind power plant for this O&M study consists of 100 NREL offshore reference turbines rated at 5 MW each to equal a 500-MW wind power plant. The onshore operations base for the baseline is located near Corpus Christi Bay, approximately 60 km northwest of the wind site. The NREL 5-MW reference turbine is a conventional, three-bladed, upwind, variable-speed, variable blade-pitch-to-feather-controlled turbine that uses IEC Class 1A design criteria (Jonkman 2009). It uses a modular, gear-driven system with full power conversion. The turbine rotor measures 126 m in diameter, and sits atop a 90-m traditional steel tubular tower that interfaces with a classic monopile substructure. The layout of the wind power plant assumes uniform rectangular array configuration with spacing of 8x8 rotor diameters. The electric power is distributed at 34 kilovolts (kV) to a centrally located substation where it is stepped up to a nominal 115 kV and transmitted to shore via an alternating current (AC) power cable.

8.1.2 Hurricane-Resilient Scenario

The hurricane-resilient wind power plant consists of 50 hurricane-resilient turbines rated at 10 MW each to equal a 500-MW wind power plant. The onshore operations base is assumed to be the same distance as the baseline scenario at 60 km. The hurricane-resilient turbine is characterized by a series of innovative technology advancements such as an advanced 218-m diameter rotor, permanent-magnet direct-drive generator, advanced IBGS substructure, hurricane-resilient designs, and wind power plant optimization and control. As with the baseline, the layout of the wind power plant assumes an 8x8 rotor-diameter spacing in a rectangular array configuration. The electrical infrastructure is similar to that of the baseline with its 34-kV lines to the centrally located substation where it is then stepped up to a nominal 115 kV and transmitted to shore via an AC power cable. A summary of the baseline and hurricane-resilient offshore wind power plant parameters are shown in Table 8-1.

Table 8-1. Turbine and Wind Power Plant Operating Parameters for Baseline and Hurricane-Resilient Scenarios

Categories	5-MW Baseline Scenario	10-MW Hurricane-Resilient Scenario
Wind power plant size (MW)	500	500
Number of turbines (units)	100	50
Machine rating (MW)	5	10
Rotor diameter (m)	126	218
Hub height (m)	90	135
Estimated wind speed @ 90 m above MSL (m/s)	8.7	-
Estimated wind speed @ 135 m above MSL (m/s)	-	9.1
Drivetrain	Geared	Direct Drive
Substructure	Monopile	IBGS

8.2 O&M Analysis Strategy

The industry-leading offshore wind O&M planning software is the ECN O&M tool v.4 (Obdam 2011). This tool is used to estimate the O&M cost, downtime, and energy production for the baseline and hurricane-resilient scenarios located in the Gulf of Mexico.

The level of effort required for O&M activities for a wind power plant can typically be characterized by a bathtub curve. The shape of the bathtub curve is derived from the unscheduled maintenance required during the commissioning, or break-in period, and again approaching the end-of-design life for the wind power plant and the relatively steady amount of scheduled maintenance throughout the lifespan of the wind power plant. Annual variation of scheduled maintenance and wind power plant overhauls also impact the shape of the bathtub curve but are not considered in this analysis. The ECN O&M tool, however, estimates the long-term annual average unscheduled and scheduled maintenance costs, which masks the trend of the bathtub curve and produces a flat average cost over the lifetime of the wind power plant (Figure 8-1). In addition to long-term annual average maintenance cost, the tool also calculates the annual average downtime due to unscheduled and scheduled maintenance that impacts plant availability.

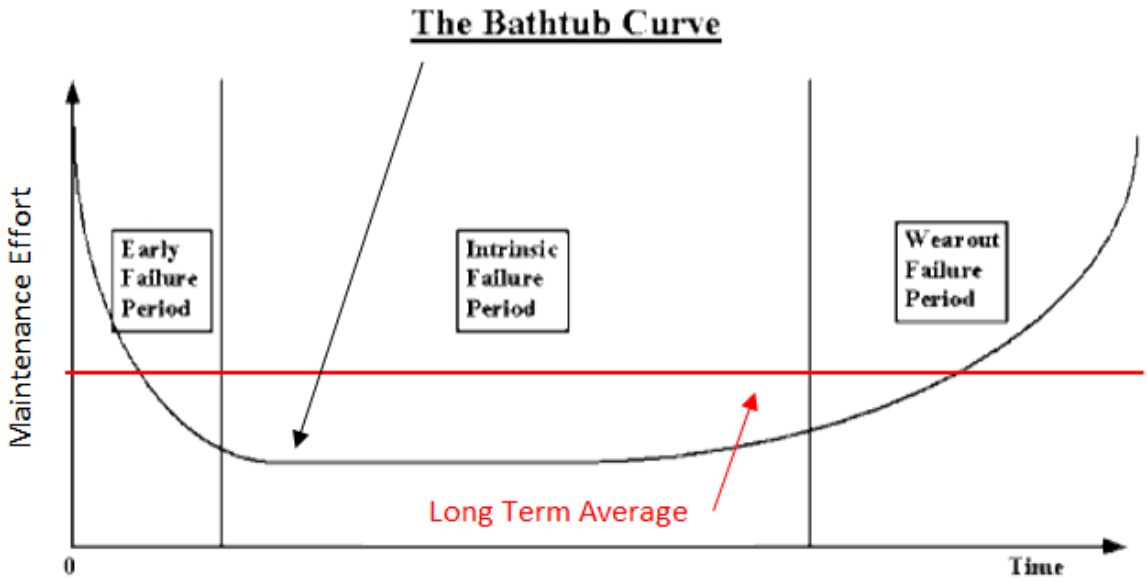

Source: Tobias (2013), modified by NREL

Figure 8-1. Example of estimated O&M efforts over the life of a wind turbine.

8.3 Baseline Scenario

The ECN O&M tool allows users to relatively easily estimate the cost and downtime of an offshore wind project. However, as with any estimating tool, there are limitations. Knowing the fundamental inputs, assumptions, and limitations is essential to understanding the validity of the results. An overview of the inputs, assumptions, and limitations are explained below.

8.3.1 Failure Frequency of Wind Turbine and Balance-of-System Components

O&M costs are highly dependent on the failure rates of the components within the wind power plant. For this analysis, both cost and downtime estimates for unscheduled wind turbine maintenance rely on the wind turbine failure rate results from the Reliawind study (Wilkinson 2010). Two sets of wind turbine component failure rates are used in this study: 1) geared drivetrain (includes a gearbox), and 2) direct-drive drivetrain (no gearbox). The failure rates for the geared drivetrain are used in the ECN model for the baseline case. However, certain wind turbine component failure rates were modified by NREL based on discussions with wind turbine original equipment manufacturers (OEMs). Data on the failure rates for balance-of-system (BOS) components are limited; therefore, the BOS component failure rates used in the ECN North Sea O&M case study (van der Zee 2011) were considered for this study.

The potential for increased failure rates at higher wind speed sites than those determined by the Reliawind study are not considered in this analysis due to limited available failure rate data for turbine components in higher wind speed sites. Recent studies have shown increased wind speed and turbulence correlate with an increase in failure rates for wind turbine blades, pitch systems, and mechanical drivetrain components (Tavner 2012). The hurricane-prone baseline site has the

potential to see hurricane wind speeds and a possible increase of wind turbine component failure rates; therefore, negatively impacting offshore wind power plant availability and O&M costs. However, the model accounts for the wind plant downtime accrued from waiting on hurricane conditions to access the wind plant for corrective maintenance. This is done by using a correlated wind and wave dataset simulating two hurricanes passing near the wind site. This wind and wave dataset is described in more detail in Section 8.3.4. Further investigation of higher wind speeds on wind turbine component failures may provide better understanding of the impacts to O&M costs and offshore wind power plant availability. Table 8-2 summarizes the wind turbine component taxonomy and failure rates used in the baseline scenario. Table 8-3 contains a summary of baseline BOS component failure rates.

Table 8-2. Baseline Wind Turbine System Component Failure Rate Assumptions

Wind Turbine System Components* (Based on RDS-PP Taxonomy)	Annual Failure Frequency of Main Turbine Components (failures/wind turbine/year)
MDA - Rotor system	0.1307
MDC - Blade adjustment	0.9778
MDK - Drivetrain	0.2888
MDL - Yaw gearbox	0.5076
MDX - Hydraulic system	0.0536
MDY - Control and protection system turbine	0.8616
MKA - Generator	0.3246
MKY - Control and projection system generator	0.6001
MSA - Generator lead/transmission cables	0.4677
MST - Transformer	0.0795
MUD - Machinery enclosure	0.0138
UMD - Turbine structure/tower	0.1512
XA - Heating, ventilation, air conditioning	0.0140
XM - Crane system	0.0144
AB - Lightning protection/grounding	0.0117
MD - Remote resets	12.000
XN - Elevator system	0.0055

*Based on the Reference Designation System for Power Plant (RDS-PP) taxonomy.

*The Reference Designation System for Power Plant (RDS-PP) taxonomy is used for the analysis (Müller et al. 2013.

Table 8-3. BOS Component Failure Rate Assumptions

BOSComponent	Annual Failure Frequency of Main BOS Components (failures/BOS component/year)
Offshore Substation Transformer 1	0.5000
Offshore Substation Transformer 2	0.5000
Foundation/scour protection	3.0000
Cables within wind power plant	0.0500

Transformer 1 and Transformer 2, identified in Table 8-3, are mounted on the offshore substation located in the center of the wind power plant.

8.3.2 Repair Strategy

Each defined component is assigned a set of repair strategies that consists of the following:

- Maintenance category (MC) estimates equipment and effort to repair the fault (Table 8-4)
- Probability of occurrence associated with each of MC
- Number of additional inspections required to complete the repair; for modeling purposes, an inspection can be characterized as a small repair
- Fault type classification (FTC) further specifies the effort required to complete the repair, which includes crew size, time needed for repair, and the cost for spare parts (Table 8-5).

Additionally, the ECN O&M tool has the capability to analyze unscheduled replacement of components known as condition-based maintenance. Condition-based maintenance is considered to be a small replacement activity based on the outcome of inspection or as a result of condition-monitoring data. In this case, the turbine would continue to generate power until the component was replaced—only accruing downtime during the time needed for replacement. The baseline and hurricane-resilient O&M scenarios both consider unscheduled condition-based maintenance.

Table 8-4. Baseline Maintenance Categories Developed by ECN

MC	MC Type	MC Description
1	Remote resets (only downtime, no visit)	Resets take 2 hours (h) and can be done remotely
2	Inspection and small repair inside	Requires workboat, 3 technicians, and consumables; repair time estimated within 2–6 h
3	Inspection and small repair outside	Requires workboat, 3 technicians, and consumables; repair time estimated within 6–10 h
4	Replacement small parts (< 2 tons (t)) using internal crane	Requires workboat, 3–4 technicians, and spare parts; repair time estimated within 8–24 h
5	Condition-based replacement of small parts (< 2 t) using internal crane	Requires workboat, 3–4 technicians, and spare parts; repair time estimated 8–24 h
6	Replacement of large parts(< 100 t) using large external crane	Requires workboat, jack-up barge, 6 technicians, and spare parts; repair time estimated within 24–40 h

Table 8-5. Baseline Fault-Type Classifications Developed by ECN

FTC	Fault-Type Classification Description	Material Costs (% of Turbine Capital Costs)	Crew Size (people)	Repair Time (h)
1	No crew, repair = 2 h, no cost	0.00%	0	2
2	Small crew, repair = 4 h, consumables	0.01%	3	4
3	Small crew, repair = 8 h, consumables	0.01%	3	8
4	Small crew, repair = 8 h, low cost	0.10%	3	8
5	Small crew, repair = 16 h, low cost	0.10%	3	16
6	Large crew, repair = 16 h, medium cost	1.00%	4	16
7	Large crew, repair = 24 h, medium cost	1.00%	4	24
8	Large crew, repair = 24 h, high cost	5.00%	4	24
9	Small crew, repair = 8 h, low cost	0.10%	3	8
10	Large crew, repair = 16 h, medium cost	1.00%	4	16
11	Large crew, repair = 24 h, medium/high cost	2.00%	6	24
12	Large crew, repair = 24 h, high cost	3.00%	6	24
13	Large crew, repair = 40 h, medium/high cost	2.00%	6	40
14	Large crew, repair = 40 h, very high cost	10.0%	6	40

8.3.3 Repair Vessels

The following access vessels and repair equipment are assumed for conducting turbine and BOS repairs:

- Workboat access vessel: transfers technicians and transports small components (< 2 t)
- Jack-up barge: transports and hoists large components (> 2 t)
- Diving support vessel: performs underwater inspection and repairs
- Cable-laying vessel: repairs cables within the wind power plant.

NREL used best estimates derived from available data (van der Zee 2011, Douglas-Westwood 2013) and estimates provided by U.S. marine contractors to represent vessel travel time, day rate, lease rate, and mobilization/demobilization (mob/demob) costs. Each vessel is also characterized by weather limitations, including maximum wind speed and maximum wave height, to account for anticipated weather-related downtime. Vessel limitations were obtained from the ECN O&M tool case study (van der Zee 2011). The model uses the wind and wave restrictions, along with correlated, long-term probability distributions characterizing site-specific metocean conditions (Table 8-6), to estimate the total duration required to complete a repair. Table 8-6 provides details on vessel specification assumptions.

Table 8-6. Vessel Limitation and Cost Assumptions

Vessel Type	Max. Wind Speed (m/s)	Max. Wave Height (m)	Equipment Logistics Time[1] (h)	Travel Time[2] (h)	Day Rate (k$/day)	Lease Rate (k$/year)	Mob/Demob Cost[3] (k$/mission)
Workboat	12	1.5	-	1.6	-	1,040	-
Jack-up barge	10	2.0	720	-	140	-	6,000
Diving support vessel	25	2.0	360	-	98	-	975
Cable-laying vessel	25	1.0	720	-	195	-	5,050

Note that additional costs are included in the O&M model that are not listed in Table 8-6 (e.g., fuel costs for the workboat). Also, during the time that a vessel is waiting on a good weather window to conduct a repair, the vessel's day rate is reduced. It is assumed that the rate while waiting is about 75% of the vessel's full day rate. Additionally, it is assumed that the workboat, jack-up barge, and diving support vessel are available in the United States, whereas the cable-laying vessel would need to be mobilized from Europe. The nacelle of the NREL 5-MW offshore reference turbine is assumed to be lifted by a U.S.-flagged jack-up barge available in the Gulf of Mexico region, whereas the nacelle of the 10-MW hurricane-resilient turbine is assumed to require a specialized heavy-lift jack-up barge that is not available in the United States. Hence, the heavy-lift jack-up barge is assumed to be mobilized from Europe for the hurricane-resilient scenario.

One of the model's attributes accounts for situations in which a failure could occur during the mobilization of the jack-up barge. In this case, the repairs would be clustered and the average logistical costs per repair will be lower. This model capability is used in the baseline and hurricane-resilient scenarios.

8.3.4 Site Wind and Wave Data

The ECN O&M Tool requires a time series wind and wave dataset whereas the AWS Truepower dataset used in Section 7.2 only considers wind speed. Therefore, analysts had to develop another dataset that includes wave height. The correlated time series wind (measured at 10 m) and wave data used as an input to the model were obtained from the Wave Information Studies (WIS) from the U.S. Army Corps of Engineers (USACE). The data was collected by a WIS buoy with the station identification number 73034, located at 27.25 latitude, -97.05 longitude, with an

[1] Denotes the period of time that elapses before the ordered personnel, equipment, and spare parts are ready to travel to the turbine for repair, and mobilization time for nonleased vessels. Therefore, the length of this interval depends on the availability of a team for inspection or repair, the availability of materials, and the availability of equipment for traveling and hoisting. This analysis does not anticipate when vessels may or may not be available based on the market.

[2] Travel time is defined as the time to travel from O&M port to site for a one-way trip, and includes the time for the technicians to access the turbine from the workboat.

[3] The mob/demob costs associated with offshore wind vessels are not well established for U.S. projects and can fluctuate depending on market conditions. This fluctuation can highly impact O&M costs; therefore, a better understanding of vessel costs and subcontracts is necessary.

estimated water depth below the buoy of 34 m MSL (USACE 2014). This buoy is determined to be the nearest to the *Hurricane-Resilient Wind Power Plant Concept Study* site. The duration of the wind and wave data set go from July 29, 1990, through December 31, 2012. During this time, the wind power plant concept site experienced two hurricanes that passed near the region. The first was Hurricane Bret in 1999, passing through the area approximately August 20, 1999, through August 24, 1999, with maximum sustainable wind speeds of 61.7 m/s recorded nearest to the site on August 22, 1999. The second hurricane was Dolly in 2008, passing through the area about July 20, 2008, through July 26, 2008, with maximum sustainable wind speeds of 38.6 m/s recorded nearest to the site on July 23, 2008 (NOAA 2014). The wind and wave data are vital to calculating the average waiting time as a function of the "mission time" based on restrictive weather constraints for a vessel's travel and various maintenance activities, whereas the mission time denotes the total time needed for the repair, including travel and overnight periods.

8.3.5 Waiting Time for Repair

The ECN O&M tool estimates the mean waiting time as a function of the mission time using polynomial functions. Each vessel is associated with a specified "weather window," defined as the time period during which the vessel can likely perform repairs given its individual operational limits. Outside the weather window the vessel is required to wait in port until the allowable weather window opens.

8.3.6 General O&M Model Assumptions

The baseline O&M analysis assumptions are primarily based on the ECN O&M North Sea Case Study (van der Zee 2011). However, there are multiple modeling assumptions specific to the baseline O&M model that vary from the ECN North Sea Case Study but are not feasible to list entirely in this report. Therefore, a select few of the high-level general assumptions used for the baseline O&M analysis are listed below:

- The NREL 5-MW reference turbine investment cost was estimated to be $1,947/kW. The cost of this turbine in the project-specific baseline was derived from a variety of resources, including NREL's Wind Turbine Cost and Scaling model (Fingersh 2006) , several recent publications (Deloitte 2011, BVG 2011, BVG 2012), and NREL conversations with U.S. offshore wind project developers.
- The kWh price is assumed to be $0.13/kWh.
- The lifetime of the wind power plant is 20 years with an estimated wind power plant efficiency of 90%.
- The burdened hourly rate for a technician is assumed at $125/h and is only calculated during travel to the repair and the time it takes to complete the repair. No annual salary costs for technicians were considered. The technicians' employment considers a 125% correction factor to account for technicians taking time off due to illness and considers enough technicians for two 12-h shifts. No technician works longer than a 12-h shift. The number of technicians employed for each season are:

    - Winter: 28 technicians
    - Spring: 52 technicians
    - Summer: 58 technicians
    - Autumn: 36 technicians.
- Technicians work during daylight periods except for repairs that require the use of a jack-up barge. In this case, two shifts of technicians work 24 h/day to complete the replacement.
- The seasonal net capacity factors (NCF) of the wind power plant are calculated using the site-specific wind data at 90 m and the NREL 5-MW reference turbine power curve (Jonkman 2009). Calculations are then used as inputs to the O&M model to obtain the lost energy production. Where NCF is defined as:

$$Seasonal\ Net\ Capacity\ Factor\ (NCF) = \frac{Seasonal\ Net\ Energy\ Production}{Seasonal\ Nameplate\ Energy\ Prodcution}$$

- The seasonal NCF used for the baseline scenario is:
    - Winter: 55%
    - Spring: 46%
    - Summer: 32%
    - Autumn: 43%.
- Small parts (< 2 t) are assumed to remain in stock; repairs can be performed with the workboat in combination with derrick cranes mounted on each offshore turbine
- Large parts are assumed not to be kept in stock and must be ordered from the manufacturer in the event of a failure. A jack-up barge is required to replace large turbine components.
- The land-based operations facility is estimated to cost about $2,630,000/year.

8.3.7 Modeling Limitations

The wind turbine component failure rates are based on the limited amount of empirical data available for onshore wind projects. The cost and downtime estimates for unscheduled maintenance rely on wind turbine failure rate assumptions determined by the Reliawind study (Wilkinson 2010). The failure rates generated by this study generally estimate drivetrain failure rates that are lower than those derived from other comparable databases for land-based turbines. This is because the Reliawind study covers relatively newer wind projects. Because of the lack of BOS component failure rate data, this analysis assumed the same BOS failure rates as ECN's North Sea Case Study (van der Zee 2011).

The model is limited to four seasonal variations within any given year. This is the highest-fidelity estimate for the offshore wind power plant O&M cost and availability. An additional modeling effort would be required to obtain monthly, or even shorter-duration, O&M cost and

availability estimates. The seasonal results considered for this analysis aggregate the following months together:

- Winter: December, January, February
- Spring: March, April, May
- Summer: June, July, August
- Autumn: September, October, November.

Additionally, it is observed that O&M costs are largely driven by specialized vessels (e.g., heavy-lift jack-up barges) cost estimates, including both vessel day rate and mob/demob costs. The mobilization cost and day rate for offshore wind power plant O&M vessels are considered to be best estimates and are inherent to a high level of variability.

8.4 Hurricane-Resilient Scenario

For this analysis, all the assumptions and inputs for the hurricane-resilient scenario are the same as for the baseline scenario except for:

- **Failure frequency of wind turbine components:** Because the 10-MW hurricane-resilient turbine utilizes a direct-drive generator, the component definitions and failure rates vary from the baseline's geared system. These failure rates were established from the Reliawind study and modified by NREL based on discussion with ECN and OEMs. As in the baseline scenario (Section 8.3), failure rates were not adjusted for higher wind speed sites than those determined by the Reliawind study due to limited available data. A summary of the direct-drive 10-MW turbine component definitions and failure rates are shown in Table 8-7.

Table 8-7. Hurricane-Resilient Wind Turbine System Component Failure Rate Assumptions

Wind Turbine System Components (Based on RDS-PP Taxonomy)	Annual Failure Frequency of Main Turbine Components (failures/wind turbine/year)
MDA10 - Rotor system – blades	0.0653
MDA20 – Rotor system – hub	0.0653
MDC - Blade adjustment	0.9779
MDK10 – Drivetrain – main shaft/bearing	0.0140
MDK30 – Drivetrain – brake system	0.0212
MDL - Yaw gearbox	0.5076
MDX - Hydraulic system	0.0536
MDY - Control and protection system turbine	0.8483
MKA - Generator	0.4252
MKY - Control and projection system generator	0.7821
MSA - Generator lead/transmission cables	0.4577
MST - Transformer	0.0770
MUD - Machinery enclosure	0.0135
UMD - Turbine structure/tower	0.1512
XA - Heating, ventilation, air conditioning	0.0140
XM - Crane system	0.0144
AB - Lightning protection/grounding	0.0117
MD - Remote resets	12.000
XN - Elevator system	0.0055

Because the hurricane-resilient turbine is using a direct-drive permanent-magnet generator, failure rates for the wind turbine are altered from the geared drivetrain. Therefore, the wind turbine component failure rates are adjusted according to the ECN North Sea O&M case study. Significant changes to the wind turbine component failure rates between the baseline's geared drivetrain and direct-drive system are:

- The direct-drive system is now divided into the main shaft/bearing and brake system, reduced to a combined failure rate of 0.0352 failures/wind turbine/year compared to the geared drivetrain failure rate of 0.2888 failures/wind turbine/year.
- Increase in generator failures for the direct-drive system of 0.4252 failures/wind turbine/year from the geared drivetrain failure rate of 0.3246 failures/wind turbine/year.
- Increase in the generator control and protection system failure rates for the direct-drive system of 0.7821 failures/wind turbine/year from the geared drivetrain failure rate of 0.6001 failures/wind turbine/year.

Less significant impacts to the direct-drive wind turbine failure rates include:

- Reduced control and protection system failure rate, reduced generator lead/transmission cables failure rate, and reduced transformer failure rate from the baseline's geared drivetrain.

- **Repair vessels:** All of the repair vessels are assumed to be the same as the baseline scenario except for the jack-up barge. Because the 10-MW hurricane-resilient direct-drive turbine sits at a hub height of 135 m in addition to an increase in nacelle mass, it would require a heavy-lift jack-up barge. It is assumed that a heavy-lift jack-up barge of this size would not be available in the United States and would need to be mobilized from Europe. Hence, a longer-estimated logistics time, higher day rate, and higher mob/demob costs compared to the baseline are applied. Table 8-8 summarizes the costs and assumptions for the heavy-lift jack-up barge.

Table 8-8. Vessel Limitation and Cost Assumptions for the Heavy-Lift Jack-Up Barge

Vessel Type	Max. Wind Speed (m/s)	Max. Wave Height (m)	Equipment Logistics Time (h)	Travel Time (h)	Day Rate (k$/day)	Lease Rate (k$/year)	Mob/Demob Cost (k$/mission)
Heavy-lift jack-up barge	10	2.0	1,440	-	170	-	9,000

- **Site wind and wave data:** The site wind and wave data inputs for the hurricane-resilient turbine scenario are considered to be the same as the baseline scenario. However, one difference between the two scenarios is the different wind speeds at hub height. The estimated wind speed at the NREL 5-MW baseline turbine's 90-m hub height is 8.7 m/s, whereas the hurricane-resilient 10-MW turbine's 135-m hub height yields an estimated wind speed of 9.1 m/s. Both hub height wind speeds are averaged over the entire input data time-series dataset (from the WIS buoy at 10 m) and extrapolated using the power law with an exponent of 0.1 for reporting purposes. This did not change the wait time estimated by the model but is considered when estimating the net annual energy production (AEP_{net}) for the two scenarios. AEP_{net} considers system losses within the offshore wind power plant—estimated to be 10% for both the baseline and hurricane-resilient scenarios. Higher wind speeds at the higher hub height make it possible to generate more energy at the same wind site and impacts the annual cost of O&M.
- **10-MW hurricane-resilient turbine:** The investment cost of the hurricane-resilient turbine is estimated to be $2,500/kW. The cost estimate is derived from scaling up the NREL 5-MW reference turbine.
- **Technicians employed:** The technicians employed for each season are different from the baseline scenario because there are fewer wind turbines in the offshore wind power plant, and changes are applied to the failure rates of the wind turbine components. The changes to the number of employed technicians are:
    - Winter: 14 technicians
    - Spring: 26 technicians
    - Summer: 30 technicians
    - Autumn: 18 technicians.

- **Seasonal Nnet capacity factors (NCF):** The seasonal NCF is calculated using the site-specific wind data at 10 m and extrapolating up to 120 m using the power law and a shear value of 0.1 as well as the hurricane-resilient 10-MW turbine power curve. The 120-m hub height was used based on the value in the proposal versus the project's current hub height of 135 m. The estimated change in wind speed at 120 m is 9.0 m/s versus 9.1 m/s at 135 m—resulting in a 1% increase in wind speed. This slight increase in wind speed does not have a significant impact on the NCF estimates. The seasonal NCF used for the hurricane-resilient scenario is:
    - Winter: 64%
    - Spring: 57%
    - Summer: 44%
    - Autumn: 53%.
- **Heavy-lift jack-up barge:** A heavy-lift jack-up barge mobilized from Europe is required to replace large turbine components on the hurricane-resilient 10-MW turbine.

8.4.1 Baseline O&M Cost and Downtime Results

The summary in Table 8-9 presents both a seasonal and annual breakdown of the downtime and costs associated with wind turbine and BOS unscheduled and scheduled maintenance. The "Total" column represents the summation of the results for each of the four seasons. Results in the "Year" column represent annual estimates that do not account for seasonal differences in wind and wave climate. This study considers the "Total" column to be more accurate because its results consider seasonal variations and, hence, are used for the calculations of O&M cost and downtime.

Table 8-9. Summary of Baseline O&M Results

Summary of downtime and costs			*Availability [%]*	94.6%					
Location	Baseline		*Costs [$ ct/kWh]*	4.51					
Type of WT	NREL 5 MW (Geared)		*Total effort [M$]*	95.8					
Wind farm	100 turbines			Winter	Spring	Summer	Autumn	Total	Year
Downtime per year									
Unscheduled WT	Logistics	hr		2,355	2,355	2,355	2,355	9,420	9,420
	Waiting	hr		4,430	2,065	537	2,647	9,679	10,395
	Travel	hr		230	230	230	230	919	919
	Repair	hr		3,097	2,201	2,201	3,097	10,597	12,081
	TOTAL unscheduled WT	hr		10,112	6,851	5,323	8,329	30,615	32,815
Unscheduled BOS	Logistics	hr		1,999	1,999	1,999	1,999	7,995	7,995
	Waiting	hr		519	267	74	347	1,207	1,373
	Travel	hr		20	20	20	20	79	79
	Repair	hr		505	254	254	505	1,517	1,849
	TOTAL unscheduled BOS	hr		3,042	2,539	2,346	2,871	10,798	11,296
Scheduled	**TOTAL scheduled**	hr		0	2,100	3,300	600	6,000	6,000
	TOTAL	hr		**13,154**	**11,490**	**10,969**	**11,800**	**47,413**	**50,111**
Availability		%		94.0%	94.8%	95.0%	94.6%	94.6%	94.3%
Loss of production per year		MWh		36,174	26,427	17,550	25,370	105,521	110,245
Energy production per year		MWh		566,076	477,273	332,850	445,480	1,821,679	1,816,955
Revenue losses per year		k$		**4,703**	**3,435**	**2,281**	**3,298**	**13,718**	**14,332**
Costs of repair per year									
Material costs									
Unscheduled WT	**TOTAL unscheduled WT**	k$		4,099	4,099	4,099	4,099	16,396	16,396
Unscheduled BOS	**TOTAL unscheduled BOS**	k$		16	16	16	16	62	62
Scheduled	**TOTAL scheduled**	k$		0	1,825	2,867	521	5,213	5,213
	TOTAL	k$		**4,114**	**5,939**	**6,982**	**4,636**	**21,671**	**21,671**
Labor costs									
Unscheduled WT	**TOTAL unscheduled WT**	k$		836	770	770	836	3,212	3,343
Unscheduled BOS	**TOTAL unscheduled BOS**	k$		2	2	2	2	8	8
Scheduled	**TOTAL scheduled**	k$		0	1,426	2,242	439	4,107	4,213
	TOTAL			**838**	**2,198**	**3,014**	**1,277**	**7,327**	**7,564**
Costs equipment									
Unscheduled WT	MOB/DEMOB	k$		9,570	9,570	9,570	9,570	38,279	38,279
	Waiting	k$		322	322	322	322	1,286	1,286
	Repair	k$		777	758	755	763	3,053	3,046
	TOTAL unscheduled WT	k$		10,668	10,649	10,647	10,655	42,619	42,612
Unscheduled BOS	MOB/DEMOB	k$		804	804	804	804	3,218	3,218
	Waiting	k$		69	69	60	71	271	263
	Repair	k$		83	81	81	83	327	322
	TOTAL unscheduled BOS	k$		957	954	945	959	3,815	3,803
Scheduled	**TOTAL scheduled**			0	498	779	171	1,448	1,542
	TOTAL			**11,625**	**12,102**	**12,371**	**11,784**	**47,882**	**47,957**
Unscheduled WT		k$		**15,603**	**15,518**	**15,516**	**15,589**	**62,227**	**62,350**
Unscheduled BOS		k$		**974**	**972**	**962**	**976**	**3,885**	**3,873**
Scheduled		k$		**0**	**3,749**	**5,888**	**1,131**	**10,768**	**10,968**
Operations (Fixed yearly costs)		k$		**1,177**	**1,437**	**1,437**	**1,177**	**5,229**	**5,749**
Total costs of repair		k$		**17,755**	**21,676**	**23,803**	**18,874**	**82,108**	**82,940**
Total cost per kWh		$ cent/kWh		**3.14**	**4.54**	**7.15**	**4.24**	**4.51**	**4.56**
Total costs of repair per kW installed		$/kW		**36**	**43**	**48**	**38**	**164**	**166**
Total cost per kW investment				**1.8%**	**2.2%**	**2.4%**	**1.9%**	**8.4%**	**8.5%**
Total effort									
Sum revenue losses & total costs of repair		k$		**22,457**	**25,112**	**26,085**	**22,172**	**95,826**	**97,272**

Two important outputs from the analysis are wind power plant availability and O&M cost. Wind power plant availability is the ratio between the actual number of operational hours and the total possible number of operational hours, shown in this equation:

$$Availability = \frac{Possible\ annual\ operating\ hours - Annual\ O\&M\ downtime\ hours}{Possible\ annual\ operating\ hours}$$

The annual availability for the baseline scenario is estimated to be 94.6%, based on the time series dataset capturing metocean characteristics of two hurricanes passing near the wind site (cf. above). The availability is calculated using the estimated wind power plant downtime from the ECN model. The total wind power plant annual downtime is subtracted from the total possible wind power plant annual operating hours (assuming 8,760 operating hours per turbine in a year) and dividing by the total possible wind power plant annual operating hours. A majority of the downtime is associated with the unscheduled wind turbine maintenance. The AEP_{net} for the scenario is estimated to be 1,822,000 MWh/year. The O&M costs are estimated at $0.0451/kWh. Most of the costs are accrued by the unscheduled wind turbine maintenance activities. The total cost includes labor hours, repair materials, vessel mob/demob, vessel usage, and rental costs for a land-based operations base. Total O&M costs do not consider the estimated revenue losses from maintenance downtime.

8.4.2 Baseline O&M Primary Cost Drivers

O&M costs are primarily driven by unscheduled wind turbine maintenance. The replacement of large wind turbine components is the main contributor (Figure 8-2) because of the high equipment costs associated with replacing large wind turbine components. The equipment costs include mob/demob costs and hourly rental costs, including time the equipment is waiting due to poor weather conditions or time the equipment is being repaired. The analysis assumes the replacement of large components for the 5-MW turbines will require the use of a jack-up barge that is available in the Gulf of Mexico region. The high mob/demob costs associated with using a jack-up barge drive the high replacement costs (Figure 8-3). This is primarily from the $6 million assumed to mob/demob each time the jack-up barge is required to replace a large turbine component. Variance in the mob/demob cost assumption highly impacts the O&M costs for the wind power plant. As offshore wind becomes more established in the United States, a better understanding of the mob/demob costs for jack-up barges can be used to refine the O&M model and potentially decrease O&M costs.

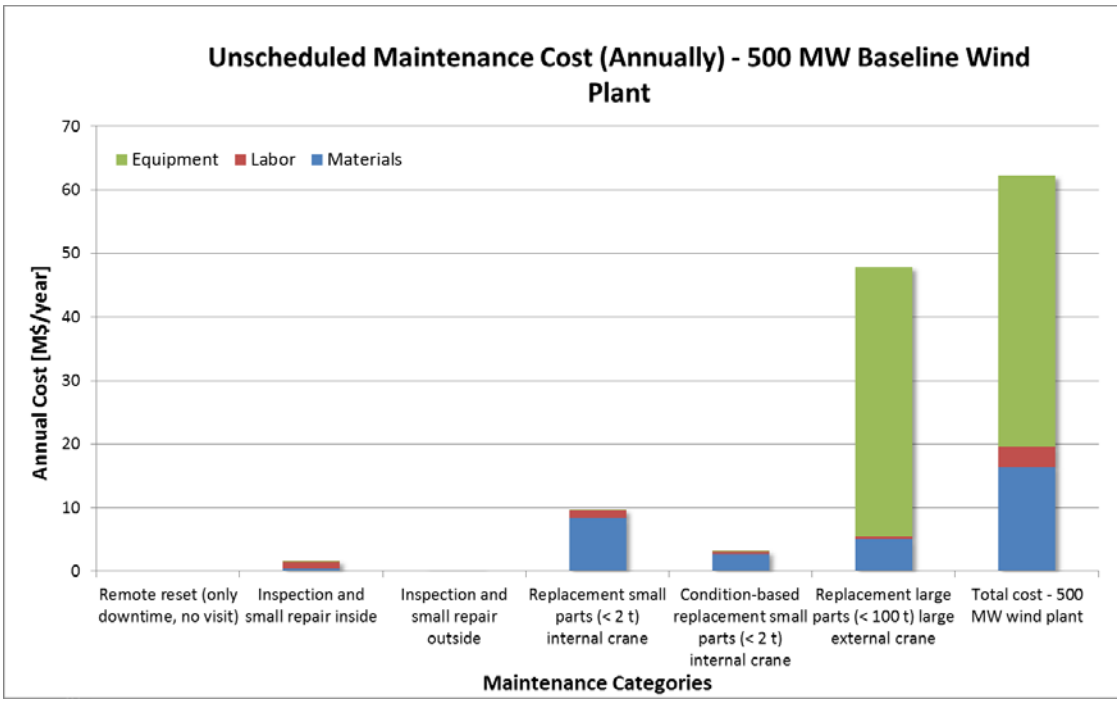

Figure 8-2. Unscheduled maintenance cost (annually) for the baseline 500-MW wind power plant

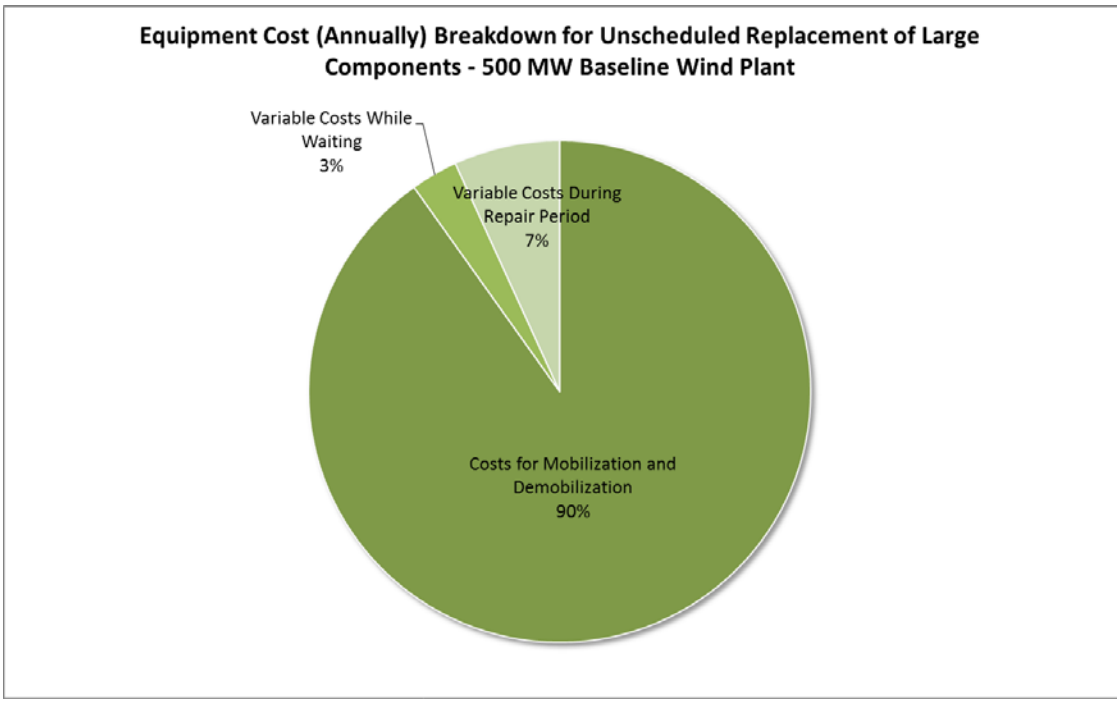

Figure 8-3. Equipment cost breakdown for unscheduled replacement of large components of the baseline 500-MW wind power plant

The second noteworthy driver of unscheduled wind turbine maintenance cost is the material cost, which includes the cost of replacement parts. This cost can be better understood by breaking down the material costs into the wind turbine components. The wind turbine component breakdown is based on the RDS-PP taxonomy (Müller et al. 2013). The drivetrain contributes the most annual average cost for replacement parts (Figure 8-4). Innovations focusing on improved reliability for the drivetrain component could reduce the number of component replacements and, thereby, reduce material costs and the need to mobilize a jack-up barge to the wind power plant. Other innovations such as direct-drive technology may further reduce O&M costs by eliminating the gearbox component of the drivetrain. This study attempts to estimate the O&M advantages of a direct-drive system over a conventional geared drivetrain. Section 8.3 describes the baseline scenario component failure rates, and Section 8.4 describes the direct-drive component failure rates and the differentiating modeling assumption for the hurricane-resilient versus the baseline scenario.

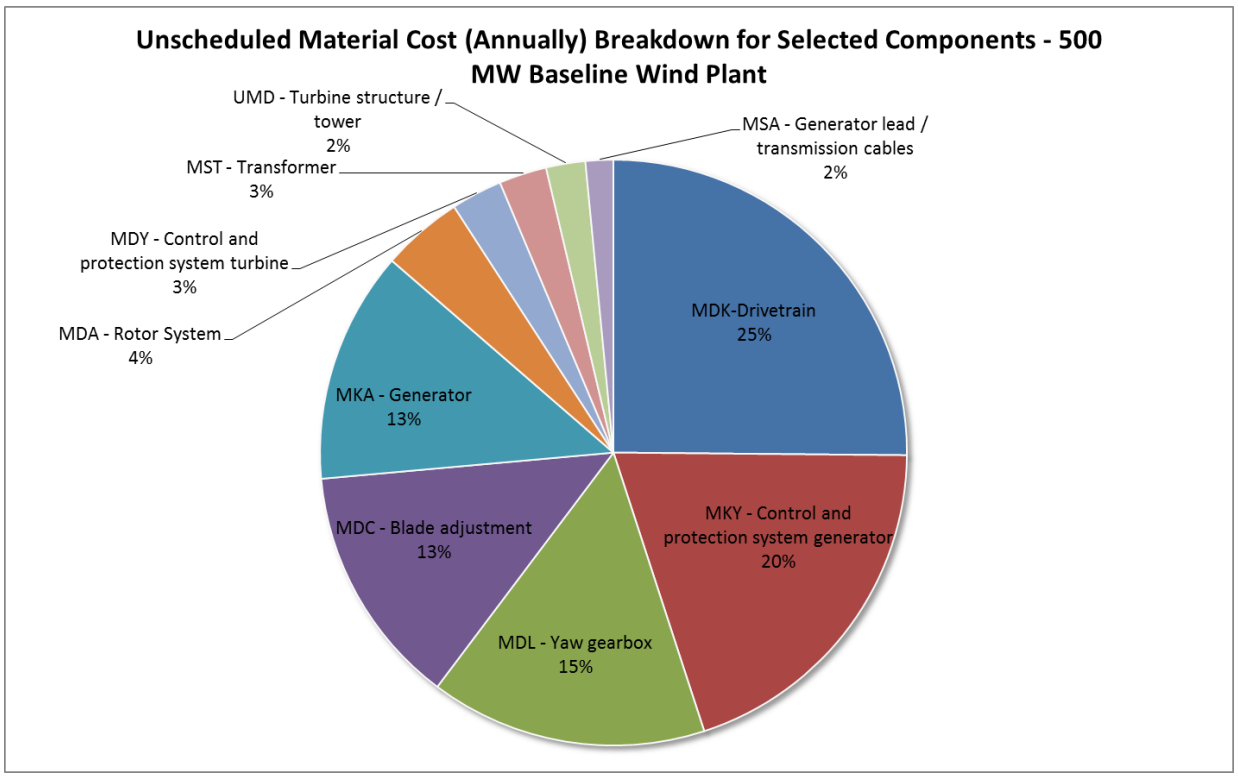

Figure 8-4. Material cost breakdown for unscheduled maintenance for the baseline 500-MW wind power plant

8.4.3 Baseline O&M Primary Downtime Drivers

Unscheduled maintenance is the primary driver for O&M downtime. Annual offshore wind power plant downtime can be broken down into four contributing factors:

- **Waiting time:** The time when the repair crew cannot depart for travel because of poor weather conditions

- **Logistical time:** The time that elapses before the personnel, equipment, and spare parts are ready to travel to the turbine for repair; includes nonleased vessel mobilization time
- **Repair Time:** The time it takes to complete the repair
- **Travel Time:** The time it takes for the access vessel to travel from the O&M operations port to the turbine and back.

A useful way of identifying the primary drivers for O&M downtime is to consider the downtime associated with each of the defined turbine repair categories (Figure 8-5). Replacing small parts is the largest contributor to unscheduled maintenance downtime. Most of the downtime is accumulated from the waiting time by the workboats not being able to depart because of poor weather conditions. Site accessibility challenges increase the downtime for offshore wind power plants and, as a result, increase O&M cost. Less restrictive workboat limitations may reduce wind power plant downtime by allowing technicians to conduct small component replacements in higher sea state conditions. However, when considering all of the maintenance categories, the downtime associated with the turbine repair time and the equipment logistics time becomes a large contributor to downtime. Improving wind turbine component reliability can potentially reduce each of these drivers that contribute to O&M downtime.

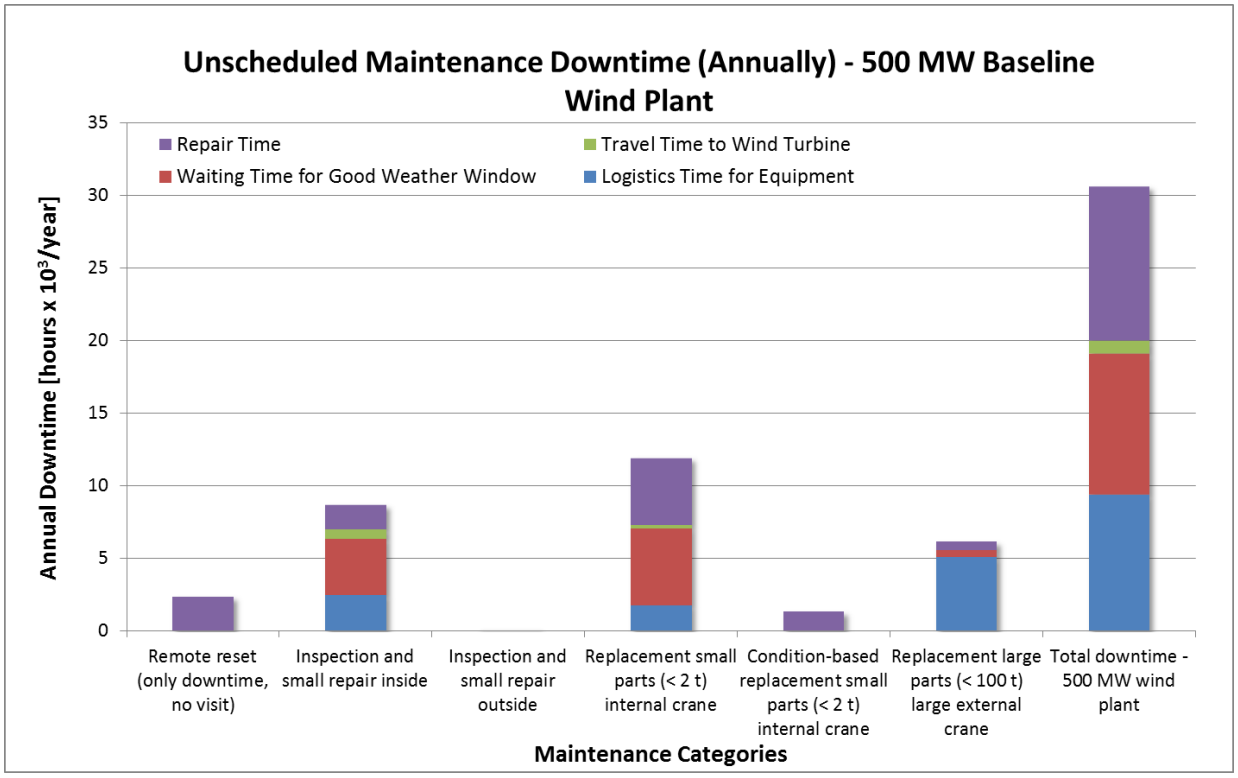

Figure 8-5. Unscheduled maintenance downtime for the 500-MW baseline wind power plant

8.4.4 Hurricane-Resilient O&M Cost and Downtime Results

This section assesses the theoretical hurricane-resilient 10-MW turbine's cost and downtime associated with offshore O&M activities in the Gulf of Mexico. We considered the same wind and wave dataset as the baseline scenario to compare the impacts on O&M costs and downtime for the two wind power plant scenarios. The summary in Table 8-10 presents both a seasonal and annual breakdown of the downtime and costs associated with wind turbine and BOS unscheduled and scheduled maintenance for the hurricane-resilient scenario.

Table 8-10. Summary of Hurricane-Resilient O&M Results

Summary of downtime and costs			*Availability [%]*	93.3%					
Location	Hurricane Site		*Costs [$ct/kWh]*	3.80					
Type of WT	10 MW Direct Drive Turbine		*Total effort [M$]*	105.8					
Wind farm		50 turbines		Winter	Spring	Summer	Autumn	Total	Year
Downtime per year									
Unscheduled WT	Logistics	hr		2,543	2,543	2,543	2,543	10,173	10,173
	Waiting	hr		2,239	1,033	268	1,334	4,874	5,236
	Travel	hr		115	115	115	115	458	458
	Repair	hr		1,555	1,101	1,101	1,555	5,312	6,061
	TOTAL unscheduled WT	hr		6,452	4,792	4,027	5,547	20,818	21,929
Unscheduled BOS	Logistics	hr		999	999	999	999	3,998	3,998
	Waiting	hr		259	133	37	174	604	687
	Travel	hr		10	10	10	10	40	40
	Repair	hr		252	127	127	252	758	924
	TOTAL unscheduled BOS	hr		1,521	1,269	1,173	1,435	5,399	5,648
Scheduled	**TOTAL scheduled**	hr		0	1,050	1,650	300	3,000	3,000
	TOTAL	hr		**7,973**	**7,111**	**6,851**	**7,282**	**29,217**	**30,577**
Availability		%		92.7%	93.5%	93.7%	93.3%	93.3%	93.0%
Loss of production per year		MWh		51,162	40,877	29,916	38,915	160,871	166,951
Energy production per year		MWh		651,499	588,529	448,270	546,253	2,234,551	2,224,529
Revenue losses per year		k$		**6,651**	**5,314**	**3,889**	**5,059**	**20,913**	**21,704**
Costs of repair per year									
Material costs									
Unscheduled WT	**TOTAL unscheduled WT**	k$		4,432	4,432	4,432	4,432	17,729	17,729
Unscheduled BOS	**TOTAL unscheduled BOS**	k$		16	16	16	16	62	62
Preventive	**TOTAL scheduled**	k$		0	915	1,437	261	2,613	2,613
	TOTAL	k$		**4,448**	**5,362**	**5,885**	**4,709**	**20,404**	**20,404**
Labor costs									
Unscheduled WT	**TOTAL unscheduled WT**	k$		409	376	376	409	1,569	1,635
Unscheduled BOS	**TOTAL unscheduled BOS**	k$		2	2	2	2	8	8
Scheduled	**TOTAL scheduled**	k$		0	713	1,121	220	2,053	2,106
	TOTAL			**411**	**1,091**	**1,499**	**630**	**3,631**	**3,750**
Costs equipment									
Unscheduled WT	MOB/DEMOB	k$		12,315	12,315	12,315	12,315	49,262	49,262
	Waiting	k$		167	167	167	167	670	670
	Repair	k$		385	383	382	380	1,530	1,540
	TOTAL unscheduled WT	k$		12,868	12,866	12,865	12,863	51,462	51,472
Unscheduled BOS	MOB/DEMOB	k$		804	804	804	804	3,218	3,218
	Waiting	k$		69	69	60	71	271	263
	Repair	k$		83	81	81	83	327	322
	TOTAL unscheduled BOS	k$		957	954	945	959	3,815	3,803
Scheduled	**TOTAL scheduled**			0	484	758	163	1,405	1,498
	TOTAL			**13,825**	**14,304**	**14,567**	**13,985**	**56,681**	**56,772**
Unscheduled WT		k$		**17,709**	**17,674**	**17,673**	**17,704**	**70,760**	**70,835**
Unscheduled BOS		k$		**974**	**972**	**963**	**976**	**3,885**	**3,873**
Scheduled		k$		**0**	**2,112**	**3,315**	**644**	**6,071**	**6,217**
Operations (Fixed yearly costs)		k$		**917**	**1,177**	**1,177**	**917**	**4,189**	**4,709**
Total costs of repair		k$		**19,600**	**21,935**	**23,128**	**20,242**	**84,904**	**85,634**
Total cost per kWh		$ cent/kWh		**3.01**	**3.73**	**5.16**	**3.71**	**3.80**	**3.85**
Total costs of repair per kW installed		$/kW		**39**	**44**	**46**	**40**	**170**	**171**
Total cost per kW investment				**1.6%**	**1.8%**	**1.9%**	**1.6%**	**6.8%**	**6.9%**
Total effort									
Sum revenue losses & total costs of repair		k$		**26,251**	**27,249**	**27,017**	**25,301**	**105,817**	**107,338**

The annual availability for the hurricane-resilient scenario is estimated to be 93.3%, based on the time series dataset simulating two hurricanes passing near the wind site, and calculated using the estimated wind power plant downtime from the ECN model. The associated AEP_{net} for the hurricane-resilient scenario is 2,235,000 MWh/year. The O&M costs are estimated to be $0.0380/kWh.

8.4.5 Hurricane-Resilient O&M Primary Cost Drivers

As with the baseline scenario, the primary O&M costs driver for the hurricane-resilient scenario is the unscheduled turbine maintenance. The equipment cost for the replacement of large wind turbine components is the main contributor (Figure 8-6) because of the high equipment costs associated with replacing large wind turbine components. Specifically, comparing Figure 8-2 and Figure 8-6, annual unscheduled maintenance costs are $62 million per year for the baseline wind power plant and $71 million per year for the hurricane-resilient wind power plant. Annual unscheduled maintenance costs are closely similar for all maintenance categories except for "replacement large parts (< 100 t) large external crane." In this category, costs are about $9 million per year higher for the hurricane-resilient wind power plant, which comprises the major portion of the overall difference between the two. This scenario assumes that the replacement of large components for the 10-MW turbines will require the use of a specialized heavy-lift jack-up barge that is not available in the United States. In this case, the heavy-lift jack-up barge will need to be mobilized from Europe to conduct the unscheduled large turbine component replacement. The high mob/demob costs associated with using a heavy-lift jack-up barge drive the high-replacement costs (Figure 8-7). This is primarily from the $9 million assumed to mob/demob the heavy-lift jack-up barge each time it is required to replace a large turbine component. Variance in the mob/demob cost assumption highly impacts the O&M costs for the wind power plant. As offshore wind becomes more established in the United States, a better understanding of the mob/demob costs for specialized heavy-lift jack-up barges can be used to refine the O&M model and potentially decrease O&M costs.

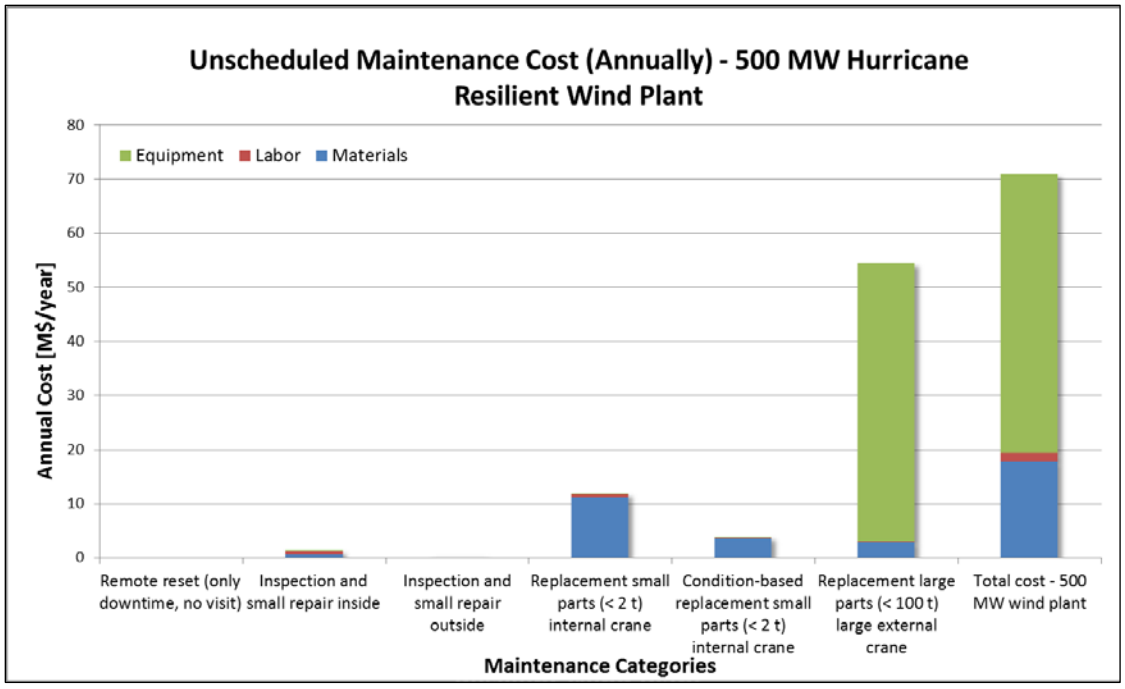

Figure 8-6. Unscheduled maintenance cost (annually) for the hurricane-resilient 500-MW wind power plant

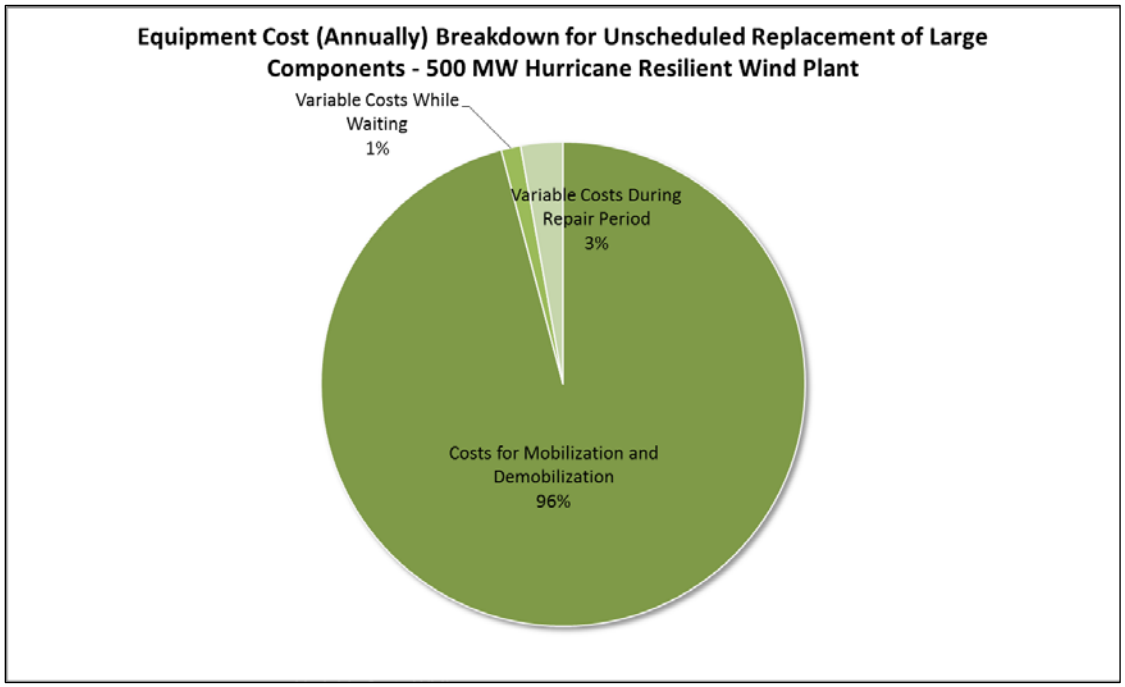

Figure 8-7. Equipment cost breakdown for unscheduled replacement of large components of the hurricane-resilient 500-MW wind power plant

The second significant driver of unscheduled maintenance costs is material cost, which includes the cost of replacement parts. This cost can be better understood by breaking down material costs by wind turbine component. The wind turbine component breakdown is based on the RDS-PP taxonomy (Müller 2012). Figure 8-8 shows the control and protection system for the direct-drive generator contributes the most annual cost for replacement materials. Improved reliability on the control and protection system for the direct-drive generator could reduce the number of replacements, thereby reducing material costs and the need to travel to the wind power plant.

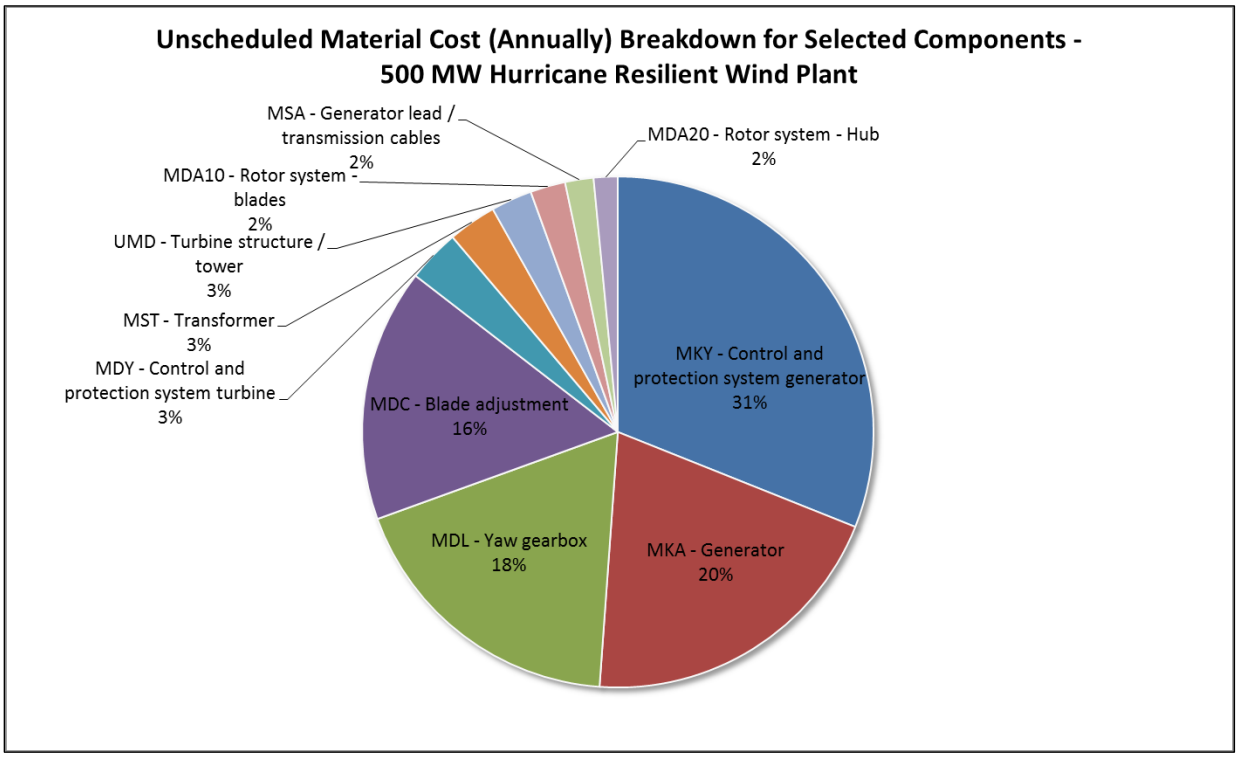

Figure 8-8. Material cost breakdown for unscheduled maintenance for the hurricane-resilient 500-MW wind power plant

8.4.6 Hurricane-Resilient O&M Primary Downtime Drivers

Unscheduled maintenance is the primary driver for O&M downtime. A useful way of identifying the primary drivers for O&M downtime is to consider the downtime associated with each of the defined turbine maintenance categories(Figure 8-9). Replacement of large parts is the biggest contributor to unscheduled maintenance downtime. This downtime is driven by the logistics and mobilization time for the heavy-lift jack-up barge to get from Europe to the Gulf of Mexico. Notably, comparing Figure 8-5 and Figure 8-9, annual unscheduled maintenance downtimes for maintenance categories "remote reset" through "condition based replacement small parts" are almost exactly halved for the hurricane-resilient wind power plant relative to the baseline wind power plant. This trend correlates with the reduction in number of turbines from the baseline wind power plant (100 turbines) to the hurricane-resilient wind power plant (50 turbines). However, this trend does not hold for the maintenance category, "replacement large parts (< 100 t)." Here, annual unscheduled maintenance downtimes are about 6,100 hours for the baseline

wind power plant and approximately 8,200 hours for the hurricane-resilient wind power plant, with this trend reversal driven by "logistics time for equipment." Thus, while "total downtime – 500 MW wind power plant" is significantly lower for the hurricane-resilient wind power plant, it is not one-half that for the baseline wind power plant, primarily because of "logistics time for equipment." Currently, there is no U.S.-flagged jack-up barge capable of conducting a large component replacement for the conceptual 10-MW turbine. As offshore wind is further developed in the United States, the availability of a U.S.-flagged heavy-lift jack-up barge may enter the U.S. market and eliminate the need to mobilize the barge from Europe.

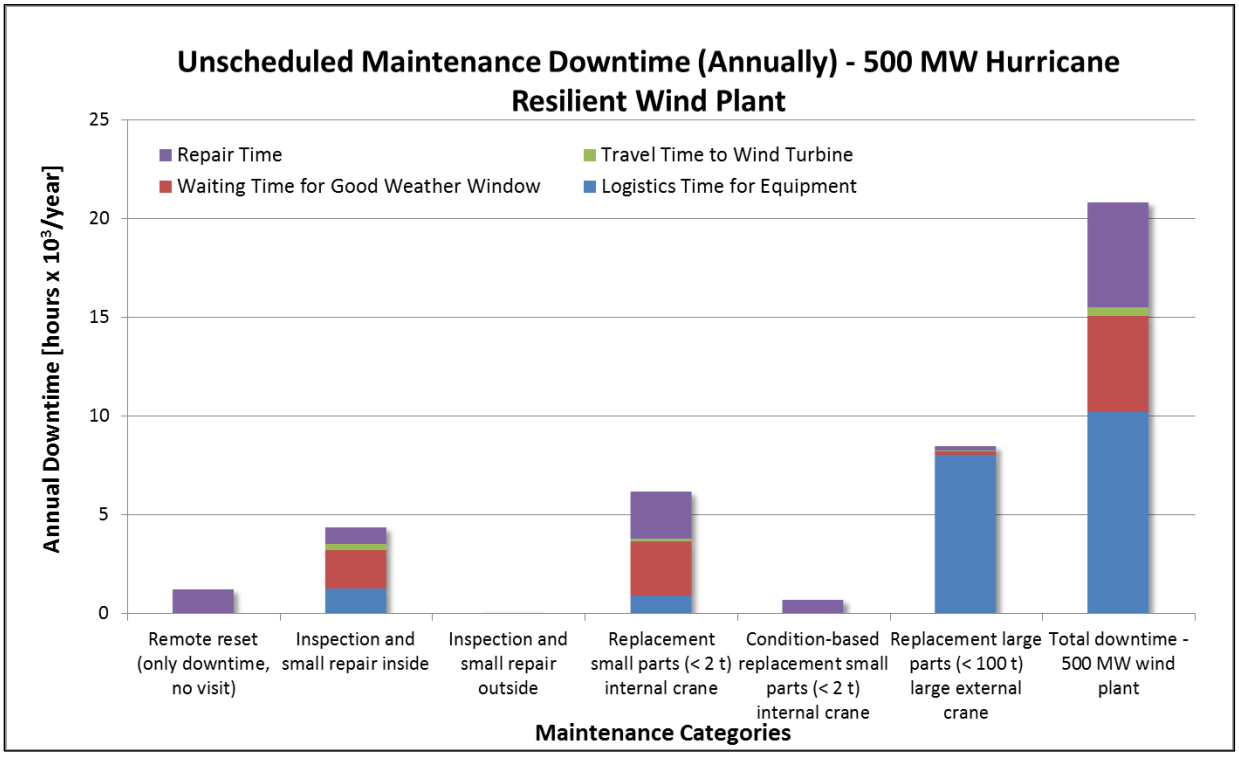

Figure 8-9. Unscheduled maintenance downtime for the 500-MW hurricane-resilient wind power plant

8.5 Conclusions

A summary of the availability, costs, and AEP_{net} for the two scenarios is shown in Table 8-11. Details for each of the scenarios are explained following the summary table of results.

Table 8-11. Summary of Results for Baseline and Hurricane-Resilient O&M Scenarios

O&M Scenario	Availability (%)	Cost ($/kWh/year)	Net Annual Energy Production (MWh/year)
Baseline	94.6	0.0451	1,822,000
Hurricane-resilient	93.3	0.0380	2,235,000

O&M costs for the baseline scenario are estimated to be approximately $0.0451/kWh/year. Of the total O&M costs, a large fraction is accrued from unscheduled maintenance, which contributes approximately 74% of the total O&M costs (Figure 8 through Figure 10). The primary driver for unscheduled maintenance is the cost mob/demob of a jack-up barge from the Gulf of Mexico region. The availability for the baseline is estimated to be 94.6%. The unscheduled maintenance drives the O&M downtime by contributing about 64% of total O&M downtime (Figure 8-11). The unscheduled maintenance downtime is driven by the waiting time for workboats waiting on good weather windows, the repair time to replace small turbine components, and the mobilization time estimated for a jack-up barge.

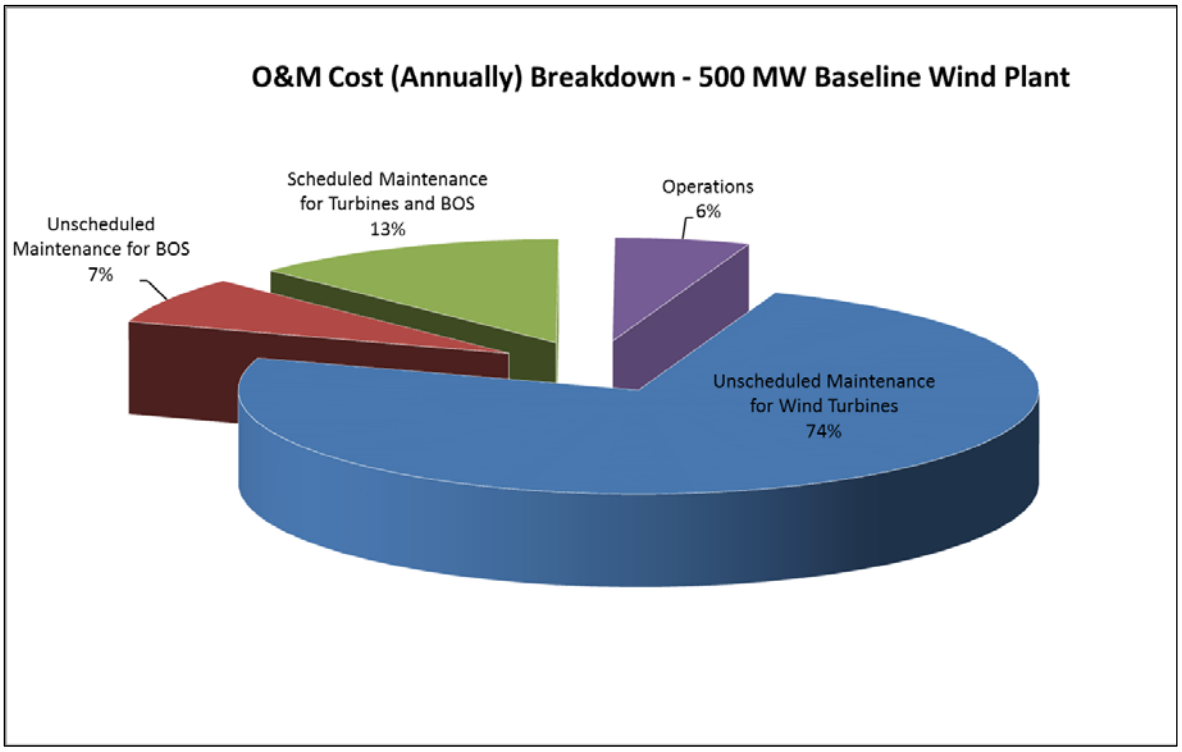

Figure 8-10. O&M cost breakdown for the baseline 500-MW wind power plant

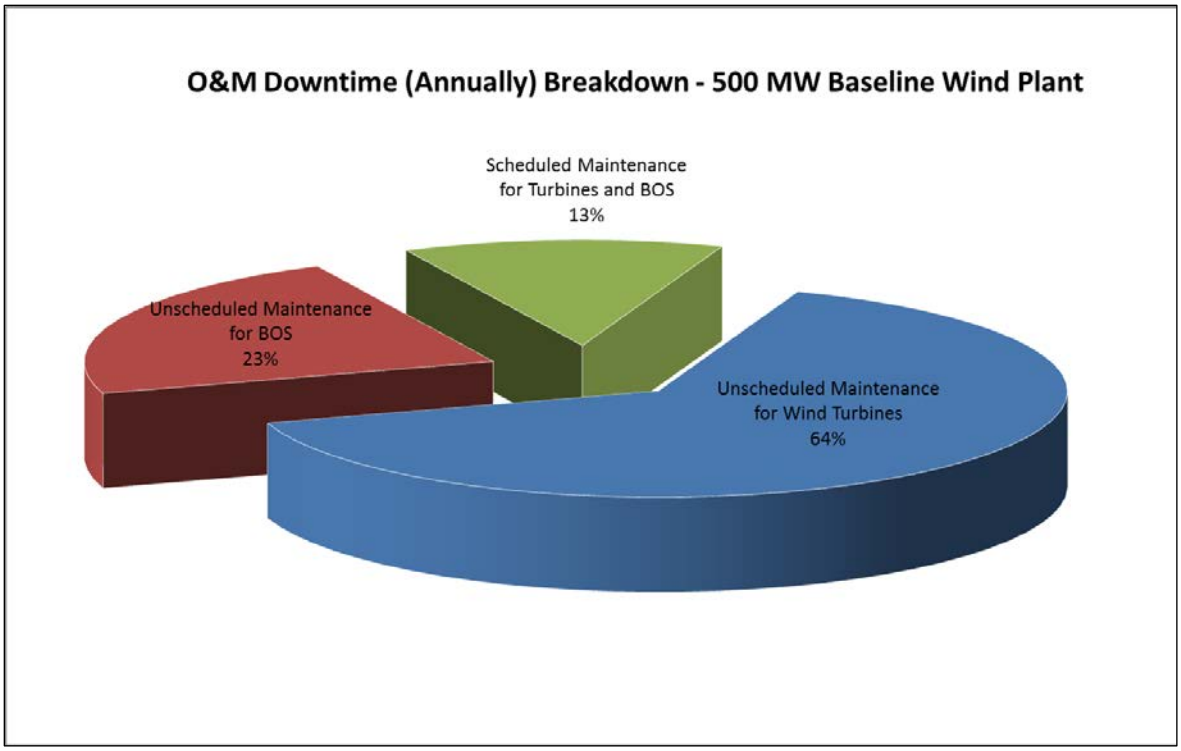

Figure 8-11. O&M downtime breakdown for the baseline 500-MW wind power plant

The hurricane-resilient scenario lowered the annual cost of O&M from the baseline's \$0.0451/kWh/year to \$0.0380/kWh/year. The lower O&M cost is because of the higher AEP_{net} generated by the 10-MW wind turbines. The estimated energy production increased from 1,822,000 MWh/year to 2,235,000 MWh/year as a result of the increased rotor diameter and higher hub height of the hurricane-resilient turbine. As with the baseline scenario, the unscheduled maintenance contributes the most to the O&M cost. Figure 8-12 shows the unscheduled maintenance being 81% of the overall O&M costs. For this scenario, the unscheduled maintenance cost is being driven by the mob/demob costs of the heavy-lift jack-up barge assumed to be mobilized from Europe.

The availability of the hurricane-resilient scenario decreased from the baseline's 94.6% to 93.3%. This is the result of the reduced number of turbines in the wind power plant (i.e., 100 to 50 turbines) and the estimated number of downtime hours for each scenario (i.e., approximately 47,000 hours for the baseline scenario versus approximately 29,000 hours for the hurricane-resilient scenario). The number of possible annual operating hours is also reduced with fewer wind turbines. For example, the baseline wind power plant's 100 turbines have a potential to operate 876,000 hours/year (8,760 hours/year x 100 turbines), whereas the hurricane-resilient wind power plant's 50 turbines have a potential to operate 438,000 hours/year (8,760 hours/year x 50 turbines). Even though the baseline wind power plant has a higher number of downtime hours from wind power plant failures, the possible number of operating hours for the baseline is double that of the hurricane-resilient wind power plant. Therefore, by definition of availability for this study, the baseline scenario results in a higher availability than the hurricane-resilient

scenario. For clarity, the availability calculation is shown below for the hurricane-resilient scenario:

$$Availability_{hurricane} = \frac{\left(\left(8{,}760\,\frac{hours}{year}\,x\ 50\ turbines\right) - 29{,}217\ plant\ downtime\ hours\right)}{8{,}760\,\frac{hours}{year}\,x50\ turbines} = 0.933$$

The unscheduled maintenance O&M downtime contributes about 71% of the total wind power plant downtime (Figure 8-13). A majority of the downtime is from the mobilization time for the heavy-lift jack-up barge from Europe to the Gulf of Mexico. As offshore wind becomes more established in the United States, a better understanding of the mob/demob costs for jack-up barges can be used to refine the O&M model and potentially decrease O&M costs. Additionally, the availability of a U.S.-flagged heavy-lift jack-up barge may enter the U.S. market and eliminate the need to mobilize the barge from Europe and further reduce O&M costs.

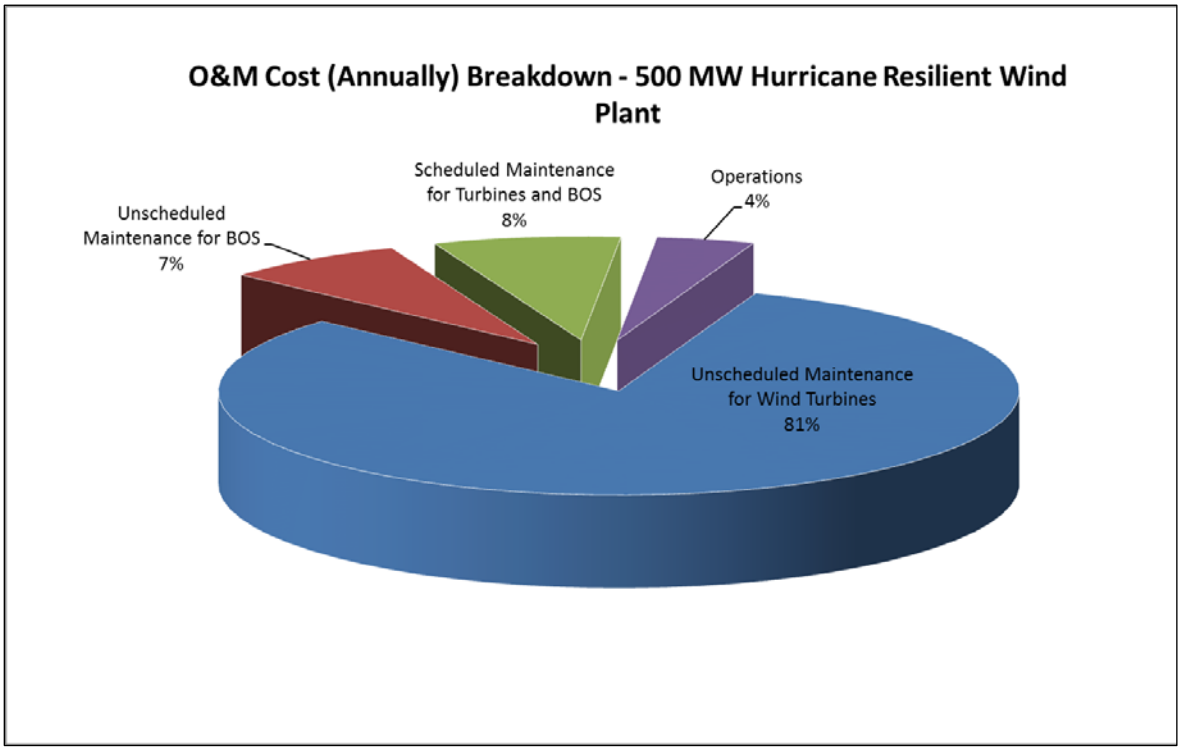

Figure 8-12. O&M cost breakdown for the hurricane-resilient 500-MW wind power plant

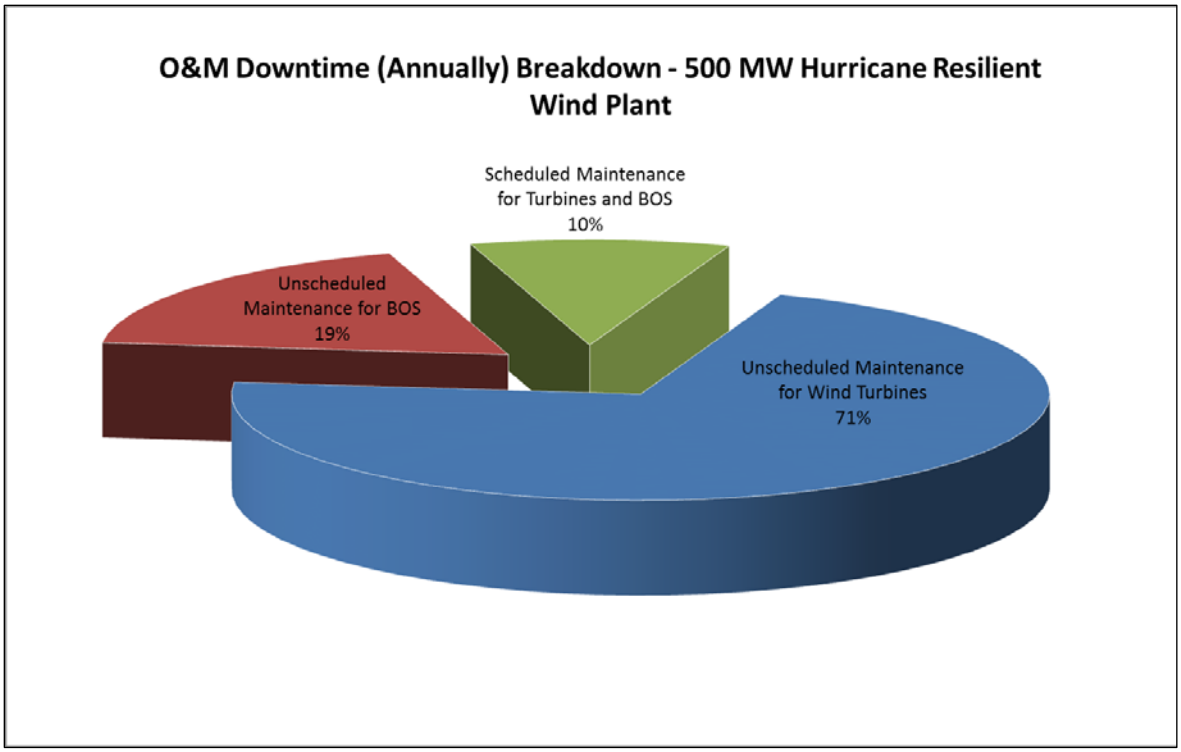

Figure 8-13. O&M downtime breakdown for the hurricane-resilient 500-MW wind power plant

8.6 Recommendations for Future O&M Analysis

This section contains recommendations for further study that could potentially improve understanding of O&M strategies for hurricane-prone regions of the United States.

The Gulf of Mexico O&M analysis suggests further investigation in a number of areas, including:

- Conduct analysis on additional O&M scenarios in nonhurricane-prone regions to gain a better sense of the impacts of costs, downtime, and energy production as compared to the hurricane site
- Consider higher wind turbine component failure rates than those in the Reliawind study to capture potential impact on O&M costs and wind power plant availability for hurricane-prone sites
- Partner with a wind industry owner/operator, or OEM, to better understand offshore wind turbine and BOS failure frequencies and repair strategies
- Explore additional vessel strategies, contracting strategies, day-rate costs, and mob/demob costs for projects in the United States. More clarity in these areas might provide more accurate cost and downtime estimates for offshore O&M. This would allow identification of areas in which to focus efforts to reduce O&M costs

- Investigate suitable repair strategies to reduce dependencies on expensive heavy-lift jack-up barges
- Conduct research on advanced vessel technologies that allow for fewer restrictions on wave and wind climates to reduce the downtime for offshore O&M activities
- Consider different turbine technology options such as Conditional Monitoring System (CMS) to assist in planning O&M activities accordingly, lower downtime, and increase AEP_{net}
- Carry out additional studies on regional hurricane and climate variations, such as wind and wave characteristics, to further understand how these site climates affect site O&M costs and downtime.

9 LCOE Analysis and Projection

This section summarizes the LCOE analysis for the *Hurricane-Resilient Wind Power Plant Concept Study* in response to Topic Area 2 of The Department of Energy's Funding Opportunity Announcement DE-FOA-0000415, U.S. Offshore Wind: Technology Development.

The *Hurricane-Resilient Wind Power Plant Concept Study* is an integrated systems approach to the feasibility-level design, performance, and cost-of-energy estimate for a notional 500-MW offshore wind project located at a site with characteristics that apply to the Gulf of Mexico and other hurricane-prone regions off the coast of the United States. The concept includes a foundation and support substructure suited for water depths of approximately 25 m.

Hurricane-resilient innovations are targeted to reduce the LCOE for large-scale offshore wind installations relative to baseline LCOE assumptions. The analyses of both the baseline and proposed configurations are customized to projects located in the Gulf of Mexico. The study focuses on the following innovations:

- Turbine innovations: Used a large advanced downwind coned rotor, specially designed carbon fiber blades, innovative permanent-magnet direct-drive (PMDD) generator with active cooling, and optimized tower design for a hurricane-resilient downwind coned rotor configuration
- Substructure innovations: Reduced foundation and substructure fabrication and installation costs by evaluating alternatives to a full-depth monopile and transition piece.
- Hurricane-resilient design: Implemented back-up generators for continuous yaw system power.

9.1 Baseline Scenario

The *Hurricane-Resilient Wind Power Plant Concept Study* benchmarked the cost and performance of proposed innovations against baseline technology representing a project installed in the Gulf of Mexico. The NREL 5-MW wind turbine was selected as the offshore baseline turbine configuration because of its wide use internationally as a reference turbine (Jonkman 2009).

As shown in Figure 9-1, to represent the baseline site and estimate cost reductions from proposed innovations, NREL used its Wind Turbine Design Cost and Scaling model, its Offshore Wind BOS model, and the ECN O&M tool (Braam et al. 2011). These estimates were validated against market data and partner experience, and adjusted as needed. The COE was calculated using DOE's LCOE formula and the prescribed financial parameters as defined in Funding Opportunity Announcement (FOA) 415.

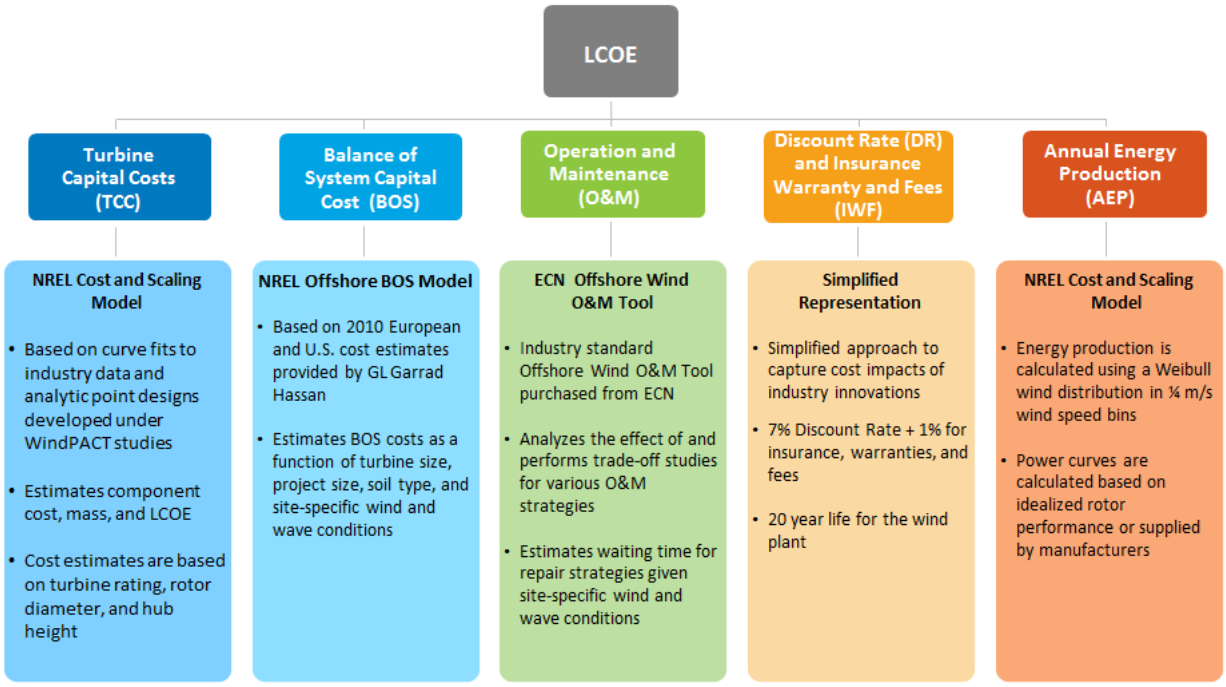

Figure 9-1. Summary of methodology used to estimate LCOE for the baseline project

9.2 Operating Parameters

Table 9-1 summarizes the operating parameters for a baseline wind power plant that consists of 100 5-MW turbines located in the Gulf of Mexico at a water depth of approximately 25 m and 50-km distance from shore. The assumed port that is accessible for large vessels is Corpus Christi Bay at an approximate distance of 60 km, which will serve as both the installation and O&M port facility.

Power production estimates were calculated using the NREL Cost and Scaling model, the published power curve of the NREL Offshore Reference Turbine, and a mean hub-height wind speed of 8.71 m/s, assuming a Weibull wind speed probability distribution and a 1/7-Power Law wind speed profile. The estimate for the baseline plant availability was obtained from the ECN O&M Tool; nondrivetrain losses were assumed to be 10%.

Table 9-1. Operating Parameters for Baseline Turbine and Wind Power Plant

Representative Categories	Offshore 5.0-MW Baseline (Geared)
Machine rating (kW)	5000
Rotor diameter (m)	126
Hub height (m)	90
Wind speed class (50 m)	8.16
Weibull K factor	2.5
Wind shear	0.11
Max rotor Cp	0.45
Max tip speed (m/s)	80
Max tip speed ratio	8
Wind power plant size (MW)	500
Total nondrivetrain losses	10%
Availability	95%
Drivetrain design (and efficiency)	3-stage planetary geared

The long-term correlated wind and wave measurements were obtained from the WIS from the USACE. The data was collected by WIS buoy station number 73034 (located at 27.25 latitude, -97.05 longitude) covering the period from July 29, 1990, through December 31, 2012. This data set was used in the ECN O&M Tool to calculate available O&M weather windows.

9.3 Turbine Capital Costs

Recommended baseline turbine capital cost estimates (Table 9-2) draw from NREL's Wind Turbine Cost and Scaling model (Fingersh et al. 2006, Maples et al. 2010), several recent publications (BVG 2011, Deloitte 2011, BVG 2012), and NREL's conversations with offshore wind project developers in the United States.

Table 9-2. Summary of Baseline Turbine Capital Costs

Component	Baseline 500 MW Plant ($/kW)
Rotor	398
Drive train, nacelle	1,024
Control, Safety system, and condition monitoring	22
Tower	328
Total	**1,772**

9.4 Balance of Station Costs

The turbines were assumed to be situated on monopiles and installed in the "bunny-ears" configuration with the tower being installed in a single lift. The bunny-ears installation strategy entails two lifts for the nacelle and rotor. The first lift is to install the nacelle in the bunny-ears configuration, where the nacelle, hub, and two blades are pre-assembled on land and transported out to sea as an assembly. The second lift is to mount the third blade on the rotor hub. Turbine

installation would be carried out by a self-propelled jack-up vessel with a supporting cast of barges, tugs, heavy lift, and crew transport vessels.

For all project layouts, turbines were assumed to be spaced eight rotor diameters apart across the prevailing wind direction and ten rotor diameters apart along the prevailing wind direction, in a simple grid. Array cables consist of a combination of sizes, all at 34.5kV in a radial layout connecting to an offshore transformer substation.

Table 9-3. Summary of Baseline BOS Costs

Category	Baseline 500-MW Wind Power Plant ($/kW)
Development	291
Substructure	733
Ports and staging	21
Turbine and substructure installation	507
Electrical infrastructure and installation	955
Total	**2,507**

9.5 Soft Costs

Soft costs include nonconstruction costs incurred before project commissioning and are mainly related to the cost of financial vehicles, including:

- Insurance—to protect against damage to components, accidents, and liability during construction. Estimated at 1% of total installed capital cost (ICC)
- Surety bond—3% of ICC
- Contingency—assumed 15% of total ICC
- Construction financing—assumes a 5.5% rate over two years.

Table 9-4 includes a summary of the soft costs for the baseline scenario.

Table 9-4. Summary of Baseline Soft Costs

Category	Baseline 500-MW Wind Power Plant ($/kW)
Insurance	57
Surety bond	170
Contingency	850
Construction financing	312
Total	**1,389**

9.6 Annual Operating Expenses

O&M costs are highly dependent on the failure frequency of turbine and BOS components; therefore, a set of generic failure frequencies was established for use in the baseline scenario, derived from the results of the Reliawind project (Wilkinson et al. 2010). Additionally, it was assumed that the following methods and equipment were the most likely option for transferring equipment and personnel and for making repairs:

- Workboat access vessel (transferring technicians and transporting small components)
- Jack-up vessel (transporting and hoisting large components)
- Cable layer (replacing cables)
- Diving support vessel (for underwater inspections and repairs).

For equipment with a long mobilization time, the situation might occur that, on average, more than one failure occurs during the mobilization time of the equipment. In reality, these repairs will be clustered and thus the average logistic time and mob/demob costs per repair will be lower. This clustering of O&M costs has been modeled in the baseline. Results of the baseline O&M scenario are presented in Table 9-5. All costs for corrective and preventative maintenance include spare parts, vessel mob/demob and day-rates, labor, and equipment to perform maintenance/repairs based on values presented in Maples et al. (2013).

Table 9-5. Summary of Baseline Annual Operating Expenses

Category	Baseline 500-MW Wind Power Plant ($/kW)
Unscheduled maintenance	132
Scheduled maintenance	22
Operations cost	10
Total	**164**

9.7 Baseline LCOE Estimate

The baseline scenario LCOE was calculated using this formula:

$$LCOE = \frac{(DR + IWF) * ICC + O\&M(1 - TR)}{AEP_{net}}$$

Where:

LCOE	=	Levelized cost of energy ($/kWh) (constant dollars)
DR	=	Discount rate (1/yr)
IWF	=	Insurance, warranty, and fees (1/yr)
ICC	=	Initial installed capital cost ($/kW)
O&M	=	Levelized O&M cost ($/kW/yr)
TR	=	Effective state and federal tax rate (%)
AEP_{net}	=	Net annual energy production (kWh/yr).

A summary of the baseline LCOE is provided in Table 9-6.

Table 9-6. LCOE Estimate for Baseline Project

Category	Baseline 500-MW Wind Power Plant
Net annual energy production (MWh)	1,709,700
Turbine capital cost ($/kW)	1,772
Balance-of-station cost ($/kW)	2,507
Soft costs ($/kW)	1,389
Annual operating expenses ($/kW/yr)	164
ICC ($/kW)	**5,668**
Baseline LCOE ($/kWh)	**$0.1614**

9.8 Proposed Hurricane-Resilient Scenario

The proposed hurricane-resilient scenario uses a set of innovations surrounding turbine, substructure, and backup generator power to obtain the lowest project cost of energy estimate.

9.9 Turbine

Nacelle, drivetrain, and hub assembly—The nacelle, drivetrain, and hub assembly design concept was investigated by Siemens. The 10-MW hurricane-resilient turbine takes full advantage of the benefits of a permanent-magnet direct-drive generator with active cooling. The analysis contains structural and mechanical model data along with information extracted from the BHawC aeroelastic code; calculation setup and simulation results corresponding to data used for the concept design case "NREL-10" (Siemens 2013). Siemens considered aeroelastic concept design models for the generator, nacelle, and hub. Rotor and tower details were not provided. Figure 9-2 shows a sketch of the nacelle and hub geometry.

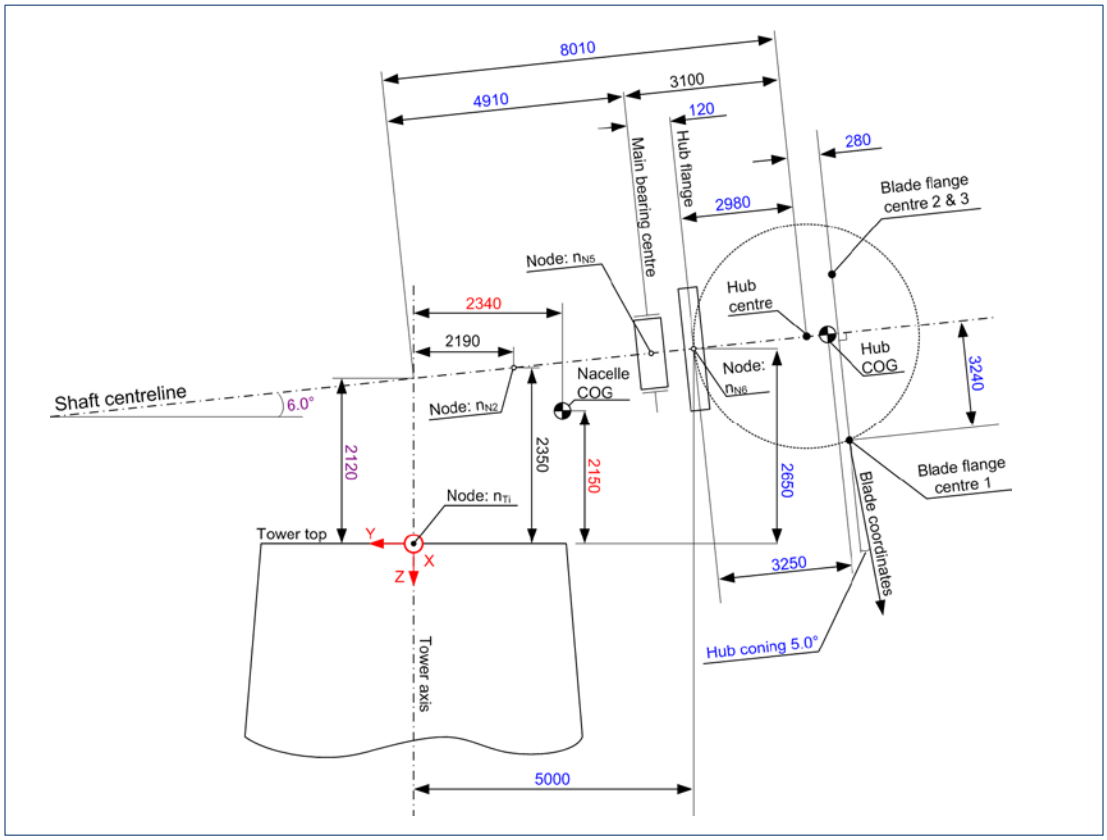

Figure 9-2. Design concept sketch of nacelle and hub geometry

Preliminary geometry, mass, aerodynamics, stiffness, and cost estimates were provided by Siemens. A summary of the nacelle, drivetrain, hub cost, and mass are presented in Table 9-7 and Table 9-8 (Siemens 2013).

Table 9-7. Hurricane-Resilient Turbine Drivetrain and Nacelle Cost and Mass

Category	Cost ($/kW)	Mass (kg/kW)
Generator	736	N/A
Main frame	562	N/A
Drivetrain, nacelle total	**1,298**	**42.9**

Table 9-8. Hurricane-Resilient Turbine Hub Cost and Mass

Category	Cost ($/kW)	Mass (kg/kW)
Hub	268	25.1

Advanced 218-m downwind coned rotor—The rotor on the 10-MW hurricane-resilient turbine is designed as a downwind rotor (Figure 9-3). The performance of the 218-m diameter rotor was

estimated by Wetzel Engineering (Wetzel et al. 2013). The estimated power curve for the 10-MW turbine generated by the NREL Turbine Cost Model using the performance data provided by Wetzel Engineering is shown in Figure 9-4.

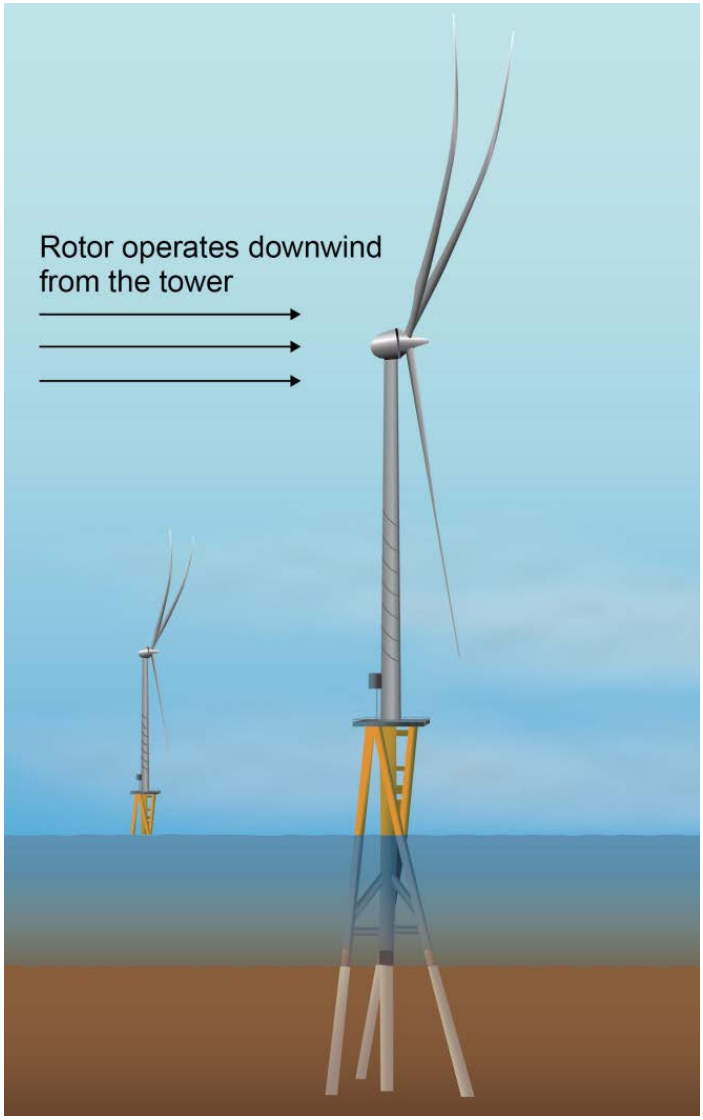

Figure 9-3. Conceptual drawing of 10-MW downwind hurricane-resilient turbine

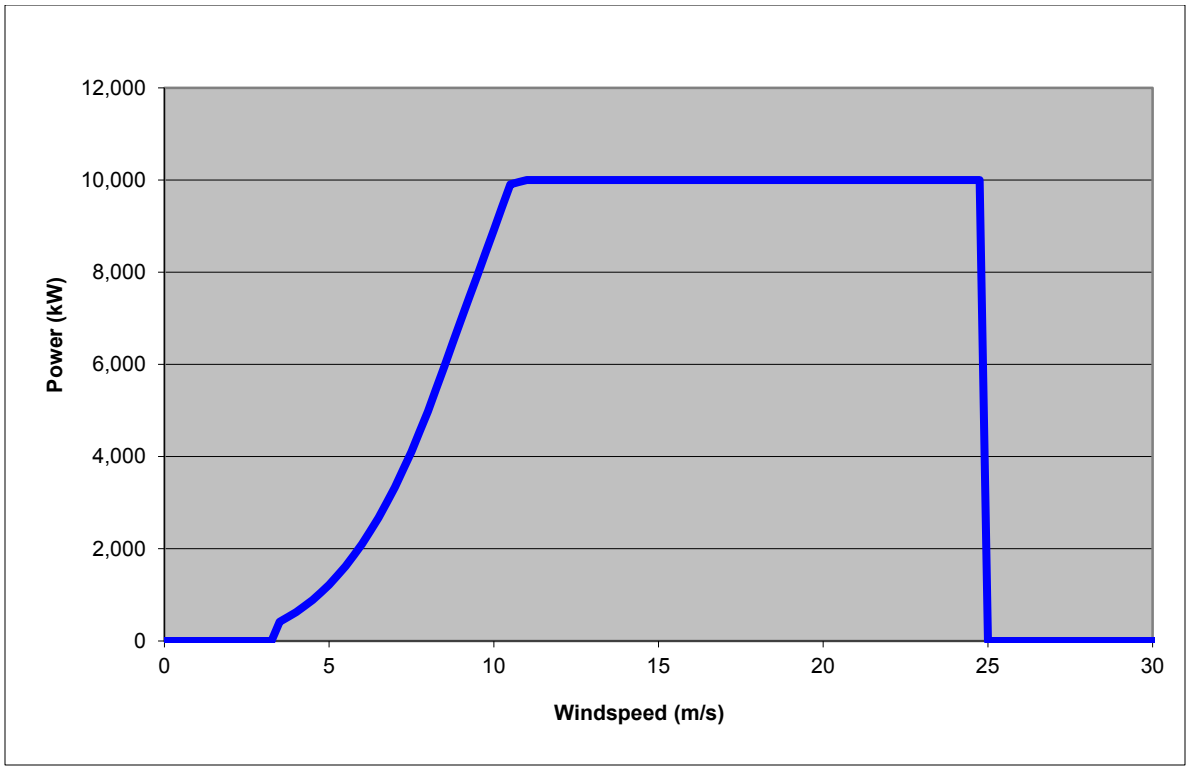

Figure 9-4. 10-MW hurricane-resilient turbine estimated power curve

105-m carbon-fiber blades—The wind turbine's 105-m blade was designed by WEI. This design process included an aerostructural optimization exercise for a 10-MW hurricane-resilient wind turbine. Results of the optimization analysis determined a 105-m blade was most optimal for the 10-MW turbine application. The mass of the carbon-fiber blades was estimated by WEI, whereas the blade cost estimate was derived from the NREL Cost and Scaling Model. A summary of the blade cost and mass is shown in Table 9-9.

Table 9-9. Hurricane-Resilient Turbine Blade Cost and Mass

Category	Cost ($/kW)	Mass (kg/kW)
Blades (includes 3 blades)	350	19.3

Optimized tower design for hurricane-resilient downwind coned rotor—The optimized tower design for the hurricane-resilient downwind coned rotors was conducted by NREL and is documented in Section 4. Based on geometric and load data produced by Siemens and WEI, NREL generated a preliminary design of the tower. Additionally, the tower design accounts for the structural qualities of the IBGS substructure. This included the creation of a FAST model to generate the complete mass matrix at the tower top and an optimization algorithm to minimize the tower mass given specified design constraints. The results of the optimized tower analysis yielded a tower mass. The tower mass was then used to calculate the cost using the $/kg unit cost

of the 5-MW baseline tower. Both the optimized tower mass and estimated cost are shown in Table 9-10.

Table 9-10. Hurricane-Resilient Turbine Tower Cost and Mass

Category	Cost ($/kW)	Mass (kg/kW)
Tower	353	65.6

9.10 Substructure and Installation

Inward battered guide structure—The substructure to support the 10-MW concept turbine is Keystone Engineering's IBGS (Figure 9-5). The substructure advancements provided by the IBGS include a less complex structure to fabricate and install. For the purposes of this study, Keystone Engineering provided a bill of materials (BOM) that details each substructure component size, mass, and fabrication cost. Additionally, the document provided transportation and installation cost estimates. A summary of the substructure mass, fabrication cost, installation and transportation time, and installation and transportation cost are presented in Table 9-11 and Table 9-12.

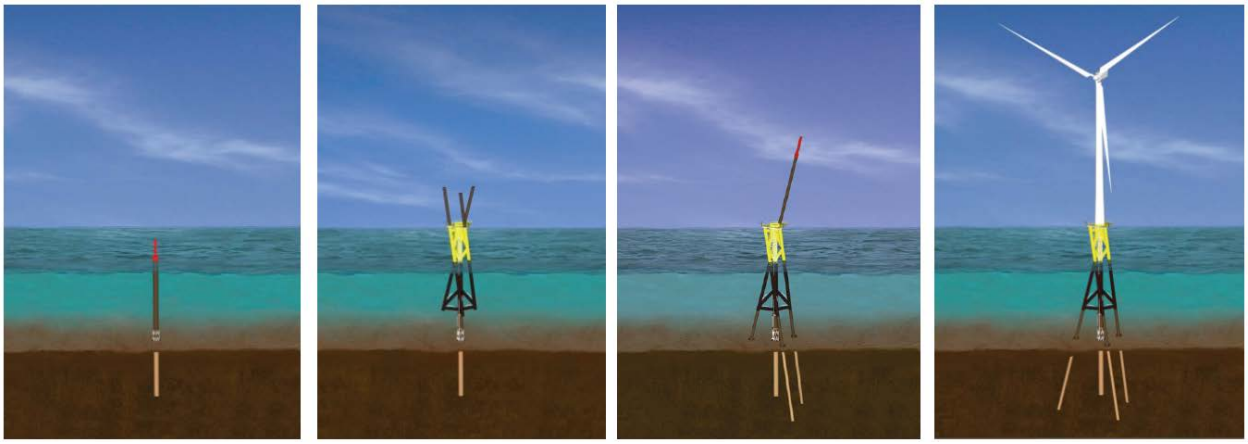

Figure 9-5. Installation sequence for the IBGS and wind turbine

Table 9-11. IBGS Mass and Fabrication Cost

Category	Mass (kg/kW)	Cost ($/kW)
IBGS substructure	121	464

Table 9-12. IBGS Transportation and Installation Time and Cost

Category	Time (h/unit)	Cost ($/kW)
IBGS substructure	74	75

9.11 Hurricane-Resilient Design

Generator backup power—The generator backup power provides uninterrupted backup power to the turbine yaw system to mitigate wind loading during hurricane conditions. The centrally located diesel-powered generator and ancillary equipment are capable of controlling a turbine array of up to 12 wind turbines. The cost estimate for this type of hurricane-resilient design was estimated from NREL resources and discussions with industry. The estimated cost for the backup power system is shown in Table 9-13.

Table 9-13. Estimated Generator Backup Power Cost

Category	Cost ($/kW)
Diesel generator and ancillary equipment	10

9.12 LCOE Estimate

Incorporating innovations in turbine, substructure, and installation into a 500-MW offshore project provides an example of the impact that these technologies have on the cost of energy.

Comparisons of the baseline and hurricane-resilient scenarios are presented in Table 9-14 and Table 9-15. Compared to the baseline, the hurricane-resilient project scenario shows a 30.4% improvement in AEP_{net}, 28% increase in TCC, 16.6% reduction in BOS, and 3.7% increase in AOE (Table 9-15). The primary increase in AEP_{net} is due to the 218-m downwind rotor. This significant increase in AEP drives the 21.5% reduction in LCOE (Table 9-14). The increase in TCC is due to the hurricane-resilient turbine's advanced technologies and its rated capacity (double that of the baseline's). The AOE for the hurricane-resilient turbine is also more expensive when considering the AOE in $/kW/yr. However, the energy production of the hurricane-resilient turbine results in a lower cost of energy ($/kWh). The BOS cost reductions are primarily driven by the IBGS substructure fabrication and installation method.

Table 9-14. Estimate for Baseline and Hurricane-Resilient Scenarios LCOE

Category	Baseline	Hurricane-Resilient Scenario
Net annual energy production (MWh/yr/turbine)	17,097	44,585
Turbine capital cost ($/kW)	1,772	2,268
Balance-of-station cost ($/kW) • Development • Substructure fabrication • Ports and staging • Turbine and substructure installation • Electrical infrastructure and installation	2,507	2,091
Soft costs ($/kW) • Insurance • Surety bond • Contingency • Construction financing	1,388	1,415
Annual operating expenses ($/kW/yr)	164	170
ICC ($/kW)	**5,667**	**5,784**
LCOE ($/kWh)	**$0.1614**	**$0.1267**

Table 9-15. Innovations Performance and Cost Impacts Summary

System	Innovations	Estimated Performance and Cost Impacts (%)			
		AEP_{net} (MWh/yr)	TCC ($/kW)	BOS ($/kW)	AOE ($/kW/yr)
Turbine system	• Advanced 218-m downwind coned rotor • 105-m carbon-fiber blades • Siemens direct-drive generator with active cooling • Optimized tower design for hurricane-resilient downwind coned rotor • Generator backup power	+30.4	+28	N/A	+3.7
Substructure & installation methods	• IBGS design • IBGS fabrication • IBGS installation strategy	N/A	N/A	-16.6	N/A

9.13 Uncertainties and Natural Variability

The range of reported costs and performances of offshore wind projects from around the world demonstrates how the natural variability and uncertainty in production from one project to the next can influence the system LCOE. Tegen et al. (2012) estimate in Figure 9-6 that, historically, the largest contributor to LCOE uncertainty is in the ICC; however, the financing terms (discount rate) and energy production (capacity factor) also play a large role in the system LCOE.

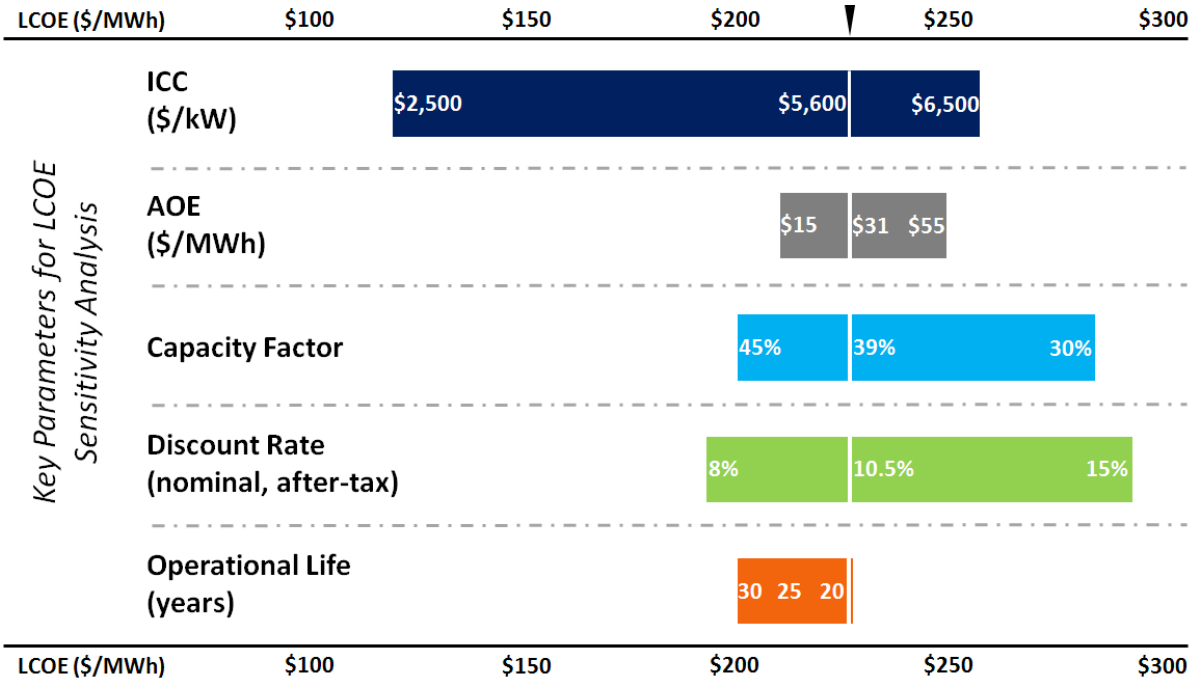

Source: Tegen et al. 2012

Figure 9-6. Representative LCOE impact of key LCOE components

Further investigation into the natural variability and uncertainties was conducted by NREL (Maples 2012, Maples 2013) to demonstrate the impact of project size, turbine size, water depth, distance to shore, installation vessel day rates, turbine installation strategies, extreme metocean conditions, and O&M strategies (among others).

It was found that the influence of any natural variability or uncertainty is variable and can range from being not very influential in one project to highly influential in another. The influence of uncertainty and natural variability in extreme metocean conditions on AOE is a good example. It was found that if a project was to be utilizing an O&M access vessel with a 1.5-m maximum wave height restriction in the mid-Atlantic region, the uncertainty and natural variability in metocean conditions would have a relatively small influence on AOE. However, if the project was to be situated in the North Sea, the uncertainty and natural variability in metocean conditions would have a relatively large influence on AOE and subsequently LCOE (Maples 2013).

Furthermore, projects are subject to many other constraints (e.g., vessel availability and regulations compliance) that can play a large role in the final cost of a project. As such, it is important for every project team to understand and investigate its own potential uncertainties well in advance.

10 Summary

Optimization of the hurricane-resilient blade and rotor carried out by Wetzel Engineering culminated in a downwind three-bladed rotor rated at 10 MW, having a swept diameter of 218 m and a hub height of 132 m. The optimization procedure produced a rotor with no precone and with the highest solidity geometry in the design space. The rotor operates at a maximum tip speed of 85 m/s and achieves a power coefficient of 0.47. The blade is constructed of glass fiber infused with epoxy resin, with the skin laminate utilizing quadraxial and triaxial glass fabric and selectively reinforced with pultruded high-modulus glass fiber composites. The main spar cap and trailing edge spar cap are composed of fiber composites that are primarily unidirectional pultruded carbon fiber composites of tailored cross-sections and unidirectional glass fabric, respectively.

The basis for the Siemens Windpower hub, nacelle, and generator design for the hurricane-resilient wind turbine is the direct drive Siemens 3.0 MW and 6.0 MW platforms, which achieves a straightforward turbine geometry. In this study, three 10-MW design concepts were created corresponding to three different blade lengths, rated rotational speeds, and rated torques. Based on input parameters obtained from other turbine component designs in this study, the main parameters for hub, generator, and nacelle were found by extrapolating from the 3.0 MW and 6.0 MW baselines to 10 MW, by applying simple physics-based scaling laws**.** The scaling relationship of the generator mass equation is based on the torque density of the SWT-6.0 MW and resulted in three concept designs. The generator mass increases with higher-rated torques and lower-rated rotational speeds.

NREL designed a minimum mass tower to support the hurricane-resilient wind turbine, which achieved a first system eigenfrequency of approximately 0.163 Hz. This preliminary design was based solely on load-bearing strength and a soft-stiff frequency approach, considering both parked and operating states. A parametric study was conducted to show what mass penalty would need to be incurred if the geometric parameters were to change, or if a higher eigenfrequency was selected. However, given the uncertainties in the soil characteristics and in the details of the design, fine-tuning the first natural frequency may not provide additional value to the current effort and a more in-depth study should be performed at a later stage in the detail design phase. It was noted that the downwind configuration forces the rotor-nacelle assembly center of mass downwind of the tower centerline and increases tower mass by some 100 tonnes, or 16%.

Keystone Engineering's goal for the substructure and foundation design was to support the hurricane-resilient wind turbine system at a Western Gulf of Mexico site where it would encounter hurricane loading conditions. A medium-consequence failure was adopted for the offshore wind turbine support structure corresponding to an L-2 exposure category. Based on that, a coupled design and analysis for the substructure and foundation were completed for ultimate limit states and robustness conditions for return periods of 50 years and 500 years, respectively. In addition, fabrication and installation cost comparisons were provided, involving the Keystone IBGS design and a typical four pile jacket, to document the reduction in capital that contributes to an overall decrease in cost of energy.

To obtain a realistic estimate of turbine system loads, NREL performed a fully coupled aero-hydro-elastic model of the integrated turbine system, which included the wind turbine, tower, and IBGS jacket substructure. Modeling was done to predict the maximum loads that the 10-MW hurricane-resilient turbine would encounter during a hurricane event. Maximum structural load values were extracted from a series of nonoperating (parked) load cases modeled for hurricane inflow conditions, for 50-, 100-, and 500-year extreme events. For integrated system modeling, only parked rotor conditions were considered because blade and rotor design optimization showed these produced higher loads than operating conditions—and because it was assumed that the turbine would be shut down during hurricane conditions.

For the NREL wind power plant layout analysis, a surrogate site was identified in the Gulf of Mexico approximately 60 km to the southeast of Corpus Christi, Texas. The site and alternative wind power plant layouts were selected to typify general development scenarios for the hurricane-resilient technology. The windTrends data base was used in connection with ancillary analyses to produce wind input files; ocean bathymetry data were obtained from the NOAA Coastal Relief Model (CRM) database. Wake losses were calculated for each layout configuration using the deep array eddy viscosity wake model in Openwind Enterprise. All other loss assumptions were manually entered into Openwind and applied to the calculation of net energy production. Using these input data, the Openwind model was applied to investigate four wind plant layouts with key criteria being energy capture, ocean depth, and export cable length.

NREL's O&M analysis compared two scenarios: 1) a baseline offshore wind power plant consisting of 100 turbines, each rated at 5 MW and, 2) a hurricane-resilient offshore wind power plant comprised of 50 turbines, each rated at 10 MW. Both the baseline and hurricane-resilient offshore wind power plant scenarios are located in the Western Gulf of Mexico, approximately 60 km southeast of Corpus Christi, Texas. This region of the United States is prone to hurricane activity that can limit access to a wind turbine for maintenance activities. Preventing access to a turbine for repair not only increases the downtime of the turbine but, ultimately, increases the LCOE. The O&M analysis for the baseline and hurricane-resilient offshore wind power plants was intended to quantify O&M costs, wind power plant availability, and energy production for a wind power plant placed in the Gulf of Mexico.

The NREL LCOE analysis showed how hurricane-resilient technology innovations reduced the LCOE for the notional 500-MW offshore wind power plant adopted for this study relative to baseline LCOE assumptions for the same size plant. The analyses of both the baseline and proposed hurricane-resilient configurations were customized to projects located in the Gulf of Mexico. This analysis characterized impacts to LCOE in response to perturbations to annual energy capture, turbine capital cost, balance-of-station costs, annual operating expenses, and operational service life. Overall, the NREL LCOE analysis predicted a 21.5% reduction in LCOE for the proposed hurricane-resilient turbine and plant technology concept.

The conceptual study documented herein shows that challenges posed by hurricanes to wind turbine survivability, operability, and cost effectiveness in the U.S. offshore environment can be successfully addressed using innovative research and development strategies. Though hurricane occurrence is possible or probable throughout most U.S. coastal regions, this need not be an insurmountable barrier to cost-effective offshore wind energy deployment and operation in these regions.

The foregoing sections have shown that this concept design study achieved robust performance levels for the hurricane resilient components, turbine, and wind plant, and that these performance levels supported significant LCOE reductions. Nonetheless, it should be emphasized that this study relied substantially on up-scaling current technologies rather than undertaking *de novo* engineering designs. In addition, while major components were optimized themselves, the current study did not carry out iterative system level optimization of the turbine or wind plant. Extrapolating from these considerations, it is reasonable to surmise that future studies employing clean-sheet engineering approaches and well integrated full system optimizations could deliver even better performance and culminate in greater LCOE reductions.

11 References

American Bureau of Shipping. *Bottom-Founded Offshore Wind Turbine Installations*. Houston: American Bureau of Shipping, 2013.

American Petroleum Institute. *API RP 2MET—Derivation of Metocean Design and Operating Conditions*. 1st ed. and 1st ed. (draft). Washington, D.C: American Petroleum Institute, 2010.

American Petroleum Institute. *RP 2A-WSD—Planning, Designing, and Constructing Fixed Offshore Platforms—Working Stress Design*. 22nd ed. Washington, D.C.: American Petroleum Institute, 2014.

American Wind Energy Association. *AWEA Offshore Compliance Recommended Practices (2012)—Recommended Practices for Design, Deployment, and Operation of Offshore Wind Turbines in the United States.* Washington, D.C.: American Wind Energy Association, 2012.

Braam H., Obdam, T.S., van de Pieterman, R.P., and Rademakers, L.W.M.M. (2011). "Properties of the O&M Cost Estimator (OMCE). https://www.ecn.nl/docs/library/report/2011/e11045.pdf

BVG Associates. *A Guide to an Offshore Wind Farm*. Published on behalf of The Crown Estate. London: BVG Associates. http://www.thecrownestate.co.uk/energy-minerals-and-infrastructure/offshore-wind-energy/

BVG Associates. *Offshore Wind Cost Reduction Pathways Study*. Published on behalf of The Crown Estate. London: BVG Associates, 2012 http://www.thecrownestate.co.uk/energy-minerals-and-infrastructure/offshore-wind-energy/

Damiani, R., and H. Song. "A Jacket Sizing Tool for Offshore Wind Turbines within the Systems Engineering Initiative." Offshore Technology Conference, Houston, TX, April 30-May 4, 2013.

Damiani, R., H. Song, and J. Jonkman. *SubDyn User's Guide and Theory Manual*, NREL/TP-5000-63062. Golden, CO: National Renewable Energy Laboratory, 2015.

Dávila, C. G., Pedro P. Camanho. *Failure Criteria for FRP Laminates in Plane Stress*, NASA/TM-2003-212663. Hampton, VA: NASA, 2003.

Deloitte. *Analysis on the furthering of competition in relation to the establishment of large offshore wind farms in Denmark*. Published on behalf of the Danish Ministry of Climate and Energy. New York: Deloitte, 2011.

Dibra, B., "NREL 10 MW Hurricane Resilient WTG sub-structure and foundation design report," Keystone Engineering Inc., Houston, TX, 2014.

Douglas-Westwood. *Assessment of Vessel Requirements for the U.S. Offshore Wind Sector*. Prepared for the U.S. Department of Energy as subtopic 5.2 of the U.S. Offshore Wind: Removing Market Barriers. 2013.

EN 1993-1-6 (2007) (English): Eurocode 3: Design of steel structures - Part 1-6: Strength and stability of shell structures.

Fingersh, L., M. Hand, and A. Laxson. *Wind Turbine Design Cost and Scaling Model*. NREL/TP-500-40566. Golden, CO: National Renewable Energy Laboratory, 2006. http://www.nrel.gov/docs/fy07osti/40566.pdf.

Jonkman, J., S. Butterfield, W. Musial, and G. Scott. *Definition of a 5-MW Reference Wind Turbine for Offshore System Development*. NREL/TP-500-38060. Golden, CO: National Renewable Energy Laboratory, 2009. http://www.nrel.gov/docs/fy09osti/38060.pdf

Germanischer Lloyd: Rules and Guidelines, IV – Industrial Services, Part 2 – Guideline for the Certification of Offshore Wind Turbines, Edition 2005.

Germanischer Lloyd. *The New Guideline for the Certification of Wind Turbines, Edition 2010*. Hamburg: Germanischer Lloyd, 2010.

Hermann, T.; Application of the Larc03 failure criterion to the analysis of wind turbine rotor blades, WEI Document 00.09.001, October 11, 2011.Chapter 2.

International Electrotechnical Commission. *IEC 61400-3 Wind Turbines – Part 3: Design Requirements for Offshore Wind Turbines*. 2009.

ISO 19902: 2007, Petroleum and natural gas industries – Fixed steel offshore structures, 2007

Jonkman, B. J. TurbSim User's Guide: Version 1.50. NREL/TP-500-46198. 2009.

Jonkman, J., S. Butterfield, W. Musial, and G. Scott. *Definition of a 5-MW Reference Wind Turbine for Offshore System Development*. NREL/TP-500-38060. 2009.

Lee, K. (a). 45.07.02.01-A. *NREL10MW WEI105.0m Blade Preliminary BOM*. Wetzel Engineering Inc. report. 2014.

Lee. K. (b). 45.04.02.01-A. *NREL 10.0MW WEI105.0m Blade Preliminary Laminate Summary*. Wetzel Engineering Inc. report. 2014.

Lee. K. (c). 45.07.01.01, Release A. *Materials Specification for NREL10MW WEI105.0m Blade*. Wetzel Engineering Inc. report. 2014.

Maples, B., M. Hand, and W. Musial. *Comparative Assessment of Direct Drive High Temperature Superconducting Generators in Multi-Megawatt Class Wind Turbines*. NREL TP-5000-49086. Golden, CO: National Renewable Energy Laboratory, 2010. http://www.nrel.gov/docs/fy11osti/49086.pdf

Maples, B., G. Saur, M. Hand, R. van de Pieterman, and T. Obdam. *Installation, Operation, and Maintenance Strategies to Reduce the Cost of Offshore Wind Energy*. NREL TP-5000-57403. Golden, CO: National Renewable Energy Laboratory, 2013. http://www.nrel.gov/docs/fy13osti/57403.pdf

Maples, Ben. "U.S. Balance-of-Station Cost Drivers and Sensitivities." Presentation at the American Wind Energy Association Offshore WindPower Conference, Virginia Beach, VA, October 2012. NREL PR-5000-56480. http://www.nrel.gov/docs/fy13osti/56480.pdf

Müller, H., J. Hantschel, J. Seiffert, J. Fröhner, and M. Brauksiepe. *VGB-Standard—RDS-PP—Application specification Part 32: Wind energy*. VGB PowerTech e.V. Accessed June 2013. http://www.vgb.org/vgbmultimedia/AKADNEU/VGB_S_823_T32_EN_2012_02_03_Draft_Final1.pdf.

National Renewable Energy Laboratory, 2014(a). NWTC Information Portal (FAST), 09 September 2014. Accessed December 2014. https://nwtc.nrel.gov/FAST.

National Renewable Energy Laboratory, 2014(b). NWTC Information Portal (BModes), 29 September 2014. Accessed December 2014. https://nwtc.nrel.gov/BModes.

National Renewable Energy Laboratory, 2014(c). NWTC Information Portal (SubDyn), 07 October 2014. Accessed December 2014. https://nwtc.nrel.gov/SubDyn.

National Renewable Energy Laboratory. Statement of Work—Hurricane Resilient Wind Plant Concept Design Study—Advanced Blade and Rotor Design. January 2012.

NIST/SEMATECH. *e-Handbook of Statistical Methods*, http://www.itl.nist.gov/div898/handbook/, updated 2012.

NOAA (2013) NOAA National Centers for Environmental Information, available at http://www.ngdc.noaa.gov/mgg/coastal/crm.html.

National Oceanic and Atmospheric Administration (NOAA), Historical Hurricane Tracks website. Accessed May 2014. https://coast.noaa.gov/hurricanes/

Obdam, T.S., H. Braam, and L.W.M.M. Rademakers. *User Guide and Model Description of ECN O&M Tool Version 4*. Energy Research Center of the Netherlands (ECN): 2011.

Raina, A. 45.00.03.03-A 10MW Cost Model-Preliminary List. Wetzel Engineering memo to author, April 10, 2013.

Raina, A. 45.08.02.01-A Cost of Energy Analysis of the WEI105.0-10.0M-A 105.0m Blade for 10.0 MW Turbine. Wetzel Engineering report. May 2014.

Raina, A. 98.01.03.002-A Airfoil Data Generic Set. Wetzel Engineering data set for airfoils. April 2013.

Raina, A. 45.03.02.01-A Aerodynamic Design of the WEI105.0-10.0M-A 105.0m Blade for 10.0 MW Turbine. Wetzel Engineering report. August 2013.

Raina, A. Cost Model for NREL 10MW Rotor Design and Analysis. Wetzel Engineering. 2013.

Raina, A. Monthly Report No. 9 (Document Number: 45.01.01.09). Wetzel Engineering report. 2013.

Siemens. "Concept Design Study: NREL Hurricane Resistant Turbine" (unpublished, 2013).

Tavner, Peter J, *Offshore Wind Turbines: Reliability, Availability and Maintenance.* London: Institution of Engineering and Technology, London, 2012.

Tegen, S., M. Hand, B. Maples, E. Lantz, P. Schwabe, and A. Smith. *2010 Cost of Wind Energy Review*. NREL TP-5000-52920. Golden, CO: National Renewable Energy Laboratory, 2012. http://www.nrel.gov/docs/fy12osti/52920.pdf

Tobias (2013). Tobias, P., et. al. *"Assessing Product Reliability"*. National Institute of Standards and Technology (NIST), Sematech, Engineering Statics Handbook. Last updated October 2013. Accessed June 2014. http://www.itl.nist.gov/div898/handbook/apr/section1/apr124.htm.

United States Army Corps of Engineers (USACE) Wave Information Studies website. Accessed May 2014. http://wis.usace.army.mil/

van der Zee, T.J.J., and T.S. Obdam. *ECN O&M Tool Case Study for a Far Offshore Wind Farm*. Energy Research Center of the Netherlands (ECN): September 2011.

Wilkinson (2010). Wilkinson, M.; Harman, K.; Hendriks, B.; Spinato, F.; van Delft, T. "Measuring Wind Turbine Reliability – Results of the Reliawind Project". https://docs.wind-watch.org/Measuring_Wind_Turbine_Reliability_-_Reliawind.pdf

Wilkinson, M. et al. (2010). Methodology and Results of the Reliawind Reliability Field Study. European Wind Energy Conference, Warszaw. http://eprints.whiterose.ac.uk/83343/1/2010%20Wilkinson,%20Hendriks,%20et%20al%20FieldReliability%20(EWEC2010).pdf

APPENDIX A

IBGS ULS Analysis Substructure Results

***** SEA STATE COMBINED LOAD CASE SUMMARY *****
GLOBAL SUBSTRUCTURE REACTIONS RELATIVE TO MUDLINE ELEVATION

*** GRAV GRAVITY LOAD

LOAD CASE	LOAD LABEL	FX (KN)	FY (KN)	FZ (KN)	MX (KN-M)	MY (KN-M)	MZ (KN-M)
88.00	GRAV	0.0	0.0	-21740.6	0.6	-122.3	0.0

*** A000-A330

*** IEC LC 1.6 : 1.1 GRAVITY LOAD + 1.35 ENVIROMENTAL LOAD

LOAD CASE	LOAD LABEL	FX (KN)	FY (KN)	FZ (KN)	MX (KN-M)	MY (KN-M)	MZ (KN-M)
89	A000	8264	-1286	-24919	20900	623184	-873
90	A030	7782	3013	-24877	-293797	550359	-242
91	A060	5264	6531	-24815	-530388	330339	1956
92	A090	1302	8294	-24901	-624521	21098	1146
93	A120	-3004	7809	-24919	-550938	-293642	-903
94	A150	-6499	5224	-24878	-330027	-530046	-258
95	A180	-8296	1290	-24815	-21182	-624884	1967
96	A210	-7832	-3002	-24902	293263	-551600	1177
97	A240	-5243	-6504	-24919	529185	-330081	-865
98	A270	-1267	-8254	-24878	623696	-20860	-219
99	A300	3017	-7838	-24815	551431	120992	1991
100	A330	6515	-5273	-24901	330388	529340	1188

*** B000-B330

*** IEC LC 1.6 : 0.9 GRAVITY LOAD + 1.35 ENVIROMENTAL LOAD

LOAD CASE	LOAD LABEL	FX (KN)	FY (KN)	FZ (KN)	MX (KN-M)	MY (KN-M)	MZ (KN-M)
101	B000	8263	-1286	-20571	20900	623209	-873
102	B030	7782	3013	-20529	-293797	550384	-242
103	B060	5264	6531	-20467	-530388	330363	1956
104	B090	1302	8293	-20553	-624521	21123	1146
105	B120	-3004	7808	-20571	-550938	-293617	-903
106	B150	-6499	5224	-20529	-330027	-530021	-258
107	B180	-8296	1290	-20467	-21183	-624860	1967
108	B210	-7832	-3001	-20554	293263	-551575	1177
109	B240	-5243	-6504	-20571	529185	-330057	-865
110	B270	-1267	-8254	-20529	623695	-20835	-219
111	B300	3017	-7838	-20467	551431	121017	1991

112	B330	6515	-5273	-20553	330388	529364	1188

*** C000-C330 50 YEAR RETURN ULS

*** IEC LC 6.1 : 1.1 GRAVITY LOAD + 1.35 ENVIROMENTAL LOAD (WAVE DOMINANT CASE)

LOAD CASE	LOAD LABEL	FX (KN)	FY (KN)	FZ (KN)	MX (KN-M)	MY (KN-M)	MZ (KN-M)
113	C000	15992	-726	-25431	83128	611385	-1308
114	C030	14297	7401	-25280	-235422	574027	3148
115	C060	8651	13519	-25360	-489571	377885	4209
116	C090	751	16071	-25550	-613828	83080	-279
117	C120	-7338	14191	-25431	-570577	-233253	-1453
118	C150	-13538	8667	-25282	-379794	-490212	3015
119	C180	-16062	747	-25360	-82937	-613777	4185
120	C210	-14286	-7358	-25550	234253	-573335	-232
121	C240	-8594	-13462	-25431	487282	-377429	-1347
122	C270	-718	-16095	-25281	615007	-82818	3176
123	C300	7357	-14264	-25360	572218	234215	4313
124	C330	13538	-8660	-25550	378402	489876	-133

*** D000-D330 50 YEAR RETURN ULS

*** IEC LC 6.1 : 0.9 GRAVITY LOAD + 1.35 ENVIROMENTAL LOAD (WAVE DOMINANT CASE)

LOAD CASE	LOAD LABEL	FX (KN)	FY (KN)	FZ (KN)	MX (KN-M)	MY (KN-M)	MZ (KN-M)
125	D000	15992	-726	-21083	83127	611410	-1308
126	D030	14297	7401	-20932	-235422	574052	3148
127	D060	8651	13519	-21011	-489571	377910	4209
128	D090	751	16071	-21202	-613828	83105	-279
129	D120	-7338	14191	-21083	-570577	-233229	-1453
130	D150	-13538	8667	-20933	-379794	-490188	3015
131	D180	-16062	747	-21012	-82937	-613752	4185
132	D210	-14286	-7358	-21202	234253	-573311	-232
133	D240	-8594	-13462	-21083	487282	-377405	-1347
134	D270	-718	-16095	-20933	615007	-82793	3176
135	D300	7357	-14264	-21012	572218	234239	4313
136	D330	13538	-8660	-21202	378401	489901	-133

*** E000-E330 50 YEAR RETURN ULS

*** IEC LC 6.1 : 1.1 GRAVITY LOAD + 1.35 ENVIROMENTAL LOAD (WIND DOMINANT CASE)

LOAD CASE	LOAD LABEL	FX (KN)	FY (KN)	FZ (KN)	MX (KN-M)	MY (KN-M)	MZ (KN-M)
137	E000	16323	-815	-25431	92876	647766	-1308
138	E030	14629	7490	-25280	-245171	610408	3148
139	E060	8894	13762	-25360	-516230	404519	4209
140	E090	840	16402	-25550	-650221	92829	-279
141	E120	-7427	14522	-25431	-606970	-243002	-1453
142	E150	-13781	8910	-25282	-406453	-516872	3015
143	E180	-16394	836	-25360	-92685	-650170	4185
144	E210	-14617	-7447	-25550	244001	-609728	-232
145	E240	-8837	-13704	-25431	513916	-404089	-1347
146	E270	-807	-16426	-25281	651389	-92566	3176
147	E300	7446	-14595	-25360	608600	243963	4313
148	E330	13689	-8810	-25550	394916	506391	-133

*** F000-F330 50 YEAR RETURN ULS

*** IEC LC 6.1 : 0.9 GRAVITY LOAD + 1.35 ENVIROMENTAL LOAD (WIND DOMINANT CASE)

LOAD CASE	LOAD LABEL	FX (KN)	FY (KN)	FZ (KN)	MX (KN-M)	MY (KN-M)	MZ (KN-M)
149	F000	16323	-815	-21083	92876	647791	-1308
150	F030	14629	7490	-20932	-245171	610433	3148
151	F060	8894	13762	-21011	-516230	404543	4209
152	F090	840	16402	-21202	-650221	92853	-279
153	F120	-7427	14522	-21083	-606970	-242978	-1453
154	F150	-13781	8910	-20933	-406453	-516847	3015
155	F180	-16394	836	-21012	-92685	-650145	4185
156	F210	-14617	-7447	-21202	244001	-609703	-232
157	F240	-8837	-13704	-21083	513916	-404065	-1347
158	F270	-807	-16426	-20933	651389	-92542	3176
159	F300	7446	-14595	-21012	608600	243988	4313
160	F330	13781	-8902	-21202	405035	516534	-133

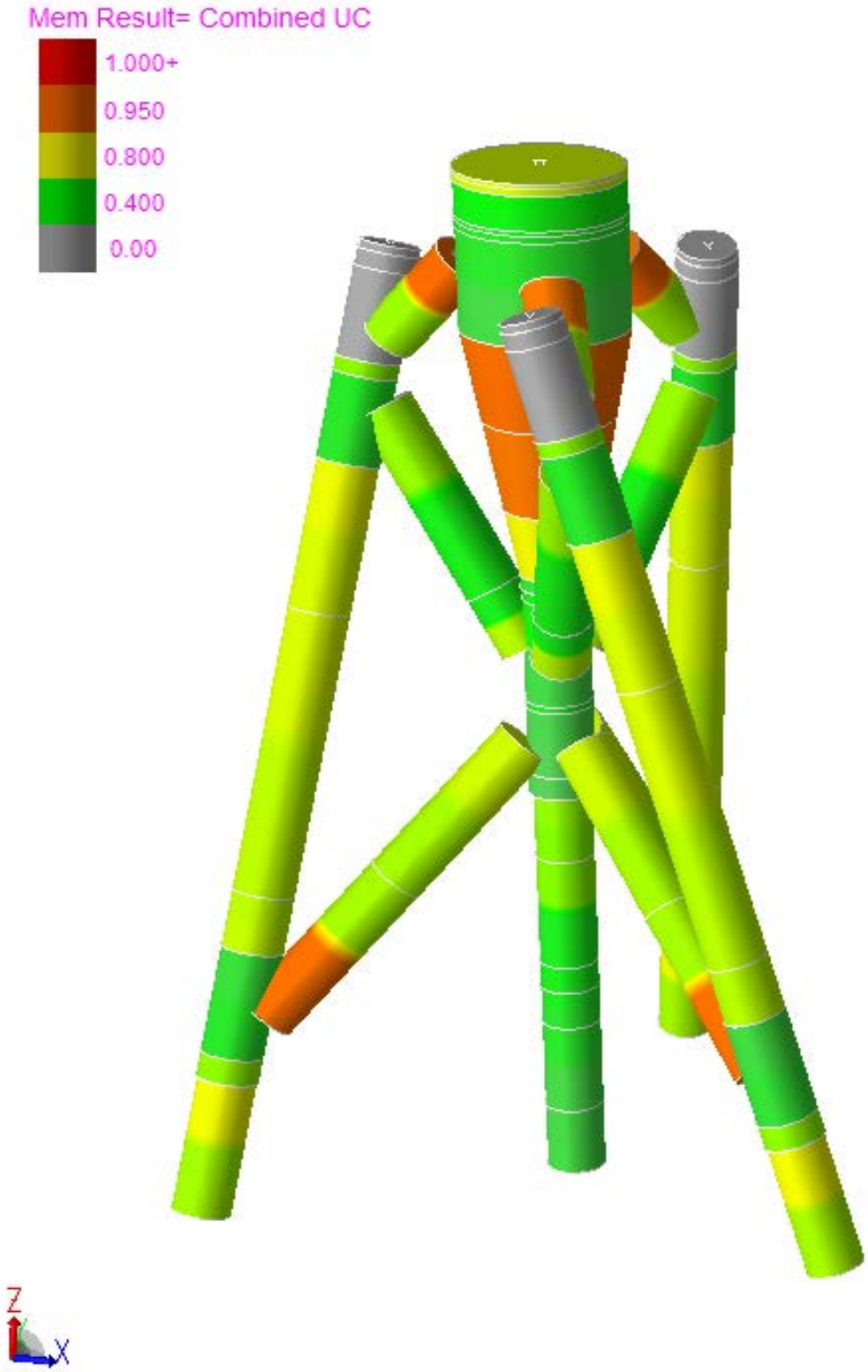

Figure A-1. IBGS ULS member unity check summary

SACS IV - MEMBER UNITY CHECK RANGE SUMMARY

GROUP I - UNITY CHECKS GREATER THAN 0.40 AND LESS THAN 0.8

MEMBER	GROUP ID	MAXIMUM COMBINED UNITY CK	LOAD COND NO.	AXIAL STRESS N/MM2	BENDING STRESS Y N/MM2	BENDING STRESS Z N/MM2	SHEAR FORCE FY KN	SHEAR FORCE FZ KN
0014-0039	Transition Conical Section	0.783	A120	-20	69	69	-5754	-7356
G101-WP1L	Pile (Above Mudline)	0.773	E000	-107	-113	110	-1842	1820
G102-WP1K	Pile (Above Mudline)	0.771	E120	-107	-113	109	-1842	1816
G103-WP1J	Pile (Above Mudline)	0.770	E240	-107	-113	109	-1837	1811
0001-0034	Pile Sleeve	0.734	A330	-129	70	69	-289	-341
0002-0031	Pile Sleeve	0.734	A210	-129	70	69	-287	-338
0003-0026	Pile Sleeve	0.734	A090	-129	70	69	-289	-344
0026-LAT4	Pile Sleeve	0.675	A090	-130	55	54	-406	-271
0031-LAT2	Pile Sleeve	0.675	A210	-130	55	54	-407	-271
0034-LAT3	Pile Sleeve	0.675	A330	-130	55	54	-407	-271
APC- X	Transition Piece	0.667	A120	-15	171	99	1596	2763
APC-WP1A	Transition Piece	0.666	A150	-15	98	-170	2763	-1594
K-0018	Lower Diagonal	0.658	E000	-46	163	24	22	-2709
K-0019	Lower Diagonal	0.657	E120	-46	163	25	18	-2706
K-0016	Lower Diagonal	0.656	E240	-46	163	24	22	-2702
LAT4-WP2F	Pile Sleeve	0.629	A060	-129	50	-39	-967	91
LAT2-WP2E	Pile Sleeve	0.628	A180	-128	50	-39	-968	88
LAT3-WP2G	Pile Sleeve	0.577	A330	-132	41	6	-674	-77
0028- Z	Intermediate Diagonal	0.544	A150	-11	-163	67	1079	-2979
0029- Z	Intermediate Diagonal	0.543	A270	-11	-163	67	1078	-2976
0030- Z	Intermediate Diagonal	0.543	A030	-11	-163	68	1079	-2979
YC01-LAT1	Caisson (Above Mudline)	0.487	A210	-55	-108	16	-200	896
WP3M-0028	Intermediate Diagonal	0.472	A210	30	116	-69	1192	-2160
WP3N-0030	Intermediate Diagonal	0.472	A060	12	141	-60	1221	-2776

WP3P-0029	Intermediate Diagonal	0.471	A330	30	116	-69	1191	-2157
WP1N-WP3N	Upper Pile Can	0.444	A060	-54	10	104	-4057	884
WP1M-WP3M	Upper Pile Can	0.443	A180	-54	10	104	-4053	886
WP1P-WP3P	Upper Pile Can	0.433	A330	-50	34	99	-4965	1919
LAT1-CNAR	Caisson (Above Mudline)	0.431	A210	-55	-88	12	-124	876

SACS-IV MEMBER UNITY CHECK RANGE SUMMARY

GROUP II - UNITY CHECKS GREATER THAN 0.80 AND LESS THAN 1.00

MEMBER	GROUP ID	MAXIMUM COMBINED UNITY CK	LOAD COND NO.	DIST FROM END	AXIAL STRESS N/MM2	BENDING STRESS Y N/MM2	BENDING STRESS Z N/MM2	SHEAR FORCE FY KN	SHEAR FORCE FZ KN	KLY/RY	KLZ/RZ	SECOND-HIGHEST UNITY CHECK	SECOND-HIGHEST LOAD COND	THIRD-HIGHEST UNITY CHECK	THIRD-HIGHEST LOAD COND
TSH0-0012	C01	0.908	A120	3.6	-13.73	65.55	55.66	-5907.40	-7574.61	6.8	6.8	0.908	A240	0.907	A000
0012-0014	C02	0.828	A120	4.0	-16.99	68.98	61.53	-5878.36	-7471.94	9.0	9.0	0.827	A240	0.827	A000
0016-WP1E	SLD	0.875	C240	8.1	-44.84	-162.32	54.55	410.38	-1854.79	17.8	17.8	0.873	E240	0.870	D240
0018-WP1G	SLD	0.876	C000	8.1	-45.08	-163.14	54.58	410.30	-1864.48	17.8	17.8	0.874	E000	0.871	D000
0019-WP1F	SLD	0.875	C120	8.1	-44.98	-162.86	54.49	405.88	-1860.56	17.8	17.8	0.873	E120	0.871	D120
TPD1-WP1M	SUD	0.911	A180	0.0	-68.37	248.64	-93.95	5952.20	********	6.8	6.8	0.901	B180	0.822	A150
TPD2-WP1P	SUD	0.821	A270	0.0	-53.28	232.40	-92.53	4477.19	********	6.8	6.8	0.813	B120	0.812	B270
TPD3-WP1N	SUD	0.911	A060	0.0	-68.41	248.71	-93.91	5956.83	********	6.8	6.8	0.902	B060	0.822	A030

SACS-IV MEMBER UNITY CHECK RANGE SUMMARY

GROUP III - UNITY CHECKS GREATER THAN 1.00 AND LESS THAN*****

** NO UNITY CHECKS IN THIS GROUP **

******* JOINT CAN SUMMARY *******
(UNITY CHECK ORDER)
******** ORIGINAL ********

JOINT	DIAMETER (CM)	THICKNESS (CM)	YLD STRS (N/MM2)	UC	LOAD COND NO.
WP1M	262.341	5.629	340	0.833	A210
WP1N	262.341	5.629	340	0.833	A090
WP1P	262.341	5.629	340	0.833	A330
K	276.801	5	325	0.752	A270
WP3M	262.341	5.629	340	0.390	A210
WP3N	262.341	5.629	340	0.390	A090
WP3P	262.341	5.629	340	0.390	A330
Z	276.801	5	325	0.380	A120
WP1F	257.341	5	340	0.326	A210
WP1E	257.341	5	340	0.326	A330
WP1G	257.341	5	340	0.326	A090

APPENDIX B

IBGS ULS Analysis Foundation Results

* * * SOIL MAXIMUM AXIAL CAPACITY SUMMARY * * *

PILE JT	GRP	********** PILE HEAD ********** O.D. CM	THK. CM	PILE ********* WEIGHT KN	PEN. M	********** COMPRESSION ********** CAPACITY (INCL. WT) KN	MAX. LOAD KN	CRITICAL LOAD CONDITION LOAD KN	LOAD CASE	SAFETY FACTOR
WP1J	PIL	243.8	4	1175	61	-57661	-32948	-32948	E210	1.75
WP1K	PIL	243.8	4	1175	61	-57661	-32956	-32956	E090	1.75
WP1L	PIL	243.8	4	1175	61	-57661	-32430	-32430	E000	1.78
WP1H	CAS	243.8	3	437	25	-30398	-13402	-13402	E090	2.27

* * * SOIL MAXIMUM AXIAL CAPACITY SUMMARY CONTD * * *

PILE JT	GRP	********** TENSION ********** CAPACITY (INCL. WT) KN	MAX. LOAD KN	CRITICAL LOAD CONDITION LOAD KN	LOAD CASE	SAFETY FACTOR
WP1J	PIL	37649	24697	24697	F030	1.52
WP1K	PIL	37649	24706	24706	F270	1.52
WP1L	PIL	37649	24662	24662	F150	1.53
WP1H	CAS	8911	0	0	A000	100

* * * PILE MAXIMUM UNITY CHECK SUMMARY * * *

PILE HEAD JOINT	GROUP	LOAD CASE	DEPTH M	** STRESSES AT MAXIMUM UC ** AXIAL	FBY	FBZ	SHEAR	COMB ********** N/MM2 **********	UNITY CHECK
WP1L	Pile (Below Mudline)	E000	19.5	-120	86	0	13	-206	0.660
WP1K	Pile (Below Mudline)	E120	19.5	-120	86	0	13	-206	0.659
WP1J	Pile (Below Mudline)	E240	19.5	-120	85	0	13	-205	0.658
WP1L	Pile (Below Mudline)	F000	19.5	-117	84	0	13	-200	0.641
WP1J	Pile (Below Mudline)	E210	19.5	-123	76	1	13	-198	0.640
WP1K	Pile (Below Mudline)	E090	19.5	-123	76	1	13	-199	0.640
WP1K	Pile (Below Mudline)	F120	19.5	-116	83	0	13	-200	0.640
WP1L	Pile (Below Mudline)	C000	19.5	-114	87	-1	13	-201	0.640
WP1J	Pile (Below Mudline)	F240	19.5	-116	83	0	13	-200	0.639
WP1K	Pile (Below Mudline)	C120	19.5	-114	87	-1	13	-200	0.639
WP1J	Pile (Below Mudline)	C240	19.5	-114	86	-1	13	-200	0.638
WP1L	Pile (Below Mudline)	E330	19.5	-120	77	1	13	-197	0.635

PILE HEAD JOINT	GROUP	LOAD CASE	DEPTH M	** STRESSES AT MAXIMUM UC ** AXIAL	FBY	FBZ	SHEAR	COMB	UNITY CHECK
				********** N/MM2 **********					
WP1K	Pile (Below Mudline)	C090	19.5	-116	79	1	14	-195	0.627
WP1J	Pile (Below Mudline)	C210	19.5	-116	79	1	14	-195	0.626
WP1L	Pile (Below Mudline)	C330	19.5	-116	79	1	14	-195	0.626
WP1K	Pile (Below Mudline)	F090	19.5	-119	74	1	13	-192	0.621
WP1L	Pile (Below Mudline)	D000	19.5	-110	85	-1	13	-195	0.621
WP1J	Pile (Below Mudline)	F210	19.5	-119	73	1	13	-192	0.620
WP1K	Pile (Below Mudline)	D120	19.5	-110	85	-1	13	-194	0.620
WP1L	Pile (Below Mudline)	F330	19.5	-119	73	1	13	-192	0.620
WP1J	Pile (Below Mudline)	D240	19.5	-110	84	-1	13	-194	0.619
WP1J	Pile (Below Mudline)	D210	19.5	-113	76	1	13	-189	0.607
WP1K	Pile (Below Mudline)	D090	19.5	-113	77	1	13	-189	0.607
WP1L	Pile (Below Mudline)	D330	19.5	-113	76	1	13	-189	0.607
WP1J	Pile (Below Mudline)	E270	19.5	-89	79	-2	13	-168	0.532
WP1L	Pile (Below Mudline)	E030	19.5	-89	79	-2	13	-168	0.532
WP1K	Pile (Below Mudline)	E150	19.5	-89	78	-2	13	-168	0.531
WP1L	Pile (Below Mudline)	F030	19.5	-86	77	-2	13	-163	0.516
WP1J	Pile (Below Mudline)	F270	19.5	-85	77	-2	13	-163	0.515
WP1K	Pile (Below Mudline)	F150	19.5	-85	77	-2	13	-163	0.514
WP1J	Pile (Below Mudline)	C270	19.5	-84	77	-2	13	-161	0.510
WP1L	Pile (Below Mudline)	C030	19.5	-84	77	-2	13	-161	0.510
WP1K	Pile (Below Mudline)	C150	19.5	-84	77	-2	13	-161	0.509
WP1L	Pile (Below Mudline)	D030	19.5	-80	76	-2	13	-156	0.494
WP1J	Pile (Below Mudline)	D270	19.5	-80	76	-2	13	-156	0.493
WP1K	Pile (Below Mudline)	D150	19.5	-80	76	-2	13	-156	0.493
WP1K	Pile (Below Mudline)	A120	19.5	-106	40	1	10	-146	0.480
WP1J	Pile (Below Mudline)	A240	19.5	-106	39	1	10	-145	0.479
WP1L	Pile (Below Mudline)	A000	19.5	-106	39	1	10	-145	0.479
WP1J	Pile (Below Mudline)	A210	8.5	-97	51	3	2	-148	0.471
WP1K	Pile (Below Mudline)	A090	8.5	-97	51	3	2	-148	0.471
WP1J	Pile (Below Mudline)	E180	11.0	-81	71	0	2	-152	0.470
WP1L	Pile (Below Mudline)	A330	8.5	-97	51	3	2	-148	0.470
WP1K	Pile (Below Mudline)	E060	11.0	-81	71	0	2	-152	0.469
WP1L	Pile (Below Mudline)	E300	11.0	-81	71	0	2	-152	0.469
WP1J	Pile (Below Mudline)	C180	19.5	-90	54	2	12	-144	0.464
WP1K	Pile (Below Mudline)	C060	19.5	-90	54	2	12	-143	0.463
WP1L	Pile (Below Mudline)	C300	19.5	-89	54	2	12	-143	0.462
WP1K	Pile (Below Mudline)	B120	19.5	-102	37	1	9	-139	0.460
WP1J	Pile (Below Mudline)	B240	19.5	-102	37	1	9	-139	0.459
WP1L	Pile (Below Mudline)	B000	19.5	-102	37	1	9	-139	0.459
WP1J	Pile (Below Mudline)	B210	7.9	-95	48	4	3	-143	0.456

PILE HEAD JOINT	GROUP	LOAD CASE	DEPTH M	** STRESSES AT MAXIMUM UC ** AXIAL	FBY	FBZ	SHEAR	COMB	UNITY CHECK
				********** N/MM2 **********					
WP1J	Pile (Below Mudline)	F180	11.0	-78	70	0	2	-148	0.456
WP1K	Pile (Below Mudline)	B090	7.9	-95	48	4	3	-143	0.456
WP1L	Pile (Below Mudline)	B330	7.9	-95	48	4	3	-143	0.456
WP1K	Pile (Below Mudline)	F060	11.0	-78	69	0	2	-147	0.455
WP1L	Pile (Below Mudline)	F300	11.0	-78	69	0	2	-147	0.455
WP1J	Pile (Below Mudline)	D180	11.6	-74	72	0	1	-146	0.448
WP1K	Pile (Below Mudline)	D060	11.6	-74	71	0	1	-145	0.447
WP1L	Pile (Below Mudline)	D300	11.6	-74	71	0	1	-145	0.446
WP1L	Pile (Below Mudline)	F180	19.5	81	-69	1	12	150	0.441
WP1J	Pile (Below Mudline)	F060	19.5	80	-69	1	12	149	0.439
WP1K	Pile (Below Mudline)	F300	19.5	80	-69	1	12	149	0.439
WP1L	Pile (Below Mudline)	A030	19.5	-71	67	0	12	-138	0.437
WP1J	Pile (Below Mudline)	A270	19.5	-71	67	0	12	-138	0.436
WP1K	Pile (Below Mudline)	A150	19.5	-71	67	0	12	-138	0.436
WP1L	Pile (Below Mudline)	E180	19.5	77	-68	1	12	145	0.427
WP1J	Pile (Below Mudline)	A180	19.5	-91	-39	4	9	-130	0.426
WP1K	Pile (Below Mudline)	A060	19.5	-91	-39	4	9	-130	0.426
WP1J	Pile (Below Mudline)	E060	19.5	77	-68	1	12	145	0.425
WP1K	Pile (Below Mudline)	E300	19.5	77	-68	1	12	145	0.425
WP1L	Pile (Below Mudline)	D180	19.5	74	-71	1	12	144	0.424
WP1J	Pile (Below Mudline)	D060	19.5	74	-70	1	12	144	0.423
WP1K	Pile (Below Mudline)	D300	19.5	74	-70	1	12	144	0.423
WP1J	Pile (Below Mudline)	B270	19.5	-67	65	0	12	-132	0.417
WP1K	Pile (Below Mudline)	B150	19.5	-67	65	0	12	-132	0.417
WP1L	Pile (Below Mudline)	B030	19.5	-67	65	0	12	-132	0.417
WP1J	Pile (Below Mudline)	B180	19.5	-87	-39	4	9	-126	0.413
WP1K	Pile (Below Mudline)	B060	19.5	-87	-39	4	9	-126	0.413
WP1L	Pile (Below Mudline)	C180	19.5	70	-70	1	12	140	0.410
WP1J	Pile (Below Mudline)	C060	19.5	70	-69	1	12	139	0.409
WP1J	Pile (Below Mudline)	F030	12.2	72	-70	1	1	142	0.409
WP1K	Pile (Below Mudline)	C300	19.5	70	-69	1	12	139	0.409
WP1K	Pile (Below Mudline)	F270	12.2	72	-70	1	1	142	0.409
WP1L	Pile (Below Mudline)	F150	12.2	72	-69	1	1	141	0.408
WP1J	Pile (Below Mudline)	E030	11.6	70	-68	1	2	138	0.398
WP1K	Pile (Below Mudline)	D270	12.2	67	-71	1	2	138	0.398
WP1K	Pile (Below Mudline)	E270	11.6	70	-68	1	2	138	0.398
WP1J	Pile (Below Mudline)	D030	12.2	67	-71	1	2	138	0.397
WP1L	Pile (Below Mudline)	E150	11.6	70	-68	1	2	138	0.397
WP1L	Pile (Below Mudline)	D150	12.2	67	-71	1	2	138	0.396
WP1H	Caisson (Below Mudline)	E090	8.2	-52	66	3	2	-119	0.391

PILE HEAD JOINT	GROUP	LOAD CASE	DEPTH M	** STRESSES AT MAXIMUM UC ** AXIAL	FBY	FBZ	SHEAR	COMB	UNITY CHECK
				********** N/MM2 **********					
WP1H	Caisson (Below Mudline)	E000	8.2	-52	66	0	2	-118	0.390
WP1H	Caisson (Below Mudline)	E120	8.2	-52	66	0	2	-118	0.390
WP1H	Caisson (Below Mudline)	E210	8.2	-52	-66	-3	2	-118	0.390
WP1H	Caisson (Below Mudline)	C090	8.2	-52	66	3	3	-118	0.389
WP1H	Caisson (Below Mudline)	C210	8.2	-52	-66	-3	3	-118	0.389
WP1H	Caisson (Below Mudline)	C330	8.2	-52	-66	-3	3	-118	0.389
WP1H	Caisson (Below Mudline)	E240	8.2	-52	-66	0	2	-118	0.389
WP1H	Caisson (Below Mudline)	E330	8.2	-52	-66	-3	2	-118	0.389
WP1J	Pile (Below Mudline)	C030	12.2	64	-70	1	2	135	0.387
WP1K	Pile (Below Mudline)	C270	12.2	64	-70	1	2	135	0.387
WP1H	Caisson (Below Mudline)	C000	8.2	-51	66	0	2	-118	0.387
WP1H	Caisson (Below Mudline)	C120	8.2	-51	66	0	2	-117	0.387
WP1L	Pile (Below Mudline)	C150	12.2	64	-70	1	1	134	0.386
WP1H	Caisson (Below Mudline)	C240	8.2	-51	-66	0	2	-117	0.386
WP1H	Caisson (Below Mudline)	F090	8.2	-44	66	3	2	-110	0.360
WP1H	Caisson (Below Mudline)	D090	8.2	-44	66	3	3	-110	0.359
WP1H	Caisson (Below Mudline)	F000	8.2	-44	66	1	2	-110	0.359
WP1H	Caisson (Below Mudline)	F210	8.2	-44	-66	-3	2	-110	0.359
WP1H	Caisson (Below Mudline)	F330	8.2	-44	-66	-3	2	-110	0.359
WP1H	Caisson (Below Mudline)	D210	8.2	-44	-66	-3	3	-110	0.358
WP1H	Caisson (Below Mudline)	D330	8.2	-44	-66	-3	3	-110	0.358
WP1H	Caisson (Below Mudline)	F120	8.2	-44	66	1	2	-110	0.358
WP1H	Caisson (Below Mudline)	F240	8.2	-44	-65	0	2	-110	0.358
WP1H	Caisson (Below Mudline)	D000	8.2	-43	66	0	2	-109	0.356
WP1H	Caisson (Below Mudline)	D120	8.2	-43	66	0	2	-109	0.356
WP1H	Caisson (Below Mudline)	D240	8.2	-43	-65	0	2	-109	0.355
WP1J	Pile (Below Mudline)	F090	12.8	46	-79	-2	2	124	0.353
WP1L	Pile (Below Mudline)	F210	12.8	46	-79	-2	2	124	0.353
WP1K	Pile (Below Mudline)	F330	12.8	46	-78	-2	2	124	0.352

APPENDIX C

IBGS Robustness Analysis Substructure Results

***** SEA STATE COMBINED LOAD CASE SUMMARY *****
GLOBAL SUBSTRUCTURE REACTIONS RELATIVE TO MUDLINE ELEVATION

*** H000-H330 500 YEAR RETURN PERIOD ROBUSTNESS CHECK
*** IEC LC 6.1 WAVE DOMINANT

CASE LOAD CASE	LOAD LABEL	FX (KN)	FY (KN)	FZ (KN)	MX (KN-M)	MY (KN-M)	MZ (KN-M)
173	H000	22401	-866	-23612	102887	928447	-1790
174	H030	19636	10295	-23693	-371994	855133	1699
175	H060	11740	18632	-23818	-745132	549630	1145
176	H090	864	22214	-23966	-928415	101749	-3660
177	H120	-10419	19808	-23612	-854978	-374605	-1941
178	H150	-18762	11817	-23693	-553924	-750996	1597
179	H180	-22044	867	-23819	-103926	-921189	1120
180	H210	-19667	-10331	-23967	375359	-855256	-3611
181	H240	-11918	-18941	-23612	751919	-553084	-1819
182	H270	-876	-22172	-23693	926912	-104870	1753
183	H300	10240	-19499	-23818	848773	369648	1268
184	H330	18804	-11827	-23966	551809	753064	-3503

*** Y000-Y330 500 YEAR RETURN PERIOD ROBUSTNESS CHECK
*** IEC LC 6.1 WIND DOMINANT CASE

LOAD CASE	LOAD LABEL	FX (KN)	FY (KN)	FZ (KN)	MX (KN-M)	MY (KN-M)	MZ (KN-M)
185	Y000	21812	-996	-23569	116313	938542	-1452
186	Y030	18958	9762	-23540	-360044	860230	2742
187	Y060	11648	18202	-23771	-746344	565537	1693
188	Y090	991	21527	-23943	-933535	115068	-3975
189	Y120	-10013	19364	-23569	-870473	-368045	-1594
190	Y150	-18308	11700	-23537	-568818	-751031	2691
191	Y180	-21622	1002	-23772	-117101	-930086	1681
192	Y210	-19135	-9877	-23943	366389	-866341	-3920
193	Y240	-11737	-18366	-23569	753975	-569812	-1472
194	Y270	-1001	-21720	-23536	934352	-117707	2839
195	Y300	9914	-19203	-23771	863103	362713	1815
196	Y330	18145	-11595	-23942	565911	750823	-3821

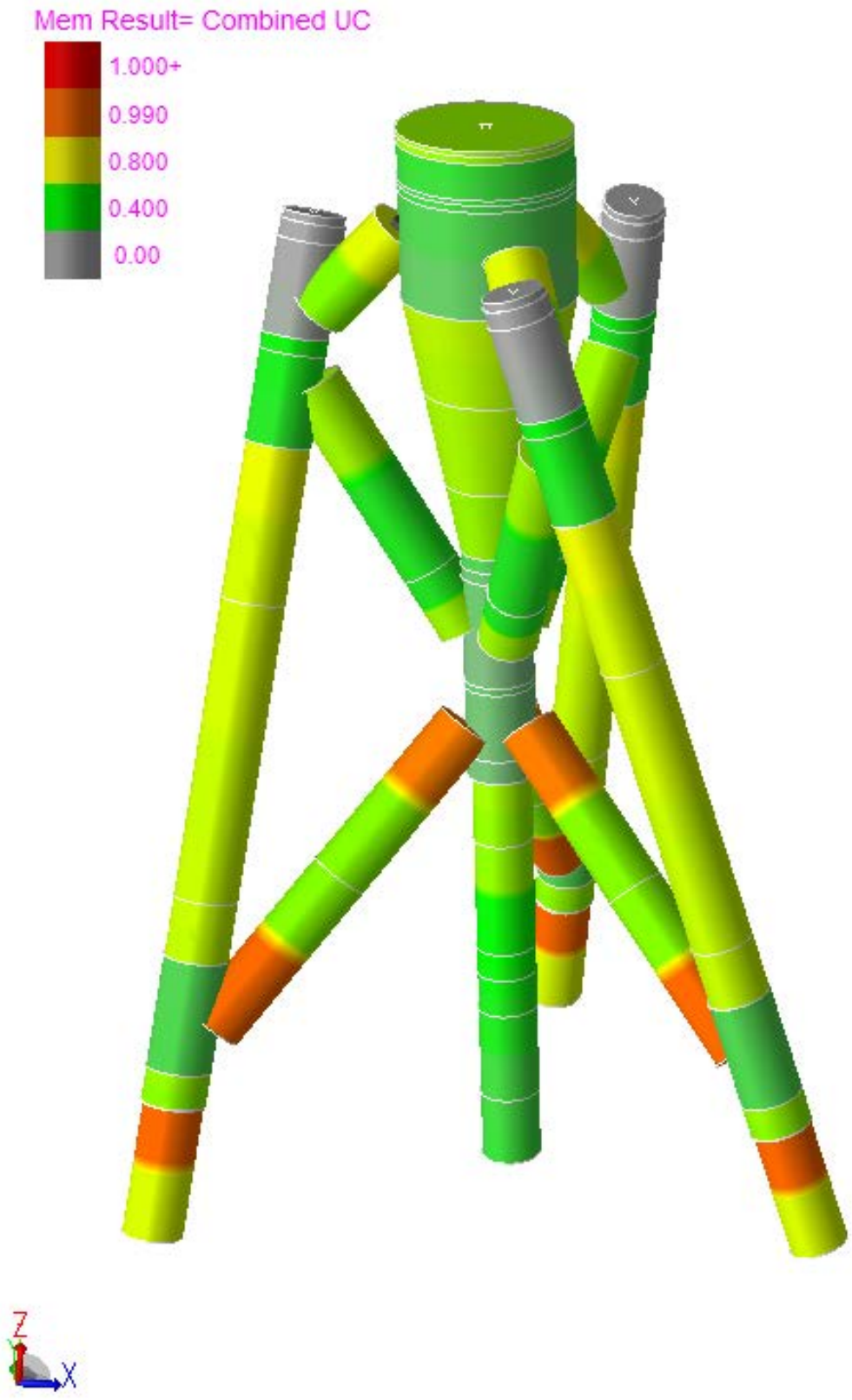

Figure C-1. IBGS robustness analysis unity check summary

SACS IV - MEMBER UNITY CHECK RANGE SUMMARY

GROUP I - UNITY CHECKS GREATER THAN 0.40 AND LESS THAN 0.8

MEMBER	GROUP ID	MAXIMUM COMBINED UNITY CK	LOAD COND NO.	AXIAL STRESS N/MM2	BENDING STRESS Y N/MM2	BENDING STRESS Z N/MM2	SHEAR FORCE FY KN	SHEAR FORCE FZ KN
0001-0034	Pile Sleeve	0.746	Y330	-151	87	46	331	-1149
0002-0031	Pile Sleeve	0.746	Y210	-151	87	46	333	-1146
0003-0026	Pile Sleeve	0.746	Y090	-151	87	46	332	-1153
TPD2-WP1P	Upper Diagonal	0.718	Y300	-61	188	-110	6380	-9335
TPD1-WP1M	Upper Diagonal	0.717	Y180	-61	188	-110	6379	-9326
TPD3-WP1N	Upper Diagonal	0.717	Y060	-61	188	-110	6378	-9328
0026-LAT4	Pile Sleeve	0.672	Y090	-152	42	55	113	-829
0031-LAT2	Pile Sleeve	0.672	Y210	-152	42	56	112	-828
0034-LAT3	Pile Sleeve	0.672	Y330	-152	42	55	111	-829
LAT2-WP2E	Pile Sleeve	0.623	H210	-149	-9	54	-201	-265
LAT3-WP2G	Pile Sleeve	0.623	H330	-149	-9	54	-199	-265
LAT4-WP2F	Pile Sleeve	0.623	H090	-149	-9	54	-198	-264
TSH0-0012	Transition Conical Section	0.599	Y210	-11	-24	43	-6926	3122
0012-0014	Transition Conical Section	0.544	Y210	-13	-25	41	-6092	2641
YC01-LAT1	Caisson (Above Mudline)	0.522	H000	-60	113	59	-192	-867
WP3M-0028	Intermediate Diagonal	0.512	Y210	65	114	-42	1008	-1701
WP3N-0030	Intermediate Diagonal	0.512	Y090	65	114	-42	1006	-1703
WP3P-0029	Intermediate Diagonal	0.512	Y330	65	114	-42	1010	-1701
0028- Z	Intermediate Diagonal	0.504	Y180	44	-125	61	962	-2672
0029- Z	Intermediate Diagonal	0.504	Y300	44	-125	61	963	-2675
0030- Z	Intermediate Diagonal	0.504	Y060	44	-125	61	961	-2675
APC- X	Transition Piece	0.487	Y000	-13	-39	-145	-4386	-1176
0014-0039	Transition Conical Section	0.486	Y090	-21	58	15	758	-5813
APC-WP1A	Transition Piece	0.485	Y270	-13	-144	-39	1176	4391
WP1G-	Lower Pile Can	0.473	H000	-65	-75	79	-	2341

G101							2443	
WP1E-G103	Lower Pile Can	0.472	H240	-65	-75	79	-2438	2334
WP1F-G102	Lower Pile Can	0.472	H120	-65	-75	79	-2441	2336
LAT1-CNAR	Caisson (Above Mudline)	0.470	H090	-63	-53	91	-828	364

SACS-IV MEMBER UNITY CHECK RANGE SUMMARY

GROUP II - UNITY CHECKS GREATER THAN 0.80 AND LESS THAN 1.00

MEMBER	GROUP ID	MAXIMUM COMBINED UNITY CK	LOAD COND NO.	DIST FROM END	AXIAL STRESS N/MM2	BENDING STRESS Y N/MM2	BENDING STRESS Z N/MM2	SHEAR FORCE FY KN	SHEAR FORCE FZ KN	KLY/RY	KLZ/RZ	SECOND-HIGHEST UNITY CHECK	SECOND-HIGHEST LOAD COND	THIRD-HIGHEST UNITY CHECK	THIRD-HIGHEST LOAD COND
G101-WP1L	P1	0.974	H000	0.0	-143.13	-147.83	155.53	-2448.97	2395.14	6.7	6.7	0.933	Y000	0.880	H030
G102-WP1K	P1	0.972	H120	0.0	-143.02	-147.40	155.26	-2447.39	2388.50	6.7	6.7	0.931	Y120	0.878	H150
G103-WP1J	P1	0.972	H240	0.0	-142.98	-147.17	155.10	-2444.38	2385.89	6.7	6.7	0.930	Y240	0.879	H270
0016-WP1E	SLD	0.962	H240	8.1	-62.40	-216.89	73.35	527.73	-2670.02	17.8	17.8	0.908	H270	0.902	Y240
0018-WP1G	SLD	0.965	H000	8.1	-62.59	-217.58	73.36	527.02	-2678.28	17.8	17.8	0.909	H030	0.904	Y000
0019-WP1F	SLD	0.963	H120	8.1	-62.44	-217.17	73.22	521.67	-2673.15	17.8	17.8	0.907	H150	0.903	Y120
K-0016	SLX	0.821	H240	0.0	-63.90	218.59	22.91	162.70	-3461.31	17.8	17.8	0.793	Y240	0.746	H210
K-0018	SLX	0.823	H000	0.0	-64.10	219.14	23.01	161.96	-3469.65	17.8	17.8	0.795	Y000	0.746	H330
K-0019	SLX	0.822	H120	0.0	-63.95	218.81	23.64	156.61	-3464.51	17.8	17.8	0.794	Y120	0.747	H090

SACS-IV MEMBER UNITY CHECK RANGE SUMMARY

GROUP III - UNITY CHECKS GREATER THAN 1.00 AND LESS THAN*****

** NO UNITY CHECKS IN THIS GROUP **

*Note: 0.98 unity checks for members G101-WP1L, G102-WP1K, and G103-WP1J occur in the pile. Therefore max jacket member unity check is 0.96.

******* JOINT CAN SUMMARY *******
(UNITY CHECK ORDER)
******** ORIGINAL ********

JOINT	DIAMETER (CM)	THICKNESS (CM)	YLD STRS (N/MM2)	UC	LOAD COND NO.
WP1N	262.341	5.629	340	0.796	Y090
WP1P	262.341	5.629	340	0.796	Y330
WP1M	262.341	5.629	340	0.796	Y210
WP3M	262.341	5.629	340	0.487	Y210
WP3P	262.341	5.629	340	0.487	Y330
WP3N	262.341	5.629	340	0.487	Y090
WP1G	260.341	6.021	340	0.320	H000
WP1F	260.341	6.021	340	0.319	H120
WP1E	260.341	6.021	340	0.318	H240
K	284.801	8.544	325	0.262	H240
Z	284.801	8.544	325	0.164	H030

APPENDIX D

IBGS Robustness Analysis Foundation Results

* * * SOIL MAXIMUM AXIAL CAPACITY SUMMARY * * *

PILE JT	GRP	********** PILE HEAD O.D. CM	THK. CM	********* PILE WEIGHT KN	PEN. M	********** COMPRESSION CAPACITY (INCL. WT) KN	MAX. LOAD KN	CRITICAL LOAD CONDITION LOAD KN	LOAD CASE	SAFETY FACTOR
WP1J	PIL	243.8	4	1175	61	-57661	-44255	-44252	Y210	1.30
WP1K	PIL	243.8	4	1175	61	-57661	-44260	-44260	Y090	1.30
WP1L	PIL	243.8	4	1175	61	-57661	-44257	-44257	Y330	1.30
WP1H	CAS	243.8	3	437	25	-30398	-14551	-14551	H090	2.09

* * * SOIL MAXIMUM AXIAL CAPACITY SUMMARY CONTD * * *

PILE JT	GRP	********** TENSION CAPACITY (INCL. WT) KN	MAX. LOAD KN	CRITICAL LOAD CONDITION LOAD KN	LOAD CASE	SAFETY FACTOR
WP1J	PIL	37649	36284	36284	H030	1.04
WP1K	PIL	37649	36444	36444	Y270	1.03
WP1L	PIL	37649	36449	36449	Y150	1.03
WP1H	CAS	8911	0	0	A000	100

* * * PILE MAXIMUM UNITY CHECK SUMMARY * * *

PILE HEAD JOINT	GROUP	LOAD CASE	DEPTH M	** STRESSES AT MAXIMUM UC ** AXIAL	FBY	FBZ	SHEAR	COMB ********** N/MM2 **********	UNITY CHECK
WP1L	Pile (Below Mudline)	H000	19.5	-168	132	0	14	-301	0.958
WP1K	Pile (Below Mudline)	H120	19.5	-168	132	0	14	-300	0.957
WP1J	Pile (Below Mudline)	H240	19.5	-168	132	0	14	-300	0.956
WP1L	Pile (Below Mudline)	Y000	19.5	-170	122	0	14	-292	0.936
WP1K	Pile (Below Mudline)	Y120	19.5	-170	122	0	14	-292	0.935
WP1J	Pile (Below Mudline)	Y240	19.5	-170	121	0	14	-291	0.934
WP1K	Pile (Below Mudline)	H090	19.5	-173	114	1	15	-287	0.924
WP1J	Pile (Below Mudline)	H210	19.5	-173	114	1	15	-287	0.923
WP1L	Pile (Below Mudline)	H330	19.5	-173	114	1	15	-287	0.923
WP1K	Pile (Below Mudline)	Y090	19.5	-173	101	2	15	-274	0.887
WP1J	Pile (Below Mudline)	Y210	19.5	-173	101	2	15	-274	0.886
WP1L	Pile (Below Mudline)	H000	19.5	-168	132	0	14	-301	0.958

PILE HEAD JOINT	GROUP	LOAD CASE	DEPTH M	** STRESSES AT MAXIMUM UC ** AXIAL	FBY	FBZ	SHEAR	COMB	UNITY CHECK
				********** N/MM2 **********					
WP1L	Pile (Below Mudline)	Y330	19.5	-173	101	2	15	-274	0.886
WP1L	Pile (Below Mudline)	H030	19.5	-122	120	-2	14	-242	0.764
WP1J	Pile (Below Mudline)	H270	19.5	-122	120	-2	14	-242	0.763
WP1K	Pile (Below Mudline)	H150	19.5	-122	120	-2	14	-242	0.762
WP1J	Pile (Below Mudline)	Y270	19.5	-124	115	-2	14	-239	0.757
WP1K	Pile (Below Mudline)	Y150	19.5	-124	115	-2	14	-239	0.756
WP1L	Pile (Below Mudline)	Y030	19.5	-123	112	-1	14	-235	0.745
WP1L	Pile (Below Mudline)	H180	19.5	128	-107	1	14	235	0.693
WP1J	Pile (Below Mudline)	H060	19.5	128	-107	1	14	235	0.691
WP1K	Pile (Below Mudline)	H300	19.5	128	-107	1	14	235	0.691
WP1J	Pile (Below Mudline)	H180	19.5	-134	74	2	15	-208	0.676
WP1L	Pile (Below Mudline)	Y180	19.5	130	-99	1	14	229	0.676
WP1J	Pile (Below Mudline)	Y060	19.5	130	-99	1	14	229	0.674
WP1K	Pile (Below Mudline)	H060	19.5	-134	74	2	15	-208	0.674
WP1K	Pile (Below Mudline)	Y300	19.5	130	-99	1	14	229	0.674
WP1L	Pile (Below Mudline)	H300	19.5	-134	74	2	15	-208	0.674
WP1J	Pile (Below Mudline)	H030	19.5	134	-88	0	14	221	0.655
WP1K	Pile (Below Mudline)	H270	19.5	134	-88	0	14	222	0.655
WP1L	Pile (Below Mudline)	H150	19.5	134	-88	0	14	221	0.655
WP1J	Pile (Below Mudline)	Y180	19.5	-134	65	1	14	-199	0.648
WP1K	Pile (Below Mudline)	Y060	19.5	-133	65	1	14	-198	0.646
WP1L	Pile (Below Mudline)	Y300	19.5	-133	65	1	14	-198	0.646
WP1K	Pile (Below Mudline)	Y270	19.5	134	-78	0	14	213	0.630
WP1L	Pile (Below Mudline)	Y150	19.5	134	-78	0	14	212	0.629
WP1J	Pile (Below Mudline)	Y030	19.5	132	-74	0	13	206	0.612
WP1L	Pile (Below Mudline)	H210	19.5	83	-111	3	14	195	0.568
WP1J	Pile (Below Mudline)	H090	19.5	83	-111	3	14	194	0.567
WP1K	Pile (Below Mudline)	H330	19.5	83	-111	3	14	194	0.566
WP1J	Pile (Below Mudline)	Y090	19.5	85	-104	2	14	188	0.551
WP1L	Pile (Below Mudline)	Y210	19.5	85	-104	2	14	189	0.551
WP1K	Pile (Below Mudline)	Y330	19.5	85	-103	2	14	188	0.550
WP1H	Caisson (Below Mudline)	H090	9.0	-57	93	9	3	-151	0.489
WP1H	Caisson (Below Mudline)	H210	9.0	-57	-93	-9	3	-150	0.489
WP1H	Caisson (Below Mudline)	H330	9.0	-57	-93	-9	3	-150	0.489
WP1H	Caisson (Below Mudline)	H000	9.0	-54	94	6	3	-149	0.482
WP1H	Caisson (Below Mudline)	H120	9.0	-54	94	6	3	-149	0.482
WP1H	Caisson (Below Mudline)	H240	9.0	-54	-94	-6	3	-149	0.482
WP1H	Caisson (Below Mudline)	Y090	8.8	-57	87	10	3	-145	0.471
WP1H	Caisson (Below Mudline)	Y210	8.8	-57	-87	-10	3	-144	0.471
WP1H	Caisson (Below Mudline)	Y330	8.8	-57	-87	-10	3	-144	0.471

PILE HEAD JOINT	GROUP	LOAD CASE	DEPTH M	** STRESSES AT MAXIMUM UC ** AXIAL	FBY	FBZ	SHEAR	COMB	UNITY CHECK
				********** N/MM2 **********					
WP1J	Pile (Below Mudline)	H000	10.4	85	-78	-1	2	163	0.470
WP1K	Pile (Below Mudline)	H240	10.4	85	-78	-1	2	162	0.469
WP1L	Pile (Below Mudline)	H120	10.4	85	-78	-1	2	162	0.469
WP1H	Caisson (Below Mudline)	Y000	8.8	-55	89	7	3	-144	0.468
WP1H	Caisson (Below Mudline)	Y120	8.8	-55	89	7	3	-144	0.468
WP1H	Caisson (Below Mudline)	Y240	8.8	-55	-89	-7	3	-144	0.467
WP1J	Pile (Below Mudline)	Y000	9.8	85	-72	-3	1	157	0.455
WP1K	Pile (Below Mudline)	Y240	9.8	85	-72	-3	1	157	0.454
WP1L	Pile (Below Mudline)	Y120	9.8	85	-72	-3	1	157	0.454
WP1H	Caisson (Below Mudline)	H030	9.0	-39	91	4	3	-130	0.414
WP1H	Caisson (Below Mudline)	H270	9.0	-39	-91	-4	3	-130	0.414
WP1H	Caisson (Below Mudline)	H150	9.0	-39	91	4	3	-129	0.413
WP1J	Pile (Below Mudline)	H150	9.8	-53	85	6	3	-138	0.412
WP1K	Pile (Below Mudline)	H030	9.8	-53	85	6	3	-138	0.412
WP1L	Pile (Below Mudline)	H270	9.8	-53	85	6	3	-138	0.412
WP1H	Caisson (Below Mudline)	H180	9.0	-40	-88	-9	3	-128	0.411
WP1H	Caisson (Below Mudline)	H060	8.8	-40	87	9	3	-128	0.410
WP1H	Caisson (Below Mudline)	H300	9.0	-40	-88	-9	3	-128	0.410
WP1H	Caisson (Below Mudline)	Y150	8.8	-39	87	4	3	-125	0.401
WP1H	Caisson (Below Mudline)	Y270	8.8	-38	-87	-4	3	-125	0.401
WP1J	Pile (Below Mudline)	Y150	9.8	-51	-82	-7	3	-134	0.399
WP1L	Pile (Below Mudline)	Y270	9.8	-51	-82	-7	3	-134	0.399
WP1J	Pile (Below Mudline)	Y300	0.0	-47	-65	59	19	-135	0.398
WP1K	Pile (Below Mudline)	Y180	0.0	-46	-65	60	19	-134	0.398
WP1H	Caisson (Below Mudline)	Y180	8.8	-40	-84	-9	3	-124	0.398
WP1L	Pile (Below Mudline)	Y060	0.0	-46	-65	59	19	-134	0.397
WP1H	Caisson (Below Mudline)	Y060	8.8	-40	84	9	3	-124	0.397
WP1H	Caisson (Below Mudline)	Y300	8.8	-40	-84	-9	3	-124	0.397

APPENDIX E

Sub/Dyn Model Validation Member End Force Summary

MEMBER END FORCES AND MOMENTS REPORT

MEMBER NUMBER	MEMB END	FORCE(X) (KN)	FORCE(Y) (KN)	FORCE(Z) (KN)	MOMENT(X) (KN-M)	MOMENT(Y) (KN-M)	MOMENT(Z) (KN-M)
X- IAL	X	-5.6	2432.2	-369.7	1.5	9048.7	-54735.6
	IAL	-5.6	2432.2	-369.7	1.5	8494.1	-51087.3
APC- X	APC	0.0	-999.8	0.0	0.0	0.0	-100190.5
	X	0.0	-999.8	0.0	0.0	0.0	-100500.3
APC-WP1A	APC	0.0	-999.2	-0.3	0.0	-0.1	100190.3
	WP1A	0.0	-999.2	-0.3	0.0	0.1	99999.8
IAL-BF02	IAL	-5.6	2432.6	-369.2	1.5	8494.1	-51087.1
	BF02	-5.6	2432.6	-369.2	1.5	8420.2	-50600.8
BF02-0038	BF02	-5.6	2432.4	-369.8	1.5	8420.2	-50601.2
	38	-5.6	2432.4	-369.8	1.5	8309.3	-49870.6
TSH0-0012	TSH0	-5.6	2432.2	-369.7	1.5	6645.7	-38926.1
	12	-5.6	2432.2	-369.7	1.5	5166.8	-29197.2
0012-0014	12	-5.6	2432.2	-369.7	1.5	5166.8	-29197.2
	14	-5.6	2432.2	-369.7	1.5	3688.0	-19468.3
0014-0039	14	-5.6	2432.2	-369.7	1.5	3688.0	-19468.2
	39	-5.6	2432.2	-369.7	1.5	2578.9	-12171.5
0039-0040	39	-5.6	2432.2	-369.7	1.5	2578.9	-12171.5
	40	-5.6	2432.2	-369.7	1.5	2357.1	-10712.2
0033-YC01	33	-57.3	195.9	-134.9	24.5	1953.9	-3627.7
	YC01	-57.3	195.9	-134.9	24.5	1819.0	-3431.8
0040-0032	40	-5.6	2432.2	-369.7	1.5	2357.1	-10712.1
	32	-5.6	2432.2	-369.7	1.5	2170.4	-9483.9
K-0033	K	-57.3	195.9	-134.9	24.5	2358.0	-4214.4
	33	-57.3	195.9	-134.9	24.5	1953.9	-3627.7
Z- K	Z	-18.5	1515.3	-1990.5	2.3	-151.8	-7677.3
	K	-18.5	1515.3	-1990.5	2.3	-759.0	-7215.1

0032- Z	32	-5.6	2432.2	-369.7	1.5	2170.4	-9483.9

MEMBER NUMBER	MEMB END	FORCE(X) (KN)	FORCE(Y) (KN)	FORCE(Z) (KN)	MOMENT(X) (KN-M)	MOMENT(Y) (KN-M)	MOMENT(Z) (KN-M)
	Z	-5.6	2432.2	-369.7	1.5	471.6	1692.3
LAT1-CNAR	LAT1	-57.3	195.9	-134.9	24.5	1414.3	-2844.0
	CNAR	-57.3	195.9	-134.9	24.5	739.7	-1864.5
YC01-LAT1	YC01	-57.3	195.9	-134.9	24.5	1819.0	-3431.8
	LAT1	-57.3	195.9	-134.9	24.5	1414.3	-2844.0
0004-WP1H	4	-57.3	195.9	-134.9	24.5	-191.2	-512.7
	WP1H	-57.3	195.9	-134.9	24.5	-595.9	75.0
0035-0004	35	-57.3	195.9	-134.9	24.5	348.5	-1296.4
	4	-57.3	195.9	-134.9	24.5	-191.2	-512.7
0036-0035	36	-57.3	195.9	-134.9	24.5	577.8	-1629.4
	35	-57.3	195.9	-134.9	24.5	348.5	-1296.4
CNAR-0036	CNAR	-57.3	195.9	-134.9	24.5	739.7	-1864.5
	36	-57.3	195.9	-134.9	24.5	577.8	-1629.4
WP3B-0020	WP3B	0.0	0.0	0.0	0.0	0.0	0.0
	20	0.0	0.0	0.0	0.0	0.0	0.0
WP3C-0027	WP3C	0.0	0.0	0.0	0.0	0.0	0.0
	27	0.0	0.0	0.0	0.0	0.0	0.0
WP3D-0006	WP3D	0.0	0.0	0.0	0.0	0.0	0.0
	6	0.0	0.0	0.0	0.0	0.0	0.0
G101-WP1L	G101	-5554.5	-107.5	-186.6	49.3	1107.4	-140.6
	WP1L	-5554.5	-107.5	-186.6	49.3	-18.2	-789.0

G102-WP1K	G102	527.1	541.4	-388.2	-775.8	3267.0	-4648.4
	WP1K	527.1	541.4	-388.2	-775.8	925.4	-1382.7
G103-WP1J	G103	5091.9	-429.2	557.1	843.5	-4348.6	4620.8
	WP1J	5091.9	-429.2	557.1	843.5	-988.0	2031.8
WP1E-G103	WP1E	5091.9	-429.3	557.1	843.4	-4986.3	5111.6
	G103	5091.9	-429.3	557.1	843.4	-4349.0	4620.5

MEMBER NUMBER	MEMB END	FORCE(X) (KN)	FORCE(Y) (KN)	FORCE(Z) (KN)	MOMENT(X) (KN-M)	MOMENT(Y) (KN-M)	MOMENT(Z) (KN-M)
WP1F-G102	WP1F	527.1	541.3	-388.2	-775.7	3711.5	-5267.4
	G102	527.1	541.3	-388.2	-775.7	3267.3	-4648.1
WP1G-G101	WP1G	-5554.5	-107.5	-186.6	49.3	1320.8	-17.6
	G101	-5554.5	-107.5	-186.6	49.3	1107.4	-140.6
WP2E-WP1E	WP2E	7031.5	215.4	-46.9	474.7	-1788.7	2587.0
	WP1E	7031.5	215.4	-46.9	474.7	-2011.0	3607.5
WP2F-WP1F	WP2F	-1444.7	-119.3	97.7	-126.6	458.1	-2616.2
	WP1F	-1444.7	-119.3	97.7	-126.6	920.8	-3181.2
WP2G-WP1G	WP2G	-5568.4	-98.1	-48.3	-316.5	1360.9	-12.4
	WP1G	-5568.4	-98.1	-48.3	-316.5	1132.1	-477.0
WP1M-WP3M	WP1M	7104.6	1009.4	-138.4	-1242.0	-274.6	-8386.5
	WP3M	7104.6	1009.4	-138.4	-1242.0	-368.2	-7704.1
WP1N-WP3N	WP1N	-2769.4	126.0	-477.1	529.9	-3449.1	2674.2
	WP3N	-2769.4	126.0	-477.1	529.9	-3771.6	2759.4

WP1P-WP3P	WP1P	-4328.2	-1130.1	609.7	735.6	3709.2	5717.6
	WP3P	-4328.2	-1130.1	609.7	735.6	4121.3	4953.6
WP2M-WP1M	WP2M	0.0	0.0	0.0	0.0	0.0	0.0
	WP1M	0.0	0.0	0.0	0.0	0.0	0.0
WP2N-WP1N	WP2N	0.0	0.0	0.0	0.0	0.0	0.0
	WP1N	0.0	0.0	0.0	0.0	0.0	0.0
WP2P-WP1P	WP2P	0.0	0.0	0.0	0.0	0.0	0.0
	WP1P	0.0	0.0	0.0	0.0	0.0	0.0

MEMBER NUMBER	MEMB END	FORCE(X) (KN)	FORCE(Y) (KN)	FORCE(Z) (KN)	MOMENT(X) (KN-M)	MOMENT(Y) (KN-M)	MOMENT(Z) (KN-M)
WP3M-0002	WP3M	7031.5	214.6	-46.3	474.6	-602.0	-2889.2
	2	7031.5	214.6	-46.3	474.6	-778.5	-2072.2
WP3N-0003	WP3N	-1444.7	-119.3	97.3	-127.0	-2024.9	422.6
	3	-1444.7	-119.3	97.3	-127.0	-1654.6	-31.6
WP3P-0001	WP3P	-5568.3	-98.1	-49.3	-316.3	2606.3	2486.7
	1	-5568.3	-98.1	-49.3	-316.3	2418.5	2113.2
0001-0034	1	-5568.3	-98.1	-49.3	-316.3	2418.4	2113.2
	34	-5568.3	-98.1	-49.3	-316.3	2095.8	1471.6
0002-0031	2	7031.5	214.6	-46.3	474.6	-778.5	-2072.2
	31	7031.5	214.6	-46.3	474.6	-1081.5	-668.9
0003-0026	3	-1444.7	-119.3	97.3	-127.0	-1654.6	-31.6
	26	-1444.7	-119.3	97.3	-127.0	-1018.4	-811.8
LAT2-	LAT2	7031.4	215.4	-46.9	474.7	-1669.4	2039.0

WP2E							
	WP2E	7031.4	215.4	-46.9	474.7	-1788.8	2587.0
LAT3-WP2G	LAT3	-5568.4	-98.1	-48.3	-316.5	1483.7	237.1
	WP2G	-5568.4	-98.1	-48.3	-316.5	1360.9	-12.4
LAT4-WP2F	LAT4	-1444.7	-119.3	97.7	-126.6	209.6	-2312.8
	WP2F	-1444.7	-119.3	97.7	-126.6	458.1	-2616.2
0006-WP2P	6	0.0	0.0	0.0	0.0	0.0	0.0
	WP2P	0.0	0.0	0.0	0.0	0.0	0.0
0020-WP2M	20	0.0	0.0	0.0	0.0	0.0	0.0
	WP2M	0.0	0.0	0.0	0.0	0.0	0.0
0027-WP2N	27	0.0	0.0	0.0	0.0	0.0	0.0
	WP2N	0.0	0.0	0.0	0.0	0.0	0.0
0026-LAT4	26	-1444.7	-119.3	97.6	-126.8	-1018.4	-811.9
	LAT4	-1444.7	-119.3	97.6	-126.8	209.7	-2312.7

MEMBER NUMBER	MEMB END	FORCE(X) (KN)	FORCE(Y) (KN)	FORCE(Z) (KN)	MOMENT(X) (KN-M)	MOMENT(Y) (KN-M)	MOMENT(Z) (KN-M)
0031-LAT2	31	7031.5	215.1	-46.7	474.7	-1081.7	-668.6
	LAT2	7031.5	215.1	-46.7	474.7	-1669.7	2038.7
0034-LAT3	34	-5568.4	-98.1	-48.6	-316.5	2095.8	1471.6
	LAT3	-5568.4	-98.1	-48.6	-316.5	1483.7	237.1
WP3M-0028	WP3M	-337.3	-287.4	670.3	846.7	-3578.7	1679.4
	28	-337.3	-287.4	670.3	846.7	2430.7	-896.9

WP3N-0030	WP3N	-1391.3	46.8	-454.7	172.9	2286.3	389.5
	30	-1391.3	46.8	-454.7	172.9	-1789.9	809.1
WP3P-0029	WP3P	1712.8	239.8	-214.4	-1021.6	1282.4	-2063.2
	29	1712.8	239.8	-214.4	-1021.6	-639.6	86.9
0028- Z	28	-337.3	-287.4	670.3	846.7	2430.7	-896.9
	Z	-337.3	-287.4	670.3	846.7	4371.9	-1729.1
0029- Z	29	1712.8	239.8	-214.4	-1021.6	-639.6	86.9
	Z	1712.8	239.8	-214.4	-1021.6	-1260.4	781.4
0030- Z	30	-1391.3	46.8	-454.7	172.9	-1789.9	809.1
	Z	-1391.3	46.8	-454.7	172.9	-3106.7	944.6
0016-WP1E	16	-2119.9	-2.0	-220.1	-142.6	-1092.1	-46.5
	WP1E	-2119.9	-2.0	-220.1	-142.6	-2864.4	-62.4
0018-WP1G	18	59.7	-76.5	-100.0	549.9	918.7	1042.7
	WP1G	59.7	-76.5	-100.0	549.9	113.5	426.9
0019-WP1F	19	2109.7	68.6	324.2	-378.1	181.5	-1033.4
	WP1F	2109.7	68.6	324.2	-378.1	2792.4	-481.0
K-0016	K	-2119.9	-2.0	-220.1	-142.6	680.2	-30.5
	16	-2119.9	-2.0	-220.1	-142.6	-1092.1	-46.5
K-0018	K	59.7	-76.5	-100.0	549.9	1723.9	1658.4
	18	59.7	-76.5	-100.0	549.9	918.7	1042.7

MEMBER NUMBER	MEMB END	FORCE(X) (KN)	FORCE(Y) (KN)	FORCE(Z) (KN)	MOMENT(X) (KN-M)	MOMENT(Y) (KN-M)	MOMENT(Z) (KN-M)
K-0019	K	2109.7	68.6	324.2	-378.1	-2429.5	-1585.9
	19	2109.7	68.6	324.2	-378.1	181.5	-1033.4
TPD1-	TPD1	6298.1	-1380.3	3152.9	-1936.6	-13277.5	5199.1

WP1M							
	WP1M	6298.1	-1380.3	3152.9	-1936.6	2435.1	-1679.9
TPD2-WP1P	TPD2	-4190.6	1051.2	-1310.1	3314.5	5224.1	-1880.2
	WP1P	-4190.6	1051.2	-1310.1	3314.5	-1304.7	3358.5
TPD3-WP1N	TPD3	-2098.2	326.5	-1844.9	-1369.5	8048.6	-3321.6
	WP1N	-2098.2	326.5	-1844.9	-1369.5	-1145.6	-1694.2
X-TPD1	X	6298.2	-1380.3	3152.9	-1936.6	-14160.2	5585.6
	TPD1	6298.2	-1380.3	3152.9	-1936.6	-13277.5	5199.1
X-TPD2	X	-4190.6	1051.2	-1310.1	3314.5	5590.2	-2174.0
	TPD2	-4190.6	1051.2	-1310.1	3314.5	5224.1	-1880.2
X-TPD3	X	-2098.2	326.4	-1844.9	-1369.4	8565.4	-3413.1
	TPD3	-2098.2	326.4	-1844.9	-1369.4	8048.6	-3321.5
0038-TSH0	38	-5.6	2432.3	-369.7	1.5	8309.3	-49871.3
	TSH0	-5.6	2432.3	-369.7	1.5	6645.6	-38926.2

APPENDIX F

Sub/Dyn Model Validation Member End Force Summary

All loads shown in Appendix F are NON FACTORIZED (no load factor is applied).

Extreme load/deflection tables for the 50-year extreme load case:

Table F-1. Extreme 50-Year Tower-Top Displacements

Parameter	Type	File Name	TTDspFA [m]	TTDspSS [m]	Time [s]	HorWindV [m/s]	Wave1Elev [m]
TTDspFA	Minimum	LC_32	- 2.0687E-002	2.4400E-003	2.9072E+003	5.4299E+001	- 1.4150E+000
TTDspFA	Maximum	LC_28	1.5276E+000	3.1520E-001	1.5579E+003	5.8497E+001	2.3120E+000
TTDspSS	Minimum	LC_48	7.7650E-001	- 8.3416E-001	1.5198E+003	4.6113E+001	1.5310E+000
TTDspSS	Maximum	LC_1	1.0650E+000	8.0738E-001	1.2406E+003	6.1426E+001	- 3.5670E+000

Table F-2. Blade 1 Extreme 50-Year Out-of-Plane Deflections (edgewise)

Parameter	Type	File Name	OoPDefl1 [m]	Time [s]	HorWindV [m/s]	Wave1Elev [m]
OoPDefl1	Minimum	LC_45	- 8.0590E-001	1.8075E+003	5.7385E+001	3.4580E+000
OoPDefl1	Maximum	LC_36	3.7041E-001	1.5167E+003	5.1185E+001	4.5280E-001

Table F-3. Blade 1 In Plane 50-Year Extreme Deflections (flapwise)

Parameter	Type	File Name	IPDefl1 [m]	Time [s]	HorWindV [m/s]	Wave1Elev [m]
IPDefl1	Minimum	LC_48	- 1.1766E+001	1.8055E+003	5.7728E+001	- 5.8530E-001
IPDefl1	Maximum	LC_60	7.2395E+000	1.5773E+003	6.0018E+001	2.1600E+000

Table F-4. Blade 1 50-Year Extreme Loads (at blade root)

Parameter	Type	File Name	RootFxc1 [kN]	RootFyc1 [kN]	RootFzc1 [kN]	RootF1 [kN]	RootM1 [kNm]	RootMzc1 [kNm]	Time [s]	HorWindV [m/s]	Wave1Elev [m]
RootFxc1	Minimum	LC_33	- 1.9039E+002	- 7.4170E+002	- 5.0710E+002	7.6575E+002	3.5223E+004	1.6310E+002	1.5664E+003	4.9999E+001	- 1.3980E+000
RootFxc1	Maximum	LC_28	1.5489E+002	- 4.9090E+002	- 3.0780E+002	5.1476E+002	2.3407E+004	- 6.8584E+001	2.4936E+003	6.4283E+001	- 1.5040E+000
RootFyc1	Minimum	LC_24	- 8.1810E+001	- 1.2162E+003	- 4.6840E+002	1.2189E+003	5.6211E+004	3.6107E+002	3.1922E+003	6.3901E+001	1.4160E+000
RootFyc1	Maximum	LC_52	4.2850E+001	1.1641E+003	- 3.2526E+002	1.1649E+003	4.1583E+004	- 4.2586E+002	4.4859E+003	6.1620E+001	- 2.0060E+000
RootFzc1	Minimum	LC_36	1.3140E+002	- 3.4820E+002	- 6.6628E+002	3.7217E+002	2.8416E+004	4.4885E+001	2.9335E+003	7.2071E+001	- 1.8740E+000
RootFzc1	Maximum	LC_12	- 7.3263E+001	3.4580E+002	6.3516E+002	3.5348E+002	1.5561E+004	- 1.4740E+002	1.3870E+003	4.9791E+001	5.0180E+000
RootF1	Minimum	LC_52	4.0640E-001	- 7.4879E-002	- 5.6541E+002	4.1324E-001	1.9452E+003	- 2.0660E+002	4.0578E+003	4.4522E+001	- 2.1440E+000
RootF1	Maximum	LC_24	- 8.1810E+001	- 1.2162E+003	- 4.6840E+002	1.2189E+003	5.6211E+004	3.6107E+002	3.1922E+003	6.3901E+001	1.4160E+000
RootM1	Minimum	LC_25	- 8.3300E+000	8.0920E+001	5.7660E+002	8.1347E+001	2.1036E+001	6.7876E+000	3.0592E+003	4.7791E+001	- 5.3120E-003
RootM1	Maximum	LC_21	- 8.8320E+001	- 1.1720E+003	- 4.4570E+002	1.1753E+003	5.6762E+004	4.2965E+002	3.1928E+003	6.0705E+001	9.9780E-001
RootMzc1	Minimum	LC_33	- 1.2130E+001	3.6735E+001	4.9331E+002	3.8686E+001	6.1878E+003	- 5.9850E+002	3.9816E+003	7.1038E+001	2.4990E+000
RootMzc1	Maximum	LC_25	- 6.9550E+001	- 9.2895E+002	4.8580E+002	9.3155E+002	3.5719E+004	5.5862E+002	2.7571E+003	6.6332E+001	9.3160E-001

Table F-5. Yaw Bearing 50-Year Extreme Loads

Parameter	Type	File Name	YawBrFxp [kN]	YawBrFyp [kN]	YawBrFzp [kN]	YawBrMxp [kNm]	YawBrMyp [kNm]	YawBrMzp [kNm]	Time [s]	HorWindV [m/s]	Wave1Elev [m]
YawBrFxp	Minimum	LC_32	-8.2941E+002	-3.5593E+001	-8.5150E+003	1.7780E+002	4.7540E+004	-9.7210E+002	2.9071E+003	5.0896E+001	-1.5250E+000
YawBrFxp	Maximum	LC_25	1.5952E+003	6.7540E+002	-8.9060E+003	5.4260E+003	5.6490E+004	6.1136E+003	1.5579E+003	5.8497E+001	2.3120E+000
YawBrFyp	Minimum	LC_48	4.6290E+002	-1.5662E+003	-8.8180E+003	-3.3690E+003	5.4630E+004	-8.8440E+003	1.5197E+003	4.6761E+001	1.1930E+000
YawBrFyp	Maximum	LC_4	6.4370E+002	1.5387E+003	-8.5138E+003	3.0330E+003	5.6420E+004	1.4360E+004	1.2405E+003	6.5491E+001	-3.7780E+000
YawBrFzp	Minimum	LC_21	4.6610E+001	-1.0790E+003	-9.4971E+003	-4.9046E+003	5.9459E+004	-1.1211E+004	3.1933E+003	6.6861E+001	1.4430E-001
YawBrFzp	Maximum	LC_60	7.8450E+001	-2.2336E+002	-8.3114E+003	-5.3590E+003	4.3050E+004	-1.7920E+003	1.0093E+003	3.8322E+001	1.8490E+000
YawBrMxp	Minimum	LC_36	1.0250E+003	5.8860E+002	-8.8453E+003	-9.6672E+003	6.0143E+004	3.3699E+003	2.3713E+003	4.8340E+001	-3.4960E+000
YawBrMxp	Maximum	LC_28	5.3290E+002	-4.3380E+002	-8.6626E+003	9.0390E+003	5.4930E+004	-5.7070E+003	2.0963E+003	4.3493E+001	-2.9110E+000
YawBrMyp	Minimum	LC_49	-3.6630E+002	2.4500E+002	-8.5512E+003	4.6998E+003	3.8213E+004	2.2070E+003	3.3470E+003	4.6914E+001	5.4690E-001
YawBrMyp	Maximum	LC_25	1.0140E+003	7.2470E+002	-9.0603E+003	6.2450E+003	6.7151E+004	1.2787E+004	3.9717E+003	6.1665E+001	3.5960E+000
YawBrMzp	Minimum	LC_33	1.0040E+003	-1.0860E+003	-8.7970E+003	-2.9997E+003	5.2210E+004	-1.6766E+004	2.5513E+003	5.4851E+001	-1.2150E+000
YawBrMzp	Maximum	LC_1	9.3222E+002	1.4611E+003	-8.8080E+003	2.3147E+003	5.1979E+004	1.5930E+004	1.2408E+003	6.8408E+001	-3.2220E+000

Table F-6. Tower Base 50-Year Extreme Loads

Parameter	Type	File Name	TwrBsFxt [kN]	TwrBsFyt [kN]	TwrBsF [kN]	TwrBsFzt [kN]	TwrBsMxt [kNm]	TwrBsMyt [kNm]	TwrBsM [kNm]	TwrBsMzt [kNm]	Time [s]	HorWindV [m/s]	Wave1Elev [m]
TwrBsFxt	Minimum	LC_36	-7.3071E+002	1.7460E+002	7.5128E+002	-1.5120E+004	-2.6643E+004	-3.1940E+004	4.1593E+004	-1.4500E+003	2.9070E+003	4.5502E+001	-1.6360E+000
TwrBsFxt	Maximum	LC_25	2.5680E+003	9.2830E+002	2.7306E+003	-1.5190E+004	-1.0780E+005	2.8740E+005	3.0695E+005	1.3200E+004	3.9834E+003	6.3829E+001	2.1970E+000
TwrBsFyt	Minimum	LC_45	9.2930E+002	-1.6615E+003	1.9037E+003	-1.5160E+004	1.7676E+005	1.2550E+005	2.1679E+005	-9.4200E+003	1.5200E+003	5.1693E+001	2.1760E+000
TwrBsFyt	Maximum	LC_25	1.2000E+003	1.5934E+003	1.9947E+003	-1.5160E+004	-1.6124E+005	1.3740E+005	2.1184E+005	8.6697E+003	2.7823E+003	4.8299E+001	-7.1570E-001
TwrBsF	Minimum	LC_56	-1.4920E-001	9.6250E-001	9.7400E-001	-1.5140E+004	5.6220E+002	1.9500E+004	1.9508E+004	-1.7590E+003	1.6742E+003	4.2393E+001	5.3990E-001
TwrBsF	Maximum	LC_25	2.5350E+003	1.0570E+003	2.7465E+003	-1.5117E+004	-1.1440E+005	2.8808E+005	3.0996E+005	1.3676E+004	3.9835E+003	6.5067E+001	2.1880E+000
TwrBsFzt	Minimum	LC_21	8.2280E+002	-1.2400E+003	1.4882E+003	-1.5940E+004	1.2680E+005	9.8606E+004	1.6063E+005	-1.1212E+004	3.1933E+003	6.6861E+001	1.4430E-001
TwrBsFzt	Maximum	LC_57	4.9260E+002	-1.6660E+002	5.2001E+002	-1.4729E+004	1.6080E+004	7.4680E+004	7.6392E+004	-1.7930E+003	1.0093E+003	3.8322E+001	1.8490E+000
TwrBsMxt	Minimum	LC_4	1.7940E+003	1.5000E+003	2.3385E+003	-1.5240E+004	-1.6927E+005	1.9410E+005	2.5754E+005	1.5090E+004	1.2406E+003	6.1426E+001	-3.5670E+000
TwrBsMxt	Maximum	LC_45	9.2930E+002	-1.6615E+003	1.9037E+003	-1.5160E+004	1.7676E+005	1.2550E+005	2.1679E+005	-9.4200E+003	1.5200E+003	5.1693E+001	2.1760E+000
TwrBsMyt	Minimum	LC_29	-5.3420E+002	8.4540E+001	5.4085E+002	-1.4940E+004	-1.1200E+003	-3.7031E+004	3.7048E+004	-9.7290E+002	2.9071E+003	5.0896E+001	-1.5250E+000
TwrBsMyt	Maximum	LC_28	2.5350E+003	1.0570E+003	2.7465E+003	-1.5117E+004	-1.1440E+005	2.8808E+005	3.0996E+005	1.3676E+004	3.9835E+003	6.5067E+001	2.1880E+000
TwrBsM	Minimum	LC_28	-1.3023E+002	1.5090E+001	1.3110E+002	-1.5080E+004	4.7396E+002	2.3470E+002	5.2889E+002	9.1820E+002	3.9986E+003	4.7669E+001	-1.6530E+000
TwrBsM	Maximum	LC_28	2.5350E+003	1.0570E+003	2.7465E+003	-1.5117E+004	-1.1440E+005	2.8808E+005	3.0996E+005	1.3676E+004	3.9835E+003	6.5067E+001	2.1880E+000
TwrBsMzt	Minimum	LC_33	1.7520E+003	-1.0740E+003	2.0550E+003	-1.5270E+004	1.1970E+005	2.1060E+005	2.4224E+005	-1.6776E+004	2.5513E+003	5.4851E+001	-1.2150E+000
TwrBsMzt	Maximum	LC_4	1.5855E+003	1.5120E+003	2.1909E+003	-1.5270E+004	-1.6730E+005	1.9750E+005	2.5883E+005	1.5940E+004	1.2408E+003	6.8408E+001	-3.2220E+000

Table F-7. Mudline Reaction 50-Year Extreme Loads

Parameter	Type	File Name	ReactFXss [N]	ReactFYss [N]	ReactFZss [N]	ReactMXss [Nm]	ReactMYss [Nm]	ReactMZss [Nm]	HorWindV [m/s]	WindVxi [m/s]	Time [s]	Wave1Elev [m]
ReactFXss	Minimum	LC_9	-9.1000E+006	-9.9796E+004	2.0566E+007	4.8488E+006	-2.6520E+008	8.7380E+006	4.4762E+001	4.4730E+001	1.4856E+003	8.0450E+000
ReactFXss	Maximum	LC_1	4.0727E+006	1.2140E+005	2.2550E+007	-8.3890E+006	5.0290E+006	-5.2490E+006	3.8426E+001	3.8409E+001	1.4889E+003	-4.7210E+000
ReactFYss	Minimum	LC_1	-1.3554E+006	-1.7272E+006	2.3050E+007	2.4181E+008	-2.6183E+008	-1.7750E+007	6.8408E+001	6.8375E+001	1.2408E+003	-3.2220E+000
ReactFYss	Maximum	LC_48	-4.4149E+006	1.6644E+006	2.1440E+007	-2.5129E+008	-2.1982E+008	1.0560E+007	5.1693E+001	5.1234E+001	1.5200E+003	2.1760E+000
ReactFZss	Minimum	LC_8	-8.8993E+006	-1.6790E+005	2.0409E+007	1.9152E+007	-2.3980E+008	5.7060E+006	4.4762E+001	4.4730E+001	1.4856E+003	8.0450E+000
ReactFZss	Maximum	LC_9	2.7560E+005	1.1960E+004	2.3921E+007	1.0470E+007	-1.2520E+008	2.4802E+005	3.8906E+001	3.8610E+001	1.4915E+003	-6.4050E+000
ReactMXss	Minimum	LC_45	-4.4149E+006	1.6644E+006	2.1440E+007	-2.5129E+008	-2.1982E+008	1.0560E+007	5.1693E+001	5.1234E+001	1.5200E+003	2.1760E+000
ReactMXss	Maximum	LC_4	-1.3554E+006	-1.7272E+006	2.3050E+007	2.4181E+008	-2.6183E+008	-1.7750E+007	6.8408E+001	6.8375E+001	1.2408E+003	-3.2220E+000
ReactMYss	Minimum	LC_25	-3.5310E+006	-1.1886E+006	2.1642E+007	1.6560E+008	-4.1707E+008	-1.2563E+007	6.5067E+001	6.5062E+001	3.9835E+003	2.1880E+000
ReactMYss	Maximum	LC_68	2.7850E+006	1.1930E+005	2.2560E+007	-2.5900E+007	6.7816E+007	-2.7378E+006	4.0994E+001	4.0990E+001	1.1932E+003	-3.4450E+000
ReactMZss	Minimum	LC_28	-3.2105E+006	-8.2217E+005	2.2470E+007	1.5339E+008	-3.7002E+008	-1.8367E+007	5.8406E+001	5.8380E+001	3.9782E+003	-2.2900E+000
ReactMZss	Maximum	LC_36	-5.2140E+006	5.7190E+005	2.1687E+007	-9.2070E+007	-3.2895E+008	1.8316E+007	5.8858E+001	5.8730E+001	1.9497E+003	3.7190E+000
HorWindV	Minimum	LC_13	-6.1120E+005	-3.5878E+005	2.2250E+007	3.7559E+007	-7.9550E+007	-4.0560E+006	1.9652E+001	1.9636E+001	3.4147E+003	-1.2290E+000
HorWindV	Maximum	LC_25	-1.4690E+006	-7.1800E+005	2.1910E+007	1.0440E+008	-1.4750E+008	-7.4188E+006	8.0924E+001	8.0923E+001	1.1667E+003	-1.3840E-001

Table F-8. Correlation of Tower Base, Tower-Top and Mudline 50-Year Extreme Loads

Parameter	Type	File Name	ReactFXss [N]	ReactFYss [N]	ReactFZss [N]	ReactMXss [Nm]	ReactMYss [Nm]	ReactMZss [Nm]	TwrBsFxt [kN]	TwrBsFyt [kN]	TwrBsFzt [kN]	TwrBsMxt [kNm]	TwrBsMyt [kNm]	TwrBsMzt [kNm]	YawBrFxp [kN]	YawBrFyp [kN]	YawBrFzp [kN]	YawBrMxp [kNm]	YawBrMyp [kNm]	YawBrMzp [kNm]	WindV [m/s]	Time [s]	eIElev [m]
ReactFXss	Minimum	LC_9	-9100041.832	-39736.421	20555555.556	48948754.957	-26520000.000	87380000.000	884.800	-18.636	694.863	-15142.000	2.034	97360.000	-2465.000	214.700	-103.200	-87227.271	-6948.000	51420.811	-2464.000	44.762	1485.600	8.045
ReactFXss	Maximum	LC_1	4072662.692	124400.000	22550000.000	-83388960.923	51029000.000	-52490000.000	114.800	-52.530	126.066	-15200.447	2048.009	55510.000	55547.767	2547.000	-7.021	95.000	1461.059	84428.000	43208.000	2545.000	38.426	1488.900	-4.721
ReactFYss	Minimum	LC_1	-3355430.509	-1727155.331	23050000.000	24912054.610	-26783919.843	-11750000.000	1585.493	1512.000	2190.874	-15270.000	-167300.000	197500.000	258834.967	15340.141	932.216	1461.059	-8008.000	2314.706	51978.882	15330.080	68.408	1240.800	-3.222
ReactFYss	Maximum	LC_48	-4414945.225	1664436.047	24400000.000	-25123201045.455	-23898421.053	10500000.000	323.300	-8661.496	1903.725	-15760.000	176764.063	125500.000	216785.110	-34201.000	386.100	-1509.937	-9716.000	-2665.000	50520.000	-3415.000	51.693	1520.000	2.176
ReactFZss	Minimum	LC_8	-8893344.037	-1678895.166	20408641.304	19152491.259	-23398000.000	57060000.000	474.600	105.320	498.146	-14979.334	-3450.000	81660.000	82209.594	1111.000	104.400	67.380	-8572.972	-251.500	57893.882	1111.000	44.762	1485.600	8.045
ReactFZss	Maximum	LC_3	275800.000	11960.000	23320833.333	1047000.000	-25220000.000	2480108.284	882.000	52.070	883.985	-15352.815	-10080.000	106700.000	107173.194	-1915.000	329.900	-24.239	-8918.201	-7160.000	53760.000	-9415.000	51.693	1520.000	2.176
ReactMXss	Minimum	LC_45	-4414945.225	1664436.047	24400000.000	-25129232045.455	-21898421.053	10500000.000	323.300	-8661.496	1903.725	-15760.000	176764.063	125500.000	216785.110	-34201.000	386.100	-1509.937	-9716.000	-2665.000	50520.000	-3415.000	51.693	1520.000	2.176
ReactMXss	Maximum	LC_4	-1355430.509	-1727155.331	23050000.000	24812054.610	-26783919.843	-11750000.000	1585.493	1512.000	2190.874	-15270.000	-167300.000	197500.000	258834.967	15340.141	932.216	1461.059	-8008.000	2314.706	51978.882	15330.080	68.408	1240.800	-3.222
ReactMYss	Minimum	LC_25	-3531000.000	-1185561.624	21642175.926	1655000.000	-41706729.630	-12562903.226	2535.000	1057.000	2746.539	-15117.083	-11440.000	288077.823	309961.537	13676.100	1502.000	1035.000	-8948.316	3784.000	55360.000	19866.100	65.067	3383.500	2.188
ReactMYss	Maximum	LC_68	2765000.000	115300.000	22555555.111	-2530000.000	67815576.072	-2737823.938	-497.128	-153.600	522.119	-15200.000	9100.000	29304.231	20304.231	303.708	-460.707	-53.702	-8793.000	269.078	46560.000	304.174	40.934	1193.200	-3.445
ReactMZss	Minimum	LC_28	-3210481.451	-822193.401	22470000.000	15338678.453	-37009896.541	-18366920.426	2271.912	1008.000	2485.487	-15230.000	-112800.000	251500.000	275837.606	14820.000	1173.000	1064.000	-8793.000	4365.000	60370.000	14810.000	58.406	3378.200	-2.230
ReactMZss	Maximum	LC_36	-5234000.000	571900.000	21688805.556	-3207000.000	-32829450.000	18315918.453	1645.393	-578.914	1744.236	-15400.000	67448.393	197500.000	208839.627	-33894.693	870.969	-794.242	-8941.000	-4556.000	55220.000	-13875.186	58.858	1943.700	3.719
TwrBsFxt	Minimum	LC_45	-4414945.225	1664436.047	24400000.000	-25129232045.455	-21898421.053	10500000.000	323.300	-8661.496	1903.725	-15760.000	176764.063	125500.000	216785.110	-34201.000	386.100	-1509.937	-9716.000	-2665.000	50520.000	-3415.000	51.693	1520.000	2.176
TwrBsFxt	Maximum	LC_4	-1355430.509	-1727155.331	23050000.000	24812054.610	-26783919.843	-11750000.000	1585.493	1512.000	2190.874	-15270.000	-167300.000	197500.000	258834.967	15340.141	932.216	1461.059	-8008.000	2314.706	51978.882	15330.080	68.408	1240.800	-3.222
TwrBsFyt	Minimum	LC_25	-3531000.000	-1185561.624	21642175.926	1655000.000	-41706729.630	-12562903.226	2535.000	1057.000	2746.539	-15117.083	-11440.000	288077.823	309961.537	13676.100	1502.000	1035.000	-8948.316	3784.000	55360.000	19866.100	65.067	3383.500	2.188
TwrBsFyt	Maximum	LC_45	-4414945.225	1664436.047	24400000.000	-25123201045.455	-21898421.053	10500000.000	323.300	-1661.496	1903.725	-15760.000	176764.063	125500.000	216785.110	-34201.000	386.100	-1509.937	-9716.000	-2665.000	50520.000	-3415.000	51.693	1520.000	2.176
TwrBsFyt	Maximum	LC_57	-5587000.000	1109000.000	20753076.923	-1723000.000	-27824362.449	-15764937.260	1734.000	1500.000	2338.469	-15240.000	-163265.441	194700.000	257537.593	15090.000	744.800	1480.000	-8772.000	2930.000	55300.000	15080.000	61.426	1240.600	-3.567
TwrBsFyt	Maximum	LC_25	-2121056.075	-1622594.783	21980000.000	23459312.397	-20680000.000	-8477000.000	1200.000	1533.397	1894.721	-15760.000	-161238.782	137400.000	211941.226	8669.667	380.349	1319.406	-8706.000	3919.631	54550.000	8665.578	48.239	2782.300	-10.776
TwrBsFyt	Minimum	LC_56	-2539864.286	507786.678	21630000.000	-4697000.000	-8065000.000	3820000.000	-0.149	0.963	0.374	-15540.000	562.200	19500.000	19508.103	-1753.000	-440.730	5.467	-8779.000	168.000	50830.000	-1759.000	42.393	1674.200	0.540
TwrBsFt	Maximum	LC_25	-3531000.000	-1185561.624	21642175.926	1655000.000	-41706729.630	-12562903.226	2535.000	1057.000	2746.539	-15117.083	-11440.000	288077.823	309961.537	13676.100	1502.000	1035.000	-8948.316	3784.000	55360.000	19866.100	65.067	3383.500	2.188
TwrBsFzt	Minimum	LC_21	-886211.603	1317021.953	22780769.231	-1850000.000	-13340000.000	11517962.963	822.800	-1040.000	1488.153	-15940.000	128800.000	98806.349	160828.304	-11212.386	46.610	-1079.000	-9497.097	-4904.615	53458.504	-11211.135	66.861	3193.300	0.144
TwrBsFzt	Maximum	LC_57	-5587000.000	1109000.000	20753076.923	-1723000.000	-27824362.449	-15764937.260	1734.000	1500.000	2338.469	-15240.000	-163265.441	194700.000	257537.593	15090.000	744.800	1480.000	-8772.000	2930.000	55300.000	15080.000	61.426	1240.600	-3.567
TwrBsMxt	Minimum	LC_4	-1652530.352	-1276103.228	23050000.000	23020000.000	-25123201045.455	-21898421.053	1734.000	1500.000	2338.469	-15240.000	-163265.441	194700.000	257537.593	15090.000	744.800	1480.000	-8772.000	2930.000	55300.000	15080.000	61.426	1240.600	-3.567
TwrBsMxt	Maximum	LC_45	-4414945.225	1664436.047	24400000.000	-25123201045.455	-21898421.053	10500000.000	323.300	-8661.496	1903.725	-15760.000	176764.063	125500.000	216785.110	-34201.000	386.100	-1509.937	-9716.000	-2665.000	50520.000	-3415.000	51.693	1520.000	2.176
TwrBsMyt	Minimum	LC_29	-588830.253	-51251.186	22030000.000	5398000.000	45074799.383	-6462000.000	-534.200	84.540	540.848	-14940.000	-1120.000	-37031.475	37048.408	-972.900	-829.409	-35.533	-8515.000	177.800	47540.000	-972.100	50.896	2907.100	-1.525
TwrBsMyt	Maximum	LC_28	-3531000.000	-1185561.624	21642175.926	1655000.000	-41706729.630	-12562903.226	2535.000	1057.000	2746.539	-15117.083	-11440.000	288077.823	309961.537	13676.100	1502.000	1035.000	-8948.316	3784.000	55360.000	19866.100	65.067	3383.500	2.188
TwrBsM	Minimum	LC_28	-2302885.246	4695.000	22044431.818	5843000.000	-31910000.000	-19082227.334	-130.228	15.090	131.093	-15080.000	473.358	234.700	528.886	918.200	-611.500	106.400	-8658.570	6236.000	45700.000	916.400	47.693	3398.600	-1.653
TwrBsM	Maximum	LC_28	-3531000.000	-1185561.624	21642175.926	1655000.000	-41706729.630	-12562903.226	2535.000	1057.000	2746.539	-15117.083	-11440.000	288077.823	309961.537	13676.100	1502.000	1035.000	-8948.316	3784.000	55360.000	19866.100	65.067	3383.500	2.188
TwrBsMzt	Minimum	LC_33	-1068000.000	1034311.404	22200000.000	-1683000.000	-28130000.000	15830000.000	1752.000	-1074.000	2054.989	-15270.000	119700.000	210600.000	242240.480	-16775.513	1004.000	-1086.000	-8797.000	-2999.663	52220.000	-16765.513	54.851	2551.300	-3.125
TwrBsMzt	Maximum	LC_4	-1355430.509	-1727155.331	23050000.000	24812054.610	-26783919.843	-11750000.000	1585.493	1512.000	2190.874	-15270.000	-167300.000	197500.000	258834.967	15340.141	932.216	1461.059	-8008.000	2314.706	51978.882	15330.080	68.408	1240.800	-3.222
YawBrFxp	Minimum	LC_32	-588830.253	-51251.186	22030000.000	5398000.000	45074799.383	-6462000.000	-534.200	84.540	540.848	-14940.000	-1120.000	-37031.475	37048.408	-972.900	-829.409	-35.533	-8515.000	177.800	47540.000	-972.100	50.896	2907.100	-1.525
YawBrFxp	Maximum	LC_25	-3476000.000	-585500.000	21659903.846	9558000.000	-39990000.000	-5764000.000	2324.000	620.900	2405.513	-15379.583	-68270.000	282700.000	290826.551	6117.699	1595.175	675.400	-8905.956	5426.000	58490.000	6113.601	58.457	1557.900	2.312
YawBrFyp	Minimum	LC_48	-4122055.046	1480000.000	21670000.000	-23930000.000	-20840000.000	10012601.463	789.700	-516.000	1709.351	-15270.000	172100.000	124700.000	212528.822	-9852.000	462.300	-1566.240	-8878.000	-3369.000	54630.000	-9844.000	46.761	1519.700	1.153
YawBrFyp	Maximum	LC_4	-1752000.000	-1345000.000	22741833.333	23160000.000	-27460000.000	-16306500.000	1846.846	1472.000	2361.543	-14965.593	-167500.000	192000.000	254794.525	14370.000	643.700	1538.667	-8513.812	3033.000	55420.000	14360.000	65.491	1240.500	-3.778
YawBrFzp	Minimum	LC_21	-886211.603	1317021.953	22780769.231	-1850000.000	-13340000.000	11517962.963	822.800	-1040.000	1488.153	-15940.000	128800.000	98806.349	160828.304	-11212.386	46.610	-1079.000	-9497.097	-4904.615	53458.504	-11211.135	66.861	3193.300	0.144
YawBrFzp	Maximum	LC_60	-5587000.000	1109000.000	20753076.923	-2150000.000	-17220000.000	20920000.000	432.800	-166.600	520.010	-14728.512	16080.000	74680.000	76391.549	-1793.000	78.450	-223.357	-8311.446	-5353.000	43950.000	-1792.000	39.322	1009.300	1.849
YawBrMxp	Minimum	LC_36	-3556000.000	-773900.000	22761038.384	12540000.000	-23510000.000	-12846398.850	1415.000	818.023	1634.438	-15321.423	-88779.277	197300.000	216876.733	3370.962	1025.000	598.600	-8845.290	-9667.171	60742.676	3363.865	48.340	2371.300	-3.496
YawBrMxp	Maximum	LC_28	-733927.346	3908867.347	22552083.333	-7583000.000	-17839000.000	4858000.000	935.500	-394.677	1070.883	-15121.023	53800.000	136400.000	148231.039	-5708.000	532.900	-433.800	-8662.641	30039.001	54930.000	-5707.000	43.493	2096.300	-2.911
YawBrMyp	Minimum	LC_49	-3678000.000	-272893.344	21679350.000	33325333.655	-44980000.000	-17410000.000	241.400	236.200	337.734	-14960.785	-20560.000	31120.883	37299.106	2208.000	-366.300	245.000	-8551.240	4938.777	38213.017	2207.000	46.914	3347.000	0.547
YawBrMyp	Maximum	LC_25	-5638000.000	-893100.000	21602250.000	11960467.049	-33330000.000	-10279004.587	1432.000	793.529	1652.123	-15523.224	-78591.418	203355.357	223620.832	12786.962	1014.000	724.700	-9060.323	6245.000	67751.125	12786.962	61.665	3371.700	3.556
YawBrMzp	Minimum	LC_33	-1068000.000	1034311.404	22200000.000	-1683000.000	-28130000.000	15830000.000	1752.000	-1074.000	2054.989	-15270.000	119700.000	210600.000	242240.480	-16775.513	1004.000	-1086.000	-8797.000	-2999.663	52220.000	-16765.513	54.851	2551.300	-1.125
YawBrMzp	Maximum	LC_1	-1355430.509	-1727155.331	23050000.000	24812054.610	-26783919.843	-11750000.000	1585.493	1512.000	2190.874	-15270.000	-167300.000	197500.000	258834.967	15340.141	932.216	1461.059	-8008.000	2314.706	51978.882	15330.080	68.408	1240.800	-3.222

Table F-9. Maximum/Minimum 50-Year Stress Levels for Selected Critical Members

Parameter	Type	File Name	ReactFXss [N]	ReactFYss [N]	ReactFZss [N]	ReactMXss [Nm]	ReactMYss [Nm]	ReactMZss [Nm]	AxialStress26 [N/mm^2]	AxialStress24 [N/mm^2]	AxialStress25 [N/mm^2]	AxialStress70 [N/mm^2]	AxialStress66 [N/mm^2]	AxialStress68 [N/mm^2]	AxialStress75 [N/mm^2]	AxialStress77 [N/mm^2]	AxialStress73 [N/mm^2]	HorWindV [m/s]	Time [s]	Wave1Elev [m]
ReactFXss	Minimum	LC_9	-9.1000E+006	-9.9796E+004	2.0566E+007	4.8488E+006	-2.6520E+008	8.7380E+006	14.8868	-46.2930	-14.4122	-6.4786	-5.8244	-38.4354	-37.8976	-5.9457	-5.3021	4.4762E+001	1.4856E+003	8.0450E+000
ReactFXss	Maximum	LC_1	4.0727E+006	1.2140E+005	2.2550E+007	8.3890E+006	5.0290E+006	-5.2490E+006	-15.8624	-19.2008	-16.1149	-10.9471	-31.4221	-4.9571	-4.4253	-10.4090	-30.8787	3.8436E+001	1.4889E+003	-4.7210E+000
ReactFYss	Minimum	LC_1	-1.3554E+006	-1.7272E+006	2.3050E+007	2.4181E+008	-2.6183E+008	-1.7750E+007	33.9187	-36.0322	-53.3282	15.3829	-22.2477	-32.1818	-31.6490	15.9256	-21.7095	6.8408E+001	1.2408E+003	-3.2220E+000
ReactFYss	Maximum	LC_48	-4.4149E+006	1.6644E+006	2.1440E+007	-2.5129E+008	-2.1982E+008	1.0560E+007	-8.5551	-60.5773	23.5392	-14.0289	-34.6931	-5.6134	-5.0779	-13.4947	-34.1655	5.1693E+001	1.5200E+003	2.1760E+000
ReactFZss	Minimum	LC_8	-8.8993E+006	-1.6790E+005	2.0409E+007	1.9152E+007	-2.3980E+008	5.7060E+006	12.5804	-42.1449	-16.8649	-7.0325	-2.9402	-38.5496	-38.0115	-6.5049	-2.4179	4.4762E+001	1.4856E+003	8.0450E+000
ReactFZss	Maximum	LC_9	2.7560E+005	1.1960E+004	2.3921E+007	1.0470E+007	-1.2520E+008	2.4802E+005	0.2543	-33.3177	-18.2484	-4.8252	-28.9584	-15.2591	-14.7155	-4.2839	-28.4150	3.8906E+001	1.4915E+003	-6.4050E+000
ReactMXss	Minimum	LC_45	-4.4149E+006	1.6644E+006	2.1440E+007	-2.5129E+008	-2.1982E+008	1.0560E+007	-8.5551	-60.5773	23.5392	-14.0289	-34.6931	-5.6134	-5.0779	-13.4947	-34.1655	5.1693E+001	1.5200E+003	2.1760E+000
ReactMXss	Maximum	LC_4	-1.3554E+006	-1.7272E+006	2.3050E+007	2.4181E+008	-2.6183E+008	-1.7750E+007	33.9187	-36.0322	-53.3282	15.3829	-22.2477	-32.1818	-31.6490	15.9256	-21.7095	6.8408E+001	1.2408E+003	-3.2220E+000
ReactMYss	Minimum	LC_25	-3.5310E+006	-1.1886E+006	2.1642E+007	1.6560E+008	-4.1707E+008	-1.2563E+007	48.3316	-60.5625	-40.5188	22.0419	-31.8758	-31.1161	-30.5833	22.5748	-31.3430	6.5067E+001	1.9835E+003	2.1880E+000
ReactMYss	Maximum	LC_68	2.7850E+006	1.1930E+005	2.2560E+007	2.5900E+007	6.7816E+007	-2.7378E+006	-25.9546	-11.1833	-13.3038	-19.2658	-21.8203	-7.0136	-6.4808	-18.7277	-21.2822	4.0994E+001	1.1932E+003	-3.4450E+000
ReactMZss	Minimum	LC_28	-3.2105E+006	-8.2217E+005	2.2470E+007	1.5339E+008	-3.7002E+008	-1.8367E+007	40.3529	-55.6047	-39.9215	20.0632	-29.2696	-30.3292	-29.7865	20.5961	-28.7368	5.8406E+001	3.9782E+003	-2.2900E+000
ReactMZss	Maximum	LC_36	-5.2140E+006	5.7190E+005	2.1687E+007	-9.2070E+007	-3.2895E+008	1.8316E+007	18.1999	-63.1177	0.6026	-2.3266	-34.6086	-21.2909	-20.7571	-1.7953	-34.0811	5.0839E+001	1.9497E+003	3.7190E+000
AxialStress26	Minimum	LC_36	1.1669E+006	1.1480E+006	2.2290E+007	-1.8240E+008	4.8362E+007	5.4006E+006	-35.8816	-23.0330	11.1734	-26.5384	-25.7507	0.4557	0.9889	-26.0003	-25.2126	4.4752E+001	1.5608E+003	-1.0350E+000
AxialStress26	Maximum	LC_28	-3.5310E+006	-1.1886E+006	2.1642E+007	1.6560E+008	-4.1707E+008	-1.2563E+007	48.3316	-60.5625	-40.5188	22.0419	-31.8758	-31.1161	-30.5833	22.5748	-31.3430	6.5067E+001	3.9835E+003	2.1880E+000
AxialStress24	Minimum	LC_21	-6.2833E+006	1.2484E+006	2.1450E+007	-1.8421E+008	-4.0527E+008	1.0411E+007	19.9508	-79.8033	14.3182	1.4415	-42.3103	-13.5586	-13.0204	1.9732	-41.7826	6.7637E+001	2.7245E+003	3.2980E+000
AxialStress24	Maximum	LC_4	-2.2820E+005	-6.6193E+005	2.1680E+007	7.4405E+007	5.1605E+007	1.4500E+005	-17.3690	-4.0952	-27.4633	-18.5677	-7.5478	-21.8784	-21.3455	-18.0348	-7.0138	5.0639E+001	4.2624E+003	1.1280E+000
AxialStress25	Minimum	LC_1	-1.5410E+006	-1.5580E+006	2.3100E+007	2.4000E+008	-2.6590E+008	-1.6720E+007	34.3132	-36.5366	-53.3282	15.8219	-21.7992	-33.4058	-32.8677	16.3600	-21.2611	6.5035E+001	1.2407E+003	-3.3560E+000
AxialStress25	Maximum	LC_48	-4.4149E+006	1.6644E+006	2.1440E+007	-2.5129E+008	-2.1982E+008	1.0560E+007	-8.5551	-60.5773	23.5392	-14.0289	-34.6931	-5.6134	-5.0779	-13.4947	-34.1655	5.1693E+001	1.5200E+003	2.1760E+000
AxialStress70	Minimum	LC_36	-3.5240E+006	1.4719E+006	2.1511E+007	2.3801E+008	-4.7278E+007	1.2858E+007	-29.5429	-36.6064	21.0393	-27.3956	-21.6354	-6.2306	-5.6978	-26.8628	-21.1075	7.0803E+001	1.5551E+003	1.4560E+000
AxialStress70	Maximum	LC_28	-3.5848E+006	-9.2684E+005	2.1850E+007	1.6880E+008	-4.1460E+008	-1.1440E+007	48.1513	-59.9984	-41.2157	22.7295	-31.8017	-32.5457	-32.0077	23.3624	-31.2689	6.4999E+001	3.9836E+003	2.1720E+000
AxialStress66	Minimum	LC_33	8.2684E+005	1.2359E+006	2.2480E+007	-1.5643E+008	-2.7950E+008	6.2780E+006	9.1451	-65.3411	8.3379	1.6882	-55.6491	-0.0896	0.4440	2.2216	-55.0731	6.2397E+001	2.4999E+003	-1.7850E+000
AxialStress66	Maximum	LC_8	-6.6083E+006	-2.6859E+005	2.0646E+007	2.8835E+007	8.4510E+007	5.1502E+006	-5.9932	-21.8656	-19.2081	-16.5921	1.9700	-34.5989	-34.0664	-16.0645	2.4933	4.6198E+001	1.4726E+003	7.6460E+000
AxialStress68	Minimum	LC_13	-8.0628E+006	-1.3109E+006	2.0980E+007	1.7198E+008	-2.9380E+008	5.6930E+005	31.1697	-39.7224	-40.2879	4.0515	-4.8183	-46.5948	-46.0576	4.5844	-4.2960	5.2465E+001	3.1446E+003	6.0360E+000
AxialStress68	Maximum	LC_60	1.5950E+006	1.2370E+006	2.2090E+007	-1.7970E+008	-1.1930E+008	4.4650E+006	-13.2940	-45.7952	11.3658	-11.6496	-43.2696	3.4354	3.9676	-11.1161	-42.7315	4.4876E+001	4.1794E+003	-3.7220E-001
AxialStress75	Minimum	LC_16	-8.0628E+006	-1.3109E+006	2.0980E+007	1.7198E+008	-2.9380E+008	5.6930E+005	31.1697	-39.7224	-40.2879	4.0515	-4.8183	-46.5948	-46.0576	4.5844	-4.2960	5.2465E+001	3.1446E+003	6.0360E+000
AxialStress75	Maximum	LC_60	1.5950E+006	1.2370E+006	2.2090E+007	-1.7970E+008	-1.1930E+008	4.4650E+006	-13.2940	-45.7952	11.3658	-11.6496	-43.2696	3.4354	3.9676	-11.1161	-42.7315	4.4876E+001	4.1794E+003	-3.7220E-001
AxialStress77	Minimum	LC_33	-3.5240E+006	1.4719E+006	2.1511E+007	-2.3801E+008	-4.7278E+007	1.2858E+007	-29.5429	-36.6064	21.0393	-27.3956	-21.6354	-6.2306	-5.6978	-26.8628	-21.1075	7.0803E+001	1.5551E+003	1.4560E+000
AxialStress77	Maximum	LC_25	-3.5848E+006	-9.2684E+005	2.1850E+007	1.6880E+008	-4.1460E+008	-1.1440E+007	48.1513	-59.9984	-41.2157	22.7295	-31.8017	-32.5457	-32.0077	23.2624	-31.2689	6.4999E+001	3.9836E+003	2.1720E+000
AxialStress73	Minimum	LC_33	8.2684E+005	1.2359E+006	2.2480E+007	-1.5643E+008	-2.7950E+008	6.2780E+006	9.1451	-65.3411	8.3379	1.6882	-55.6491	-0.0896	0.4440	2.2216	-55.0731	6.2397E+001	2.4999E+003	-1.7850E+000
AxialStress73	Maximum	LC_8	-6.6083E+006	-2.6859E+005	2.0646E+007	2.8835E+007	8.4510E+007	5.1502E+006	-5.9932	-21.8656	-19.2081	-16.5921	1.9700	-34.5989	-34.0664	-16.0645	2.4933	4.6198E+001	1.4726E+003	7.6460E+000

Extreme load/deflection tables for the 100-year extreme load case:

Table F-10. Extreme 100-Year Tower-Top Displacements

Parameter	Type	File Name	TTDspFA [m]	TTDspSS [m]	Time [s]	HorWindV [m/s]	Wave1Elev [m]
TTDspFA	Minimum	LC_56	- 1.9918E-001	1.3590E-001	2.5190E+003	3.1007E+001	2.1120E+000
TTDspFA	Maximum	LC_29	1.8825E+000	- 8.4480E-002	1.5579E+003	6.6626E+001	2.2350E+000
TTDspSS	Minimum	LC_33	6.7820E-001	- 1.1990E+000	3.7058E+003	7.1469E+001	- 3.5740E+000
TTDspSS	Maximum	LC_40	8.8130E-001	1.1370E+000	4.4213E+003	6.9546E+001	- 2.6640E+000

Table F-11. Blade 1 Extreme 100-Year Out-of-Plane Deflections (edgewise)

Parameter	Type	File Name	OoPDefl1 [m]	Time [s]	HorWindV [m/s]	Wave1Elev [m]
OoPDefl1	Minimum	LC_60	- 1.0183E+000	1.5752E+003	6.8696E+001	- 2.2260E+000
OoPDefl1	Maximum	LC_72	5.6287E-001	2.4145E+003	6.4659E+001	2.9140E+000

Table F-12. Blade 1 In-Plane 100-Year Extreme Deflections (flapwise)

Parameter	Type	File Name	IPDefl1 m	Time s	HorWindV (m/s)	Wave1Elev m
IPDefl1	Minimum	LC_33	- 1.2890E+001	4.4033E+003	7.0019E+001	8.2240E-001
IPDefl1	Maximum	LC_45	8.5703E+000	1.4062E+003	7.3878E+001	1.2920E+000

Table F-13. Blade 1 100-Year Extreme Loads (at blade root)

Parameter	Type	File Name	RootFxc1 kN	RootFyc1 kN	RootFzc1 kN	RootF1 (kN)	RootM1 (kNm)	RootMxc1 kN-m	RootMyc1 kN-m	RootMzc1 kN-m	Time s	HorWindV (m/s)	Wave1Elev m
RootFxc1	Minimum	LC_69	- 2.4122E+002	- 9.0360E+002	- 5.1783E+002	9.3524E+002	4.0874E+004	3.8682E+004	- 1.3205E+004	2.7912E+002	2.7593E+003	6.5147E+001	- 1.8330E+000
RootFxc1	Maximum	LC_32	2.1862E+002	- 8.2080E+002	- 2.5112E+002	8.4942E+002	3.5693E+004	3.5170E+004	6.0870E+003	2.7550E+001	1.5574E+003	7.5436E+001	2.7890E+000
RootFyc1	Minimum	LC_60	- 8.1200E+001	- 1.4268E+003	- 3.4149E+002	1.4291E+003	5.8696E+004	5.8340E+004	- 6.4560E+003	4.4740E+002	3.4114E+003	8.4452E+001	- 9.1190E-001
RootFyc1	Maximum	LC_36	- 6.2400E+001	1.4330E+003	- 3.5570E+001	1.4344E+003	5.4284E+004	- 5.3810E+004	- 7.1570E+003	- 5.0160E+002	3.9813E+003	8.2020E+001	1.9150E+000
RootFzc1	Minimum	LC_45	- 5.4040E+001	- 7.1810E+002	- 6.8341E+002	7.2013E+002	4.5303E+004	4.4692E+004	- 7.4212E+003	1.2773E+002	4.3216E+003	6.7101E+001	- 4.7850E-001
RootFzc1	Maximum	LC_9	- 5.8440E+001	1.0851E+002	6.4779E+002	1.2325E+002	8.0878E+003	- 6.7310E+003	- 4.4840E+003	- 1.6580E+002	1.8050E+003	4.6990E+001	1.5760E+000
RootF1	Minimum	LC_32	5.6370E-002	- 1.0706E-001	6.1434E+002	1.2100E-001	4.4308E+003	3.9767E+003	- 1.9540E+003	- 1.3470E+002	1.9856E+003	5.7017E+001	1.1780E+000
RootF1	Maximum	LC_36	- 6.2400E+001	1.4330E+003	- 3.5570E+001	1.4344E+003	5.4284E+004	- 5.3810E+004	- 7.1570E+003	- 5.0160E+002	3.9813E+003	8.2020E+001	1.9150E+000
RootM1	Minimum	LC_37	4.3190E+001	- 1.2560E+002	- 4.0760E+002	1.3282E+002	4.3186E+001	3.4100E+001	- 2.6500E+001	- 3.5540E+002	3.0558E+003	6.2417E+001	2.3210E+000
RootM1	Maximum	LC_9	- 4.5970E+000	- 1.1870E+003	- 5.5819E+002	1.1870E+003	6.2114E+004	6.1957E+004	- 4.4090E+003	3.9630E+002	3.1293E+003	8.2422E+001	- 2.6710E+000
RootMxc1	Minimum	LC_52	- 3.8770E+001	1.3340E+003	- 5.3410E+002	1.3346E+003	5.4905E+004	- 5.4552E+004	- 6.2180E+003	- 3.8692E+002	1.2118E+003	6.9917E+001	- 2.9400E+000
RootMxc1	Maximum	LC_12	- 4.5980E+000	- 1.1870E+003	- 5.5819E+002	1.1870E+003	6.2114E+004	6.1957E+004	- 4.4090E+003	3.9630E+002	3.1293E+003	8.2422E+001	- 2.6710E+000
RootMyc1	Minimum	LC_69	- 2.1906E+002	1.1384E+003	2.6420E+002	1.1593E+003	4.6933E+004	- 4.4800E+004	- 1.3987E+004	- 8.7257E+001	2.4111E+003	7.5274E+001	- 1.8070E+000
RootMyc1	Maximum	LC_57	1.4937E+002	4.9060E+002	- 4.3616E+002	5.1284E+002	1.6289E+004	- 1.4218E+004	7.9477E+003	- 1.9893E+002	1.8184E+003	4.7666E+001	- 3.2100E-001
RootMzc1	Minimum	LC_52	7.6450E+001	1.0735E+003	- 5.7580E+002	1.0762E+003	4.3263E+004	- 4.3260E+004	- 5.2300E+002	- 7.9282E+002	1.4454E+003	7.3630E+001	8.8710E-001
RootMzc1	Maximum	LC_49	- 7.6250E+001	- 1.0580E+003	5.3330E+002	1.0607E+003	4.9622E+004	4.9350E+004	- 5.1850E+003	7.8360E+002	1.1206E+003	6.1043E+001	1.5430E+000

Table F-14. Yaw Bearing 100-Year Extreme Loads

Parameter	Type	File Name	YawBrFxp kN	YawBrFyp kN	YawBrFzp kN	YawBrMxp kN·m	YawBrMyp kN·m	YawBrMzp kN·m	Time s	HorWindV (m/s)	Wave1Elev m
YawBrFxp	Minimum	LC_28	**-1.1196E+003**	7.9720E+001	-8.6360E+003	7.1370E+003	4.8570E+004	-1.7850E+003	2.9069E+003	4.8810E+001	-1.8120E+000
YawBrFxp	Maximum	LC_32	**2.0345E+003**	-1.5540E+002	-9.1690E+003	7.6170E+002	6.5900E+004	-4.1740E+003	1.5579E+003	6.6626E+001	2.2350E+000
YawBrFyp	Minimum	LC_33	3.0060E+002	**-2.1550E+003**	-9.1342E+003	-1.5480E+003	5.3700E+004	-1.3882E+004	3.7061E+003	7.0601E+001	-4.6750E+000
YawBrFyp	Maximum	LC_40	4.4020E+002	**2.0671E+003**	-9.0170E+003	1.2687E+003	5.5310E+004	1.9970E+004	4.4212E+003	6.3912E+001	-2.7640E+000
YawBrFzp	Minimum	LC_57	3.9940E+002	-9.6570E+002	**-9.7136E+003**	-4.5910E+003	5.7290E+004	-1.1990E+004	1.2100E+003	7.0901E+001	-2.9680E+000
YawBrFzp	Maximum	LC_9	8.9960E+001	-1.6730E+002	**-8.2196E+003**	-5.6883E+003	4.6080E+004	-3.4860E+003	3.8228E+003	4.4971E+001	2.5300E+000
YawBrMxp	Minimum	LC_12	4.8410E+002	4.2120E+002	-8.8284E+003	**-9.9244E+003**	6.2940E+004	3.8219E+003	1.1005E+003	5.4736E+001	3.5150E+000
YawBrMxp	Maximum	LC_28	4.0010E+002	-6.4280E+002	-8.9530E+003	**9.7324E+003**	5.8861E+004	-2.9020E+003	2.2197E+003	4.3213E+001	-1.2730E+000
YawBrMyp	Minimum	LC_36	-5.9670E+002	-2.7035E+002	-8.5270E+003	-4.7022E+003	**3.5257E+004**	1.7090E+003	2.9077E+003	5.1672E+001	-1.1390E+000
YawBrMyp	Maximum	LC_52	1.0870E+003	1.4660E+003	-9.2581E+003	5.2057E+003	**7.3419E+004**	1.6444E+004	3.4310E+003	6.4975E+001	-9.0110E-001
YawBrMzp	Minimum	LC_48	9.1880E+002	-1.0040E+003	-9.2070E+003	-3.3185E+003	5.6122E+004	**-2.0851E+004**	2.1277E+003	6.8966E+001	-5.8190E-001
YawBrMzp	Maximum	LC_37	2.2640E+002	1.9850E+003	-8.8460E+003	1.5610E+003	5.6120E+004	**2.0586E+004**	4.4210E+003	6.2772E+001	-2.7500E+000

Table F-15. Tower Base 100-Year Extreme Loads

Parameter	Type	File Name	TwrBsFxt kN	TwrBsFyt kN	TwrBsF (kN)	TwrBsFzt kN	TwrBsMxt kN·m	TwrBsMyt kN·m	TwrBsM (kNm)	TwrBsMzt kN·m	Time s	HorWindV (m/s)	Wave1Elev m
TwrBsFxt	Minimum	LC_56	**-1.1354E+003**	1.6370E+002	1.1471E+003	-1.5210E+004	-2.3560E+004	-7.8616E+004	8.2070E+004	1.8880E+002	2.5189E+003	3.0654E+001	2.1030E+000
TwrBsFxt	Maximum	LC_32	**3.2677E+003**	-3.2030E+002	3.2833E+003	-1.5352E+004	3.7940E+004	3.5150E+005	3.5354E+005	-5.7000E+001	3.9836E+003	7.4409E+001	2.0060E+000
TwrBsFyt	Minimum	LC_36	7.6723E+002	**-2.3460E+003**	2.4682E+003	-1.5390E+004	2.5282E+005	1.0990E+005	2.7567E+005	-1.2761E+004	3.7059E+003	7.2739E+001	-4.0010E+000
TwrBsFyt	Maximum	LC_37	1.3750E+003	**2.3113E+003**	2.6894E+003	-1.5298E+004	-2.4150E+005	1.5940E+005	2.8936E+005	1.6620E+004	4.4214E+003	6.7392E+001	-2.4540E+000
TwrBsF	Minimum	LC_44	9.4600E-001	-1.3251E+000	**1.6281E+000**	-1.5252E+004	-1.2540E+004	1.5760E+004	2.0140E+004	1.3485E+003	3.2981E+003	6.1637E+001	-1.9200E+000
TwrBsF	Maximum	LC_25	3.1090E+003	1.5489E+003	**3.4735E+003**	-1.5690E+004	-1.5621E+005	3.3280E+005	3.6764E+005	9.3480E+003	3.9830E+003	6.9633E+001	1.9270E+000
TwrBsFzt	Minimum	LC_60	1.2180E+003	-7.5590E+002	1.4335E+003	**-1.6190E+004**	9.1637E+004	1.4420E+005	1.7085E+005	-1.1990E+004	1.2100E+003	7.0901E+001	-2.9680E+000
TwrBsFzt	Maximum	LC_9	6.3582E+002	-1.8890E+002	6.6328E+002	**-1.4641E+004**	1.1200E+004	8.2528E+004	8.3285E+004	-3.4870E+003	3.8228E+003	4.4971E+001	2.5300E+000
TwrBsMxt	Minimum	LC_37	1.3750E+003	2.3113E+003	2.6894E+003	-1.5298E+004	**-2.4150E+005**	1.5940E+005	2.8936E+005	1.6620E+004	4.4214E+003	6.7392E+001	-2.4540E+000
TwrBsMxt	Maximum	LC_33	7.6723E+002	-2.3460E+003	2.4682E+003	-1.5390E+004	**2.5282E+005**	1.0990E+005	2.7567E+005	-1.2761E+004	3.7059E+003	7.2739E+001	-4.0010E+000
TwrBsMyt	Minimum	LC_53	-1.1354E+003	1.6370E+002	1.1471E+003	-1.5210E+004	-2.3560E+004	**-7.8616E+004**	8.2070E+004	1.8880E+002	2.5189E+003	3.0654E+001	2.1030E+000
TwrBsMyt	Maximum	LC_32	3.1187E+003	-1.2630E+002	3.1212E+003	-1.5581E+004	1.9100E+004	**3.5494E+005**	3.5545E+005	-7.2430E+002	1.5577E+003	6.9152E+001	2.5460E+000
TwrBsM	Minimum	LC_37	-2.6019E+002	5.7560E+001	2.6648E+002	-1.5432E+004	-3.0810E+002	6.6430E+002	**7.3227E+002**	7.7580E+003	2.0940E+003	7.4126E+001	2.7390E-002
TwrBsM	Maximum	LC_25	3.0340E+003	1.5487E+003	3.4064E+003	-1.5840E+004	-1.5768E+005	3.4718E+005	**3.8131E+005**	9.4220E+003	3.9835E+003	7.4506E+001	1.9970E+000
TwrBsMzt	Minimum	LC_48	1.8440E+003	-9.2520E+002	2.0631E+003	-1.5670E+004	1.0420E+005	2.0750E+005	2.3219E+005	**-2.0861E+004**	2.1277E+003	6.8966E+001	-5.8190E-001
TwrBsMzt	Maximum	LC_37	1.1970E+003	2.0350E+003	2.3609E+003	-1.5310E+004	-2.2590E+005	1.2980E+005	2.6054E+005	**2.0596E+004**	4.4210E+003	6.2772E+001	-2.7500E+000

Table F-16. Mudline Reaction 100-Year Extreme Loads

Parameter	Type	File Name	ReactFXss N	ReactFYss N	ReactFZss N	ReactMXss Nm	ReactMYss Nm	ReactMZss Nm	HorWindV (m/s)	WindVxi m/s	Time s	Wave1Elev m
ReactFXss	Minimum	LC_9	**-1.1373E+007**	-5.9230E+004	1.9978E+007	5.4180E+006	-3.5800E+008	6.0650E+006	5.1014E+001	5.0970E+001	1.4856E+003	9.6940E+000
ReactFXss	Maximum	LC_1	**5.4398E+006**	-2.6146E+005	2.2508E+007	6.0033E+007	6.2970E+007	-6.9610E+006	4.3040E+001	4.3020E+001	1.4889E+003	-6.1850E+000
ReactFYss	Minimum	LC_40	-2.5130E+006	**-2.4771E+006**	2.2145E+007	3.5062E+008	-2.3920E+008	-1.5724E+007	6.7392E+001	6.7360E+001	4.4214E+003	-2.4540E+000
ReactFYss	Maximum	LC_33	1.1318E+006	**2.4322E+006**	2.2790E+007	-3.5940E+008	-1.1176E+008	1.2058E+007	6.5151E+001	6.5066E+001	3.7060E+003	-4.4300E+000
ReactFZss	Minimum	LC_21	-9.2460E+006	2.6336E+005	**1.9976E+007**	-5.2953E+007	-2.7450E+008	6.8100E+006	5.4475E+001	5.4468E+001	2.2003E+003	7.8250E+000
ReactFZss	Maximum	LC_16	3.2630E+006	-1.5220E+005	**2.4173E+007**	3.9060E+007	-2.4530E+006	-7.1670E+006	4.8324E+001	4.7690E+001	2.1948E+003	-6.7780E+000
ReactMXss	Minimum	LC_36	9.8510E+005	2.3560E+006	2.2647E+007	**-3.6160E+008**	-1.1581E+008	1.0070E+007	7.2739E+001	7.2558E+001	3.7059E+003	-4.0010E+000
ReactMXss	Maximum	LC_37	-2.5130E+006	-2.4771E+006	2.2145E+007	**3.5062E+008**	-2.3920E+008	-1.5724E+007	6.7392E+001	6.7360E+001	4.4214E+003	-2.4540E+000
ReactMYss	Minimum	LC_21	-7.9570E+006	1.0820E+006	2.0900E+007	-1.6070E+008	**-5.2302E+008**	1.0263E+007	7.6742E+001	7.6640E+001	2.7245E+003	4.1310E+000
ReactMYss	Maximum	LC_56	-7.8913E+005	-2.8790E+005	2.1080E+007	3.3810E+007	**1.0855E+008**	3.0760E+005	3.0654E+001	2.8968E+001	2.5189E+003	2.1030E+000
ReactMZss	Minimum	LC_28	-4.1090E+006	-9.9590E+005	2.1860E+007	1.5510E+008	-4.3470E+008	**-2.3555E+007**	7.4397E+001	7.3660E+001	2.4941E+003	-1.0820E+000
ReactMZss	Maximum	LC_60	-7.7980E+006	6.0190E+005	2.0930E+007	-1.0900E+008	-3.5970E+008	**2.7249E+007**	6.2111E+001	6.1960E+001	3.0063E+003	4.2290E+000
HorWindV	Minimum	LC_24	-1.1480E+006	2.5300E+005	2.1970E+007	-2.1457E+007	-1.4511E+008	1.1140E+006	**2.0812E+001**	2.0796E+001	3.4147E+003	-1.3010E+000
HorWindV	Maximum	LC_25	-1.8660E+006	-1.4930E+006	2.1360E+007	2.2950E+008	-1.7330E+008	-1.3240E+007	**9.2952E+001**	9.2950E+001	1.1667E+003	5.5680E-001
WindVxi	Minimum	LC_36	-3.4329E+006	3.7030E+004	2.1020E+007	-1.1810E+007	-1.0497E+008	-1.5216E+006	2.2982E+001	**2.0062E+001**	3.3267E+003	1.6910E+000
WindVxi	Maximum	LC_36	-2.0040E+006	9.3480E+005	2.1380E+007	-1.3870E+008	-1.8820E+008	7.2224E+005	9.2952E+001	**9.2950E+001**	1.1667E+003	5.5680E-001

Table F-17. Maximum/Minimum 100-Year Stress Levels for Selected Critical Members

Parameter	Type	File Name	ReactFXss N	ReactFYss N	ReactFZss N	ReactMXss Nm	ReactMYss Nm	ReactMZss Nm	AxialStress26 (N/mm^2)	AxialStress24 (N/mm^2)	AxialStress25 (N/mm^2)	AxialStress70 (N/mm^2)	AxialStress66 (N/mm^2)	AxialStress68 (N/mm^2)	AxialStress75 (N/mm^2)	AxialStress77 (N/mm^2)	AxialStress73 (N/mm^2)	HorWindV (m/s)	Time s	Wave1Elev m
ReactFXss	Minimum	LC_9	-1.1373E+007	-5.9230E+004	1.9978E+007	5.4180E+006	-3.5800E+008	6.0650E+006	2.5934E+001	-5.7764E+001	-1.3991E+001	-1.1931E+000	-3.5077E+000	-4.4160E+001	-4.3622E+001	-6.6524E-001	-2.9890E+000	5.1014E+001	1.4856E+003	9.6940E+000
ReactFXss	Maximum	LC_1	5.4398E+006	-2.6146E+005	2.2508E+007	6.0033E+007	6.2970E+007	-6.9610E+006	-1.7479E+001	-7.3969E+000	-2.6906E+001	-1.0868E+001	-2.7824E+001	-7.4523E+000	-6.9247E+000	-1.0335E+001	-2.7281E+001	4.3040E+001	1.4889E+003	-6.1850E+000
ReactFYss	Minimum	LC_40	-2.5130E+006	-2.4771E+006	2.2145E+007	3.5062E+008	-2.3920E+008	-1.5724E+007	3.9225E+001	-2.4305E+001	-6.9524E+001	1.5199E+001	-1.0114E+001	-4.5134E+001	-4.4601E+001	1.5736E+001	-9.5754E+000	6.7392E+001	4.4214E+003	-2.4540E+000
ReactFYss	Maximum	LC_33	1.1318E+006	2.4322E+006	2.2790E+007	-3.5940E+008	-1.1176E+008	1.2058E+007	-2.8565E+001	-5.6912E+001	3.8528E+001	-2.0828E+001	-5.1156E+001	1.5547E+001	1.6080E+001	-2.0290E+001	-5.0618E+001	6.5151E+001	3.7060E+003	-4.4300E+000
ReactFZss	Minimum	LC_21	-9.2460E+006	2.6336E+005	1.9976E+007	-5.2953E+007	-2.7450E+008	6.8100E+006	1.1572E+001	-5.1370E+001	-5.4423E+000	-7.6076E+000	-1.0119E+001	-3.1612E+001	-3.1074E+001	-7.0747E+000	-9.6018E+000	5.4475E+001	2.2003E+003	7.8250E+000
ReactFZss	Maximum	LC_16	3.2630E+006	-1.5220E+005	2.4173E+007	3.9060E+007	-2.4530E+006	-7.1670E+006	-1.2617E+001	-1.6928E+001	-2.3873E+001	-9.0320E+000	-2.6452E+001	-9.5833E+000	-9.0446E+000	-8.4939E+000	-2.5909E+001	4.8324E+001	2.1948E+003	-6.7780E+000
ReactMXss	Minimum	LC_36	9.8510E+005	2.3560E+006	2.2647E+007	-3.6160E+008	-1.1581E+008	1.0070E+007	-2.8161E+001	-5.7478E+001	3.8941E+001	-2.0732E+001	-5.0394E+001	1.5368E+001	1.5906E+001	-2.0193E+001	-4.9855E+001	7.2739E+001	3.7059E+003	-4.0010E+000
ReactMXss	Maximum	LC_37	-2.5130E+006	-2.4771E+006	2.2145E+007	3.5062E+008	-2.3920E+008	-1.5724E+007	3.9225E+001	-2.4305E+001	-6.9524E+001	1.5199E+001	-1.0114E+001	-4.5134E+001	-4.4601E+001	1.5736E+001	-9.5754E+000	6.7392E+001	4.4214E+003	-2.4540E+000
ReactMYss	Minimum	LC_21	-7.9570E+006	1.0820E+006	2.0900E+007	-1.6070E+008	-5.2302E+008	1.0263E+007	3.6862E+001	-9.3137E+001	1.1515E+001	9.7671E+000	-4.4490E+001	-1.8971E+001	-1.8439E+001	1.0299E+001	-4.3962E+001	7.6742E+001	2.7245E+003	4.1310E+000
ReactMYss	Maximum	LC_56	-7.8913E+005	-2.8790E+005	2.1080E+007	3.3810E+007	1.0855E+008	3.0760E+005	-2.8232E+001	1.1899E+000	-2.1391E+001	-2.4305E+001	-3.9003E+000	-2.0520E+001	-1.9988E+001	-2.3772E+001	-3.3701E+000	3.0654E+001	2.5189E+003	2.1030E+000
ReactMZss	Minimum	LC_28	-4.1090E+006	-9.9590E+005	2.1860E+007	1.5510E+008	-4.3470E+008	-2.3555E+007	4.8151E+001	-6.4146E+001	-3.9988E+001	2.4802E+001	-3.3100E+001	2.9285E+001	-2.8747E+001	2.5339E+001	-3.2567E+001	7.4397E+001	2.4941E+003	-1.0820E+000
ReactMZss	Maximum	LC_60	-7.7980E+006	6.0190E+005	2.0930E+007	-1.0900E+008	-3.5970E+008	2.7249E+007	2.0571E+001	-6.6337E+001	4.4534E+000	-5.1164E+000	-2.9744E+001	-2.8260E+001	-2.7727E+001	-4.5856E+000	-2.9222E+001	6.2111E+001	3.0063E+003	4.2290E+000
AxialStress26	Minimum	LC_33	1.4302E+006	1.0368E+006	2.2029E+007	-1.8670E+008	9.5840E+007	1.3510E+007	-4.1387E+001	-1.6153E+001	1.2577E+001	-3.2468E+001	-2.3619E+001	1.4109E-001	6.7427E-001	-3.1929E+001	-2.3084E+001	4.8263E+001	1.5607E+003	-1.0820E+000
AxialStress26	Maximum	LC_25	-4.3260E+006	-1.7187E+006	2.2220E+007	2.3273E+008	-5.0375E+008	-7.9068E+006	6.4336E+001	-6.7066E+001	-5.0159E+001	2.8655E+001	-3.5198E+001	-3.8349E+001	-3.7816E+001	2.9193E+001	-3.4671E+001	7.4506E+001	3.9835E+003	1.9970E+000
AxialStress24	Minimum	LC_21	-7.9570E+006	1.0820E+006	2.0900E+007	-1.6070E+008	-5.2302E+008	1.0263E+007	3.6862E+001	-9.3137E+001	1.1515E+001	9.7671E+000	-4.4490E+001	-1.8971E+001	-1.8439E+001	1.0299E+001	-4.3962E+001	7.6742E+001	2.7245E+003	4.1310E+000
AxialStress24	Maximum	LC_37	7.0040E+005	-1.5062E+006	2.1965E+007	2.1930E+008	7.3617E+007	-5.6050E+006	8.8642E+000	8.3884E+000	-4.9943E+001	-1.2773E+001	-2.3907E+000	3.1443E+001	3.0905E+001	-1.2235E+001	-1.8576E+000	4.4501E+001	2.9192E+003	-2.0870E+000
AxialStress25	Minimum	LC_37	-2.5130E+006	-2.4771E+006	2.2145E+007	3.5062E+008	-2.3920E+008	-1.5724E+007	3.9225E+001	-2.4305E+001	-6.9524E+001	1.5199E+001	-1.0114E+001	-4.5134E+001	-4.4601E+001	1.5736E+001	-9.5754E+000	6.7392E+001	4.4214E+003	-2.4540E+000
AxialStress25	Maximum	LC_36	9.8510E+005	2.3560E+006	2.2647E+007	-3.6160E+008	-1.1581E+008	1.0070E+007	-2.8161E+001	-5.7478E+001	3.8941E+001	-2.0732E+001	-5.0394E+001	1.5368E+001	1.5906E+001	-2.0193E+001	-4.9855E+001	7.2739E+001	3.7059E+003	-4.0010E+000
AxialStress70	Minimum	LC_36	1.4302E+006	1.0368E+006	2.2029E+007	-1.8670E+008	9.5840E+007	1.3510E+007	-4.1387E+001	-1.6153E+001	1.2577E+001	-3.2468E+001	-2.3619E+001	1.4109E-001	6.7427E-001	-3.1929E+001	-2.3084E+001	4.8263E+001	1.5607E+003	-1.0820E+000
AxialStress70	Maximum	LC_25	-4.3230E+006	-9.1700E+005	2.2127E+007	1.9675E+008	-5.0300E+008	-9.8280E+006	6.1504E+001	-6.9670E+001	-4.5226E+001	3.1155E+001	-3.7134E+001	3.7758E+001	-3.7225E+001	3.1687E+001	-3.6596E+001	7.0662E+001	3.9833E+003	1.9910E+000
AxialStress66	Minimum	LC_12	-1.8360E+006	1.9974E+006	2.2980E+007	-2.8143E+008	-3.7490E+008	1.6970E+007	1.1075E+001	-8.4788E+001	2.8490E+001	-6.0274E-001	-6.1441E+001	2.3793E+000	2.9175E+000	-6.8471E-002	-6.0920E+001	7.7371E+001	3.1296E+003	-2.5880E+000
AxialStress66	Maximum	LC_1	-7.6765E+006	-1.1378E+006	2.0480E+007	1.0223E+008	-5.8772E+007	7.9595E+006	-4.1315E+000	-1.2617E+001	-2.9876E+001	-2.0063E+001	1.2543E+001	-4.3390E+001	-4.2863E+001	-1.9529E+001	1.3065E+001	5.7019E+001	1.4724E+003	8.4960E+000
AxialStress68	Minimum	LC_1	-1.1080E+007	-7.6405E+005	1.9980E+007	1.1500E+008	-3.4730E+008	1.2291E+006	3.2710E+001	-4.9114E+001	-3.1048E+001	3.4730E+000	1.8449E+000	-5.1691E+001	-5.1159E+001	4.0016E+000	2.3662E+000	4.9660E+001	1.4855E+003	8.7660E+000
AxialStress68	Maximum	LC_33	1.1318E+006	2.4322E+006	2.2790E+007	-3.5940E+008	-1.1176E+008	1.2058E+007	-2.8565E+001	-5.6912E+001	3.8528E+001	-2.0828E+001	-5.1156E+001	1.5547E+001	1.6080E+001	-2.0290E+001	-5.0618E+001	6.5151E+001	3.7060E+003	-4.4300E+000
AxialStress75	Minimum	LC_1	-1.1080E+007	-7.6405E+005	1.9980E+007	1.1500E+008	-3.4730E+008	1.2291E+006	3.2710E+001	-4.9114E+001	-3.1048E+001	3.4730E+000	1.8449E+000	-5.1691E+001	-5.1159E+001	4.0016E+000	2.3662E+000	4.9660E+001	1.4855E+003	8.7660E+000
AxialStress75	Maximum	LC_36	1.1318E+006	2.4322E+006	2.2790E+007	-3.5940E+008	-1.1176E+008	1.2058E+007	-2.8565E+001	-5.6912E+001	3.8528E+001	-2.0828E+001	-5.1156E+001	1.5547E+001	1.6080E+001	-2.0290E+001	-5.0618E+001	6.5151E+001	3.7060E+003	-4.4300E+000
AxialStress77	Minimum	LC_36	1.4302E+006	1.0368E+006	2.2029E+007	-1.8670E+008	9.5840E+007	1.3510E+007	-4.1387E+001	-1.6153E+001	1.2577E+001	-3.2468E+001	-2.3619E+001	1.4109E-001	6.7427E-001	-3.1929E+001	-2.3084E+001	4.8263E+001	1.5607E+003	-1.0820E+000
AxialStress77	Maximum	LC_25	-4.3230E+006	-9.1700E+005	2.2127E+007	1.9675E+008	-5.0300E+008	-9.8280E+006	6.1504E+001	-6.9670E+001	-4.5226E+001	3.1155E+001	-3.7134E+001	3.7758E+001	-3.7225E+001	3.1687E+001	-3.6596E+001	7.0662E+001	3.9833E+003	1.9910E+000
AxialStress73	Minimum	LC_9	-1.8360E+006	1.9974E+006	2.2980E+007	-2.8143E+008	-3.7490E+008	1.6970E+007	1.1075E+001	-8.4788E+001	2.8490E+001	-6.0274E-001	-6.1441E+001	2.3793E+000	2.9175E+000	-6.8477E-002	-6.0920E+001	7.7371E+001	3.1296E+003	-2.5880E+000
AxialStress73	Maximum	LC_1	-7.6765E+006	-1.1378E+006	2.0480E+007	1.0223E+008	-5.8772E+007	7.9595E+006	-4.1315E+000	-1.2617E+001	-2.9876E+001	-2.0063E+001	1.2543E+001	-4.3390E+001	-4.2863E+001	-1.9529E+001	1.3065E+001	5.7019E+001	1.4724E+003	8.4960E+000
HorWindV	Minimum	LC_24	-1.1480E+006	2.5300E+005	2.1970E+007	-2.1457E+007	-1.4511E+008	1.1140E+006	4.4368E-001	3.6724E+001	-1.2428E+001	-5.3413E+000	-2.8151E+001	1.5305E+001	-1.4772E+001	-4.8031E+000	-2.7613E+001	2.0812E+001	3.4147E+003	-1.3010E+000
HorWindV	Maximum	LC_25	-1.8660E+006	-1.4930E+006	2.1360E+007	2.2950E+008	-1.7330E+008	-1.3240E+007	2.2187E+001	-2.3800E+001	-5.1105E+001	7.2172E+000	-1.4487E+001	-3.4308E+001	-3.3775E+001	7.7500E+000	-1.3954E+001	9.2952E+001	1.1667E+003	5.5680E-001

Extreme load/deflection tables for the 500-year extreme load case:

Table F-18. Extreme 500-Year Tower-Top Displacements

Parameter	Type	File Name	TTDspFA m	TTDspSS m	Time s	HorWindV (m/s)	Wave1Elev m
TTDspFA	Minimum	LC_28	- 7.1558E-001	8.8810E-002	2.9068E+003	6.1374E+001	- 2.0630E+000
TTDspFA	Maximum	LC_32	2.7765E+000	9.5290E-002	1.5577E+003	8.4628E+001	2.9890E+000
TTDspSS	Minimum	LC_33	1.3640E+000	- 1.6473E+000	4.4012E+003	1.0297E+002	- 8.5320E-001
TTDspSS	Maximum	LC_28	1.3410E+000	1.6258E+000	1.8741E+003	8.7410E+001	- 1.6740E+000

Table F-19. Blade 1 Extreme 500-Year Out-of-Plane Deflections (edgewise)

Parameter	Type	File Name	OoPDefl1 m	Time s	HorWindV (m/s)	Wave1Elev m
OoPDefl1	Minimum	LC_12	- 1.5611E+000	4.3433E+003	8.0992E+001	2.8290E+000
OoPDefl1	Maximum	LC_28	8.1665E-001	2.9097E+003	5.9191E+001	3.4440E+000

Table F-20. Blade 1 In-Plane 500-Year Extreme Deflections (flapwise)

Parameter	Type	File Name	IPDefl1 m	Time s	HorWindV (m/s)	Wave1Elev m
IPDefl1	Minimum	LC_36	- 2.0171E+001	3.9823E+003	1.0053E+002	1.5850E+000
IPDefl1	Maximum	LC_52	1.3590E+001	4.1507E+003	9.3855E+001	4.5100E+000

Table F-21. Blade 1 500-Year Extreme Loads (at blade root)

Parameter	Type	File Name	RootFxc1 kN	RootFyc1 kN	RootFzc1 kN	RootF1 (kN)	RootM1 (kNm)	RootMzc1 kN·m	Time s	HorWindV (m/s)	Wave1Elev m
RootFxc1	Minimum	LC_25	**- 4.1492E+002**	6.9008E+002	- 5.3402E+002	8.0521E+002	4.1344E+004	- 3.5010E+002	2.9185E+003	7.0801E+001	- 3.1360E+000
RootFxc1	Maximum	LC_36	**3.5712E+002**	- 1.0570E+003	- 4.0620E+002	1.1157E+003	5.2234E+004	2.6063E+002	2.4929E+003	8.5024E+001	- 3.7520E-001
RootFyc1	Minimum	LC_36	- 2.1280E+002	**- 1.9303E+003**	- 7.2760E+002	1.9420E+003	1.0151E+005	9.8670E+002	3.9804E+003	9.0746E+001	2.6620E-001
RootFyc1	Maximum	LC_61	2.7498E+001	**1.9779E+003**	- 4.5360E+002	1.9781E+003	7.3860E+004	- 6.7820E+002	2.7000E+003	8.1359E+001	- 8.3800E-001
RootFzc1	Minimum	LC_48	3.3300E+001	- 9.2580E+002	**- 8.0615E+002**	9.2640E+002	6.4867E+004	1.1240E+002	4.2947E+003	7.4525E+001	1.7680E+000
RootFzc1	Maximum	LC_32	1.2720E+002	8.5394E+001	**6.6283E+002**	1.5321E+002	2.0060E+003	- 3.5230E+002	4.0123E+003	7.4202E+001	- 1.4570E+000
RootF1	Minimum	LC_5	3.3900E-001	3.0830E-001	5.9430E+002	**4.5822E-001**	4.1632E+003	- 3.1870E+002	4.5131E+003	8.3307E+001	- 1.1520E-001
RootF1	Maximum	LC_64	2.7498E+001	1.9779E+003	- 4.5360E+002	**1.9781E+003**	7.3860E+004	- 6.7820E+002	2.7000E+003	8.1359E+001	- 8.3800E-001
RootM1	Minimum	LC_21	2.7810E+001	2.1830E+002	- 4.6370E+002	2.2006E+002	**1.8402E+001**	- 1.2800E+001	1.6576E+003	4.3382E+001	- 2.7490E+000
RootM1	Maximum	LC_36	- 2.1280E+002	- 1.9303E+003	- 7.2760E+002	1.9420E+003	**1.0151E+005**	9.8670E+002	3.9804E+003	9.0746E+001	2.6620E-001
RootMzc1	Minimum	LC_28	1.8347E+002	5.8410E+002	- 5.7380E+002	6.1224E+002	2.3773E+004	**- 1.2040E+003**	1.1747E+003	8.7885E+001	- 2.8470E-002
RootMzc1	Maximum	LC_4	- 1.7535E+001	- 1.7375E+003	3.3794E+002	1.7376E+003	8.3145E+004	**1.2475E+003**	1.1091E+003	9.3532E+001	6.4260E+000

Table F-22. Yaw Bearing 500-Year Extreme Loads

Parameter	Type	File Name	YawBrFxp kN	YawBrFyp kN	YawBrFzp kN	YawBrMxp kN·m	YawBrMyp kN·m	YawBrMzp kN·m	Time s	HorWindV (m/s)	Wave1Elev m
YawBrFxp	Minimum	LC_25	**- 2.1534E+003**	3.0000E+002	- 8.8530E+003	7.3310E+003	5.2490E+004	5.2180E+002	2.9068E+003	6.1374E+001	- 2.0630E+000
YawBrFxp	Maximum	LC_25	**3.3378E+003**	1.2228E+003	- 9.1078E+003	2.7750E+003	5.1370E+004	8.6171E+003	2.9157E+003	6.8578E+001	- 3.4400E+000
YawBrFyp	Minimum	LC_33	1.0810E+003	**- 3.0326E+003**	- 9.3241E+003	9.3906E+002	5.4535E+004	- 1.8938E+004	4.4012E+003	1.0297E+002	- 8.5320E-001
YawBrFyp	Maximum	LC_49	4.8320E+002	**3.0370E+003**	- 9.4870E+003	9.5070E+002	6.5178E+004	1.6454E+004	1.2101E+003	8.9257E+001	- 4.9910E+000
YawBrFzp	Minimum	LC_12	8.9180E+002	- 2.5179E+003	**- 1.0433E+004**	2.9720E+002	5.8750E+004	- 2.8702E+004	1.1428E+003	9.1557E+001	- 2.1770E+000
YawBrFzp	Maximum	LC_36	- 6.5218E+002	- 3.5810E+002	**- 8.0899E+003**	- 5.2380E+003	3.8760E+004	4.1434E+003	3.3565E+003	6.4658E+001	- 3.5680E-001
YawBrMxp	Minimum	LC_57	1.9190E+003	6.6550E+002	- 9.2509E+003	**- 1.1090E+004**	7.1400E+004	2.9690E+003	3.2852E+003	6.7941E+001	4.4860E+000
YawBrMxp	Maximum	LC_1	1.1000E+003	- 5.3880E+002	- 9.1600E+003	**1.1524E+004**	7.3057E+004	- 5.1272E+003	4.2934E+003	5.0211E+001	1.4190E+000
YawBrMyp	Minimum	LC_25	- 1.7142E+003	1.5950E+003	- 8.6448E+003	1.4234E+002	**2.6920E+004**	7.1300E+003	2.9185E+003	7.0801E+001	- 3.1360E+000
YawBrMyp	Maximum	LC_64	2.5170E+003	9.7350E+002	- 9.1952E+003	8.1607E+003	**8.3653E+004**	7.9440E+003	1.0973E+003	6.8398E+001	- 5.5570E-001
YawBrMzp	Minimum	LC_57	1.5745E+003	- 1.9069E+003	- 9.4940E+003	- 9.3259E+002	6.2280E+004	**- 3.2117E+004**	2.9189E+003	7.6440E+001	- 2.5530E+000
YawBrMzp	Maximum	LC_4	1.4270E+003	2.3290E+003	- 8.9137E+003	6.4310E+002	6.5280E+004	**3.1072E+004**	4.0292E+003	7.6935E+001	- 5.3850E+000

Table F-23. Tower Base 500-Year Extreme Loads

Parameter	Type	File Name	TwrBsFxt kN	TwrBsFyt kN	TwrBsF (kN)	TwrBsFzt kN	TwrBsMxt kN·m	TwrBsMyt kN·m	TwrBsM (kNm)	TwrBsMzt kN·m	Time s	HorWindV (m/s)	Wave1Elev m
TwrBsFxt	Minimum	LC_25	**-1.8570E+003**	2.1260E+002	1.8691E+003	-1.5394E+004	-2.7280E+004	-1.7920E+005	1.8126E+005	2.5353E+003	2.9070E+003	6.2632E+001	-1.9280E+000
TwrBsFxt	Maximum	LC_28	**5.2490E+003**	1.2951E+003	5.4064E+003	-1.5590E+004	-1.4190E+005	5.3176E+005	5.5036E+005	8.3580E+003	2.9158E+003	7.9218E+001	-3.5980E+000
TwrBsFyt	Minimum	LC_36	2.5880E+003	**-3.2248E+003**	4.1348E+003	-1.5373E+004	3.3950E+005	2.2530E+005	4.0746E+005	-1.8220E+004	4.4015E+003	9.6878E+001	-8.7420E-001
TwrBsFyt	Maximum	LC_13	3.3180E+003	**3.0788E+003**	4.5264E+003	-1.5840E+004	-3.2856E+005	3.4740E+005	4.7816E+005	1.8529E+004	3.1321E+003	7.8930E+001	1.4290E+000
TwrBsF	Minimum	LC_41	-3.4097E+000	-7.7155E-001	**3.4959E+000**	-1.5331E+004	1.4730E+004	1.5870E+004	2.1652E+004	-2.1750E+003	2.2515E+003	6.6734E+001	-1.2410E+000
TwrBsF	Maximum	LC_25	5.2490E+003	1.2951E+003	**5.4064E+003**	-1.5590E+004	-1.4190E+005	5.3176E+005	5.5036E+005	8.3580E+003	2.9158E+003	7.9218E+001	-3.5980E+000
TwrBsFzt	Minimum	LC_12	2.1350E+003	-2.4384E+003	3.2410E+003	**-1.6986E+004**	2.7590E+005	2.2940E+005	3.5881E+005	-2.8732E+004	1.1428E+003	9.1557E+001	-2.1770E+000
TwrBsFzt	Maximum	LC_36	4.8780E+002	-2.6850E+002	5.5681E+002	**-1.4480E+004**	2.6330E+004	2.2650E+004	3.4732E+004	4.1412E+003	3.3565E+003	6.4658E+001	-3.5680E-001
TwrBsMxt	Minimum	LC_25	2.6310E+003	3.0223E+003	4.0070E+003	-1.5426E+004	**-3.3671E+005**	2.6250E+005	4.2694E+005	2.2062E+004	1.8741E+003	8.7410E+001	-1.6740E+000
TwrBsMxt	Maximum	LC_36	2.6595E+003	-3.1800E+003	4.1455E+003	-1.5450E+004	**3.4014E+005**	2.3880E+005	4.1560E+005	-1.9440E+004	4.4014E+003	1.0260E+002	-8.7020E-001
TwrBsMyt	Minimum	LC_25	-1.7850E+003	1.5167E+002	1.7914E+003	-1.5360E+004	-2.4150E+004	**-1.8275E+005**	1.8434E+005	8.5430E+002	2.9069E+003	5.9090E+001	-1.9960E+000
TwrBsMyt	Maximum	LC_36	4.9485E+003	-1.3170E+003	5.1208E+003	-1.5530E+004	1.3690E+005	**5.3606E+005**	5.5326E+005	-1.1125E+004	1.5579E+003	8.1522E+001	2.6250E+000
TwrBsM	Minimum	LC_53	2.2323E+002	2.9650E+001	2.2520E+002	-1.5442E+004	1.3690E+002	-2.7980E+002	**3.1150E+002**	3.1814E+003	2.1643E+003	6.9435E+001	-7.8790E-001
TwrBsM	Maximum	LC_25	5.0634E+003	1.2940E+003	5.2262E+003	-1.5460E+004	-1.5880E+005	5.3272E+005	**5.5589E+005**	2.5090E+004	1.5576E+003	9.0488E+001	3.0880E+000
TwrBsMzt	Minimum	LC_57	2.9230E+003	-1.8018E+003	3.4337E+003	-1.6020E+004	1.9870E+005	3.1946E+005	3.7621E+005	**-3.2137E+004**	2.9189E+003	7.6440E+001	-2.5530E+000
TwrBsMzt	Maximum	LC_4	3.1160E+003	2.1350E+003	3.7773E+003	-1.5420E+004	-2.5220E+005	3.1790E+005	4.0579E+005	**3.1102E+004**	4.0292E+003	7.6935E+001	-5.3850E+000

Table F-24. Mudline Reaction 500-Year Extreme Loads

Parameter	Type	File Name	ReactFXss N	ReactFYss N	ReactFZss N	ReactMXss Nm	ReactMYss Nm	ReactMZss Nm	HorWindV (m/s)	WindVxi m/s	Time s	Wave1Elev m
ReactFXss	Minimum	LC_24	**-1.5213E+007**	1.2270E+006	2.0330E+007	-2.2240E+008	-3.5909E+008	1.6789E+007	6.9329E+001	6.8790E+001	2.1997E+003	1.3390E+001
ReactFXss	Maximum	LC_16	**8.4190E+006**	-4.3510E+005	2.5665E+007	8.8500E+007	-4.5220E+006	-6.9676E+006	5.7343E+001	5.6997E+001	2.1956E+003	-1.4000E+001
ReactFYss	Minimum	LC_13	-5.8740E+006	**-3.3718E+006**	2.1750E+007	4.7578E+008	-5.3520E+008	-1.8762E+007	7.8930E+001	7.8576E+001	3.1321E+003	1.4290E+000
ReactFYss	Maximum	LC_36	-4.9233E+006	**3.5200E+006**	2.1760E+007	-4.8274E+008	-4.9150E+008	1.6240E+007	8.9838E+001	8.9590E+001	4.4009E+003	-8.8800E-001
ReactFZss	Minimum	LC_37	-1.1170E+007	-7.3591E+005	**1.9570E+007**	7.2710E+007	-2.4360E+008	-8.1929E+005	7.1029E+001	7.0892E+001	3.1443E+003	8.2150E+000
ReactFZss	Maximum	LC_16	8.4190E+006	-4.3510E+005	**2.5665E+007**	8.8500E+007	-4.5220E+006	-6.9676E+006	5.7343E+001	5.6997E+001	2.1956E+003	-1.4000E+001
ReactMXss	Minimum	LC_33	-4.2840E+006	3.2074E+006	2.2060E+007	**-4.8790E+008**	-3.8110E+008	2.2583E+007	1.0260E+002	1.0250E+002	4.4014E+003	-8.7020E-001
ReactMXss	Maximum	LC_13	-5.8740E+006	-3.3718E+006	2.1750E+007	**4.7578E+008**	-5.3520E+008	-1.8762E+007	7.8930E+001	7.8576E+001	3.1321E+003	1.4290E+000
ReactMYss	Minimum	LC_28	-7.5230E+006	-1.0760E+006	2.1240E+007	2.1270E+008	**-7.9529E+008**	-2.4610E+007	9.0488E+001	9.0320E+001	1.5576E+003	3.0880E+000
ReactMYss	Maximum	LC_25	4.7382E+005	-3.1480E+005	2.2242E+007	3.8980E+007	**2.4757E+008**	-1.9936E+006	6.2632E+001	6.2100E+001	2.9070E+003	-1.9280E+000
ReactMZss	Minimum	LC_1	-3.2040E+006	-1.9150E+006	2.3210E+007	3.4380E+008	-4.6110E+008	**-3.7663E+007**	7.6935E+001	7.6930E+001	4.0292E+003	-5.3850E+000
ReactMZss	Maximum	LC_72	-7.1880E+006	1.9902E+006	2.1370E+007	-2.9954E+008	-3.4520E+008	**3.6699E+007**	7.8740E+001	7.7020E+001	3.1079E+003	6.5920E+000
HorWindV	Minimum	LC_24	-1.3076E+006	1.5670E+005	2.2270E+007	3.0649E+006	-1.4150E+008	4.5050E+005	**2.4971E+001**	2.4956E+001	3.4147E+003	-1.2670E+000
HorWindV	Maximum	LC_49	-4.7330E+006	-8.4403E+005	2.2160E+007	1.3790E+008	-5.5190E+008	-1.3220E+007	**1.1565E+002**	1.1551E+002	4.1405E+003	-8.4740E-001
WindVxi	Minimum	LC_13	-1.2471E+006	-4.7064E+005	2.2100E+007	2.3742E+007	-1.5269E+008	-9.0850E+006	2.4971E+001	**2.4956E+001**	3.4147E+003	-1.2670E+000
WindVxi	Maximum	LC_60	-5.0750E+006	1.4440E+006	2.1630E+007	-2.1880E+008	-6.0130E+008	9.8372E+006	1.1565E+002	**1.1551E+002**	4.1405E+003	-8.4740E-001

Table F-25. Maximum/Minimum 500-Year Stress Levels for Selected Critical Members

Parameter	Type	File Name	ReactFXss N	ReactFYss N	ReactFZss N	ReactMXss Nm	ReactMYss Nm	ReactMZss Nm	AxialStress26 (N/mm^2)	AxialStress24 (N/mm^2)	AxialStress25 (N/mm^2)	AxialStress70 (N/mm^2)	AxialStress66 (N/mm^2)	AxialStress68 (N/mm^2)	AxialStress75 (N/mm^2)	AxialStress77 (N/mm^2)	AxialStress73 (N/mm^2)	HorWindV (m/s)	Time s	Wave1Elev m
ReactFXss	Minimum	LC_24	-1.5213E+007	1.2270E+006	2.0330E+007	- 2.2240E+008	- 3.5909E+008	1.6789E+007	6.7782E+000	- 7.1018E+001	2.1152E+001	- 1.7981E+001	- 8.0232E-001	- 3.7084E+001	- 3.6546E+001	- 1.7453E+001	- 2.8878E-001	6.9329E+001	2.1997E+003	1.3390E+001
ReactFXss	Maximum	LC_16	8.4190E+006	-4.3510E+005	2.5665E+007	8.8500E+007	- 4.5220E+006	- 6.9676E+006	- 6.2587E+000	- 1.6377E+001	3.2110E+001	- 8.0173E-001	- 4.6871E+001	1.1132E+000	1.6534E+000	- 2.5630E-001	- 4.6311E+001	5.7343E+001	2.1956E+003	- 1.4000E+001
ReactFYss	Minimum	LC_13	- 5.8740E+006	- 3.3718E+006	2.1750E+007	4.7578E+008	- 1.8762E+007	8.5883E+001	- 5.4191E+001	- 8.7186E+001	4.0127E+001	- 1.9077E+001	- 6.0612E+001	- 6.0084E+001	- 6.0084E+001	4.0665E+001	- 1.8544E+001	3.1321E+003	1.4290E+000	
ReactFYss	Maximum	LC_36	-4.9233E+006	3.5200E+006	2.1760E+007	- 4.8274E+008	- 4.9150E+008	1.6240E+007	9.7265E+000	- 1.1263E+002	5.9579E+001	- 7.3016E-001	- 6.9115E+001	1.1397E+001	1.1935E+001	- 2.0111E-001	- 6.8587E+001	8.9838E+001	4.4009E+003	- 8.8800E-001
ReactFZss	Minimum	LC_37	- 1.1170E+007	- 7.3591E+005	1.9570E+007	7.2710E+007	- 2.4360E+008	- 8.1929E+005	1.5793E+001	- 3.7930E+001	- 2.4802E+001	- 7.2172E+000	7.3280E+000	- 4.6927E+001	- 4.6399E+001	- 6.6896E+000	7.8503E+000	7.1029E+001	3.1443E+003	8.2150E+000
ReactFZss	Maximum	LC_16	8.4190E+006	-4.3510E+005	2.5665E+007	8.8500E+007	- 4.5220E+006	- 6.9676E+006	- 6.2587E+000	- 1.6377E+001	- 3.2110E+001	- 8.0173E-001	- 4.6871E+001	1.1132E+000	1.6534E+000	- 2.5630E-001	- 4.6311E+001	5.7343E+001	2.1956E+003	- 1.4000E+001
ReactMXss	Minimum	LC_33	-4.2840E+006	3.2074E+006	2.2060E+007	- 4.8790E+008	3.8110E+008	2.2583E+007	- 4.8483E+000	- 9.8393E+001	6.0302E+001	- 1.1775E+001	- 6.2263E+001	1.2514E+001	1.3047E+001	- 1.1243E+001	- 6.1686E+001	1.0260E+002	4.4014E+003	- 8.7020E-001
ReactMXss	Maximum	LC_13	- 5.8740E+006	- 3.3718E+006	2.1750E+007	4.7578E+008	- 5.3520E+008	- 1.8762E+007	8.5883E+001	- 5.4191E+001	- 8.7186E+001	4.0127E+001	- 1.9077E+001	- 6.0612E+001	- 6.0084E+001	4.0665E+001	- 1.8544E+001	3.1321E+003	1.4290E+000	
ReactMYss	Minimum	LC_28	- 7.5230E+006	- 1.0760E+006	2.1240E+007	2.1270E+008	- 7.9529E+008	2.4610E+007	9.8061E+001	- 1.0722E+002	- 4.7255E+001	5.4756E+001	- 4.9149E+001	- 4.0107E+001	- 3.9574E+001	5.5283E+001	- 4.8621E+001	9.0488E+001	1.5576E+003	3.0880E+000
ReactMYss	Maximum	LC_25	4.7382E+005	- 3.1480E+005	2.2242E+007	3.8980E+007	2.4757E+008	- 1.9936E+006	- 4.6028E+001	1.9080E+001	- 2.3561E+001	- 3.3826E+001	5.4684E+000	- 1.9424E+001	- 1.8887E+001	- 3.3287E+001	6.0061E+000	6.2632E+001	2.9070E+003	- 1.9280E+000
ReactMZss	Minimum	LC_1	- 3.2040E+006	- 1.9150E+006	2.3210E+007	3.4380E+008	- 4.6110E+008	- 3.7663E+007	6.5341E+001	- 5.6481E+001	7.0153E+001	3.8871E+001	- 2.5271E+001	- 4.2575E+001	- 4.2037E+001	3.9410E+001	- 2.4733E+001	7.6935E+001	4.0292E+003	- 5.3850E+000
ReactMZss	Maximum	LC_72	- 7.1880E+006	1.9902E+006	2.1370E+007	- 2.9954E+008	- 3.4520E+008	3.6699E+007	4.8516E+000	- 7.7785E+001	3.3434E+001	- 1.3923E+001	- 4.0707E+001	- 1.3133E+001	- 1.2599E+001	- 1.3395E+001	- 4.0180E+001	7.8740E+001	3.1079E+003	6.5920E+000
AxialStress26	Minimum	LC_57	1.2553E+006	1.8110E+006	2.1730E+007	- 2.9870E+008	1.2170E+008	7.2420E+006	- 5.4306E+001	- 2.1020E+001	2.8745E+001	- 3.7653E+001	- 2.6125E+001	9.9816E+000	1.0509E+001	- 3.7120E+001	- 2.5587E+001	6.0648E+001	3.2879E+003	- 1.1120E+000
AxialStress26	Maximum	LC_28	- 6.4075E+006	- 2.3082E+006	2.1688E+007	3.4795E+008	- 7.2709E+008	- 1.8510E+007	1.0093E+002	- 8.8804E+001	- 6.7294E+001	5.1713E+001	- 3.9594E+001	- 4.9586E+001	- 4.9048E+001	5.2246E+001	- 3.9061E+001	9.1692E+001	3.9835E+003	1.6550E+000
AxialStress24	Minimum	LC_33	- 6.8057E+006	1.5330E+006	2.1490E+007	- 2.0220E+008	- 7.8242E+008	1.4053E+007	6.8129E+001	- 1.3221E+002	1.8491E+001	3.1301E+001	- 7.7289E+001	- 1.0673E+001	- 1.0140E+001	3.1829E+001	- 7.6762E+001	8.1522E+001	1.5579E+003	2.6250E+000
AxialStress24	Maximum	LC_61	9.0606E+005	1.8220E+006	2.2880E+007	2.8400E+008	1.8205E+008	- 1.6972E+007	- 1.9617E+001	2.6214E+001	- 6.1724E+001	- 1.6074E+001	1.1585E+001	- 3.5857E+001	- 3.5320E+001	- 1.5531E+001	1.2118E+001	7.2818E+001	1.1404E+003	- 4.1590E+000
AxialStress25	Minimum	LC_25	- 6.1961E+006	- 2.9970E+006	2.1900E+007	4.7562E+008	- 4.3490E+008	- 2.2199E+007	7.2044E+001	- 4.0419E+001	- 8.8024E+001	3.4165E+001	- 8.1140E+000	- 6.2781E+001	- 6.2253E+001	3.4698E+001	- 7.5812E+000	8.7410E+001	1.8741E+003	- 1.6740E+000
AxialStress25	Maximum	LC_33	- 4.2840E+006	3.2074E+006	2.2060E+007	- 4.8790E+008	- 3.8110E+008	2.2583E+007	- 4.8483E+000	- 9.8393E+001	6.0302E+001	- 1.1775E+001	- 6.2263E+001	1.2514E+001	1.3047E+001	- 1.1243E+001	- 6.1686E+001	1.0260E+002	4.4014E+003	- 8.7020E-001
AxialStress70	Minimum	LC_57	- 3.2032E+006	1.9821E+006	2.2523E+007	- 3.4510E+008	2.3226E+007	2.3851E+007	- 4.6558E+001	- 3.4242E+001	3.7381E+001	- 4.0352E+001	- 2.3444E+001	1.0919E-001	6.4067E-001	- 3.9813E+001	- 2.2911E+001	7.2964E+001	3.2817E+003	- 1.8040E+000
AxialStress70	Maximum	LC_28	- 7.5230E+006	- 1.0760E+006	2.1240E+007	2.1270E+008	- 7.9529E+008	- 2.4610E+007	9.8061E+001	- 1.0722E+002	- 4.7255E+001	5.4756E+001	- 4.9149E+001	- 4.0107E+001	- 3.9574E+001	5.5283E+001	- 4.8621E+001	9.0488E+001	1.5576E+003	3.0880E+000
AxialStress66	Minimum	LC_12	- 3.4610E+006	2.9384E+006	2.3428E+007	- 4.2308E+008	- 5.8819E+008	2.7780E+007	2.7802E+001	- 1.2217E+002	5.1279E+001	7.2812E+000	- 8.2308E+001	9.2099E+000	9.7480E+000	7.8135E+000	- 8.1728E+001	9.8896E+001	3.1295E+003	- 2.6520E+000
AxialStress66	Maximum	LC_1	- 1.1343E+007	- 1.2845E+006	1.9970E+007	1.4980E+008	- 9.0804E+007	2.3800E+006	1.8824E+000	- 1.2049E+001	- 3.7200E+001	- 1.8534E+001	2.8836E+001	- 5.7757E+001	- 5.7183E+001	- 1.8001E+001	2.9333E+001	7.2103E+001	1.4724E+003	1.0520E+001
AxialStress68	Minimum	LC_61	- 1.0659E+007	2.6450E+006	2.0769E+007	4.1429E+008	- 4.6618E+008	- 1.6838E+007	6.9522E+001	- 4.5912E+001	- 7.7484E+001	2.7655E+001	3.2672E+000	- 7.1641E+001	7.1113E+001	2.8188E+001	3.7901E+000	7.8033E+001	4.2129E+003	3.4170E+000
AxialStress68	Maximum	LC_12	4.8991E+005	2.7352E+006	2.3180E+007	- 4.6142E+008	- 1.6764E+008	1.6360E+007	- 2.9567E+001	- 7.1342E+001	5.4434E+001	- 2.3128E+001	- 5.8138E+001	2.2657E+001	2.3183E+001	- 2.2590E+001	- 5.7611E+001	8.4255E+001	4.3371E+003	- 2.8060E+000
AxialStress75	Minimum	LC_61	- 1.0659E+007	2.6450E+006	2.0769E+007	4.1429E+008	- 4.6618E+008	- 1.6838E+007	6.9522E+001	- 4.5912E+001	7.7484E+001	2.7655E+001	3.2672E+000	- 7.1641E+001	- 7.1113E+001	2.8188E+001	3.7901E+000	7.8033E+001	4.2129E+003	3.4170E+000
AxialStress75	Maximum	LC_9	4.9000E+005	2.7352E+006	2.3180E+007	- 4.6142E+008	- 1.6764E+008	1.6360E+007	- 2.9570E+001	- 7.1342E+001	5.4434E+001	- 2.3128E+001	- 5.8138E+001	2.2657E+001	2.3183E+001	- 2.2590E+001	- 5.7611E+001	8.4255E+001	4.3371E+003	- 2.8060E+000
AxialStress77	Minimum	LC_57	- 3.2032E+006	1.9821E+006	2.2523E+007	- 3.4510E+008	2.3226E+007	2.3851E+007	- 4.6558E+001	- 3.4242E+001	3.7381E+001	- 4.0352E+001	- 2.3444E+001	1.0919E-001	6.4067E-001	- 3.9813E+001	- 2.2911E+001	7.2964E+001	3.2817E+003	- 1.8040E+000
AxialStress77	Maximum	LC_25	- 7.5230E+006	- 1.0760E+006	2.1240E+007	2.1270E+008	- 7.9529E+008	- 2.4610E+007	9.8061E+001	- 1.0722E+002	- 4.7255E+001	5.4756E+001	- 4.9149E+001	- 4.0107E+001	- 3.9574E+001	5.5283E+001	- 4.8621E+001	9.0488E+001	1.5576E+003	3.0880E+000
AxialStress73	Minimum	LC_9	- 3.4610E+006	2.9384E+006	2.3428E+007	- 4.2308E+008	- 5.8819E+008	2.7780E+007	2.7802E+001	- 1.2217E+002	5.1279E+001	7.2812E+000	- 8.2308E+001	9.2099E+000	9.7480E+000	7.8135E+000	- 8.1728E+001	9.8896E+001	3.1295E+003	- 2.6520E+000
AxialStress73	Maximum	LC_4	- 1.1343E+007	- 1.2845E+006	1.9970E+007	1.4980E+008	- 9.0804E+007	2.3800E+006	1.8824E+000	- 1.2049E+001	- 3.7200E+001	- 1.8534E+001	2.8836E+001	- 5.7757E+001	- 5.7183E+001	- 1.8001E+001	2.9353E+001	7.2103E+001	1.4724E+003	1.0520E+001
HorWindV	Minimum	LC_24	- 1.3076E+006	1.5670E+005	2.2270E+007	3.0649E+006	- 1.4150E+008	4.5050E+005	1.7031E+000	- 3.4634E+001	- 1.6494E+001	- 4.5392E+000	- 2.6326E+001	- 1.8712E+001	- 1.8174E+001	- 4.0027E+000	- 2.5788E+001	2.4971E+001	3.4147E+003	- 1.2670E+000
HorWindV	Maximum	LC_49	- 4.7330E+006	- 8.4403E+005	2.2160E+007	1.3790E+008	- 5.5190E+008	- 1.3220E+007	6.2720E+001	- 8.0341E+001	- 3.6271E+001	3.1148E+001	- 4.1140E+001	- 3.1364E+001	- 3.0826E+001	3.1681E+001	- 4.0602E+001	1.1565E+002	4.1405E+003	- 8.4740E-001